Methapyrilene: Metabolism and Macromolecular Binding

by

Janine Estelle Rose

DISSERTATION

Submitted in partial satisfaction of the requirements for the degree of

DOCTOR OF PHILOSOPHY

in

Pharmaceutical Chemistry

in the

GRADUATE DIVISION

of the

UNIVERSITY OF CALIFORNIA

San Francisco

Abstract

The antihistamine methapyrilene was recently found to be a liver carcinogen in rats. Metabolic studies utilizing rat liver microsomes led to a degradation of approximately 35% of the drug in one hour at 37° in the presence of NADPH as determined by gas chromatography. Specifically ^{3}H-labeled methapyrilene was used to determine that the majority of the metabolites distributed into the aqueous phase upon organic extraction of the incubate. The metabolites were purified by preparative reverse phase high pressure liquid chromatography. With the aid of deuterium labeled methapyrilene, the structures of the metabolites were identified through GC-EIMS and ^{1}H-NMR analysis as well as total synthesis. A total of seven metabolites were identified and quantitated, with the major route of metabolism being oxidation of a carbon alpha to a tertiary amine.

Additionally, a significant percentage was found to bind covalently to microsomal proteins upon metabolic activation. The interaction was inhibited by sulfur nucleophiles such as cysteine ethyl ester and glutathione while other nucleophiles such as cyanide and BSA did not effect the binding. The protein-bound adduct(s) was found to be labile to acid and stable in the presence of base. Preliminary analysis of interactions with exogenous DNA have found a covalent attachment of approximately 250 pmol/mg DNA of microsomally activated ^{3}H-methapyrilene.

The consequences of the metabolic oxidation and macromolecular binding demonstrated by methapyrilene in vitro has been discussed with respect to its carcinogenicity.

Acknowledgments

I sincerely acknowledge Dr. Neal Castagnoli, Jr. for his guidance and encouragement in this research. It has been a pleasure to work with him and his many excellent colleagues.

I would like to thank Dr. A. Burlingame and the entire staff of the Bio-organic, Biomedical Mass Spectrometry Resource for their assistance in running mass spectra. Ms. Sydell Lewis and Dr. Ken Straub taught me how to operate the Kratos MS-25. Dr. Yoshihiko Shinohara and Mrs. Kay Castagnoli operated the MS-9 obtaining chemical ionization mass spectra. Drs. T. Baillie, R. Ketcham and C.-T. Peng provided numerous stimulating discussions on drug metabolism, synthesis and radiochemistry, respectively.

I also want to acknowledge all the graduate students, post doctoral fellows and visiting professors who helped me appreciate many areas of science outside of my own research.

Lastly, I would like to acknowledge my parents, Silviano and Jean Marin, for their continued interest in my research and science in general. I respect them for their everlasting pursuit of knowledge.

To those who have shared the many good restaurants, ski slopes and ice creams with me, it's been fun.

Dedication

To Allan

for his love,

patience

and unending support.

Table of Contents

List of Tables

List of Schemes

List of Figures

Figure

I. Introduction

Methapyrilene (1) is an ethylenediamine antihistamine recently found to be carcinogenic in rats. When fed to rats at 0.1 - 0.2% of their diet over a lifetime, methapyrilene was found to cause a high incidence of liver tumors.[1] Thus it was removed from numerous over-the-counter formulations such as Compoz, Excedrin- PM, Nytol, Sleep-eze, Sominex and others.[2] As a representative of a large class of highly prescribed competitive H1-histamine antagonists, the mechanism by which methapyrilene initiates carcinogenesis is of extreme interest and importance. This thesis considers the possible metabolic formation of a methapyrilene derived "ultimate carcinogen" and the interaction of metabolically activated methapyrilene with biologically important nucleophiles and macromolecules.

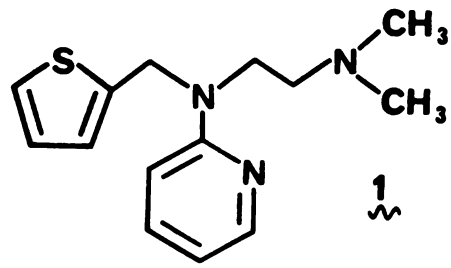

1

The relationship between cancer and chemicals has long been recognized. One of the earliest records is that by John Hill in 1761.[3] As a physician, he noted the development of nasal cancer as a result of excessive use of tobacco snuff. Similarly, Percival Pott later recorded the high incidence of scrotal cancer among young men who at some

time had been chimney sweeps.[4] Through the years, many carcinogens of biological and synthetic origin have been discovered.

The mechanism(s) by which chemical carcinogens elicit their response is variable and in many cases not well understood. In general terms, the non-carcinogenic xenobiotic or "precarcinogen" is believed to undergo metabolic activation in vivo to yield the "ultimate carcinogen." As shown in Figure I,[5] the precarcinogen may be transformed directly to the carcinogenic species or may require numerous metabolic reactions to reach the ultimate carcinogen. The ultimate carcinogen is in most cases an electrophilic intermediate which can covalently interact with nucleophiles present in DNA, RNA, various proteins and/or an inactivating nucleophile such as glutathione.

Figure 1. Metabolic Activation and Inactivation of Chemical Carcinogens.

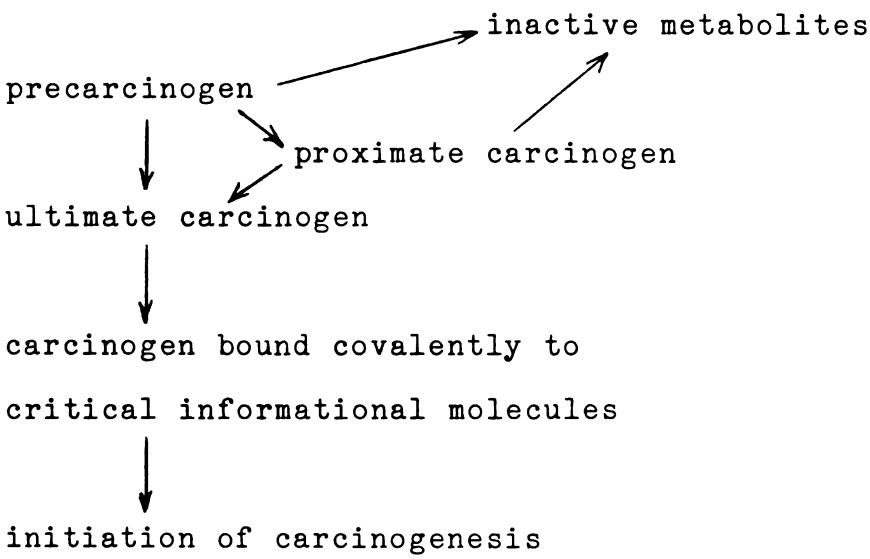

Carcinogens representative of different structural classes are shown in Table 1. A great deal of research has gone into determining the structures of the ultimate carcinogens shown here and will not be discussed in detail. In each case, however, specific metabolic transformations have occurred. In the case of benzo(a)pyrene (2), stereospecific metabolism by mixed function oxidase and epoxide hydrase leads to the proximate carcinogen, 7β,8α -dihydroxy-7,8-dihyrobenzo(a)pyrene.[6] Through subsequent stereoselective epoxidation, the benzo(a)pyrene backbone is further transformed to the carcinogenic diol-epoxide (3). Similarly, aflatoxin B1 (4), one of the most carcinogenic compounds known, undergoes epoxidation to form 5.[9,10] These two epoxides are representative of a large class of aromatic and olefinic compounds which undergo metabolic epoxidation. The epoxide carcinogens may be inactivated by either attack with an endogenous nucleophile such as glutathione or by an additional metabolic reaction with epoxide hydrase.

N-Acetylaminofluorene (AAF, 6) is another well studied carcinogen. The first step in its activation requires amide oxidation to the N-hydroxy-AAF.[5] Subsequent conjugation of this hydroxamic acid leads to the O-sulfate metabolite 7 which is believed to be the ultimate carcinogenic species.[5,11]

Dimethylnitrosamine (8), a small molecule in comparison

Table I. Formation of Ultimate Carcinogens.

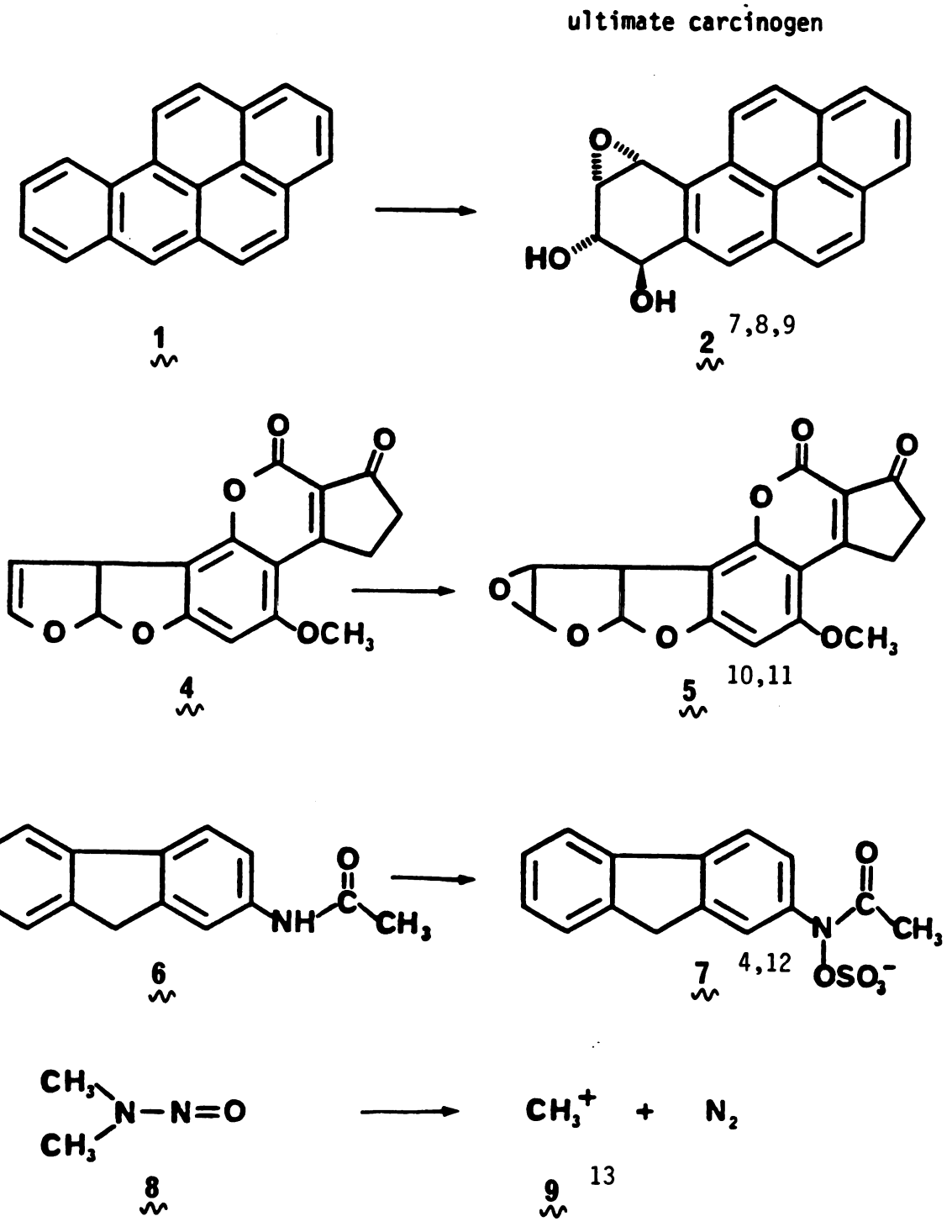

to the others discussed, gains activity by first undergoing oxidative dealkylation followed by dehydration and elimination of nitrogen to yield the methyl carbocation 9.[13]

Each of the electrophilic species in Table I is known to react with DNA[14] but this is not true for all carcinogens. In general, carcinogens can be classified into two types: genotoxic and epigenetic. Genotoxic carcinogens are those which damage DNA through covalent interactions. Epigenetic carcinogens include those compounds which do not directly alter DNA function but instead promote the growth of altered cells by interfering in some way with the transmission of regulatory factors. Among the many carcinogens being studied, benzo(a)pyrene, aflatoxin B1, safrole, 4-dimethylaminoazobenzene, 2-AAF and dimethylnitrosamine are known genotoxic carcinogens while DDT and phenobarbital are epigenetic carcinogens.[14]

Many carcinogens produce primarily liver tumors. Hepatic drug metabolism may be responsible in these cases for producing the electrophilic ultimate carcinogen. As reviewed by E.C. Miller,[12] the electron rich bases G, A, and C present in DNA as well as the phosphate moieties in the backbone represent nucleophiles which attack the electrophilic intermediates, causing an alteration in genomic information. Nucleophiles present in proteins include methionine, cysteine, histidine, tyrosine and lysine.[12] The biological consequences of DNA, RNA and

protein alkylation are believed to result in cellular mutation by mechanisms not well understood. In the case of epigenetic carcinogens, the interactions with the cell may be slow acting and sometimes reversible, thus increasing the difficulty of researching these mechanisms.

The structure of methapyrilene contains two tertiary amine centers, a pyridine ring and a benzylic thiophene moiety. By reviewing the known metabolism of these functionalities, as presented in the following sections, we can postulate the following electrophilic derivatives of methapyrilene as potential carcinogenic intermediates.

Metabolic dealkylation of tertiary amines appears to involve the formation of an iminium ion in equilibrium with its corresponding carbinolamine. The two tertiary amines present within methapyrilene have the potential to form the four iminium ions 10, 11, 12 and 13. Methapyrilene may undergo N-demethylation through the intermediate 10 or oxidative deamination via 11. The iminium ions 12 and 13 would result in dealkylation of the 2-aminopyridine nitrogen. To postulate which of these iminium ions might be the "ultimate carcinogen", one must consider the fact that not all tertiary amines are carcinogenic. Thus, the toxic iminium ion must have a particular stability uncommon to the majority of iminium ions generated in N-dealkylation. For this reason, iminium ion 11 is of special interest. The neighboring nitrogen of the pyridine ring has the potential for intramolecular cyclization to yield the stabilized

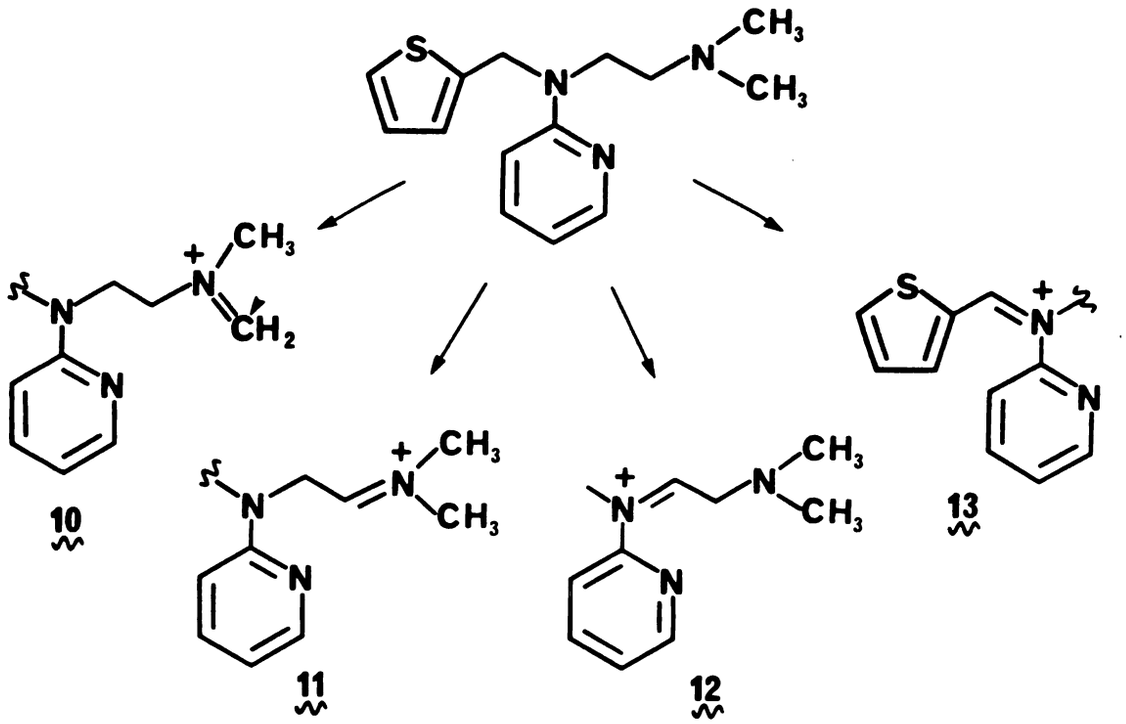

iminium ion 14. This process would enable the electrophilic iminium 11 to dissociate from the activating enzyme without hydrolysis and thus initiate carcinogenesis by interacting with other macromolecules. Such a stabilized electrophilic iminium ion may thus serve as a carcinogenic intermediate.

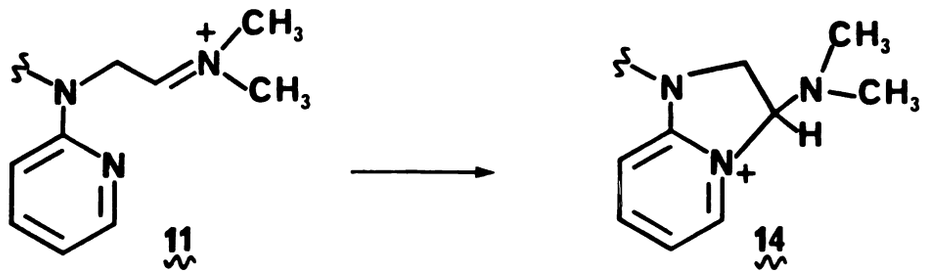

The presence of two heteroaromatic rings presents the potential for forming arene oxide derivatives of methapyrilene. The pyridine and thiophene rings may both undergo metabolic hydroxylation through electrophilic

epoxides such as 15 and 16. The electron-rich thiophene moiety is more likely to undergo epoxidation than the pyridine moiety but either one of these epoxides could react with biomacromolecules as does the carcinogenic diol-epoxide of benzo(a)pyrene.

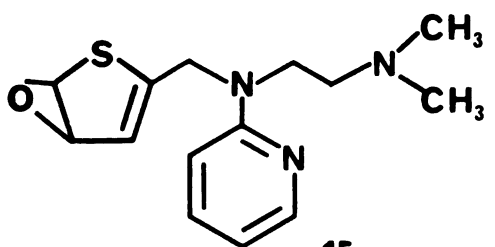

15

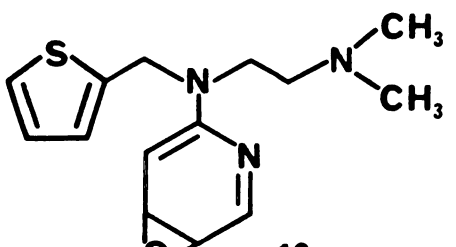

16

Additionally, N-dealkylation coupled with pyridine ring hydroxylation could lead to an iminoquinone 17 which itself could react with macromolecules resulting in toxicity. Such an intermediate derived from acetaminophen has been shown to interact with cellular nucleophiles leading to hepatotoxicity at high levels.

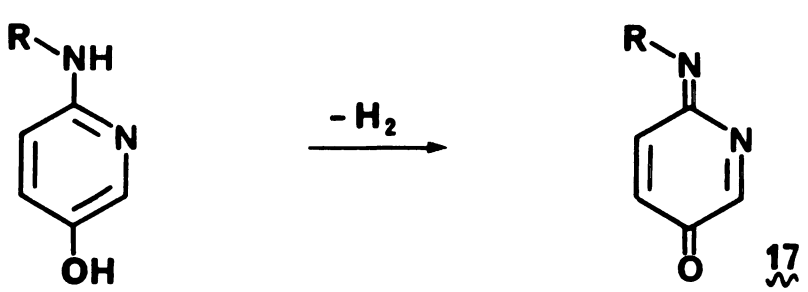

17

Thus, methapyrilene has the potential to form a number of different electrophilic intermediates, all of which might be carcinogenic. This research has been conducted in an attempt to aid the identification of the "ultimate carcinogen" derived metabolically from methapyrilene.

Reviews on the metabolism of tertiary amines, pyridine rings and thiophene analogs will be presented. The background on methapyrilene carcinogenesis and metabolism will also be discussed followed by our findings from rat microsomal metabolism of methapyrilene. Finally, the covalent binding of metabolically activated methapyrilene to macromolecules will be discussed along with concluding remarks concerning the overall findings of this thesis.

II. Drug Metabolism

Drug metabolism is the biochemical mechanism by which mammals transform xenobiotics and foreign compounds. Metabolism varies from one species to the next and in many cases is age-dependent. For most drugs, the liver is the primary site for metabolism in vivo although other tissues such as the kidney, lung and gastrointestinal tract contribute to the overall metabolism.

Metabolites themselves are an important aspect of drug therapy. In some cases, the activity of the metabolite(s) may resemble that of the parent compound. Lipophilic drugs, while easily absorbed, are not easily eliminated and can accumulate in the body tissues. Metabolism increases the polarity of lipid soluble drugs and enhances their excretion into urine and bile. These properties of the body have been utilized in the design of new drugs. Lipophilic prodrugs are metabolized to the polar, biologically active drug which would ordinarily not be absorbed. Many disease states show altered metabolism, for which reason drug and metabolite level monitoring has become important.

Metabolic processes have been divided into two basic categories. Type I metabolism generally includes such reactions as oxidation, reduction and hydrolysis of chemical functionalities present in drugs. Type II metabolic reactions involve conjugation with various ligands which highly increase the polarity of the overall molecule. A wide range of compounds can induce various enzymes important to

drug metabolism by mechanisms not well understood. Phenobarbital, 3-metylcholanthrene, β-naphthoflavone and pregnenolone-16α-carbonitrile are all inducers of mixed function oxidases.

Oxidation is a very important metabolic reaction. Unlike most enzyme catalyzed reactions, a wide variety of compounds including hydrocarbons, halogenated hydrocarbons, olefins, aromatic hydrocarbons and aliphatic and aromatic amines are metabolically oxidized to a variety of products. Not one but a group of enzymes is responsible for these oxidations. The majority of hepatic metabolic activity is contained within the microsomal enzymes and of these the smooth endoplasmic reticulum (SER) contains the oxidative enzymes as well as glucuronidase activity. For this reason, microsomal metabolism is often used for rapid in vitro assessment of metabolism. The cofactors required by mixed function oxidases include reduced nicotinamide adenine dinucleotide phosphate (NADPH) and oxygen. Microsomal glucuronidation requires uridine diphosphoglucuronic acid (UDPGA) and is present in both the liver and kidney.

Other metabolic processes are also very important but are not present within the microsomal fraction. The soluble enzymes are those leading to reduction, hydrolysis and conjugation (sulfation, acetylation, etc.). The following sections will describe what is known about the metabolism of tertiary amines, and pyridine rings and thiophene containing compounds.

A. Tertiary Amine Metabolism

1). Introduction

Methapyrilene contains two tertiary amine nitrogen centers linked together by a two carbon bridge. In addition to methapyrilene, the tertiary amine functionality is an important chemical component present in many drugs including antihistamines, analgesics, local anesthetics and tricyclic antidepressants. Its basicity and polar character are important for drug action as well as for drug detoxication. This chapter reviews the metabolic fate of tertiary alkyl and aryl amines reported in the literature during the past decade. A number of earlier reviews may be consulted for literature published prior to 1971.[15,16,17] We have selected examples that illustrate structural requirements of substrates in an attempt to develop a rationale for interpreting the metabolism of tertiary amines.

We must first consider the classical routes of tertiary amine metabolism shown in Scheme 1. Tertiary amines (18) are susceptible to two routes of oxidation. Alpha-carbon (α-C) oxidation leads to carbinolamine intermediates (19) which in general undergo spontaneous cleavage to form secondary amines (20) and the corresponding carbonyl products (21). Carbinolamines also may be further oxidized to amides (22). Alternatively, tertiary amines may be oxidized to form dipolar N-oxides (23) which in certain limited cases may undergo dealkylation to yield the

corresponding secondary amines (20). Additionally, tertiary amine N-oxides are readily reduced to the parent drug, particularly in vivo.

Scheme 1. Metabolism of Tertiary Amines.

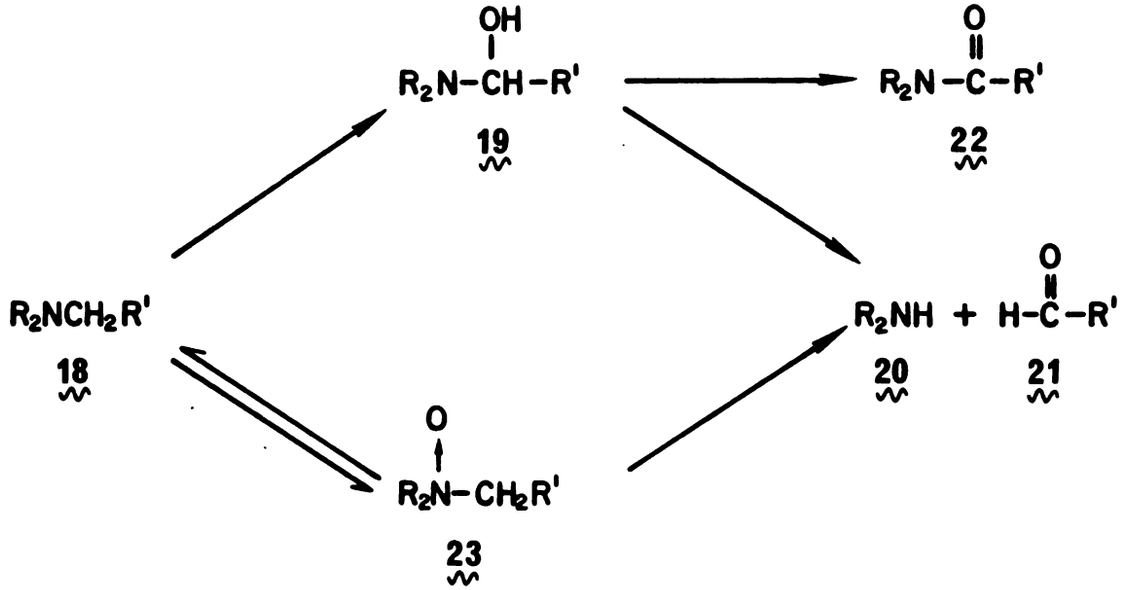

Both α-C oxidation (leading to N-dealkylation) and N-oxidation reactions of tertiary amines are catalyzed by hepatic mixed function oxidases which require NADPH and dioxygen (O_2). Evidence derived from studies on enzyme induction, inhibition, and species and age differences supports the argument that these two reaction pathways are catalyzed by different enzyme systems. Phenobarbital,[18,19] 3-methylcholanthrene[20] and pregnenolone-16 α-carbonitrile,[21] which induce cytochrome P-450 enzymes, also facilitate N-dealkylation but have little or no effect on N-oxidation. Similarly, SKF 525A, a well known inhibitor of cytochrome P-450 enzymes,[22] inhibits N-dealkylation but has no effect on

N-oxidation.[20,23] Other cytochrome P-450 inhibitors[20,24,25] selectively inhibit N-dealkylation. Conversely, cysteamine and dithiothreitol inhibit N-oxide formation with little effect on N-dealkylation.[20,25] Also, NADH enhances the rate of some N-dealkylation reactions without altering the rate of N-oxide formation.[25]

Differences in N- vs α-C oxidation also depend on age and species. N-oxidation of N,N-dimethylaniline by lung tissue obtained from newborn rabbits was found to be approximately 50% of that expected for adults whereas N-demethylation was only 10-20% of that expected for adults.[26] N-oxidation but not N-dealkylation of chlorpromazine has been demonstrated with human fetal liver microsomes.[20] Pretreatment with SKF 525A inhibits by 54% the demethylation of N,N-dimethylaniline in rats but is without effect in pigs.[27] Imipramine undergoes more extensive N-oxidation in lung tissue derived from rats than from rabbits.[28] Cyproheptadine N-oxide was found to be a major urinary metabolite in dogs, a minor urinary metabolite in cats, and was not detected in rat urine.[29]

Based on the results of studies such as those described above, α-C oxidation and N-oxidation appear to be mediated by separate mixed function oxidases. Alpha-C oxidation and therefore oxidative N-dealkylation is catalyzed by the heme protein cytochrome P-450 and N-oxidation by the FAD-containing mixed function oxidase (MFAO).[16] This

chapter will summarize the salient features associated with the reactions catalyzed by these enzymes. Several physical and biological parameters, as discussed above, influence the overall outcome of tertiary amine metabolism. Consequently, it is difficult to develop well defined concepts that generally apply to tertiary amine metabolism.

2). N-Dealkylation

Cytochrome P-450 catalyzed N-dealkylation of a variety of tertiary amine xenobiotics has been investigated. The reaction can be assayed by measuring the formation of the secondary amine metabolite or, in the case of N-demethylation, the formation of formaldehyde.[30] Mechanistically N-dealkylation (Figure 2) may proceed directly via carbinolamine (19) formation by an oxene insertion reaction. Alternatively, the substrate may undergo dehydrogenation to an iminium ion (24) which then adds the equivalent of hydroxide to form the carbinolamine. The carbinolamine then cleaves to yield the corresponding secondary amine (20) and aldehyde or ketone (21). We will consider the mechanism of this reaction in further detail in a later section.

Table 2 includes a selected group of tertiary amines which have been reported to undergo N-dealkylation. Additionally, examples of cyclic tertiary amines which are oxidized to the corresponding lactams are included since these transformations also proceed by a cytochrome P-450 mediated α-C oxidation. Although the examples cited

Table 2. Compounds Undergoing N-Dealkylation

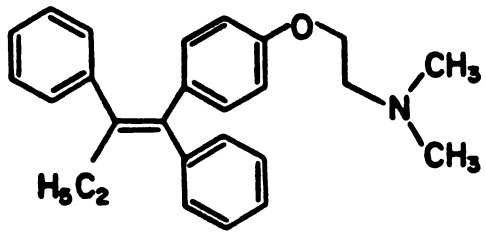

25 [31,32]

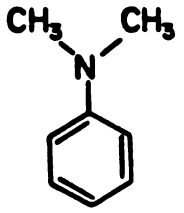

26 [19,27]

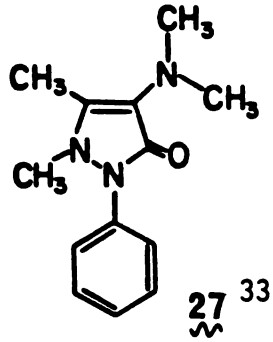

27 [33,34,35,36]

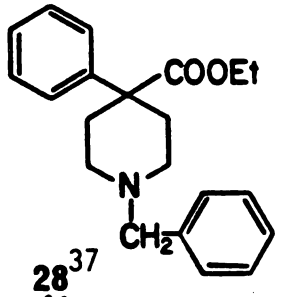

28 [37]

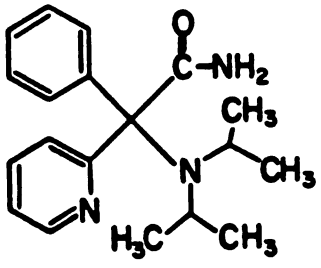

29 [38]

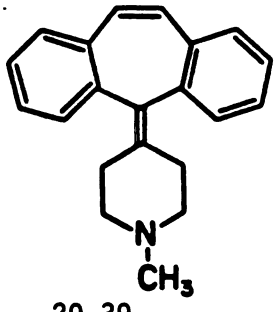

30 [29,39]

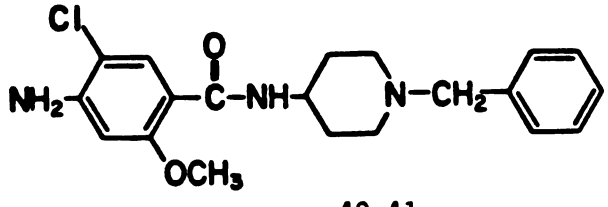

31 [40,41]

Figure 2. Mechanism of N-Dealkylation.

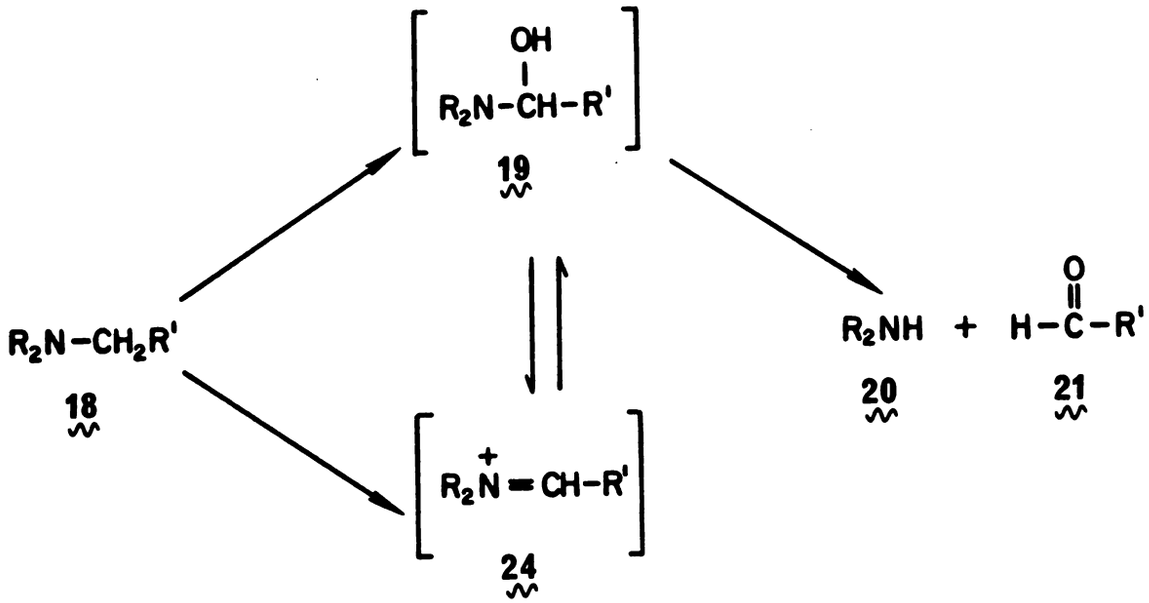

display a broad range of structural types, a common feature is the basicity and lipophilic character of the various substrates.[42,43] Considering the lipoidal nature of the endoplasmic reticulum where the cytochrome P-450 mixed function oxidase system is located, one would expect lipid soluble molecules to be favored substrates.[15]

The active site of the enzyme(s) appears to make few structural demands on substrates. In some cases, steric hindrance to N-dealkylation has been observed.[20] As demonstrated in Table 2, however, the dealkylation reaction is nonspecific. In the case of various dialkyl substituted amphetamine derivatives no selectivity in the cleavage of N-methyl, ethyl or isopropyl substituents has been observed.[44] The lack of substrate specificity may be explained by a flexible active site that can accommodate a broad range of substrates and/or by multiple forms of

cytochrome P-450. The multiplicity of this enzyme is well established,[45] although little is known about the structural features of the active site other than the presence of the heme moiety in a presumably lipophilic environment.[46]

In a few instances semistable carbinolamines have been isolated as metabolic products of trisubstituted nitrogen containing compounds. For the most part the nitrogen atoms in these systems are sp^2 hybridized and only weakly basic due to delocalization of the lone pair electrons. The first well characterized example of carbinolamine formation involved the isolation of N-hydroxymethylcarbazole (32) from N-methylcarbazole (33).[47] The metabolic conversions of medazepam (34) to 2-hydroxymethylpentamethylmedazepam (35)[48] and hexamethylmelamine (36) to N-hydroxymethylpentamethylmelamine (37)[49,50,51] are analogous to the N-methylcarbazole system in that spontaneous cleavage of the carbinolamines is retarded presumably because the weakly basic nitrogen atoms are not significantly protonated at pH 7.4. Cleavage of carbinolamines undoubtedly is facilitated by N-protonation according to Scheme 2.

Scheme 2. Acid Catalyzed Degradation of Carbinolamines.

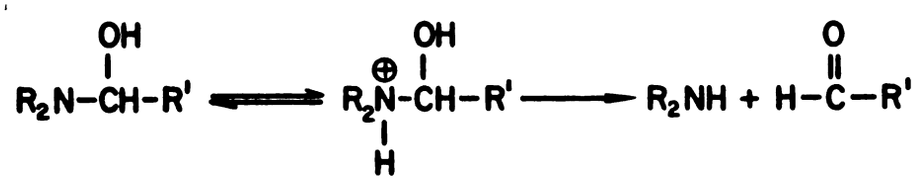

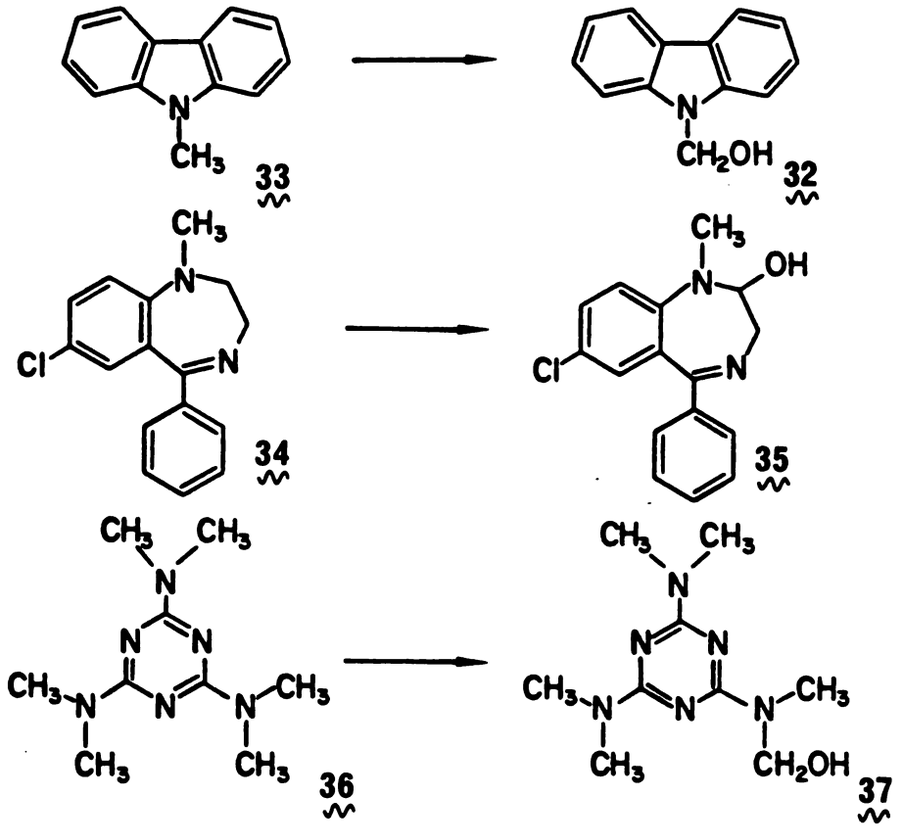

33 32

34 35

36 37

A somewhat similar situation is encountered with amides and lactams. For example the lactams cotinine (38),[52] 1-benzyl-2-pyrrolidinone (39)[53] and chloridiazepam (40)[54] are metabolized to the corresponding carbinolamides 41, 42, and 43, respectively. The weakly basic character of the sp^2 hybridized nitrogen atoms in these molecules favors the carbinolamide structures over the corresponding acyclic structures.

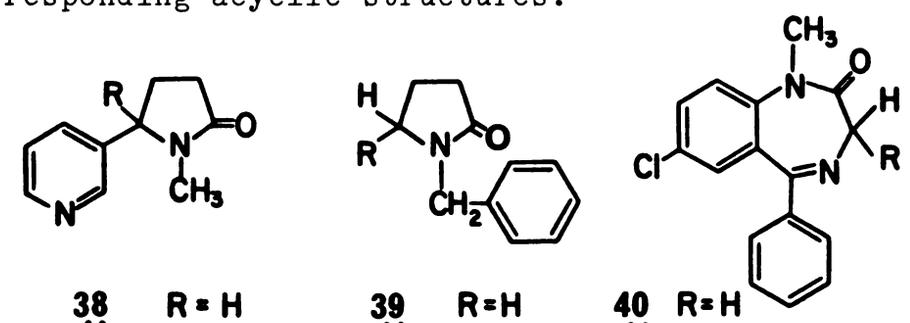

38 R = H 39 R=H 40 R=H

41 R = OH 42 R=OH 43 R=OH

Enantioselective N-dealkylation reactions are well documented. For example, in rats the S-(+) enantiomer of chlorpheniramine undergoes demethylation 35% faster than the R-(-) enantiomer.[55] Evidence has been presented to suggest that the S-(+) enantiomer inhibits the demethylation of the R-(-) enantiomer. On the other hand, S-(+) and R-(-) N,N-dimethylamphetamine showed no difference in rates of N-demethylation.[44] Thus, generalization with respect to stereochemical requirements in the N-dealkylation of tertiary amines cannot be made.

Essentially all tertiary amines of interest bear more than one type of N-substituent. In general, however, "N-dealkylation" leading to cleavage of a small alkyl group appears to occur more readily than "deamination" - that is cleavage of an N,N-dialkylamino moiety to generate the dialkylamine and a carbonyl containing fragment bearing the major structural unit. Exceptions to this generalization include the oxidative removal of the dimethylamino group of chlorpheniramine (44)[56] and the diethylamino group of metoclopramide (45),[57] both of which also undergo N-dealkylation. The monomethylamino groups of 46 and 47 are similarly deaminated by 9000 x g supernatants to yield the

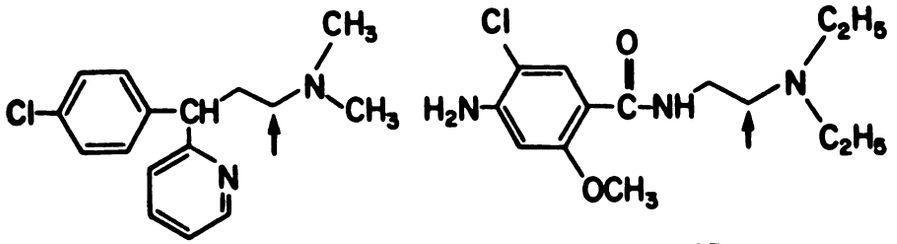

44 45

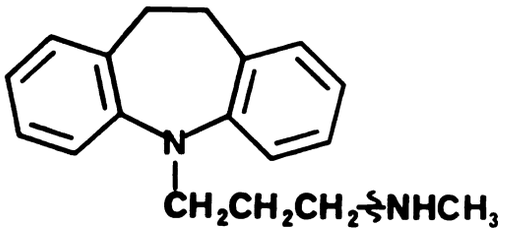

46

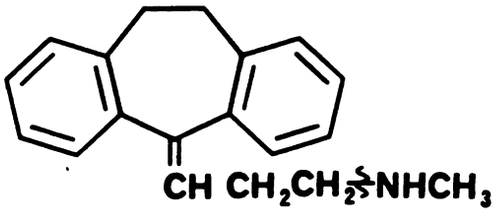

47

corresponding propionic acid metabolites.[58] Additionally, a number of cyclic tertiary amines are preferentially oxidized at a ring α-carbon atom. For example, the principal mammalian metabolites of nicotine[59] and phencyclidine[60] involve ring oxidation. Multiple conversions also may occur. For example, clebopride (31) undergoes N-debenzylation to give the desbenzyl metabolite which is further oxidized to the corresponding lactam (48).[40,41]

31 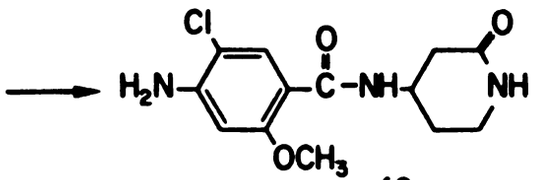

48

The mechanism(s) by which cytochrome P-450 catalyzed oxidations proceed is not fully understood. A number of review articles dealing with the chemistry and biochemistry of the cytochrome P-450 mixed function oxidase system may be consulted for detailed discussion of this subject.[45,46] Suffice it to say that the overall stoichiometry of the reaction involves a two electron oxidation of the substrate by dioxygen which is coupled to a two electron oxidation of

NADPH and the formation of one mole of water. The process is illustrated in Scheme 3 with the oxidation of a model tertiary amine to the corresponding carbinolamine. A key aspect of the overall process involves the activation of dioxygen (O_2) to an oxenoid species such as oxene ($\ddot{O}:$) which is capable of establishing new bonds to carbon, nitrogen, and sulfur.[46] Present evidence suggests that the substrate (R_2NCH_2R') binds to a hydrophobic region of cytochrome P-450 which is situated in close proximity to the oxidized (Fe^{3+}) iron containing heme group. Once the substrate is bound, the iron is reduced to Fe^{2+} in a reaction catalyzed by the NADPH requiring enzyme cytochrome P-450 reductase. This reduced form of cytochrome P-450 now accepts dioxygen as an axial ligand on the surface to which the substrate is bound. This system is reduced by a second electron to form a species which may cleave the oxygen-oxygen bond and yield, with the addition of two protons, one mole of water and "active oxygen" - namely a ferric-oxene complex ($Fe^{3+}:\ddot{O}$).

Scheme 3. Stoichiometry of Cytochrome P-450 Catalyzed Oxidations.

$$R_2NCH_2R' + NADPH + O_2 + H^{\oplus} \rightleftharpoons R_2\overset{\overset{OH}{|}}{N}CHR' + NADP^{\oplus} + H_2O$$

In the absence of the reducing equivalents supplied by NADPH, no reaction occurs. It is possible, however, to "bypass" this part of the cycle by providing "resting", that

is the Fe^{3+} form of cytochrome P-450, with a peroxy species such as H_2O_2 or cumene hydroperoxide.[61-64] In the absence of NADPH, cytochrome P-450 will oxidize various substrates when coincubated with such "oxene donors".[61,62,65] Consistent with the view that cytochrome P-450 catalyzes α-C oxidation and not N-oxidation of tertiary amines, cumene hydroperoxide supports the microsomal oxidative N-demethylation of aminopyrene but not its N-oxidation.[61]

The details concerning the pathway by which $Fe^{3+}:\ddot{O}$ converts a tertiary amine to the corresponding α -carbinolamine are far from clear. Direct oxygen insertion into the C-H bond has been proposed by analogy with carbene insertion reactions.[68] An alternate pathway proceeds by initial electron transfer from nitrogen to oxygen to form bound oxene radical anion ($Fe^{3+}:\ddot{O}\cdot^{-}$) and the radical cationic nitrogen species ($R_2\dot{\overset{+}{N}}-CH_2R'$) (Scheme 4). Hydrogen radical abstraction from $R_2\dot{\overset{+}{N}}-CH_2R'$ leads to

Scheme 4. Proposed Mechanism of Tertiary Amine Oxidation by P-450.

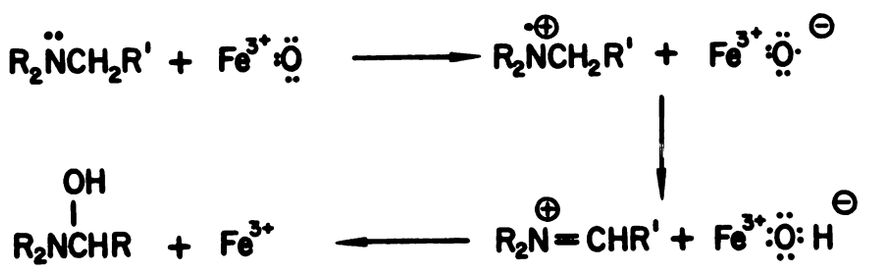

Fe^{3+}:$\ddot{O}$:H^- and the iminium ion $R_2\overset{+}{N}$=CHR'. Final transfer of the hydroxide group to the iminium ion would yield the carbinolamine product. Consistent with this proposed pathway, the H_2O_2-cytochrome P-450 catalyzed N-demethylation of aminopyrene leads to an aminopyrene radical species which has been detected by EPR.[63,64] Metyrapone, a P-450 inhibitor, was found to inhibit the formation of aminopyrene radicals by 46% in incubations containing cumene hydroperoxide.[69] Finally, nitrosobenzene was found to be an efficient trap of free radicals generated in this reaction mixture.[69] Although these results support the production of a radical intermediate during oxidative N-dealkylation, no comparable evidence has been reported with the complete reconstituted system involving NADPH-cytochrome P-450 reductase as the electron donor source.

Additional indirect evidence for the involvement of iminium ion intermediates in the microsomal α-C oxidation of tertiary amines is the isolation of α-aminonitriles following the co-incubation of certain tertiary amines with cyanide ion in the presence of NADPH. For example, N-cyanomethylnornicotine (49) and N-cyanomethylnormethapyrilene (50) have been characterized from such incubation mixtures.[59,70,71] Similarly, 5'-cyanonicotine (51),[72] 1-benzyl-2-cyanopyrrolidine (52),[53] and 1-(1-phenylcyclohexyl)-2-cyanopiperidine (53)[73] are produced when the corresponding tertiary

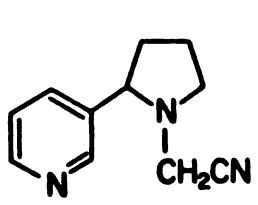

49

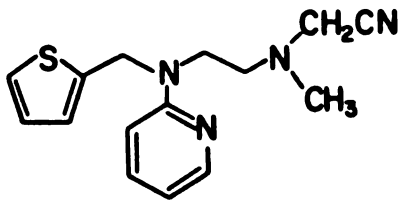

50

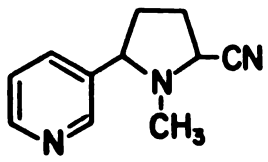

51

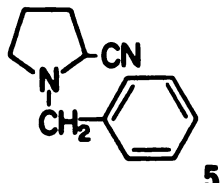

52

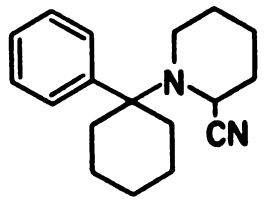

53

amines are incubated with liver microsomal preparations containing sodium cyanide. The $\Delta^{1',5'}$-iminium ion 54 of nicotine[74,75,76] and the iminium ion derived from azapetine (55)[77] have been shown to be good

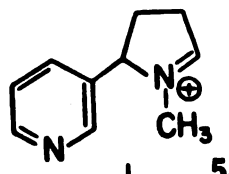

54

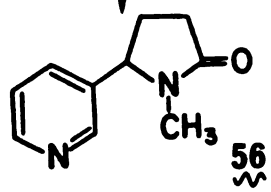

56

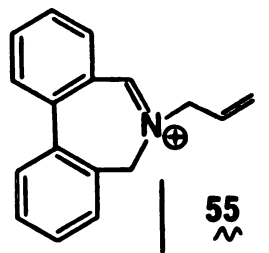

55

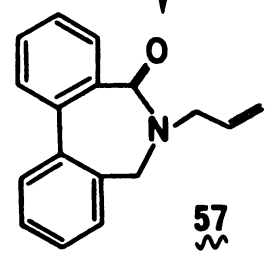

57

substrates for the soluble oxidase responsible for the formation of the corresponding lactams 56 and 57, respectively. Intramolecular trapping of iminium intermediates also has been reported. For example Bisolvon

(58)[78] and trifluralin (59)[79] are converted to the corresponding cyclic metabolites 60 and 61, respectively, presumably via the pathways summarized below (Scheme 5).

Scheme 5. Intramolecular Cyclization of Iminium Ions.

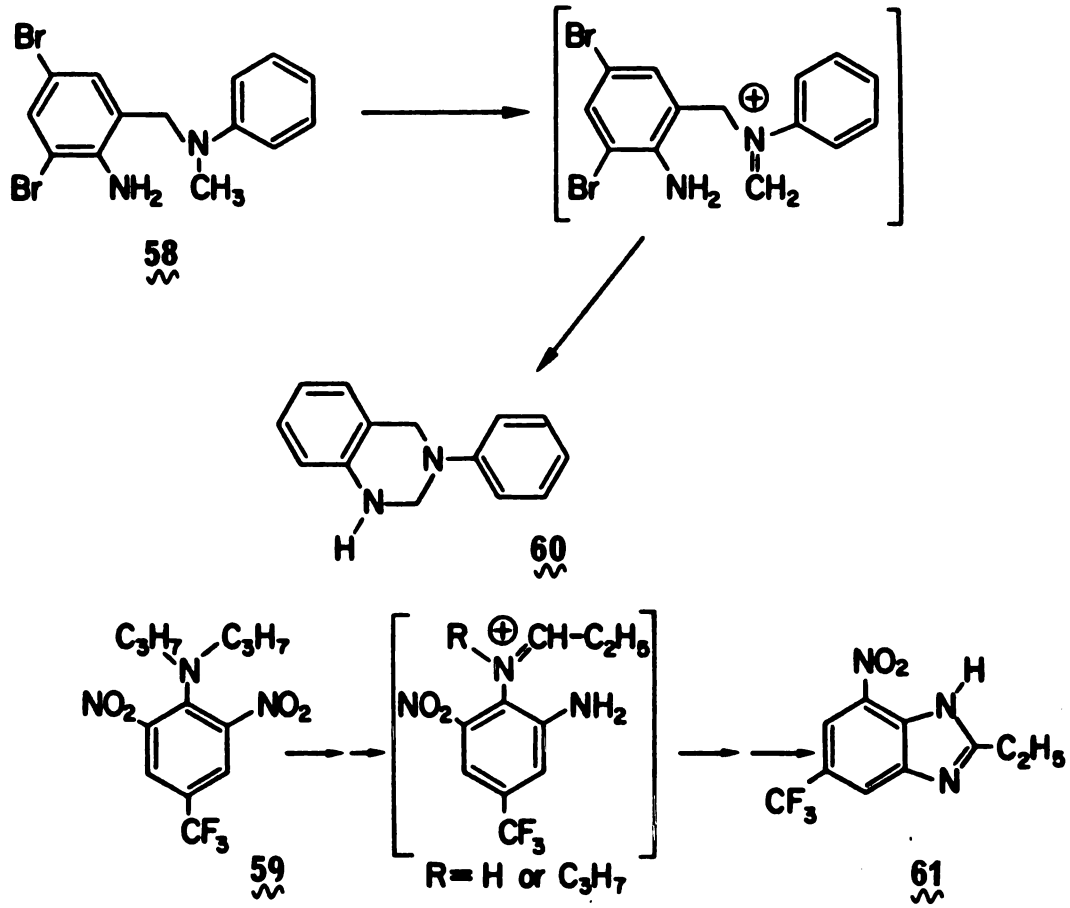

Additionally, the N-glutathione-S-methylene adduct of 4-aminoazobenzene 62 has been trapped following metabolic activation of the N-methyl group of N,N-dimethylaminoazobenzene (63).[80]

Although suggestive, the data do not prove that iminium ions are obligatory intermediates in cytochrome P-450 catalyzed oxidative N-dealkylation reactions. An alternate pathway involving direct oxene insertion to generate a

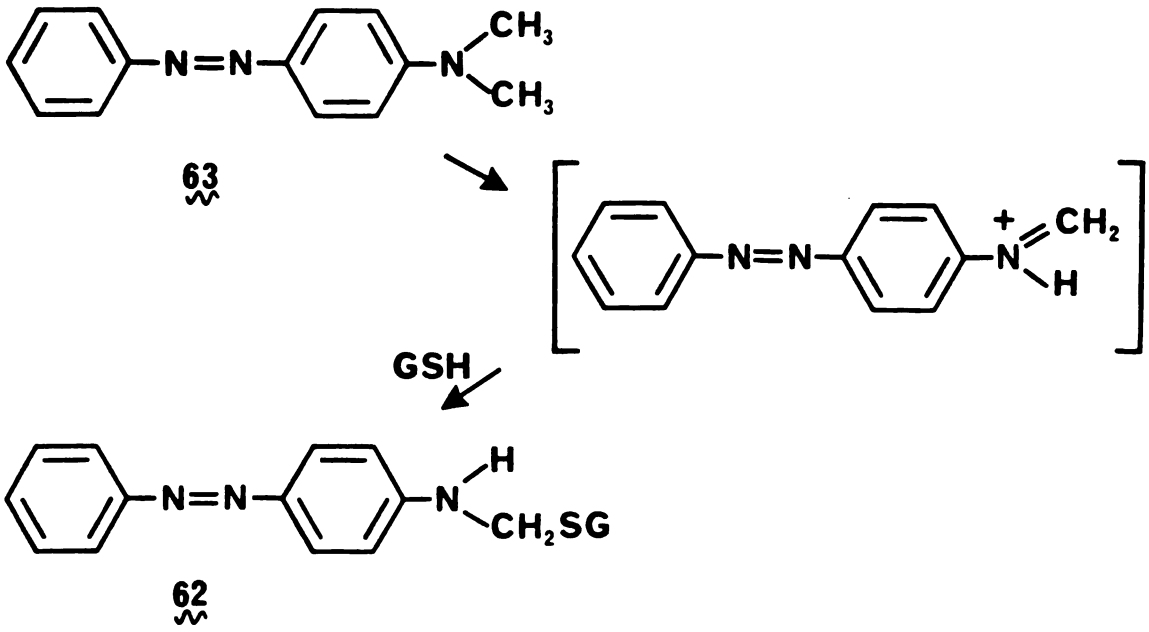

cabinolamine which might be in equilibrium with the corresponding iminium ion also could accommodate the majority of these data. Kinetic isotope effect studies with deuterium labeled substrates for the most part have revealed values ranging between 1.0 and 1.6.[81-86] Such low values do not support a reaction pathway that would involve carbon-hydrogen bond cleavage as the rate determining step in the net reaction leading to N-dealkylation. Such values would be consistent with an oxene insertion mechanism in which oxygen activation or electron transport steps are rate determining. Unfortunately too little is known about the electron transport steps involved in the cytochrome P-450 cycle to formulate definitive statements concerning the rate limiting step or steps which determine the kinetics of oxidative N-dealkylation. Arguments describing multiple partially rate determining steps[87] and multiple active

site[88,89,90] have been advanced. The addition of the first or second electron to the heme of cytochrome P-450 via cytochrome P-450 reductase may control the overall kinetics of the process.[91,92] Consequently, clarification of the kinetic and mechanistic details involved in the cytochrome P-450 catalyzed two electron oxidation of a carbon atom attached to the nitrogen atom of a tertiary amine must await further experimental results.

3). N-Oxidation

As with N-dealkylation, a broad range of tertiary amines is susceptible to N-oxidation. Unlike α-carbon oxidation, N-oxide formation is a reversible process and some N-oxides may undergo a rearrangement to the corresponding α-carbinolamines. These factors plus the highly polar character of N-oxides have made difficult a full appreciation of the extent to which N-oxidation of tertiary amines occurs in mammalian systems. The quantitative importance of N-oxidation in some instances is illustrated by the fact that 34% of the chlorpromazine incubated with rat liver microsomes is converted to the corresponding N-oxide.[93] A select group of compounds known to form N-oxide metabolites is shown in Table 3. As with N-dealkylation, lipophilicity, steric hindrance, and stereochemistry are important in determining the extent to which N-oxidation occurs. Species and sex differences also may effect N-oxide formation.

Lipophilic tertiary amines containing N,N-dimethylalkylamine moieties with 8-12 carbons in the side chain are oxidized faster than compounds with shorter alkyl chains.[99] Tertiary amines with nearby polar groups in general are not metabolized via N-oxidation.[99] Contrary to this, oxycodone (67) forms an N-oxide while morphine does not.[98] Increased steric hindrance about the nitrogen atom also may cause a decrease in the extent of N-oxide formation. As demonstrated with analogs of

Table 3. Compounds Forming N-Oxides

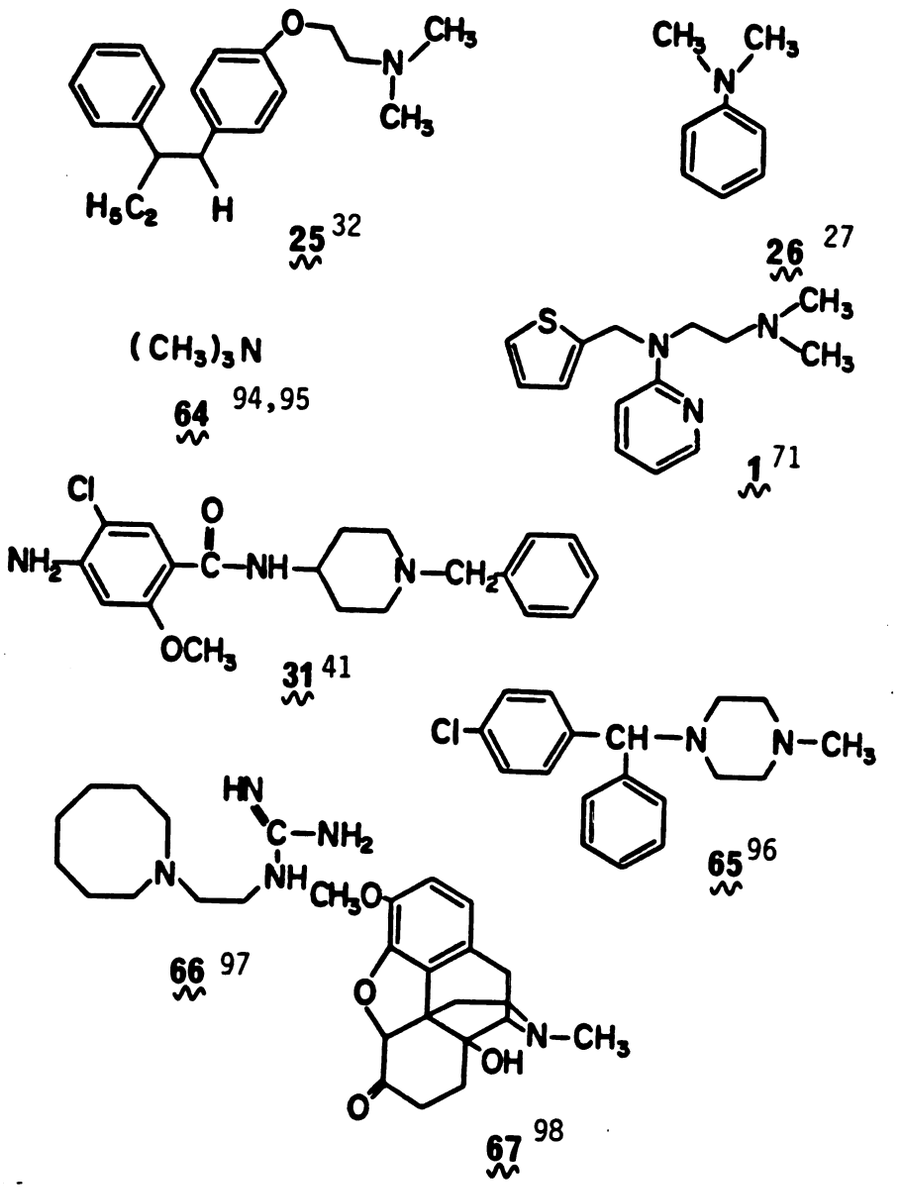

methadone, N-oxidation decreases in the order of normethadone > isomethadone > methadone.[20] Similarly, tamoxifen (25) forms an N-oxide while the sterically more hindered N,N-diethyl analog enclimophene does not.[100]

Stereochemical factors also contribute to the course of N-oxidation. Both (R)- and (S)-nicotine undergo oxidation to form the cis and trans-1'-nicotine N-oxide metabolite.[101] N-oxidation of nicotine by lung tissue has been reported to be stereoselective with the 2'-center of the pyrrolidine ring dictating the stereochemistry of N-oxidation.[102,103] It now appears that the pyrrolidine ring dictates the binding to the enzyme yielding a preferred 1'-R-N-oxide of nicotine.[104]

Differences in N-oxidation also are dependent on the species and sex. For instance, cyproheptadine N-oxide is a major metabolite in dogs, minor in cats and nonexistent in rats.[29] N-Oxidation is apparently under hormonal control. Two weeks after gonadectomy, the specific activity of enzymatic N-oxidation of N,N-dimethylaniline doubled in male mice and treatment with testosterone returned the activity to normal.[105] Similarly, administration of estradiol to female mice lowered the N-oxidation of N,N-dimethylaniline.[105]

The conversion of tertiary amines to their corresponding N-oxides is primarily catalyzed by the flavoprotein enzyme mixed function amine oxidase (MFAO).[106,107] Some evidence also exists for cytochrome

P-450 mediated N-oxidation.[19,108,109,110] Gorrod et al.[101] observed that the formation of nicotine N-oxide was not inhibited by SKF 525A, a well known P-450 inhibitor, while pregnenolone-16 α-carbonitrile, an inducer of P-450 and cytochrome P-450 reductase, was found to increase the formation of N,N-dimethylaniline N-oxide.[108] On the other hand, pretreatment of animals with cobalt chloride led to a 75% reduction in cytochrome P-450 content and an approximate 50% reduction of N-oxide formation.[108] Up to 60% of the N-oxide formed from N,N-dimethylaniline has been attributed to cytochrome P-448[109,110] or P-450.[108] Formation of the remaining portion of this N-oxide is mediated by MFAO. In as much as the MFAO is extremely susceptible to post mortum deactivation, one would expect to observe a greater ratio of MFAO/P-450 mediated N-oxidation in vivo than in vitro.

Mixed function amine oxidase has been isolated and purified from pig liver[99] but the activity is also present in pig lung.[28] This flavoprotein enzyme requires NADPH and O_2 and catalyzes the N-oxidation of both secondary and tertiary amines. N-oxide formation is activated by the addition of N-octylamine[99] which appears to bind to a regulatory site of the enzyme.[106] Cyanide, SKF 525A and CO do not inhibit MFAO while 1-(1-naphthyl)-2-thiourea competitively inhibits (through sulfur oxidation to the sulfinic acid) N-oxide formation by as much as 92%.[106] In one case, SKF 525A led to an

increase in N,N-dimethylaniline N-oxide formation, presumably by inhibiting cytochrome P-450 mediated α-C oxidation and thereby increasing the amount of tertiary amine available for N-oxidation.[27]

The mechanism of MFAO catalyzed N-oxidation is fairly well understood. Direct incorporation of O_2 into trimethylamine N-oxide by liver microsomes has been demonstrated with $^{18}O_2$.[94,95] The catalytic reaction appears to require the reduced flavin-peroxide form of the enzyme where no covalent interaction occurs between the substrate and the flavin moiety.[111] The reaction kinetics are consistent with a Ter-Bi mechanism in which the NADPH first binds to the enzyme followed by O_2 and then substrate.[112,113] The hydroperoxyflavin form of the enzyme is believed to be the active oxygenating species. The possible involvement of a radical intermediate has been eliminated since 4a-hydroperoxyflavin radical anion[114] was ineffective in the N-oxidation of N,N-dimethylaniline. The free radical trap 2,6-di-tert-butyl-p-cresol (BHT) also was found to have no inhibitory effect on N-oxide formation.[115] Additionally 4a-flavinperoxy anion did not catalyze the formation of N,N-dimethylaniline N-oxide.[114] Instead, the N-oxide apparently donates an oxenoid specie to the heme which subsequently catalyzes N-dealkylation.[115a] Thus the oxygenation of tertiary amines is believed to occur through direct nucleophilic displacement of the terminal oxygen of the hydroperoxyflavin

Scheme 6. Proposed Mechanism of N-Oxide Formation by a 4a-Hydroperoxyflavin.

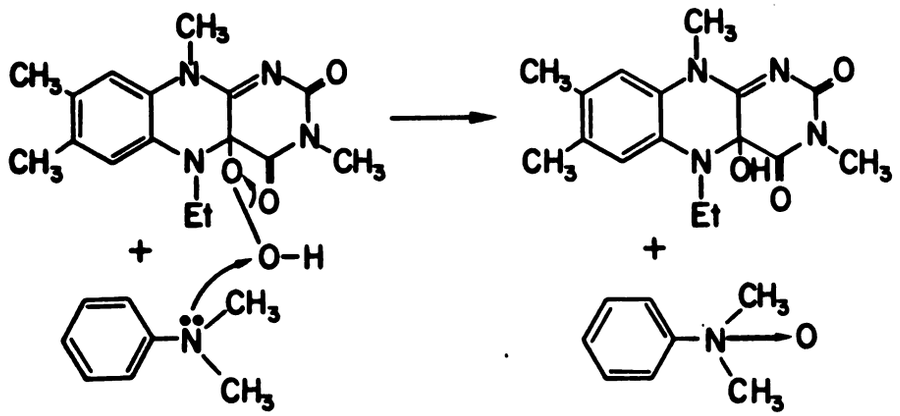

form of the enzyme as shown in Scheme 6.[114]

The lack of formation of N-oxide metabolites in many cases may be due to the post mortem inactivation of MFAO and the presence of an N-oxide reducing enzyme. The enzyme system involved in N-oxide reduction is unknown. Stereochemically, the enzyme prefers to reduce the levo isomer of nicotine N-oxide.[103] An inducible tertiary amine N-oxide reductase has been isolated from E. coli.[116] Similar to the mammalian enzyme xanthine oxidase,[117] this bacterial enzyme possibly contains a molybdate in the active site.[116] Additionally, strong evidence exists for cytochrome P-450 mediated N-oxide reduction. Tiaramide N-oxide was found to undergo microsomal reduction under anaerobic conditions in the presence of NADPH.[118] The reduction was induced by phenobarbital and 3-methylcholanthrene while O_2 and CO

inhibited the reaction.[118] Later studies utilizing purified P-450, NADPH-cytochrome P-450 reductase and NADPH gave similar results.[119] Spectral analysis indicates that the N-oxide binds to cytochrome P-450 in a manner similar to O_2 and CO.[119] A similar conclusion was obtained with studies on N,N-dimethylaniline N-oxide reduction.[19] Reduction of N,N-dimethylaniline N-oxide may be linked to the formation of N-methylaniline.[19] Consequently tertiary amine N-oxide reduction and α-carbon oxidation of the resulting tertiary amine may be catalyzed by the same enzyme. Such a reaction sequence is suggested by the model system chlorotetraphenylporphyrinatoiron(III) where N,N-dimethylaniline N-oxide was found to be an oxene donor capable of supporting the N-dealkylation of N,N-dimethylaniline.[120]

Evidence against P-450 catalyzed N-oxide reduction also has been reported. For example, various rat tissue homogenates catalyzed the reduction of imipramine N-oxide without added cofactors. Additionally the reductive activity was neither inhibited by CO, SKF 525A nor cyanide.[121] The activity was present in the extramicrosomal 9000g pellet.[121] In vivo studies on imipramine N-oxide reduction revealed that there was no first pass effect in its metabolism, and therefore it was concluded that extrahepatic mechanisms were involved.[122] Chlorcyclizine N-oxide is metabolized to chlorcyclizine and norchlorcyclizine.[96] Pretreatment with SKF 525A in this

case led to a decreased amount of norchlorcyclizine and an increase in chlorcyclizine formation.[96] Based on these results it would appear that P-450 is not the only enzyme involved in N-oxide reduction.

In general N-oxides do not appear to be direct substrates for N-dealkylation[20] even though N,N-dimethylaniline N-oxide is reported to undergo N-dealkylation more readily than N,N-dimethylaniline.[19,27] Therefore, the rearrangement of N-oxides to carbinolamines is, at best, a minor pathway.[25] The bulk of the available evidence supports the following two step reaction pathway leading to the N-dealkylation of tertiary amine N-oxides: 1) reduction of the N-oxide and 2) the cytochrome P-450 mediated N-dealkylation of the resulting tertiary amine.

4). Summary

The metabolism of tertiary amines is mediated primarily by cytochrome P-450 and MFAO, leading to α-C oxidation and N-oxidation, respectively. We have discussed how lipophilicity, basicity, steric hindrance and stereochemistry can effect the outcome of metabolism as well as species, sex and age. The proposed oxidation of tertiary amines to iminium ions by cytochrome P-450 may explain the isolation of various intramolecular and cyanide-trapped metabolites. N-oxides may represent a smaller percentage of the overall in vitro metabolism of tertiary amines due to

the post mortum inactivation of MFAO. In addition N-oxide reducing enzymes present in vivo and in vitro may influence the extent of N-oxide formation. In general, definite conclusions about substrate requirements have been difficult to formulate because of the numerous biological and physical parameters affecting the outcome of metabolism. More singularly directed research on a single species of animal and a wide variety of substrates or vice versa would greatly increase our understanding of the potential metabolism of tertiary amine xenobiotics.

B. Metabolism of Pyridine and Thiophene.

Methapyrilene also contains two heteroaromatic rings, namely pyridine and thiophene. The pyridine ring is a fairly prevalent constituent of many drugs while the electron-rich thiophene moiety has been incorporated into fewer compounds of biological interest. The metabolism of a few substituted pyridine and thiophene compounds will be discussed to illustrate the potential sites of aromatic oxidation within methapyrilene.

The majority of pyridine biotransformation occurs at the nitrogen atom to form pyridine N-oxide.[123-125] This oxidation appears to be cytochrome P-450 mediated and formation of N-oxides in vitro and in vivo is induced by phenobarbital.[123,125] 3-Substituted pyridines such as 3-methyl- and 3-chloropyridine yield lesser quantities of N-oxides than pyridine itself.[125] Other 3-substituted pyridine rings behave differently. Metyrapone (68)[126] and cotinine (38)[127] both undergo pyridine ring

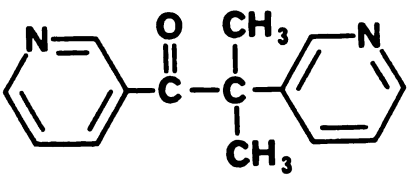

68

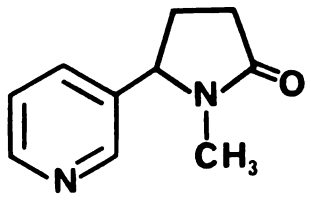

38

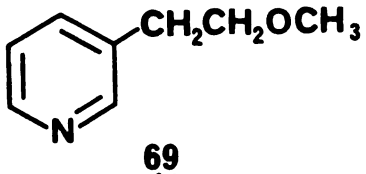

69

N-oxidation while methyridine (69) does not.[128] Similarly, the 2-substituted pyridine, oxisuran, does not undergo N-oxidation.[129,130] Ring oxidation alpha to the nitrogen atom has been observed for both metyrapone[126] and nicotinamide[131] but this oxidation is believed to be mediated by a soluble molybdenum hydroxylase-aldehyde oxidase type enzyme.[132] Oxidation of nitrogen heterocycles β to the nitrogen atom is thought to be a cytochrome P-450 catalyzed reaction.[132]

The metabolism of thiophene (70) and substituted thiophene derivatives has received limited interest. When administered to rabbits, 35 percent of the thiophene was recovered unchanged in the urine while 40% was converted to 2- and 3-substituted mercapturic acid metabolites.[133] Further studies revealed that both rats and rabbits metabolized thiophene to 2-thienylmercapturic acid (71),[134] as illustrated in Figure 3. Thiophene is

Figure 3. Postulated Mechanism of Thiophene Metabolism.

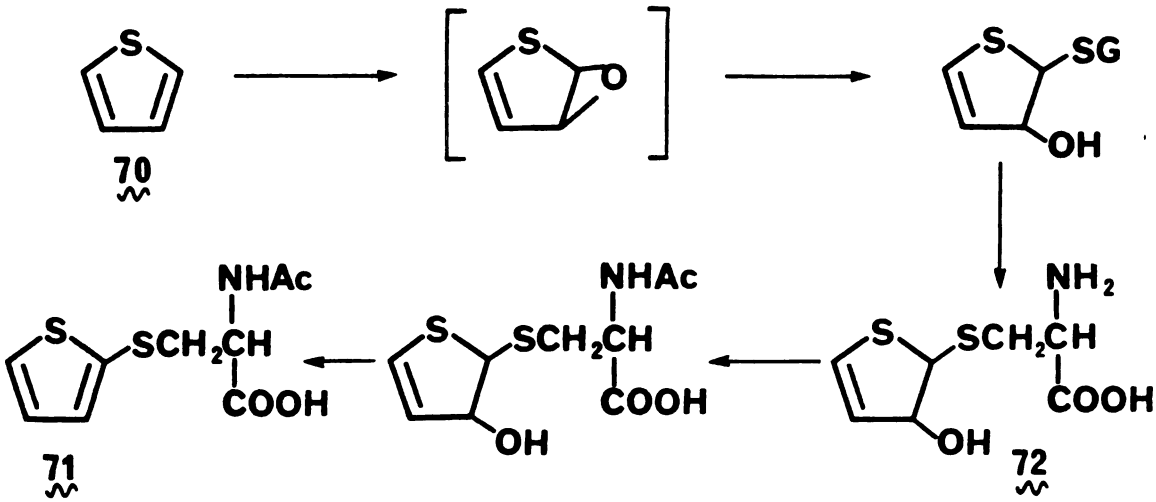

proposed to undergo epoxidation followed by nucleophilic attack with glutathione, the relative amount at each position being determined by the relative electron densities at C-2 and C-3. Glutathione peptidase then hydrolyzes the peptide bonds in the glutathione moiety followed by N-acetylation to yield 3-hydroxy-2,3-dihydro-2-thienyl mercapturic acid (72), as confirmed by isolation from the metabolic sample. Subsequent loss of water resulted in the observed 2-thienylmercapturic acid (71).

Thiophene-2-carboxylic acid (73) is metabolized microbially by a somewhat different pathway (Figure 4).[135] Through feeding experiments with ^{14}C-labeled thiophene-2-carboxylic acid, the radiolabeled acetyl CoA ester 74 of 2-oxoglutarate was isolated. The initial step of esterification of the carboxylic acid is believed to be followed by ring hydroxylation in the C-5 position to yield

Figure 4. Proposed Mechanism of Microbial Metabolism of Thiophene-2-carboxylic Acid.[135]

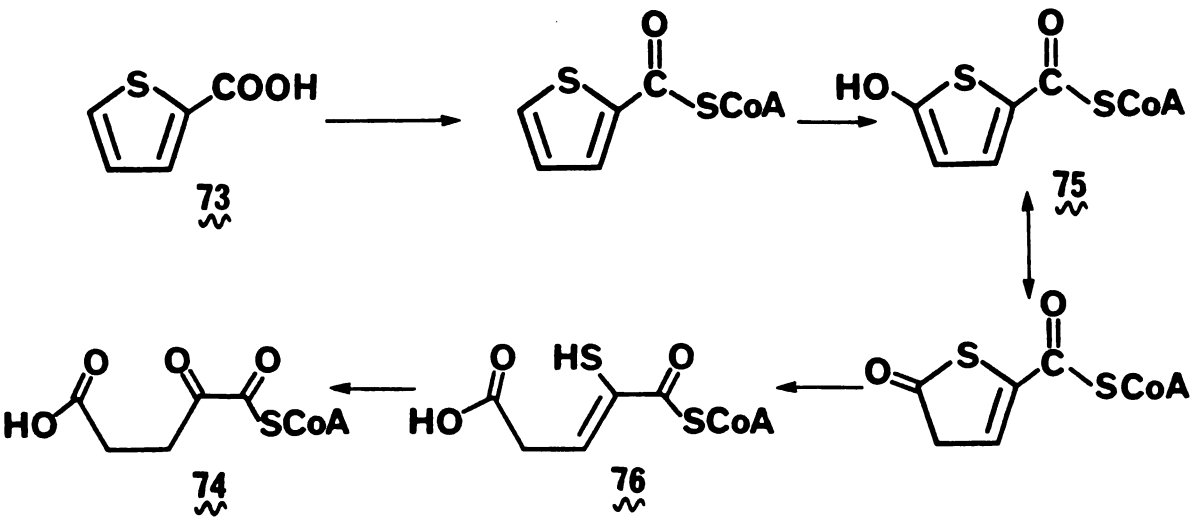

75. Hydroxy thiophenes are not stable structures and the thiolactone is thought to undergo hydrolysis to yield the corresponding thiol-carboxylic acid 76. The thiol then undergoes exchange with water to yield 2-oxoglutarate acetyl CoA ester (74). Thus the carbonyl containing substituent at the C-2 position of thiophene alters the metabolic fate of ring oxidation.

The metabolism of another C-2 substituted thiophene, PG-501 (77), has been investigated. As shown by analysis of rat urinary metabolites, the ester of PG-501 has undergone hydrolysis and the thiophene containing moiety 78 metabolized to more polar derivatives (Figure 5).[136]

Figure 5. Rat Urinary Metabolites of PG-501.

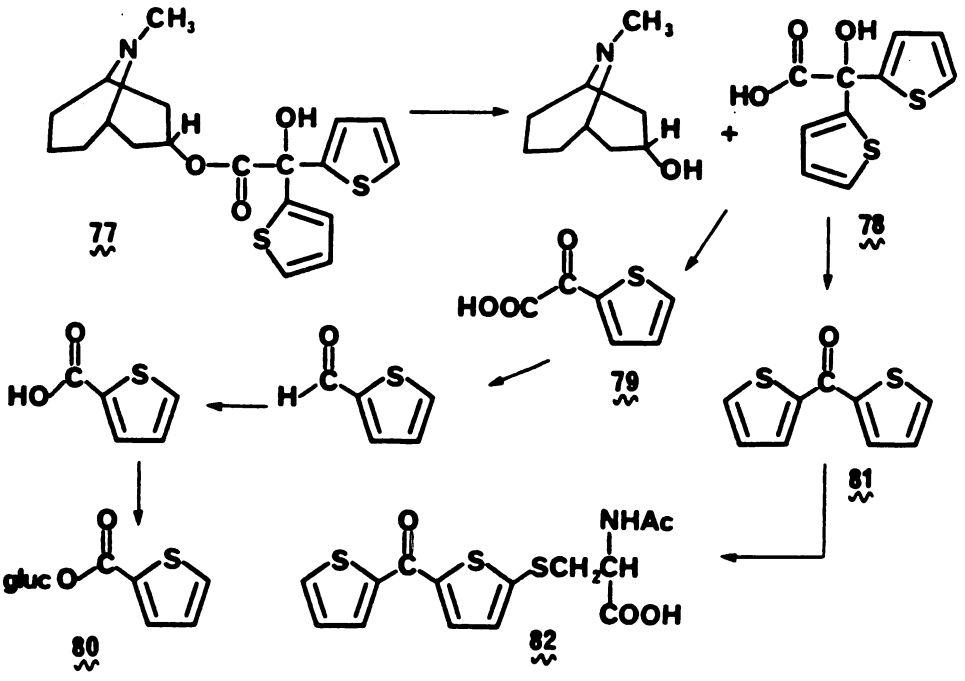

In one case, the α-hydroxy acid eliminates thiophene to yield the unstable ketoacid 79. Loss of CO_2 leads to thiophene-2-carboxylic acid, isolated as the glucuronide conjugate 80. Alternatively, the initial loss of CO_2 can results in the ketone 81 which is then susceptible to mercapturic acid conjugation to yield 82 by a mechanism similar to that shown in Figure 3.

Benzo(b)thiophene analogs represent a 2,3-disubstituted electron rich thiophene ring system. When benzo(b)thiophene (83) was administered to rats, mercapturic acid compounds were isolated in high yields from urine.

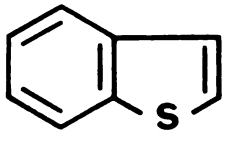

83

Unlike the previously discussed thiophene analogs, N-methylbenzo(b)thiophene carbamate, Mobam,[137] undergoes sulfur oxidation to the sulfone which has been isolated as a urinary metabolite of dairy goats and lactating cows. On the other hand, 3-(2-dimethylaminoethyl)benzo(b)thiophene (84) does not undergo sulfur oxidation in vivo or in vitro in rats.[138] The major metabolite was the 6-hydroxylated species 85 and deamination to the carboxylic acid 86 and alcohol 87 as well as lesser amounts of the N-desmethyl compound 88.[138] Alternatively, the benzo(b)thiophene analog of trytophan[139] was found to undergo side chain

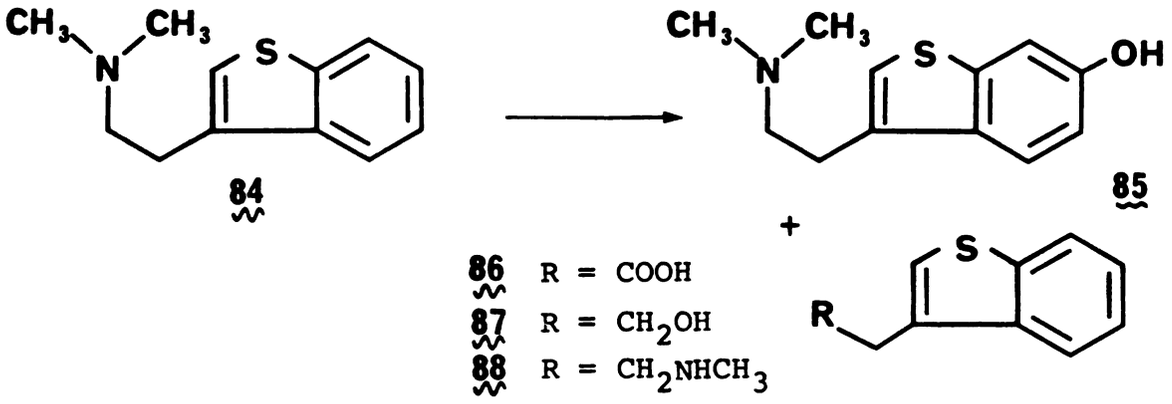

metabolism without demonstrating ring or sulfur oxidation. Other aromatic ring systems containing sulfur such as chlorpromazine, bis-desmethylchlorpromazine and perazine are converted to sulfoxide and sulfone metabolites.[140,141] In these systems, the sulfur is associated via thioether linkage to aromatic rings and the electrons of sulfur are accessible for oxidation. Sulfone metabolites of most thiophene derivatives have not been observed.

From these results, in vitro metabolism of the pyridine ring within methapyrilene might result in nitrogen oxidation or ring hydroxylation beta to the nitrogen. Thiophene ring oxidation in vivo would most likely result in a 2-mercapturic acid conjugate of methapyrilene. The glutathione required for the biosynthesis of mercapturates is present in negligible amounts in in vitro metabolic incubates. Thus the metabolism through the alternate pathway to the highly polar 2-oxoglutarate derivative of methapyrilene might be expected.

III. Background on Methapyrilene Carcinogenicity.

Methapyrilene (1) acts as a competitive H1-histamine antagonist in addition to having mild sedative hypnotic effects. As an ethylenediamine antihistamine, methapyrilene is a representative of a large class of compounds with similar structures. Numerous over-the-counter drugs such as Compoz, Excedrin-PM, Nytol, Sleep-eze and Sominex contained varying quantities of methapyrilene in their formulation.[142] A few fatalities have been attributed to methapyrilene overdose, as a consequence of the sedative activity.[143] Methapyrilene was removed from the market in July 1979[2] when rats fed methapyrilene in their diet at 0.1-0.2% over a lifetime demonstrated a high incidence of hepatocellular carcinoma and cholangiocarcinoma.[1] Numerous metastatic carcinomas were observed in the lungs, portahepatic lymph nodes, omentum and peritonium. No sex differences were observed.

Various in vitro assays on methapyrilene showed none of the activities common to other known carcinogens. Methapyrilene was found to be nonmutagenic by the Ames test after S-9 activation but led to a lower number of revertants than the control assay.[144] Methapyrilene also did not transform Hamster embryo cells[145] and did not induce sister-chromatid exchange.[146] Additionally, methapyrilene was found to be ineffective in inducing unscheduled DNA synthesis in primary hepatocyte

culture,[147] while two structurally similar antihistamines, pyrilamine maleate and tripelennamine hydrochloride, were active in the assay. All of these in vitro studies seem to indicate that methapyrilene is not genotoxic, i.e. does not produce DNA damage through covalent interaction. Contrary to these studies, Althaus and coworkers[148] found that methapyrilene stimulated DNA-repair synthesis in primary rat hepatocyte cultures by at least seven-fold as measured by an increased incorporation rate of radiolabeled nucleotides into DNA. In these studies, methapyrilene appeared to interact with the DNA in such a way as to result in alkaline-labile lesions in the hepatocellular DNA. A dose dependent rate of DNA repair synthesis was observed with the maximum dose of methapyrilene being 10^{-3} M, a concentration ten times that used in the previously reported studies.[147] At higher concentrations of methapyrilene, marked cytotoxicity as determined by light microscopy caused a decrease in DNA interaction with methapyrilene. Most interestingly, neither SKF 525A, a cytochrome P-450 inhibitor, or isonicotinamide, a preserver of P-450 activity, had an effect on DNA interaction. Additionally, a dose-response relationship exists between the hepatic γ-glutamyl transpeptidase activity of methapyrilene treated rats similar to that observed for aflatoxin B1 and phenobarbital.[149] From these results, one would conclude that methapyrilene is in fact genotoxic. Our efforts to clarify this situation will

be discussed in later sections.

Three basic approaches to understanding methapyrilene carcinogenicity have been taken. The possibility of nitrosamine involvement in methapyrilene carcinogenesis has been extensively investigated as have the ultrastructural changes within the liver of animals treated with methapyrilene. The in vivo and in vitro metabolism have been investigated as mechanisms towards formation of the ultimate carcinogen.

Initially Lijinsky and coworkers promoted the idea that methapyrilene's carcinogenicity arose through nitrosamine formation.[150] As a dimethylamino containing tertiary amine, methapyrilene has the potential to form nitrosamines. A fairly large group of male and female rats were subjected to a long term feeding study. After 90 weeks, almost 50% of the rats drinking water containing methapyrilene and sodium nitrite showed necrotic and other degenerative changes in the liver.[1] The autopsies of 14 female rats showed four liver cholangiocarcinomas, one hepatocellular carcinoma, and one haemangioendothelial sarcoma. In the 15 male rats that were autopsied, a slightly lower number of carcinomas was observed, i.e. one liver cholangiocarcinoma, two hepatocellular carcinomas and one spinal cord neurofibrosarcoma. Although the survival rates of the methapyrilene/sodium nitrite fed rats were the same as the control sodium nitrite rats, the incidence of liver tumors was much higher.[1]

Model chemical studies in which methapyrilene was treated with sodium nitrite at 37° in acetate buffer at pH 3.3 led to the formation of only 0.7% dimethylnitrosamine(DMNA).[150] This is in contrast to aminopyrine which under the same conditions led to a 40% conversion to DMNA.[150] At 90°, the formation of DMNA from methapyrilene was more favorable[150] but a number of other oxidative products were then observed.[151] As shown in Figure 6, a number of nitrogen containing products of methapyrilene oxidation can undergo nitration. Nitration of the dimethylamine nitrogen (89) can yield DMNA in addition to an aziridinium species (90) which itself might be considered a potential electrophilic carcinogen. Alternatively, oxidative dealkylation of the 2-aminopyridine exocyclic nitrogen leads to two secondary amines, 91 and 92, which can be nitrated to yield 93 and 94, respectively. Interestingly, when methapyrilene and sodium nitrite were allowed to stand in aqueous solution,[151] approximately 1% degraded per day with the product being N-(N',N'-dimethylaminoethyl)-2-aminopyridine (92). This product, in turn, was more rapidly converted to its nitrosamine than was methapyrilene due to the reactivity of a secondary amine compared to a tertiary amine.

Thus the feeding studies were repeated with methapyrilene and methapyrilene plus sodium nitrite being administered in the diet.[152] The results indicated that sodium nitrite did not increase the incidence of

Figure 6. Possible Nitrosamines Derived From Methapyrilene

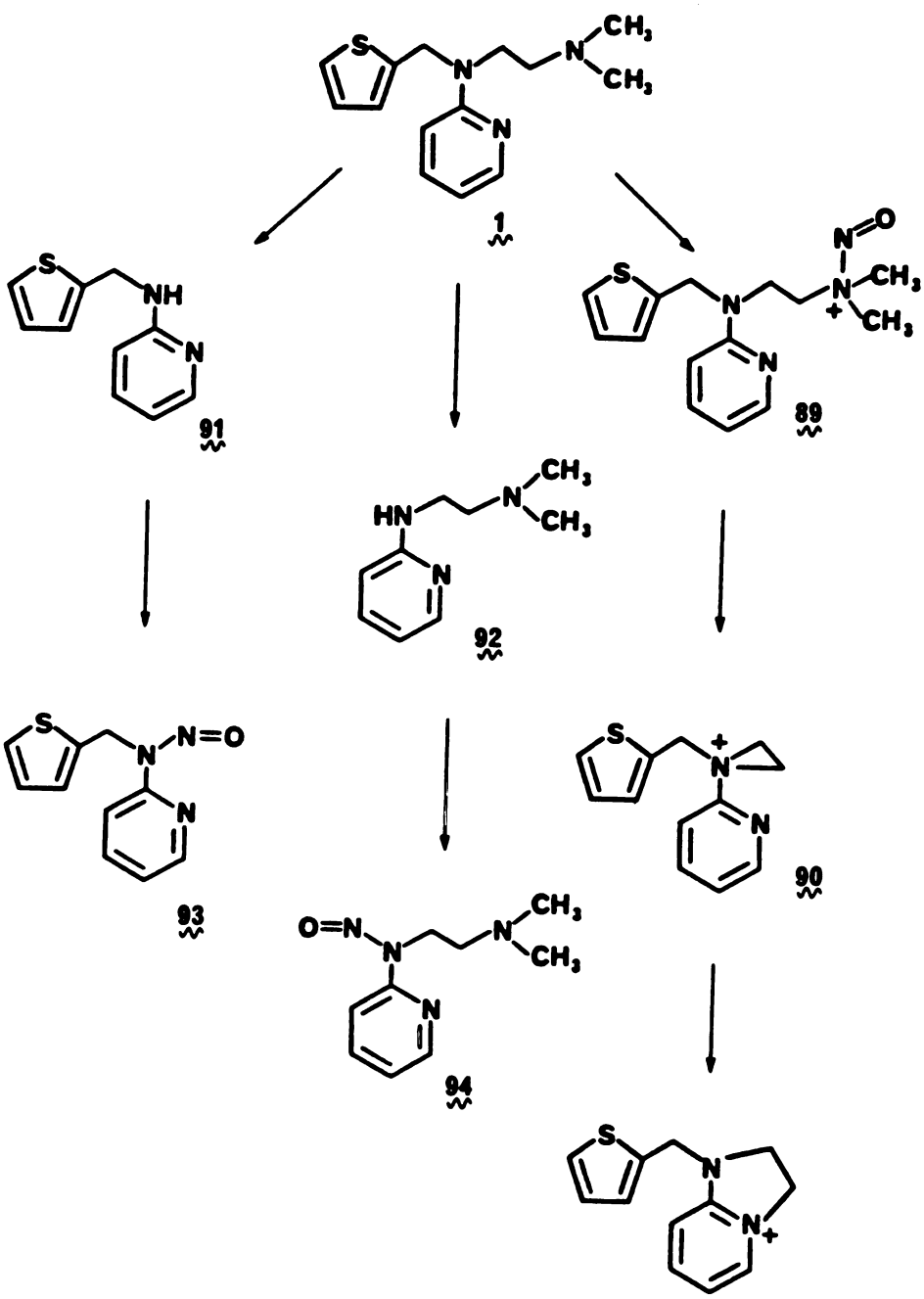

methapyrilene induced tumorigenesis and thus nitrosamines derived from methapyrilene are not the ultimate carcinogenic species. These results were confirmed by results from an Ames test where a mixture of methapyrilene and sodium nitrite led to mutagenesis but the type of mutagenesis indicated that it was not a result of DMNA.[144]

An analysis of the in vivo tissue damage caused by methapyrilene administration was conducted. After one week on a diet containing 1000 ppm methapyrilene, enlarged, pale-staining nuclei, prominent and multiple nucleoli and a pale-staining cytoplasm were observed in hepatocytes in the periportal region.[153] Most noticeably, a significant increase in the number of mitochondria with a concommitant decrease in the amount of both rough and smooth endoplasmic reticulum was observed.[153] After two weeks on this diet, a large increase in the number of mitochondria per cell was seen with the mitochondria appearing swollen and deformed to a ring-shape. An increased ratio of nuclear to cytoplasmic area as well as nucleolar area per cell was found. When randomly radiolabeled methapyrilene was introduced in the diet, 67% of the radiolabel was incorporated into the mitochondria within the hepatocyte while 20% was excreted in the urine.[153] Only background levels were detected in the nucleus and lipid, while 23% of the radioactivity was associated with the smooth endoplasmic reticulum. A small but significant amount (9%) was incorporated into the rough endoplasmic reticulum. Further

studies compared the ultrastructural changes resulting from methapyrilene and a few structurally related analogs shown in Figure 7.[154] Methapyrilene was the only compound to cause increased numbers of mitochondria in rat hepatocytes located in the portal region. This result was observed in rats but not in Syrian golden hamsters or guinea pigs. Methafurylene (95), the furan analog of methapyrilene, demonstrated some of the other changes observed with methapyrilene. An augmentation of the smooth endoplasmic reticulum in hepatocytes in the portal region was seen as well as an increase in mitotic rate in liver cells.[154] None of the other analogs demonstrated pronounced effects except for general swelling of cytoplasmic organelles, indicative of toxic effects.

These ultrastructural changes have been previously observed for genotoxic carcinogens and in certain disease states. Oncocytes, those cells which develop into tumors, have been found to contain increased numbers of normal sized mitochondria.[155] These mitochondria generally lack the dense granuales of divalent cations such as calcium and magnesium, indicative of abnormal membrane ionic transport.[155] 2-AAF and 4-dimethylaminoazobenzene lead to altered hepatocytes containing prominent nuclei, increased mitochondria, decreased parallel-arrayed rough endoplasmic reticulum and increased levels of glycogen.[156] An increase in mitotic index in altered hepatocyte foci was also observed, indicative of increased

Figure 7. Noncarcinogenic analogs of methapyrilene

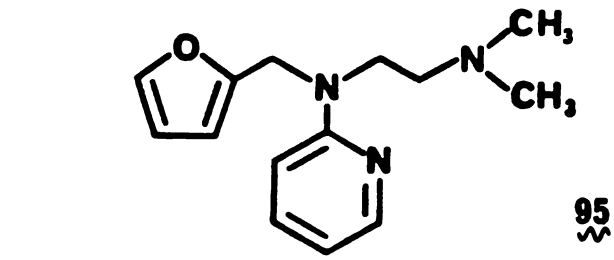

95

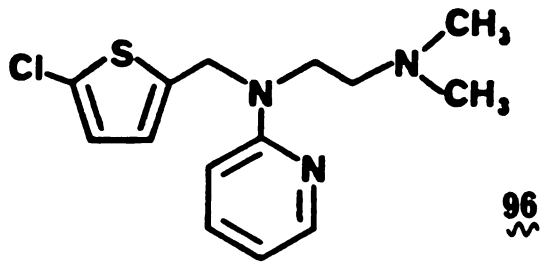

96

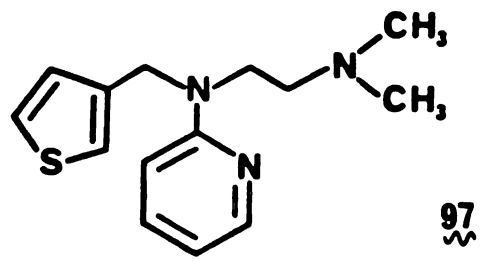

97

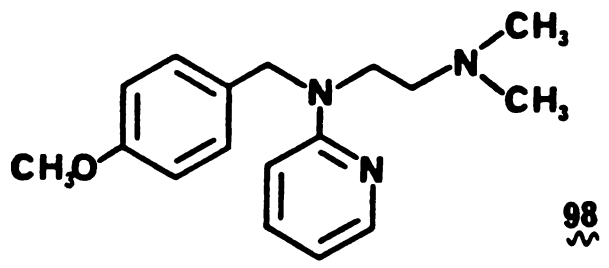

98

DNA synthesis.[156] In certain instances, the mitochondrial genetic system is believed to be the primary target of chemical carcinogens.[157] A study of the effects of 16 carcinogens and 3 noncarcinogens on haploid yeast strains under fermentable and non-fermentable conditions indicated that the mitochondria were prime in vivo targets for many carcinogens.[158] Mitochondrial toxicity was observed by the decrease in synthesis of cytochromes aa3 and b in Saccharomyces.[159] This may be a result of reaction with DNA ending in altered DNA transcription.[159] Early studies by Wunderlich and coworkers[160] found that N-nitrosomethylurea and N-nitrosodimethylamine showed preferential methylation of hepatic mitochondrial DNA when administered to rats. Analogously, six different polycyclic aromatic hydrocarbons bound 50-500 times more to mitochondrial DNA than nuclear DNA.[161] Benzo(a)pyrene diol epoxide binds 40-90 times more efficiently to mitochondrial DNA than nuclear, as does benzo(a)pyrene itself.[162] Aflatoxin B1 also attacks mitochondrial DNA preferentially during hepatocarcinogenesis.[163] The reasons for mitochondrial mutagenesis may include the following:[158] 1) the preferential localization of the mitochondria, 2) the activity of short-lived species within the organelle, 3) greater accessibility of the relatively naked mitochondrial DNA compared to chromatin DNA and 4) the intrinsic differences in DNA binding sites. Mitochondrial mutagenesis

is also believed to occur through changes in the cellular membrane.[164,165] Epigenetic carcinogens, such as phenobarbital and DDT, may act through an alteration of the cell membrane which in turn interferes with the transmission of regulatory factors.[165] In this way, epigenetic carcinogens affect gene expression and promote cell growth and proliferation. Other commonly observed changes in cancerous or precancerous livers include deficiency in the accumulation of iron, altered γ-glutamyl transpeptidase activity, deficiency in ATPase and G6Pase.[156] Tumor bearing animals exhibit increased levels of cAMP, serum calcium and decreased levels of cGMP and drug metabolism.[166] Methapyrilene demonstrates many of the above mentioned cellular alterations observed for genotoxic and epigenetic carcinogens. Thus, the classification of methapyrilene as a genotoxic or epigenetic carcinogen cannot yet be made.

Early metabolism studies showed that methapyrilene was extensively metabolized by the guinea pig liver.[167] In later studies,[168,169] little or no parent methapyrilene could be detected in the urine and plasma of patients using methapyrilene as assayed by gas chromatography. More recent studies[170] have found that the half-life of methapyrilene in man is only 1-2 hours and that only 0.04-1.3% of the dose is excreted in the urine unchanged. Pharmacokinetic studies indicated that methapyrilene has a high volume of distribution and the total body clearance

exceeds the hepatic blood flow, demonstrating extrahepatic metabolism in man.[170] In vitro metabolic studies utilizing rabbit liver microsomes (100,000x g pellet) showed that 50% of the methapyrilene was consumed in one hour at 37° in the presence of NADPH.[71] Thus, methapyrilene is extensively metabolized both in vivo and in vitro.

Thus we have evidence that methapyrilene forms nitrosamines but that these are not involved in carcinogenesis. Methapyrilene also effects the constituents of the hepatic cell with the predominent effect being an increase in the number of mitochondria. From the reported results, it is difficult to ascertain if this proliferation of mitochondria is due to a direct interaction of methapyrilene or one of its metabolites with the mitochondrial DNA or if there is some alteration in the cell wall which by some indirect mechanism leads to an altered regulatory mechanism of genetic expression. A fair amount of evidence suggests that methapyrilene is extensively metabolized in a number of species and the end metabolic intermediates or the metabolites themselves may be the ultimate carcinogen(s) resulting from methapyrilene.

With the above information in mind, we set out to study the metabolism of methapyrilene in rats. Utilizing rat liver microsomes, we have determined the extent of metabolism in control and induced rats as well as studied the distribution of specifically radiolabeled methapyrilene. We have determined the structures of numerous organic and

aqueous soluble metabolites and extimated the quantities of their formation by HPLC utilizing synthetic metabolite standards. We have also determined whether radiolabeled methapyrilene binds covalently to microsomal proteins and exogenous calf thymus DNA and have examined the effects of model nucleophiles on that binding. Through these studies we have developed a better understanding of the possible route(s) of methapyrilene induced carcinogenesis.

IV. Overall Rate of Methapyrilene Metabolism

Until recently, very little was known about the in vivo and in vitro metabolism of methapyrilene. As discussed earlier, methapyrilene has a half-life of one to two hours in humans as determined by a gas chromatographic (gc) assay.[170] In our laboratory, R. Ziegler etal.[71] developed a method for analyzing the in vitro metabolism of methapyrilene. To monitor the extent of metabolism in rabbit liver microsomal incubations, a quantitative gc assay was developed in which pyrilamine maleate was added as an internal standard. In the presence of reduced nicotinamide adenine dinucleotide phosphate (NADPH), 33-50% of the methapyrilene was consumed in one hour at 37°.[71] In the absence of NADPH, methapyrilene was recovered from microsomal incubates in nearly quantitative yields. Metabolic studies utilizing phenobarbital (Pb) induced rats yielded liver microsomes that were capable of metabolizing only 20% of the parent drug.[71]

On the basis of these studies, methapyrilene appears to be extensively metabolized in vivo and in vitro. The enzymes present in rabbit liver microsomes seem to be more active in metabolizing methapyrilene than those in rat liver microsomes. To better understand the enzymes involved, the overall level and rate of methapyrilene metabolism by rat liver microsomes was investigated with phenobarbital, 3-methylcholanthrene and methapyrilene induced rats.

Utilizing microsomes prepared from rat livers (see experimental) and diluted to a concentration of 2-3 mg protein/ml buffer as determined by Lowry assay,[171] metabolic incubations were conducted to various time points. In each study two different controls were run. In one sample, no methapyrilene or NADPH was added to the microsomes to observe the background. In the other control, methapyrilene but no NADPH was added to view the metabolism not requiring NADPH. The remaining metabolic samples contained methapyrilene, and NADPH was added every 20 minutes. At the endpoint of each incubation, the microsomal mixture was pipeted into 5 ml methylene chloride (CH_2Cl_2) and shaken to kill the microsomal enzymes. Pyrilamine maleate (1mg/sample) was then added to the partitioning mixture as an internal standard and the resulting mixture was shaken for 20 minutes. After low speed centrifugation, the CH_2Cl_2 was pipeted away from the remaining aqueous layer and protein pellet and directly subjected to gc analysis. On a 3% OV 25 on Chromasorb W, AW, DMSC (100/120 mesh), the sample was chromatographed on a temperature program of 6°/min and the compounds detected by flame ionization detection.

This assay differs slightly from that of Ziegler.[71] First, the incubate was not basified prior to CH_2Cl_2 extraction. When comparing the gc trace of basic incubate extraction versus neutral extractions, we found that there was no difference in the peaks obtained. As amines, the

extraction efficiency would be higher at basic pH but, for the purpose of quantitation, a standard curve determined from the same isolation procedure eliminates this problem. Secondly, the CH_2Cl_2 resulting from extraction was not dried over potassium carbonate prior to gc analysis. Because of the nature of CH_2Cl_2, very little water is present in the CH_2Cl_2 layer and should not alter the gc analysis. Additionally, amines are known to adsorb onto drying agents. Thus, both of these steps were eliminated in an effort to minimize experimental error.

A standard curve was determined by spiking inactivated microsomes with varying known amounts of methapyrilene followed by the extraction procedure described above. A sample standard curve is shown in Figure 8 where the methapyrilene (MP) and pyrilamine (IS) were assayed both by peak height ratio (MP/IS) and by ratio of the areas under the curves. An Apple computer area computing program was utilized since triangulation could not account for the slight tailing of the peaks. As seen in the graph, very good agreement exists between the two methods of analysis but the points arising from the peak height ratios appear to be more linear. Perhaps the area computing program was not exact enough for such small areas. Based on these results, the use of peak height ratios seemed more than adequate for the analysis of metabolic samples.

The extraction yield was found to be quite high for both methapyrilene and pyrilamine. In comparing the peak

Figure 8. Standard Curve of Peak Height Ratio versus Area Under the Curve Analysis.

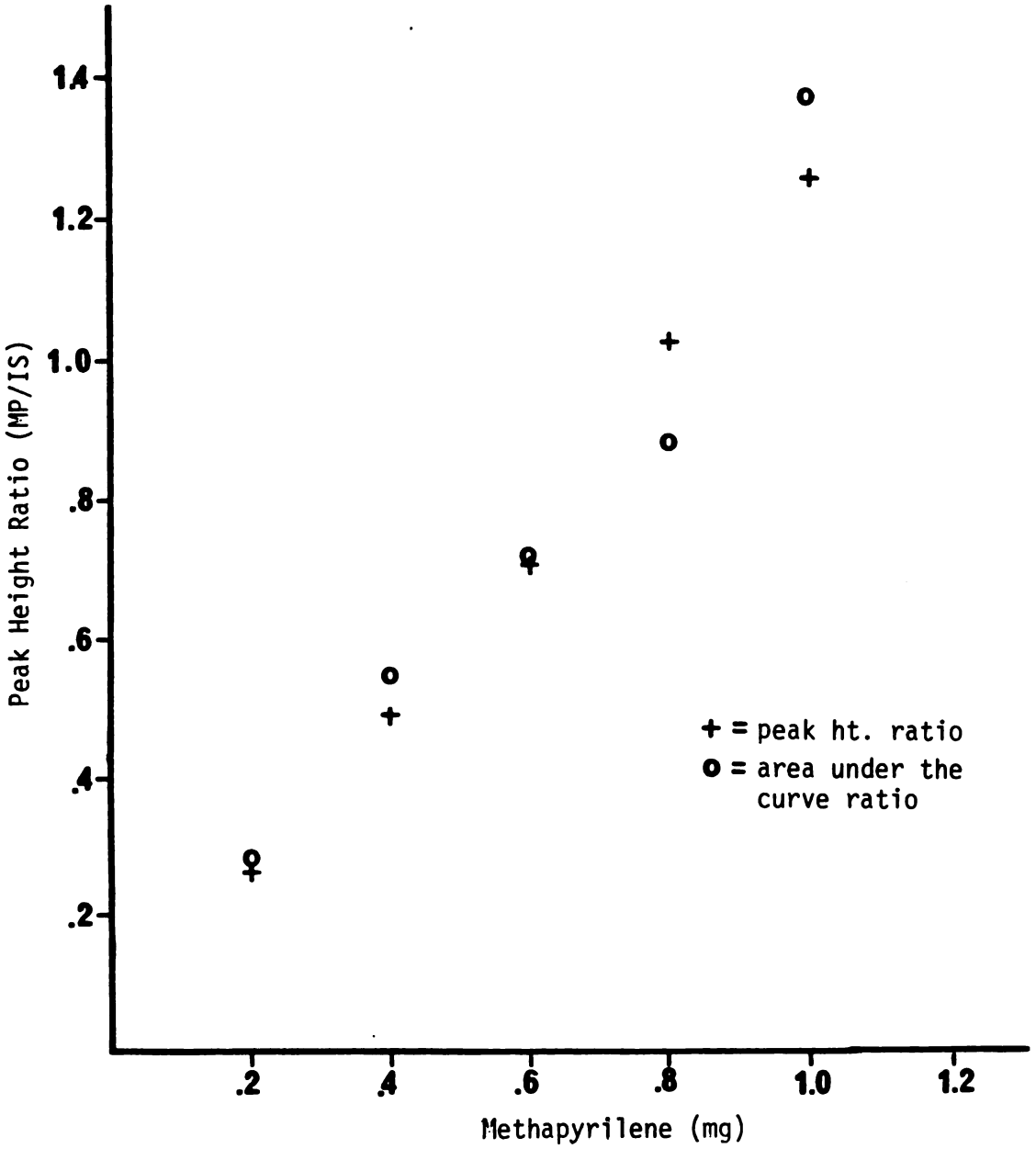

height ratios of a standard CH_2Cl_2 solution of MP and IS versus a solution derived from extraction of spiked microsomes, the peak height ratios (MP/IS) were 1.04 and 1.15, respectively. Apparently, methapyrilene extracts more readily than pyrilamine at pH 7.4. Because of this high extraction efficiency, the metabolic incubates were only extracted once with CH_2Cl_2.

A) Rate of Metabolism in Pb-induced and Control Rats.

Male Sprague Dawley rats (180-200g) were induced with Pb for three days prior to sacrifice as judged by their deep anesthesia following i.p. injections. As illustrated in Figure 9, the disappearance of methapyrilene with respect to time was nearly identical for the induced and control incubates. These results indicate one of two things. Either the phenobarbital inducible enzymes may not be responsible for a majority of methapyrilene metabolism or the aerobic degradation of the microsomes themselves may lead to slowed metabolism independent of induction. A closer examination of the gc tracings indicated that the N-desmethylmethapyrilene peaks were larger in the samples obtained from Pb-induced animals. The peak heights and the ratios derived therefrom for Pb-induced versus control incubates are given in Table 4. Although the experimental error is probably great, the difference between the Pb-induced and control metabolic formation of N-desmethylmethapyrilene appears to be substantial.

Figure 9. Pb-Induced versus Control Metabolism.

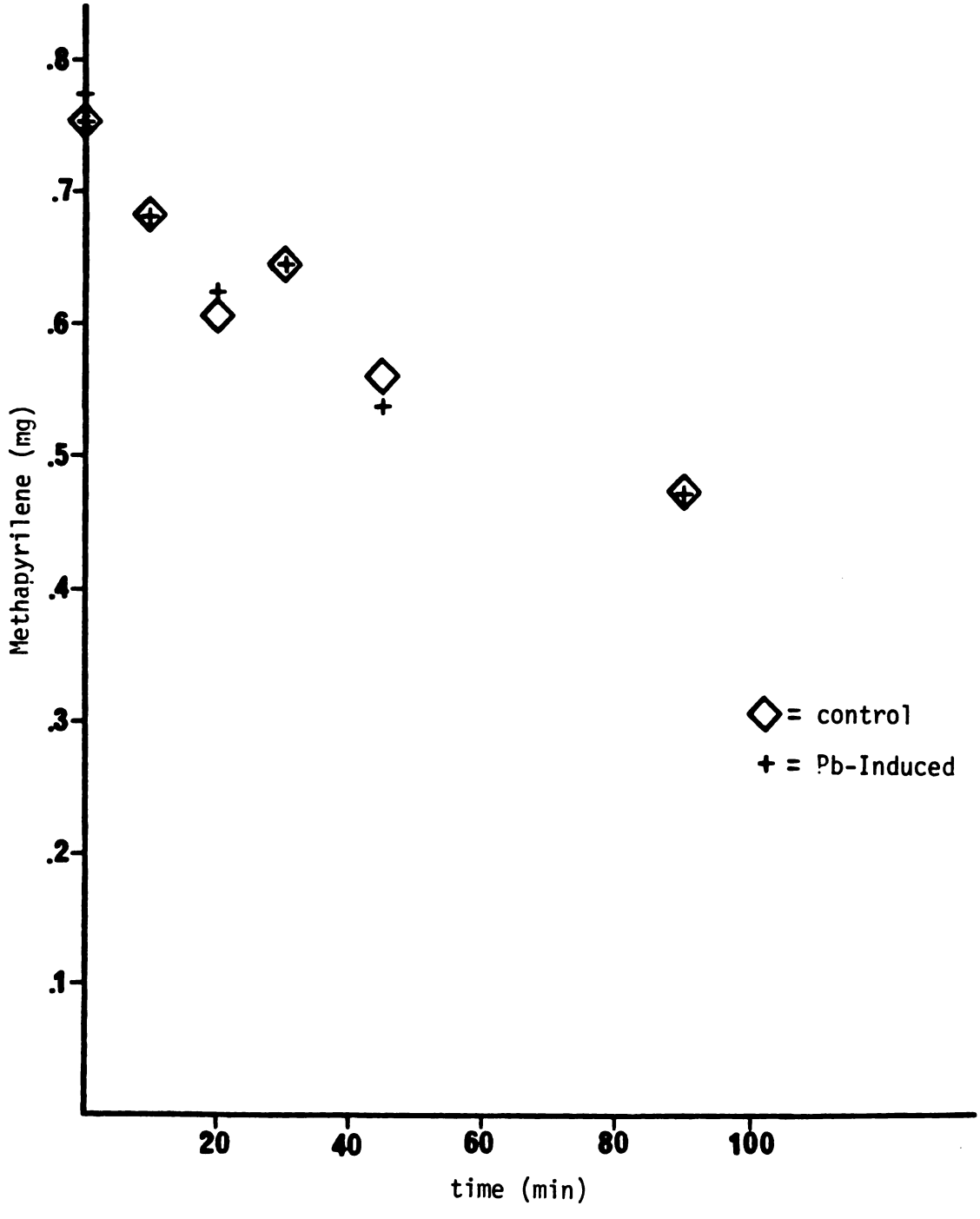

Table 4. Pb-Induction of N-Desmethylmethapyrilene Formation

	peak heights (cm)		
	N-des	IS	Ratio
Pb-induced	1.0	11.0	0.09
	1.25	12.0	0.104
Control	0.25	12.0	0.021

Different induction studies carried out at various times illustrated that the curves were highly reproducible (Figure 10). The reproducibility of results seems to be well within the limits of biological variation. To judge the overall metabolism of methapyrilene in Pb-induced rats, the peak height ratios of methapyrilene incubates containing NADPH were compared to similar incubates not containing NADPH. In one case, the Pb-induced microsomes yielded 48% metabolism and in another only 39% metabolism. The major differences in these two studies was in the zero time point or non-metabolic peak height ratio as seen in Figure 10. Otherwise, the metabolism was nearly identical in the two separate studies. The control rats demonstrated 37% metabolism in a study conducted in conjunction with the Pb-induced metabolism leading to 39% consumption.

In obtaining 35-45% metabolism with Pb-induced rat liver microsomes, these results have differed significantly from the 20% reported previously.[71] We later found that the quality of the NADPH is very important to the extent of metabolism. When old NADPH was used, only 20% metabolism

Figure 10. Overall Metabolism by Pb-Induced Rats

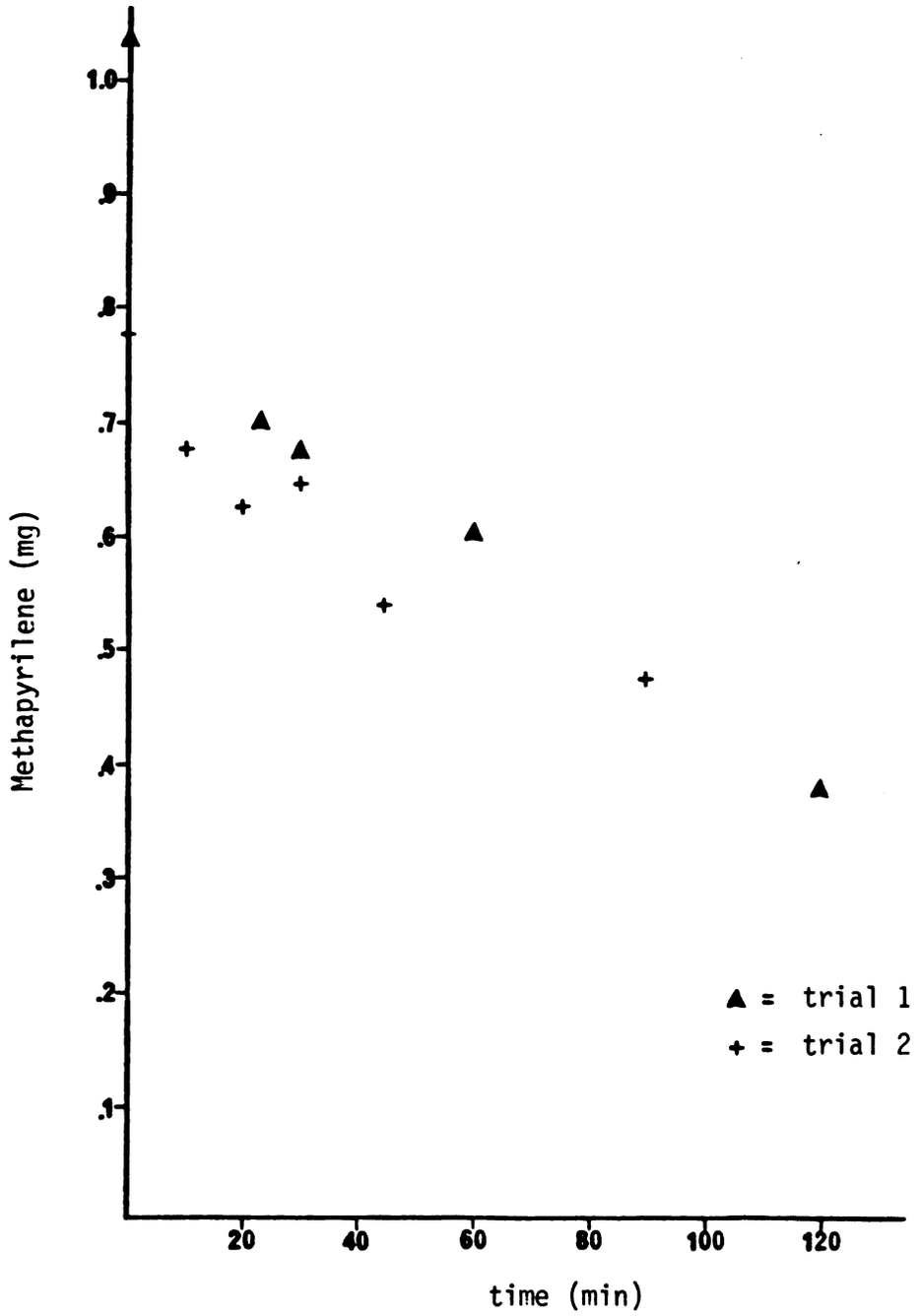

was observed. Thus, in all subsequent studies, the NADPH used was purchased just prior to the studies.

B). 3-Methylcholanthrene Induction of Methapyrilene Metabolism

3-Methylcholanthrene (3-MC), when injected i.p. as an oil suspension 24 hours prior to sacrifice, is known to lead to increased levels of cytochrome P-448. Utilizing male Sprague Dawley rats in this manner, the overall microsomal metabolism of methapyrilene was found to be 34% in one hour from induced livers and 41% from control livers, as assayed by the previously discussed gc-peak height ratio analysis. Unlike the Pb-induced studies, the production of N-desmethylmethapyrilene was not altered by 3-MC induction. Thus, cytochrome P-448 does not appear to be responsible for the majority of methapyrilene's metabolism.

C). Methapyrilene Induction of Microsomal Metabolism.

To determine whether methapyrilene induces or inhibits its own metabolism, methapyrilene was fed to rats over a one to two week period at 0.05% of their diet prior to studying the microsmal metabolism rates. The original carcinogenesis studies were conducted with methapyrilene at 0.1% of the diet.[152] The rats, in general, did not like the powdered diet and would not eat enough of the 0.1% diet to sustain their weight. Thus, the diet was diluted to 0.05% methapyrilene.

In the initial study, two rats on the normal pelleted rat chow were compared to four rats on the 0.05% methapyrilene powdered rat chow. After two weeks on the diet, the rats were starved for 24 hours to cleanse their bodies of ingested methapyrilene. The same study was repeated for one week where the control rats were fed unadulterated powdered rat chow. The standard curves were nearly identical for both MP-induced and control rats (Figure 11). The overall metabolism from these two studies is given in Table 5. After two weeks on the methapyrilene diet, in vitro microsomal metabolism consumed 48% of the methapyrilene incubated while the control metabolized 53%. The difference in the two studies has been attributed to the different batches on NADPH used in the incubations. Based on these results, the metabolism of methapyrilene was not induced but, if anything, slightly inhibited by pretreatment of the rats with methapyrilene for 1 to 2 weeks.

Table 5. Overall Metabolism in Methapyrilene Induced Rats.

	2 weeks	1 week
MP-induced	48%	35%
Control	53%	40%

The peak height ratios for N-desmethylmethapyrilene were compared for MP-induced and control animals. As is shown in Table 6, the formation of N-desmethylmethapyrilene was not significantly different in the induced incubates.

Figure 11. Standard Curve of Methapyrilene Induced versus Control Rats

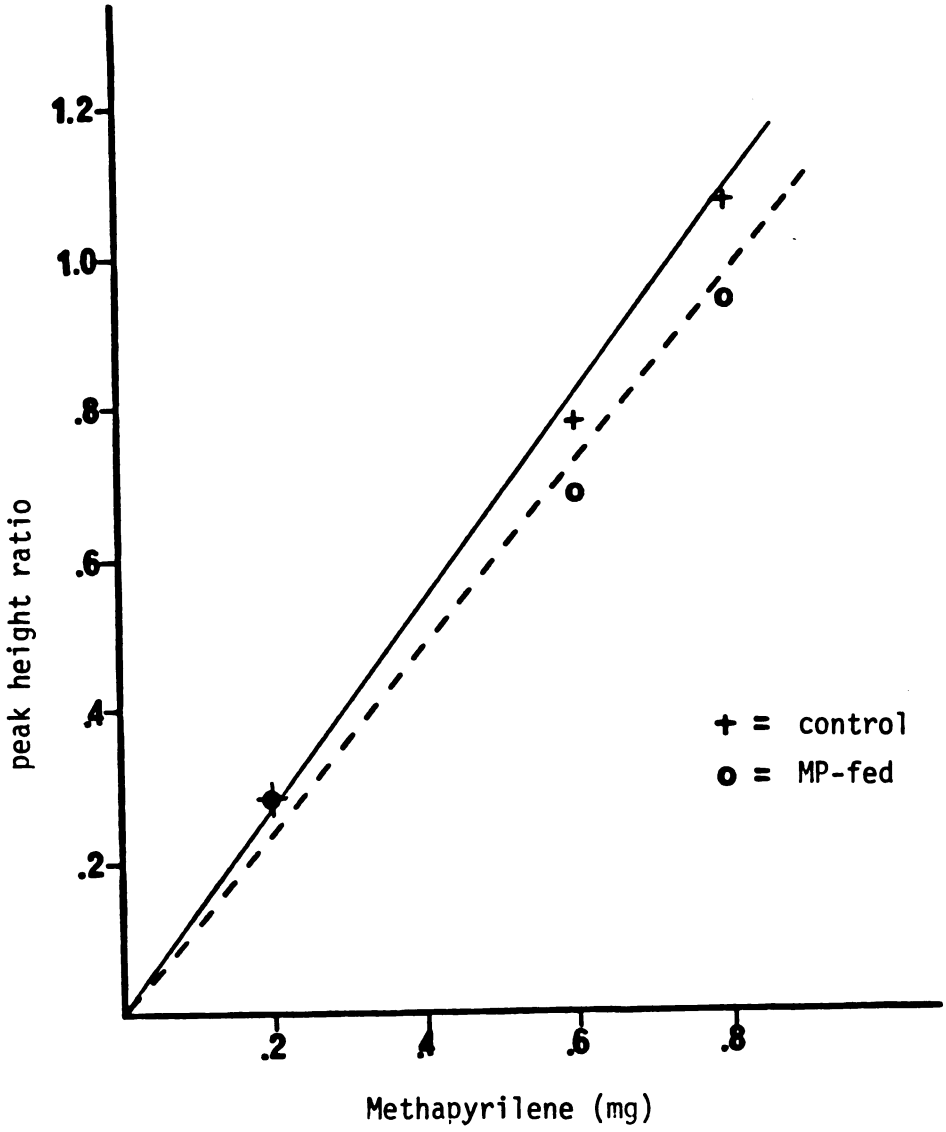

Table 6. Formation of N-Desmethylmethapyrilene from Methapyrilene-Induced Rats.

	peak heights (cm)		
	N-des	IS	Ratio
MP-induced	0.30	12.9	0.023
Control	0.20	11.4	0.018

The amount of N-desmethyl metabolite formed was in good agreement with that found for controls from the previous Pb-induced studies (Table 4).

Conclusions:

These results indicate that phenobarbital, 3-methylcholanthrene and methapyrilene are not significant inducers of rat liver microsomal methapyrilene metabolism. The overall levels of methapyrilene metabolism in one hour at 37° range between 35-45% and require the presence of NADPH. The profile of metabolism was altered by Pb-induction to yield increased amounts of N-desmethylmethapyrilene. From these results, one can conclude that the majority of methapyrilene metabolism does not occur through the Pb-inducible cytochrome P-450. Similarly, 3-methylcholanthrene induced cytochrome P-448 does not account for a major pathway of metabolism.

These results also show that methapyrilene does not induce but, if anything, slightly inhibits its own metabolism. Perhaps some other cytochrome P-450 enzyme(s) is involved in oxidative methapyrilene metabolism.

Microsomal flavin-containing monooxygenase[172] may also contribute to the observed metabolism. With the knowledge of structures of metabolites we hoped to have a better idea as to the types of enzymatic transformations occurring in vitro.

V. Radiochemical Synthesis and Metabolic Distribution of Methapyrilene and its Metabolites.

The use of radiolabeled drug can be extremely important in tracing the drug and its metabolites through isolation and purification procedures. In the case of methapyrilene, it was important to consider the possible sites of metabolism prior to designing a synthetic approach for incorporating tritium and ^{14}C into the structure. The oxidative metabolism of the ethylenediamine portion of methapyrilene has already been established,[71] whereas the metabolism in the thiophene and pyridine rings has gone unmapped. For this reason we chose to incorporate the two labels in the areas designated A and B in 99. For synthetic reasons that will be discussed below, we designed syntheses in which the ^{14}C-label could be incorporated into the A portion of methapyrilene and the ^{3}H-label into the B portion. The two labels would be introduced separately resulting in ^{3}H-methapyrilene and ^{14}C-methapyrilene so that the two radiolabels could be used separately or together to map the structural content of the various metabolites isolated. In the progress of this research, the actual synthesis of ^{14}C-methapyrilene was never carried out.

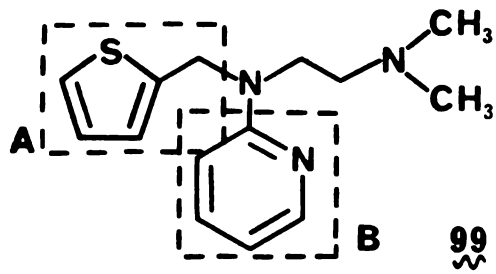

99

A). Incorporation of Tritium.

Given that the tritium had to be incorporated into the pyridine ring with specific knowledge of the location of the label, we chose to introduce the tritium into the 5-position based on known chemistry. Based on previous studies on the structural analog of methapyrilene, tripelennamine,[173] and what is currently known about pyridine ring metabolism (Section IIB) the 5-position of the pyridine ring is expected to undergo limited ring hydroxylation. This type of metabolism could be detected in our studies by the loss of tritium but not ^{14}C label. Otherwise, the tritium label should be present in all metabolites containing the pyridine ring.

The simplest method of introducing the tritium seemed to be through catalytic hydrogenation to remove a halogen in the 5-position. Under the mild conditions necessary for this reaction, we felt that little or no tritiated impurities would be produced. Two methods were tried to achieve 5-bromomethapyrilene. Initially, precedence for direct bromination of methapyrilene was obtained when the precursor, N-(N',N'-dimethylaminoethyl)-2-aminopyridine (92) was converted in low yield to N-(N',N'-dimethylaminoethyl)-2-amino-5-bromoyridine (100) in the presence of bromine and acetic acid[174] as determined by NMR. Incorporation of the bromine into the 5 position was evident by the aromatic signal at δ8.10 (J= 2.5 Hz)

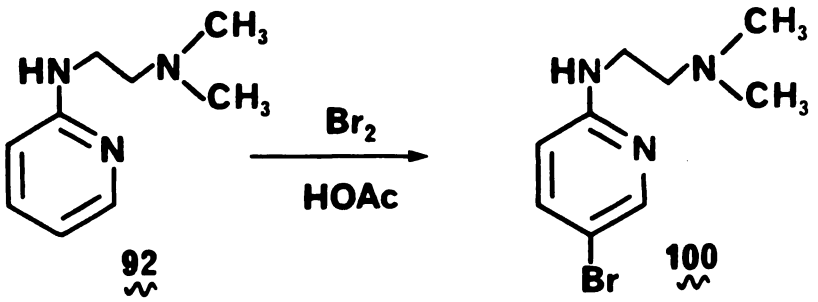

exhibiting only meta coupling and the integration of the aromatic peaks accounted for only three protons.

Direct bromination of methapyrilene, however, did not yield the 5-bromo adduct alone but instead yielded a mixture of both thiophene and pyridine brominated products. Although the chemical ionization mass spectrum gave only the brominated thiophene fragment at m/e 175/177, the GC-EIMS gave both m/e 175/177 and 156/158, the bromopyridine ions. These results are in contradiction to those obtained by D.H. Marrian and coworkers[175] in which bromination of methapyrilene was reported to have given only C-5 pyridine bromination. On the basis of reactivity of the two aromatic rings towards aromatic electrophilic substitution, one would expect the thiophene to be brominated more readily because pyridine rings are in general deactivated towards

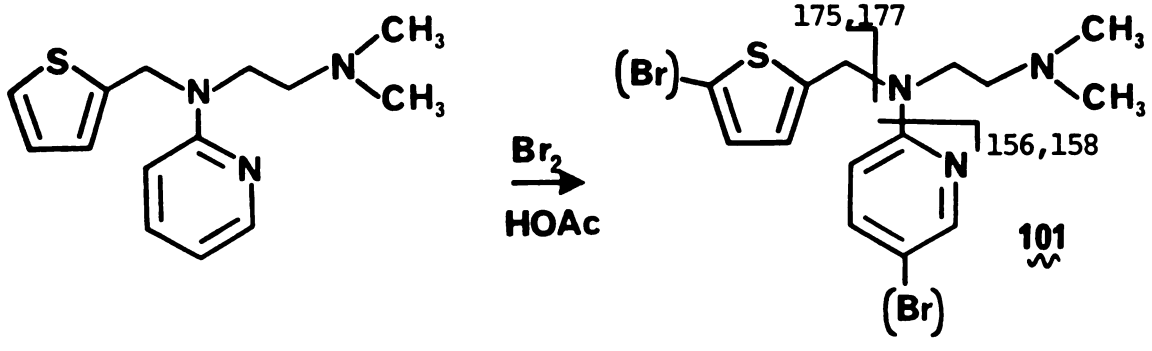

electrophilic substitution. The position of bromination of the thiophene ring would be difficult to assign by NMR but is predicted to be in the 5'-position as shown in 101.[176]

An alternative and more direct route to 5-bromomethapyrilene is shown in Scheme 7. 2-Amino-5-bromopyridine (102) is ionized with sodium hydride[177] in anhydrous dioxane and then coupled to N,N-dimethylaminoethyl chloride to yield N-(N',N'-dimethylaminoethyl)-2-amino-5-bromopyridine (100) as an oil in 24% yield. The formation of the anion of 2-amino-5-bromopyridine was required due to the ambident nature of the two nitrogens. Under neutral conditions, 2-aminopyridine is in equilibrium between the following two forms, with the exocyclic amine donating electrons to the pyridine ring.[178] To reverse this polarity and favor alkylation of the exocyclic nitrogen, a strong base such as sodium hydride[177] or sodium amide[174] has been used to generate the anion under anhydrous conditions followed by alkylation with the desired alkyl halide. The desired 5-bromomethapyrilene (103) was formed by coupling the anion of 100 with 2-chloromethylthiophene. After vacuum distillation and thin layer chromatography, the product was obtained in 11% yield.

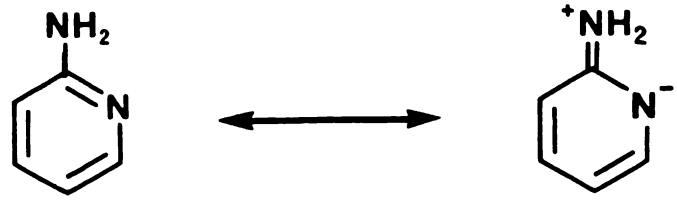

Scheme 7. Synthesis of ^{3}H-Methapyrilene

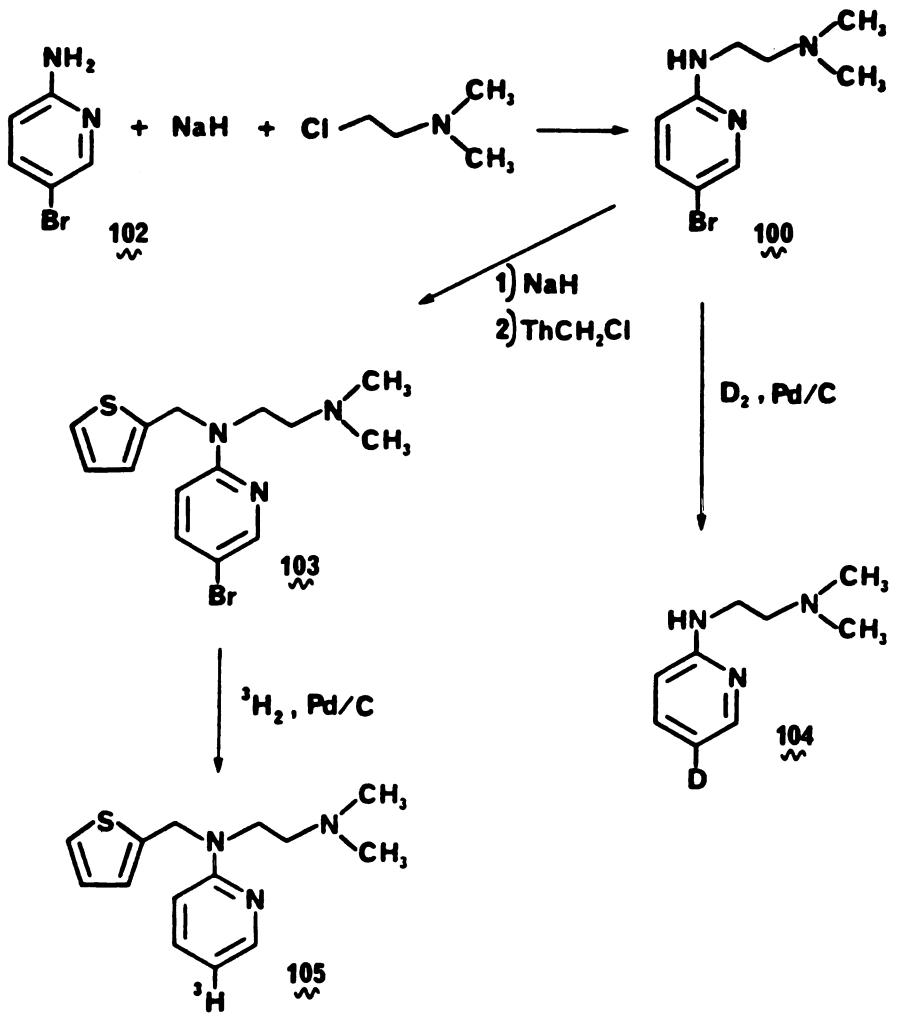

The NMR spectrum of 5-bromomethapyrilene is shown in Figure 12. Whereas the aliphatic and most of the aromatic regions closely resemble those of methapyrilene, the 5-H does not appear at δ6.5 and the doublet for 6-H at δ8.1 now shows only meta coupling. The HR-EIMS was also characteristic of this structure showing the following fragmentation.

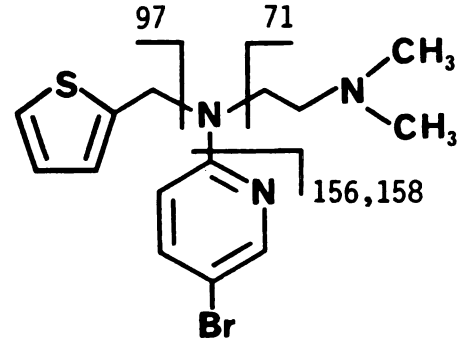

Conditions for the catalytic incorporation of tritium were determined by deuterogenation of 100 to give 104. After 24 hours in the presence of Pd/C and D_2 in ethanol, 100 was converted to 104 in good yield as determined by NMR and EIMS. The signals for the aromatic protons of the deutero derivative 104 differ in shift with respect to the bromo compound (100). The most distinctive shift was in the C-3 proton, from δ6.30 (d, J = 11 Hz) in 100 to δ6.59 (d, J = 10 Hz) in 104. The mass spectrum of the deutero compound showed a similar fragmentation pattern with respect to the proteo derivative, except for being one mass unit higher.

To ascertain the efficiency of catalytic tritiation of

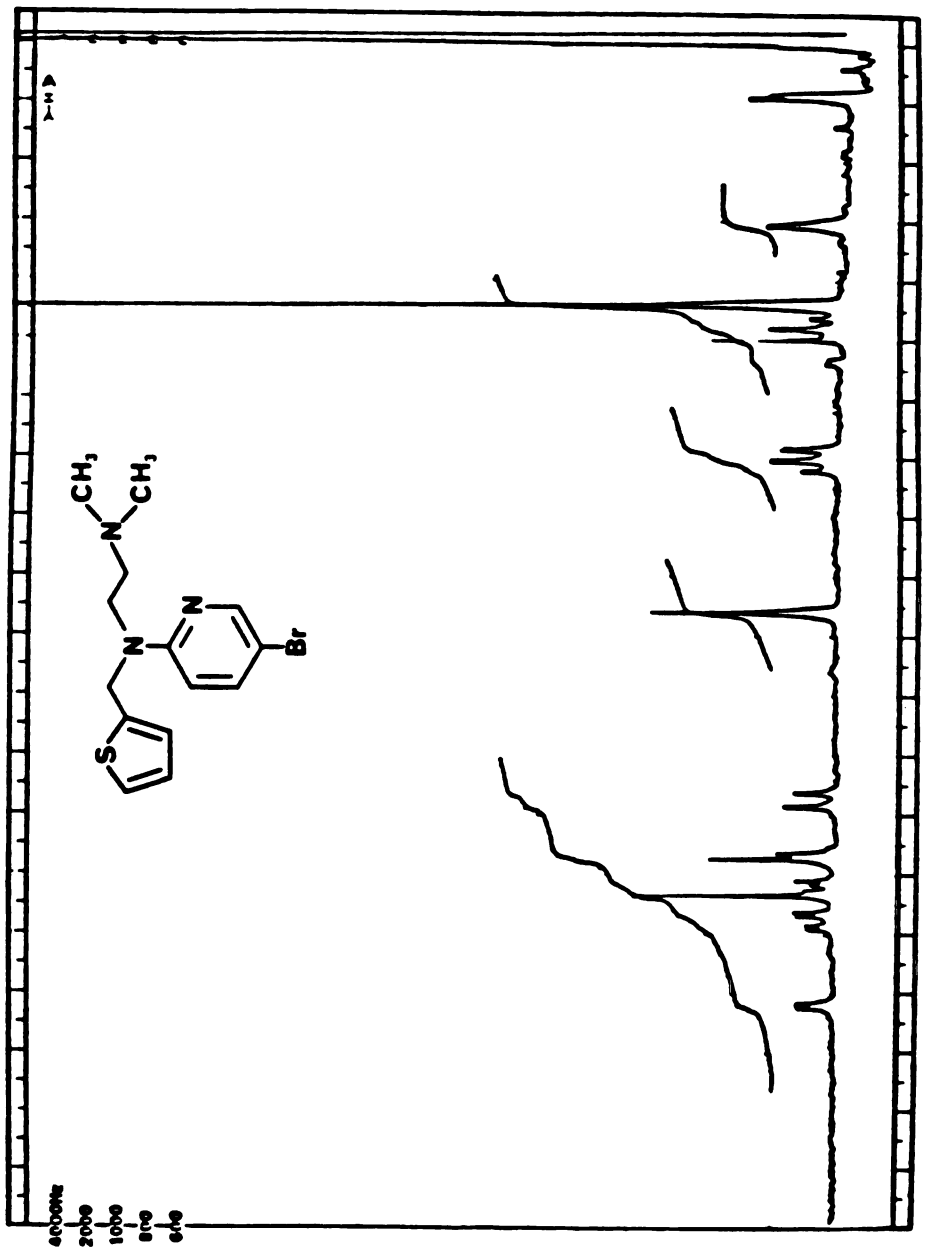

Figure 12. NMR Spectrum of 103.

5-bromomethapyrilene (103), 12 mg of the oil were dissolved in ethanol and treated with deuterium gas and Pd/C.[179] After two hours at atmospheric pressure, the reaction mixture showed both the bromo- and deuteromethapyrilene by NMR. Hydrogenation overnight, however, yielded 100% incorporation as seen by NMR (Figure 13). Similarly, the EIMS of the deuterated methapyrilene showed the same fragmentation pattern observed for methapyrilene except for those fragments containing the deuterated pyridine ring which were one mass unit higher.

Based on this information, it appeared that tritium could be incorporated specifically without production of side products. Hydrogenation of the aromatic rings should not occur in as much as these reactions require elevated temperatures and higher pressures of hydrogen.[180] Subsequently, 5-bromomethapyrilene was tritated at the Lawrence Berkeley Laboratory in the presence of our Pd/C catalyst in their glassware. Since we desired a specific activity in the range of 2-4 Ci/ mmol prior to any dilution, 10 Ci of tritium gas in a 1:10 mixture with hydrogen was used. After three hours at room temperature, the reaction mixture was frozen in liquid nitrogen and the tritium gas removed under vacuum. This procedure was repeated twice and then the catalyst was removed by centrifugation. The ethanolic solution was then placed in a scintillation vial, frozen and lyophilized.

To isolate and purify the ^{3}H-methapyrilene (105),

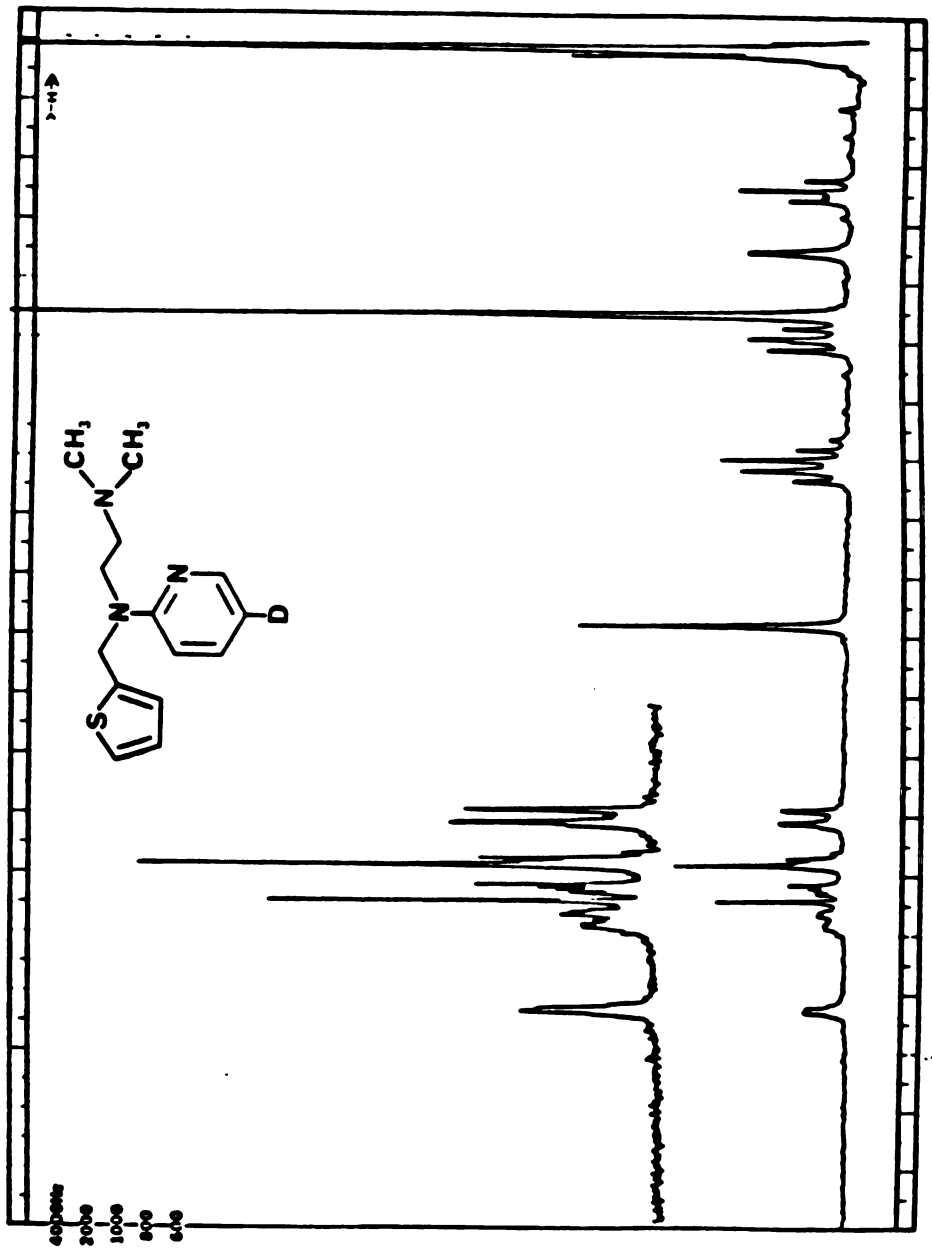

Figure 13. NMR Spectrum of 5-Deuteromethapyrilene.

the material was dissoved in 5% $NaHCO_3$ (1 ml). During the exchange of tritium for bromine, one equivalent of ^3HBr was produced and could easily form the salt of the amine. Thus $NaHCO_3$ was required to neutralize the salt and EtOAc was used to extract the amine. By using a small aliquot of the NaHCO3 solution, EtOAc was found to extract 91% of the tritiated material with three extractions. Thus, the major portion of ^3H-methapyrilene was extracted into 7ml of EtOAc. With approximately 40% counting efficiency by external standard channels ratio, scintillation counting determined that the EtOAc solution contained 2.27×10^{11} dpm or approximately 100 mCi.

Purification of the tritiated material was then pursued. Although thin layer chromatography would have been preferable for such a small quantity, silica gel chromatography proved inappropriate for separating 5-bromomethapyrilene from methapyrilene. Solvent systems such as acetone, EtOAc, 10% MeOH in EtOAc, 10% MeOH in EtOAc plus a small quantity of Et_3N and other systems gave nearly identical, low Rf's for both compounds. Prepurification of the plates gave higher Rf's but still no separation. Thus normal phase silica gel was judged inappropriate for the purification. Reverse phase chromatography also proved ineffective in separating the bromo- from proteomethapyrilene.

The remaining alternative was to convert the amine to its corresponding hydrochloride salt and recrystallize it to

a constant specific activity, although constant specific activity cannot always be used as a measure of purity. A specific activity of 4-5 mCi/ mmol was utilized for metabolic studies and by using approximately 10 mCi of tritiated material in one mmol of unlabeled methapyrilene, the resulting oil was concentrated to dryness and treated with one equivalent of HCl gas dissolved in anhydrous ether. A milky white solid was obtained and the residual HCl and ether were removed under vacuum. The resulting solid was then dissolved in warm EtOAc and MeOH and crystallized upon addition of ether. At this point, the hygroscopic crystals were filtered under nitrogen and subjected to further recrystallization. A constant specific activity of 3.83 mCi/mmol was obtained after three crystallizations.

B). Incorporation of ^{14}C.

As discussed earlier, the methylthiophene side chain was chosen as the site for ^{14}C incorporation. The commercial availability and cost governed in favor of the use of ^{14}C-formaldehyde or ^{14}C-paraformaldehyde in the synthesis of an activated 2-methylthiophene equivalent. The cost and low specific activity of ^{14}C-thiophene argued against incorporation in the thiophene ring itself.

Our first approach is shown in Scheme 8,[181] where thiophene was treated with formaldehyde and HCl gas to produce 2-chloromethylthiophene (106) in 50% yield. The major drawback in this synthesis was the production of

Scheme 8. Synthesis of 2-Chloromethylthiophene from $^{14}CH_2O$.[181]

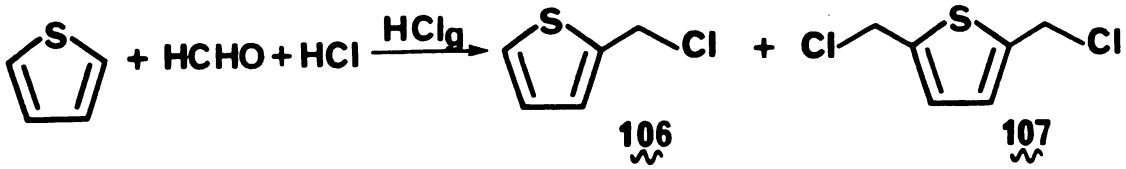

2,5-bischloromethylthiophene (107) which on large scale can be removed by distillation. On small scale, however, this side-product would have to be removed by preparative gas chromatograhy since 2-chloromethylthiophene reacts irreversibly with silica gel. The major drawback in this approach was that approximately 66% of the ^{14}C-formaldehyde would be lost to undesirable side products.

A more successful approach is outlined in Scheme 9. In the first step, nBuLi and TMEDA in ether were added to thiophene to synthesize the 2-lithio salt (108).[182] The salt was generated at room temperature to avoid formation of the kinetically favored 3-lithiothiophene. Approximately one half hour was required to produce the thiophene anion at which time freshly dried paraformaldehyde was added. This reaction mixture was allowed to stir overnight under nitrogen after which time a reddish precipitate formed. The reaction was then partitioned between water and ether. By washing with dilute acid, the TMEDA was easily removed, leaving 2-hydroxymethylthiophene 109 in the ether. The beauty of this reaction was that the side products were

Scheme 9. Synthesis of 2-Chloromethylthiophene from ^{14}C-Paraformaldehyde.

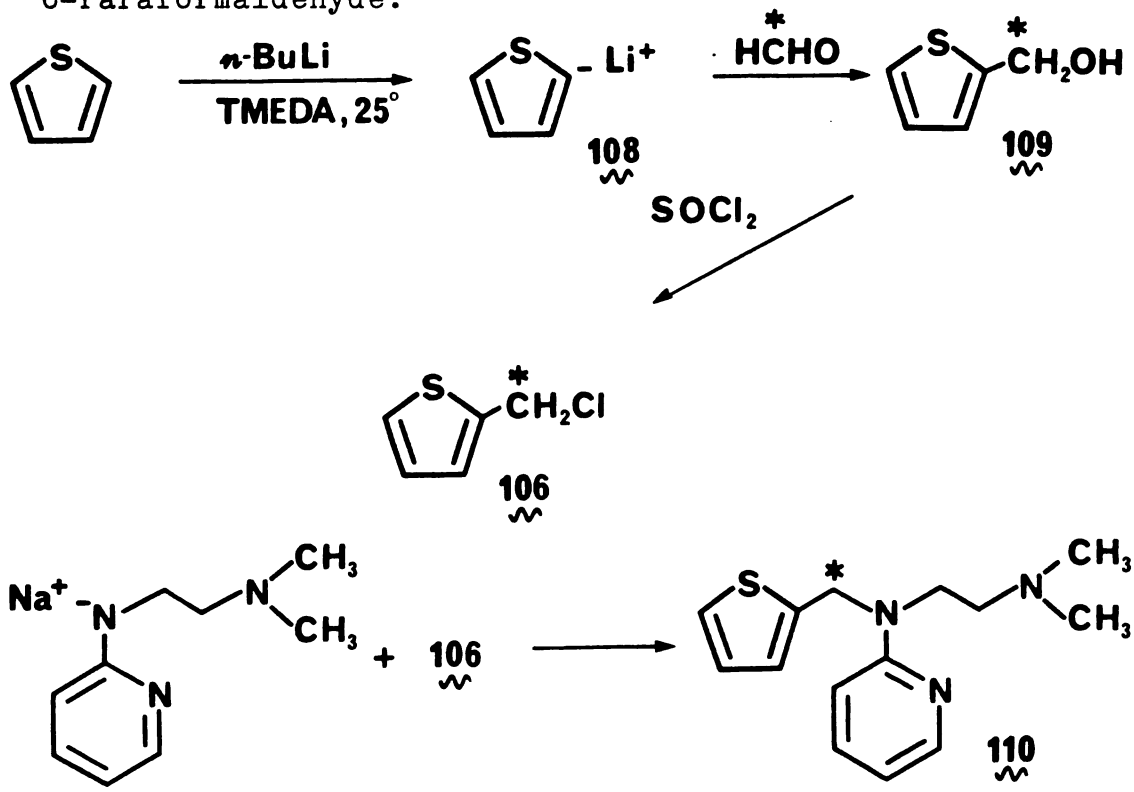

thiophene and paraformaldehyde which are easily removed by evaporation and aqueous extraction, respectively. A preliminary yield of 40% has been obtained but the yield could certainly be increased.

The next step involved the conversion of 2-hydroxymethylthiophene to 2-chloromethylthiophene. Although HCl gas could have been used, it was found that thionyl chloride readily converted the alcohol to alkyl chloride as determined by TLC (2-chloromethylthiophene reacts irreversibly with silica gel to form a red color) and by comparative NMR with authentic 2-chloromethylthiophene. The reaction was worked up by extracting the ethereal reaction mixture with water and drying the ether over

$MgSO_4$ prior to concentration under reduced pressure. The desired product was obtained in approximately 95% yield. Again the solvent and reagents were chosen for their high volatility and easy removal as well as clean product formation. The coupling of 2-chloromethylthiophene with the anion of N-(N',N'-dimethylaminoethyl)-2-aminopyridine yielded the desired methapyrilene, as described earlier. The above synthesis therefore represents an easy, clean method of producing ^{14}C-methapyrilene (110). The actual synthesis of 110 has not as yet been carried out.

C). Radiochemical Distribution of Methapyrilene.

In the case of methapyrilene, previous studies were unable to account for approximately 25% of the initially incubated drug.[71] For this reason, synthetically tritiated methapyrilene has been used as a substrate for microsomal metabolism to ascertain the distribution of the drug and its metabolites according to their solubility, i.e. organic, aqueous or protein bound. The radiolabel has also been extremely helpful in the isolation and analysis of the polar methapyrilene metabolites.

Table 7 illustrates the effects of incubation and extraction conditions on radiochemical distribution. In each case, the incubate was extracted with 5 mls of CH_2Cl_2 followed by low speed centrifugation to separate the two layers from the protein emulsion. At pH 7.4, 73% of the radioactivity was in the CH_2Cl_2, 24%

in the aqueous and 2.4% was covalently bound to the protein pellet. As indicated by the control incubation, NADPH was required for metabolism as well as protein binding. Without NADPH, 97% of the radiolabel was distributed into the organic phase and from previous studies is known to be methapyrilene. With only 3% of the methapyrilene distributed into the aqueous phase in the control, we can deduce that the 24% radioactivity present in the aqueous layer of an NADPH fortified incubate represents methapyrilene metabolites. This was an important finding in that this represents the exact percent unaccounted for in the previous studies.[71] In basifying the incubate prior to extraction, the distribution changes to 81% organic and 14% aqueous. Thus, about 8% of the water soluble

Table 7. Radiochemical Distribution of Methapyrilene and its Metabolites.

	Org	Aq	Protein
extraction conditions			
pH 7.4	73%	24%	2.4%
10	81%	14%	4.5%
7.4, HCl pellet	---	---	1.5%
7.4, TCA pellet	---	---	0.7%
incubation conditions			
- NADPH	97%	3%	0%

metabolites must be basic in nature. Interestingly, the amount of radioactivity bound to protein was reduced upon treating the pellet with trichloroacetic acid or 0.1 M HCl. Apparently the interaction between the radiolabeled metabolite and protein is acid labile. This point will be discussed further in the section on macromolecular binding.

The overall results indicate that the labeled products are largely organic soluble, although 25-30% distributes into the aqueous and protein fractions. As established by gc studies, methapyrilene was metabolized to the extent of 35-45% in one hour and therefore the radioactivity present in the aqueous layer represents the majority of the metabolites. The protein bound adduct requires NADPH and is labile to acid and stable to base. Each of these results will be discussed in more detail in the following sections on organic and aqueous soluble metabolites and macromolecular binding.

VI. Metabolites and Synthesis.

Methapyrilene belongs to a class of antihistamines where the structures contain two aromatic rings linked by a two or three atom chain to a tertiary amine, as illustrated in 111. The X atom may be carbon, oxygen or, as in methapyrilene, nitrogen. As tertiary amines, most antihistamines undergo N-dealkylation and N-oxidation by the mechanisms discussed in Section IIA. To assess the potential pathways of methapyrilene metabolism and the relative amounts derived therefrom, the metabolism of a few antihistamines containing structural units similar to those of methapyrilene will be reviewed. Thus, antihistamines containing ethylenediamine, pyridine and/or benzylic moieties will be discussed.

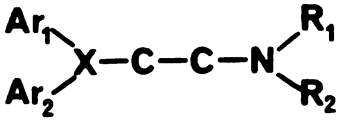

111

Tripelennamine (112) is an antihistamine which differs in structure from methapyrilene by a benzene instead of a thiophene aromatic ring. Although tripelennamine is not carcinogenic, 6% of the administered dose was converted to N-nitrosodesmethyltripelennamine in rats,183 similar to those results obtained with methapyrilene. The N-nitroso

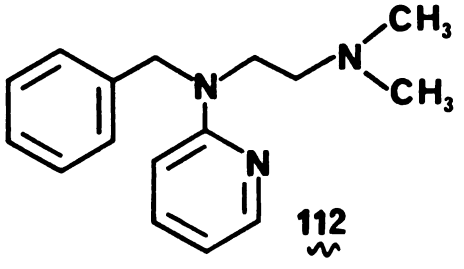

112

derivative of tripelennamine, in turn, led to neither liver nor kidney necrosis.

Tripelennamine radiolabeled at the benzylic methylene with ^{14}C was extensively metabolized by guinea pigs with 90% of the administered radiolabel being excreted in the urine.[184] The majority of the urinary metabolites were found to be conjugates while only a small percentage was hydrophobic material.[184] Similarly, 78% of the administered radiolabel was excreted into the urine by rats in 24 hours.[185] Upon hydrolysis of the rat urinary conjugates and subsequent derivatization with N,O-bistrimethylsilyltrifluoroacetamide (BSTFA), the following metabolic products were observed by GC-MS. The major metabolic routes included N-demethylation (113 and 114) and benzene ring oxidation (115). Derivatized metabolites arising from multiple metabolic hydroxylation were less prevalent, but the pyridine hydroxylated metabolites (116 & 117) demonstrate the capacity

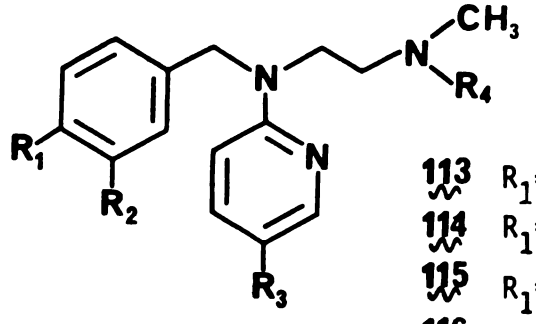

113 R_1= R_2= R_3= H, R_4= TMS
114 R_1= OTMS, R_2= R_3=H, R_4= TMS
115 R_1= OTMS, R_2= R_3= H, R_4=CH_3
116 R_1= R_3= OTMS, R_2=H, R_4= TMS
117 R_1= R_3= OTMS, R_2= H, R_4= CH_3
118 R_1= R_2= OTMS, R_3= H, R_4= TMS

for oxidation beta to the nitrogen as discussed previously.

Tripelennamine was found to undergo N-oxidation and pyridine ring hydroxylation in man with N-demethylation occurring to a lesser extent.[173] A quaternary N-glucuronide of tripelennamine was also detected.[173] Thus, the metabolism of tripelennamine is highly species dependent.

Dual radiolabeled tripelennamine, with ^{14}C in the benzylic position and ^{3}H in the N-methyl groups, was found to bind covalently to proteins in vivo[185] and in vitro.[186] The carbon and tritium labels were equally incorporated into the protein, indicating that neither N-demethylation nor N-debenzylation can occur prior to binding. In rats, non-localized tissue binding led to an incorporation of approximately 25 pmol/mg protein.[173] This binding was induced by pretreatment with phenobarbital and inhibited by 3-methylcholanthrene.[186] Thus, P-450 activation of tripelennamine is thought to be required for binding. Because of the structural similarity, this point will be important in the discussion of methapyrilene's macromolecular binding.

Brompheniramine (119) and chlorpheniramine (44) are aminopropyl-2'-pyridine antihistamines. Metabolic studies on brompheniramine demonstrated high levels of N-desmethyl and N-didesmethyl derivatives in the urine of both dogs and humans.[187] In contrast to tripelennamine, brompheniramine N-oxidation and pyridine ring hydroxylation

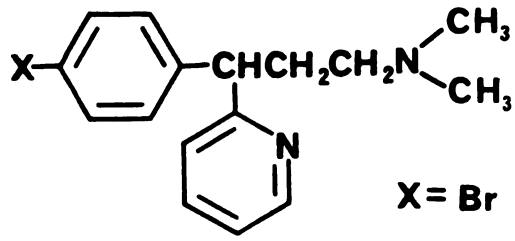

X= Br 119

X= Cl 44

were not observed in man,[187] while metabolic deamination leading to the glycine conjugate of the resulting propionic acid was detected.[187]

Chlorpheniramine (44), like brompheniramine, was excreted in the urine as desmethyl and bisdesmethyl derivatives in man, dog and rat.[188-190,55,56] Metabolic deamination of 44 in dog led to both the alcohol and carboxylic acid analogs.[56]

Orphenadrine (120) and diphenhydramine (121) are ethanolamine antihistamines. The major route of metabolism of 120 and 121 results in ether cleavage to yield the corresponding substituted diphenylmethanols 122 and 123, respectively.[191,192] N-Demethylation and bisdemethylation products have also been observed but in lesser quantities.

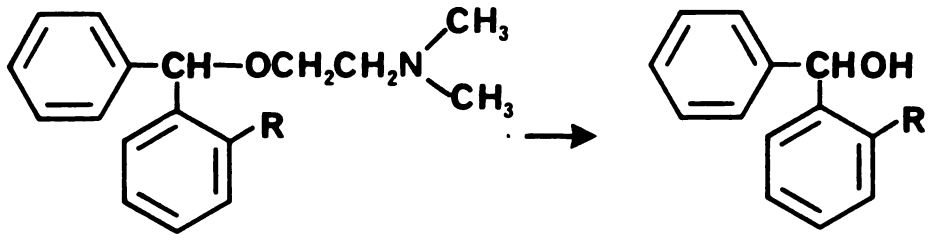

R= CH_3 120

R= H 121

122

123

The piperazine antihistamines chlorcyclizene (65) and meclizine (124) were found to have strong teratogenic effects in rats.[193] Both chlorcyclizine and meclizine are susceptible to N-dealkylation to yield norchlorcyclizine (125) in rats, while chlorcyclizine also undergoes N-oxidation in man.[96] A unique metabolite was isolated from tissue extracts of rats treated with either 65 or 124. The piperazine of norchlorcyclizine underwent further oxidation

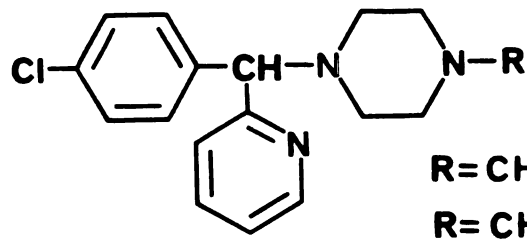

R= CH_3 65
R= CH_2Bz 124
R= H 125

to open the ring, resulting in the ethylenediamine 126.[194] Additionally, no aromatic hydroxylated metabolites were observed.

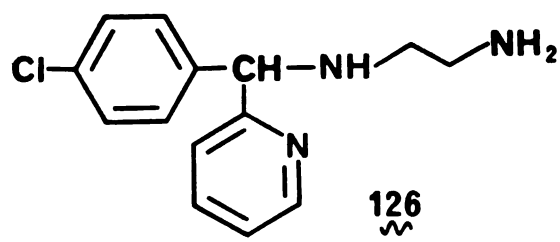

126

Previous studies on the rabbit microsomal metabolism of methapyrilene[71] led to the isolation of five organic extractable metabolites (Figure 14). N-Demethylation accounted for the majority of metabolism but N-oxidation was also detected. The remaining products (91, 129 and 130)

occurred through oxidation of the ethylenediamine protion of methapyrilene. Oxidative dealkylation to yield the secondary amine 91 presumably occur through the same mechanism as N-demethylation. Formation of amide 129 is analogous to the metabolism of nicotine to yield cotinine (38), where the intermediate carbinolamine undergoes further oxidation to the amide.

The N-formyl metabolite 130 is a more difficult structure to rationalize biochemically. The authors

Figure 14. Rabbit Microsomal Metabolites of Methapyrilene.

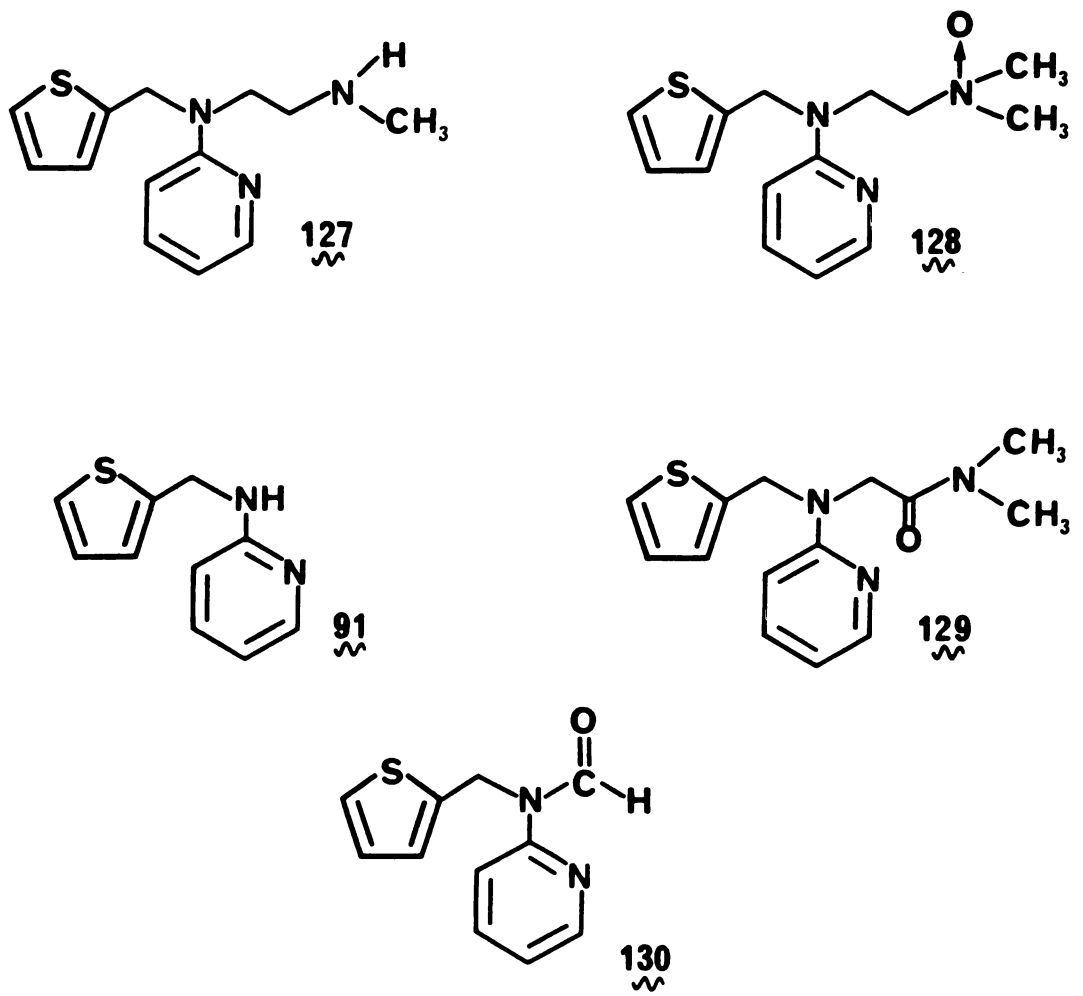

proposed[71] that further oxidation of the aldehyde 131 resulting from metabolic deamination could yield the formylamine. The synthetic aldehyde was found to yield 130 upon treatment with mild aqueous base in the presence of dioxygen.[71] The formation of 130 may, therefore, have resulted from either oxidative metabolism or from the conditions of incubate analysis.

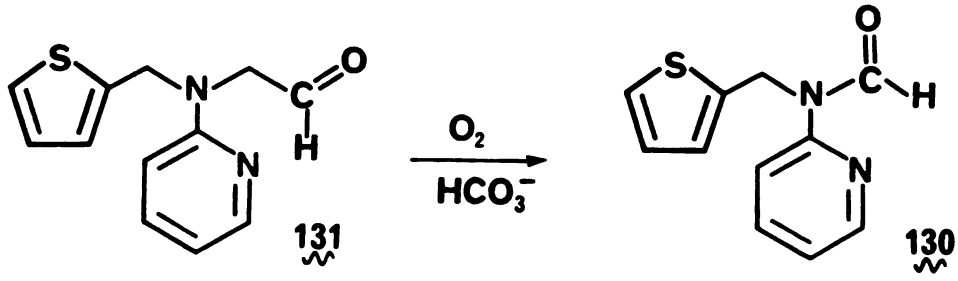

From these results we expect methapyrilene to undergo N-demethylation and N-oxidation with rat liver microsomes. Additionally, we might expect to observe pyridine ring hydroxylation. Most of the above studies were conducted on urinary metabolites, but we decided to investigate rat liver microsomal metabolism since the original carcinogenesis studies yielded liver tumors in rats.

Methapyrilene metabolites may be categorized as to their solubility in organic or aqueous solvent. Due to the fairly polar character of methapyrilene, the finding of some metabolites in both the organic and aqueous fractions was not unexpected. As discussed in Section IV, the microsomal incubates were extracted with an equal volume of CH_2Cl_2 to yield an aqueous phase devoid of methapyrilene but containing 20-25% of the metabolized drug.

The organic phase, in turn, holds approximately 10-15% of the transformed methapyrilene. In the following pages the analytical and synthetic analysis of the organic and aqueous soluble methapyrilene metabolites will be discussed with special emphasis on the possible function of electrophilic intermediates.

Although a gas chromatographic assay had been useful in the quantitation of methapyrilene metabolism, the polar and perhaps thermally labile nature of the expected metabolites deemed this method inappropriate for studying the metabolites of methapyrilene. An assay utilizing high pressure liquid chromatography was developed to aid in the isolation and quantitation of organic and aqueous soluble metabolites. An ion-pairing reverse phase chromatography system was pursued since the majority of metabolites should contain a minimum of two nitrogens.[195] Aqueous acetonitrile (20%) buffered to pH 2.5 with 0.08 M potassium perchlorate[196] gave good separation and peak shape on a RP-18 (Altex) column. As shown in Figure 15, separation of the organic phase from biological extracts, monitored at 254 nm, gave four smaller peaks in addition to the large methapyrilene peak. The corresponding radioactivity trace for the samples demonstrated that a poorly absorbing compound was eluting very early in the chromatography.

The chromatogram of the aqueous soluble metabolites, as shown in Figure 16, illustrates the complexity of the mixture. The radioactivity trace, however, simplifies the

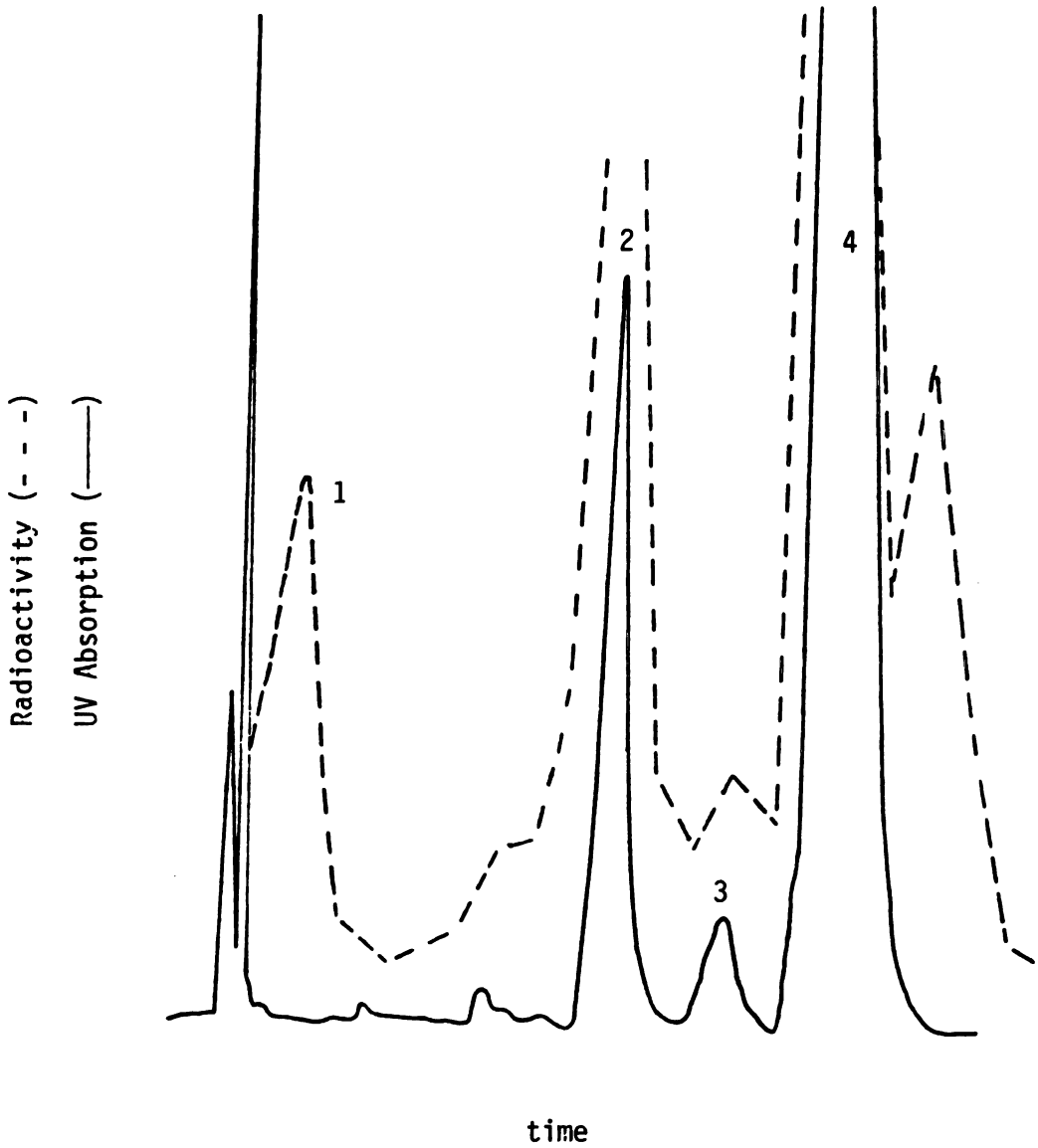

Figure 15. HPLC of Organic Soluble Metabolites

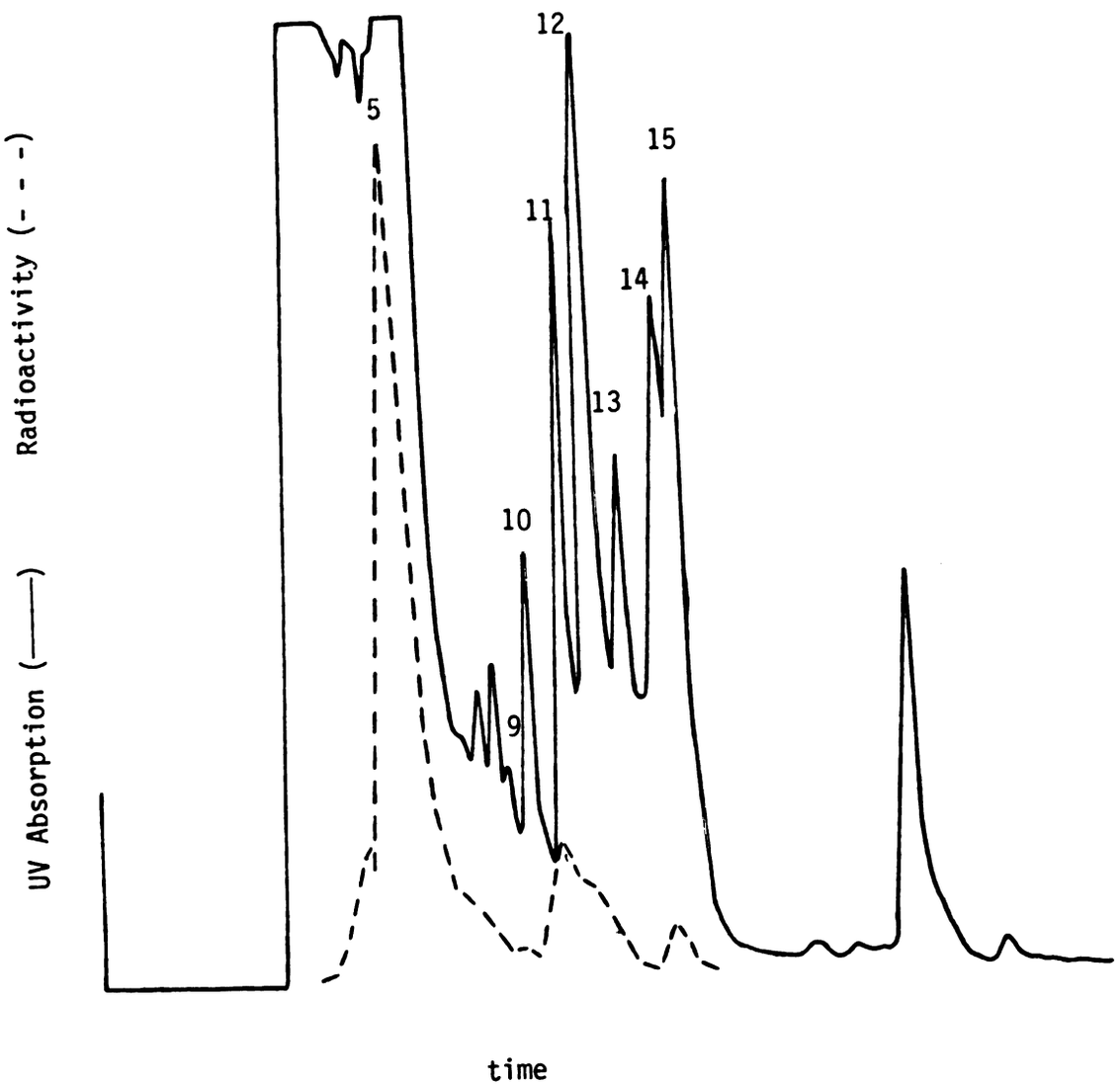

Figure 16. HPLC of Water Soluble Metabolites

situation by determining the 5-hydroxypyridine or non-pyridine containing peaks. To account for hydroxylated pyridine metabolites, all of the peaks were analyzed by mass spectrometry. The assignment of structures to the above peaks will be given in the following sections.

Mass spectral analysis of the metabolites was also a very useful technique. With the organic soluble metabolites, gas chromatography electron ionization mass spectrometry (GC-EIMS) was helpful in both separating and analyzing the spectra of the metabolites present. Analysis of the aqueous soluble metabolites, however, was a different problem. Numerous derivatization techniques with trimethylsilyl-, trifluoroacetyl-, and pentafluoropropionyl derivatizing agents were attempted on the mixture of aqueous metabolites with no obvious success. The chromatograms and the spectra therein were very complex. In the end, success was obtained by direct probe EIMS analysis of aqueous soluble samples collected from preparative scale HPLC. In a few cases, enough sample was obtained to allow for proton magnetic resonance analysis.

A specifically deuterated methapyrilene was needed where the deuterium could act as a mass spectral marker for those peaks arising from methapyrilene. Although deuterium could have been incorporated into the pyridine ring as was tritium, we decided on the benzylic hydrogen. The location of deuterium in this position, although enzymatically more labile, would lead to structural information separate and

unique compared to the tritiated methapyrilene studies. For instance, pyridine hydroxylated metabolites could be easily recognized from an incubate containing a 50:50 mixture of benzylic deutero to proteo methapyrilene.

As shown in Scheme 10, the synthesis of deuterated methapyrilene was similar to that designed for radiolabeled methapyrilene. Thiophene-2-carboxaldehyde (132) was condensed with 2-aminopyridine with the concomitant removal of water via a Dien Stark trap.[197] The resulting Schiff base 133, without further purification, was subsequently reduced with lithium aluminum deuteride to yield the desired deuterated 2-thienymethylaminopyridine (134). The NMR spectrum of 134 (see Figure 17 and 18) before and after exchange with D_2O was that of the proteo analog except that the benzylic hydrogens integrated for only 1.1-1.3 protons. The secondary amine was then treated with one equivalent of NaH and alkylated with 1-chloro-2-dimethylaminoethane, to produce deuterated methapyrilene 135. After chromatography, the deuterated methapyrilene was converted to the dihydrochloride salt with a yield of 12% The NMR spectrum (Figure 19) and EIMS (Figure 20) confirm the structure as the deuterated methapyrilene. The EIMS parent ion at mass 262 with no significant ion at 261 indicates that deuterium has been incorporated in nearly 100% yield. The position of the deuterium is clearly benzylic as indicated by the benzylic fragment at m/e 98 (C_4H_3S-CHD).

Figure 17. ^{1}H-NMR Spectrum of 134.

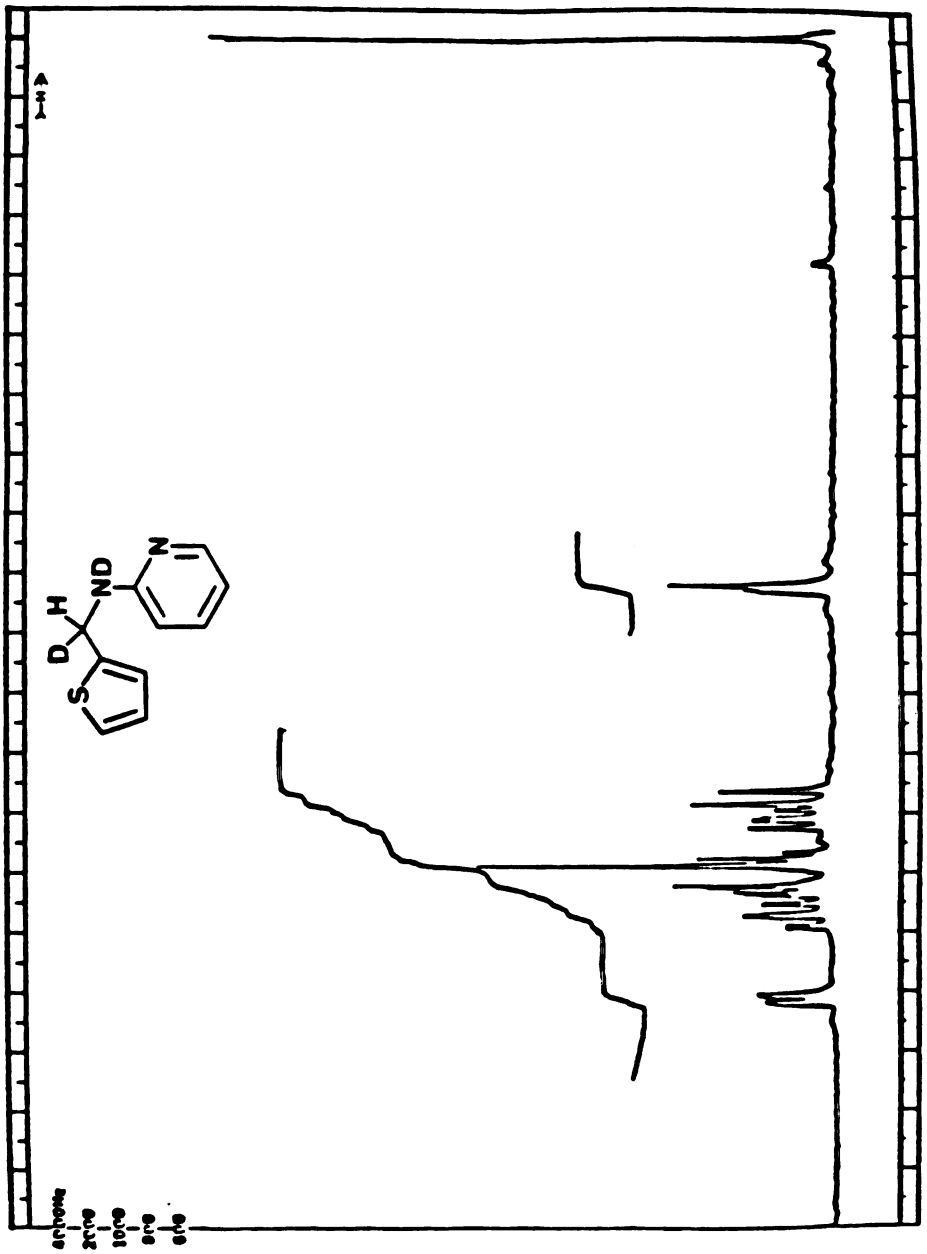

Figure 18. ^{1}H-NMR Spectrum of 134 plus D_2O.

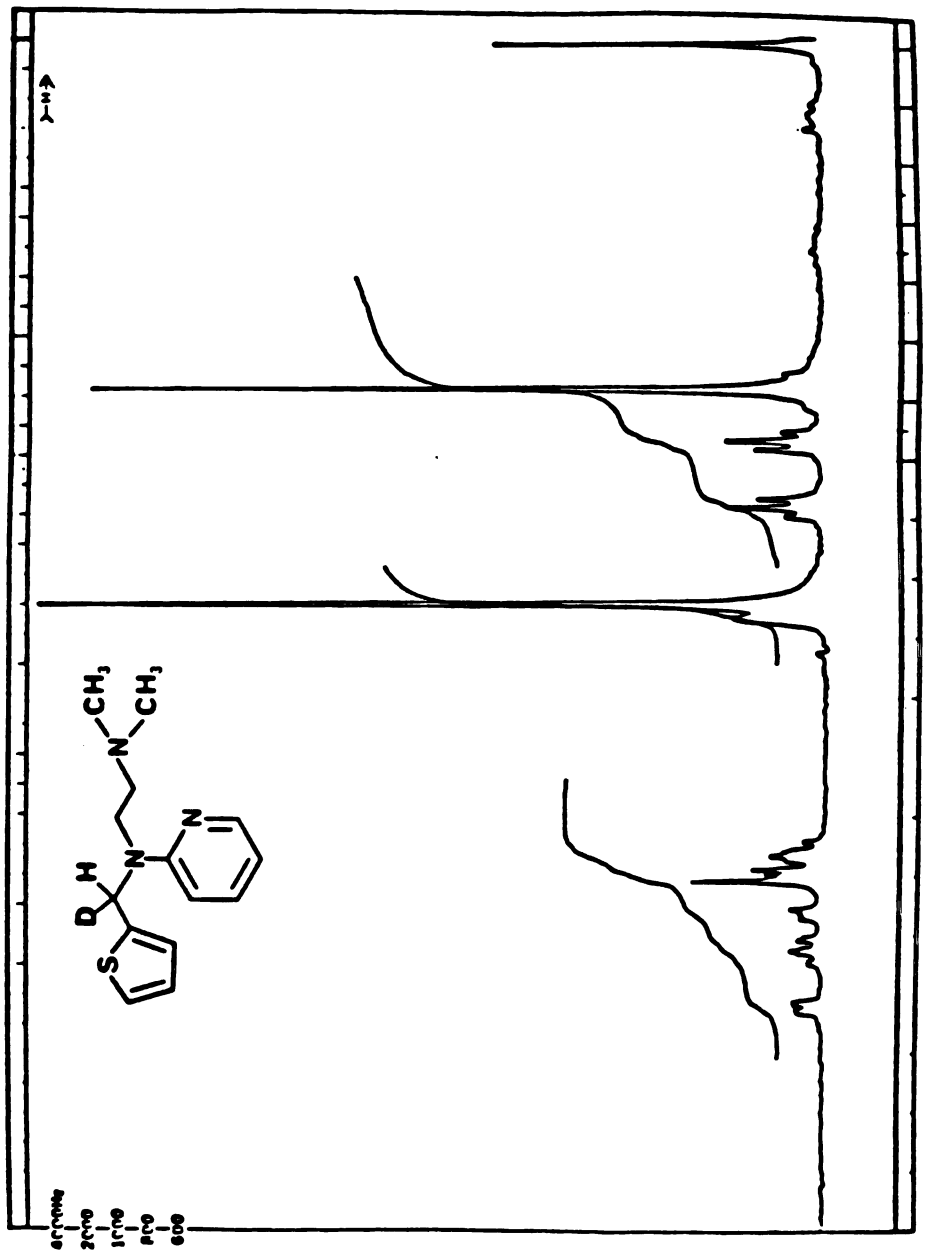

Figure 19. ^{1}H-NMR Spectrum of 135.

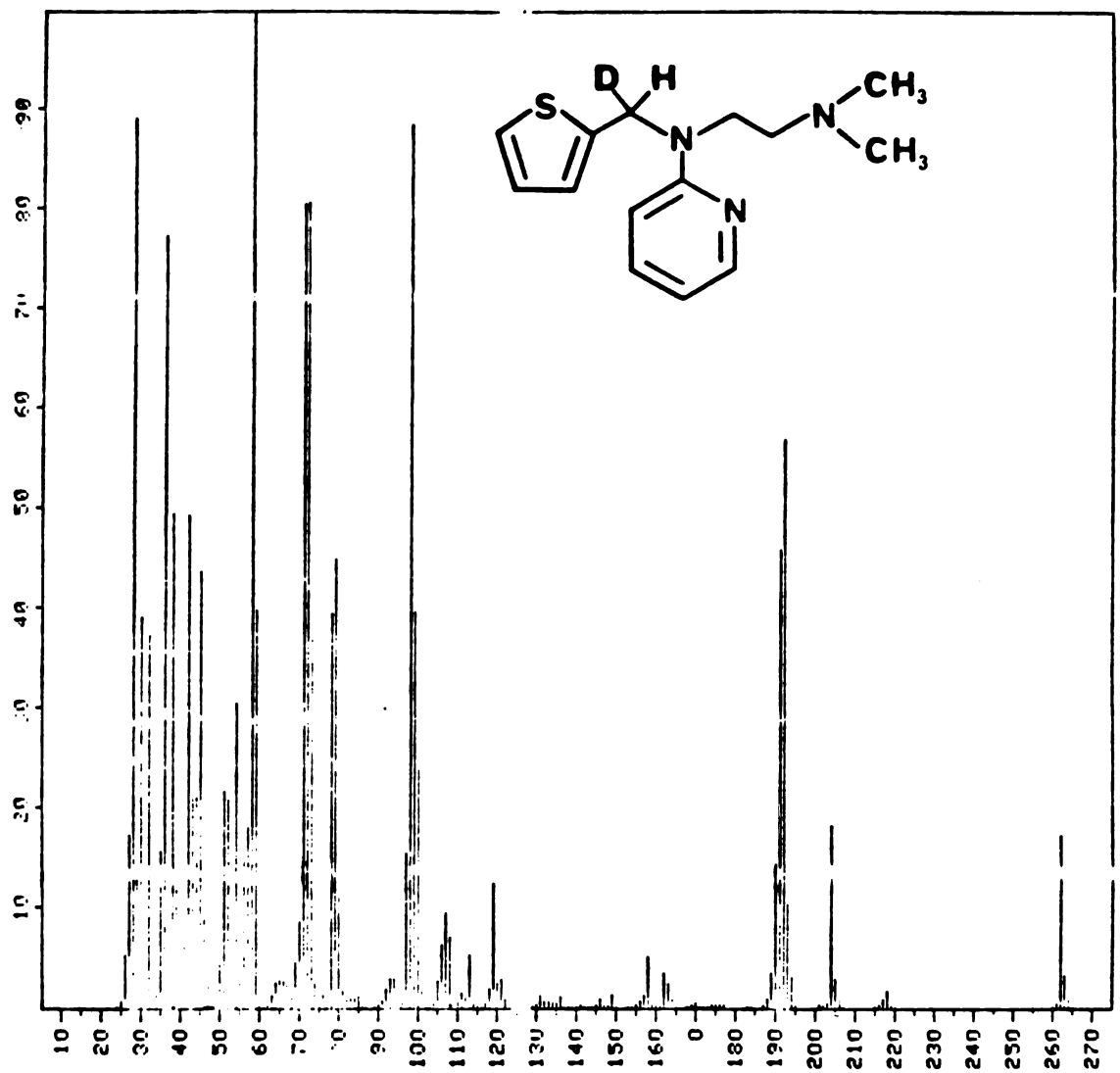

Figure 20. EIMS of 135.

Scheme 10. Synthesis of Deuteromethapyrilene.

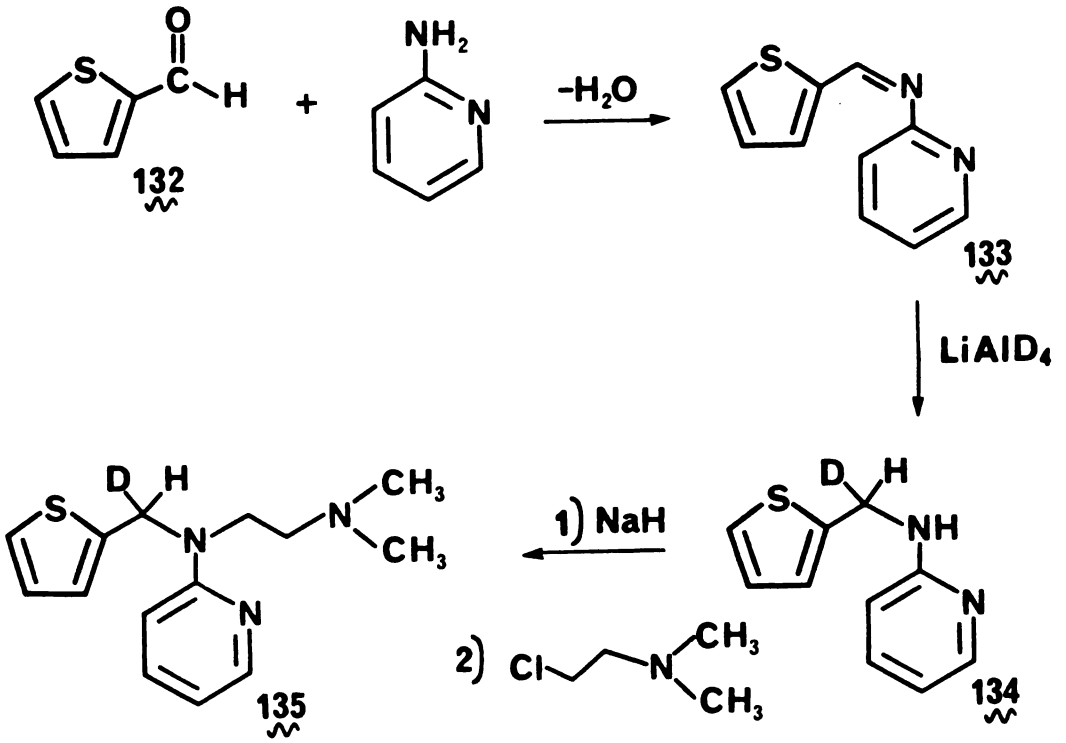

An alternate synthetic approach to deuterated methapyrilene was unsuccessful. In this case, methapyrilene was treated with n-butyllithium and TMEDA as shown in Scheme 11 under anhydrous conditions to form the aromatic litium salt of the thiophene ring.[198] The anion was then quenched with D_2O but under no reaction conditions was the deuterated methapyrilene (136) recovered.

Scheme 11. Alternate Approach to Deuteromethapyrilene.

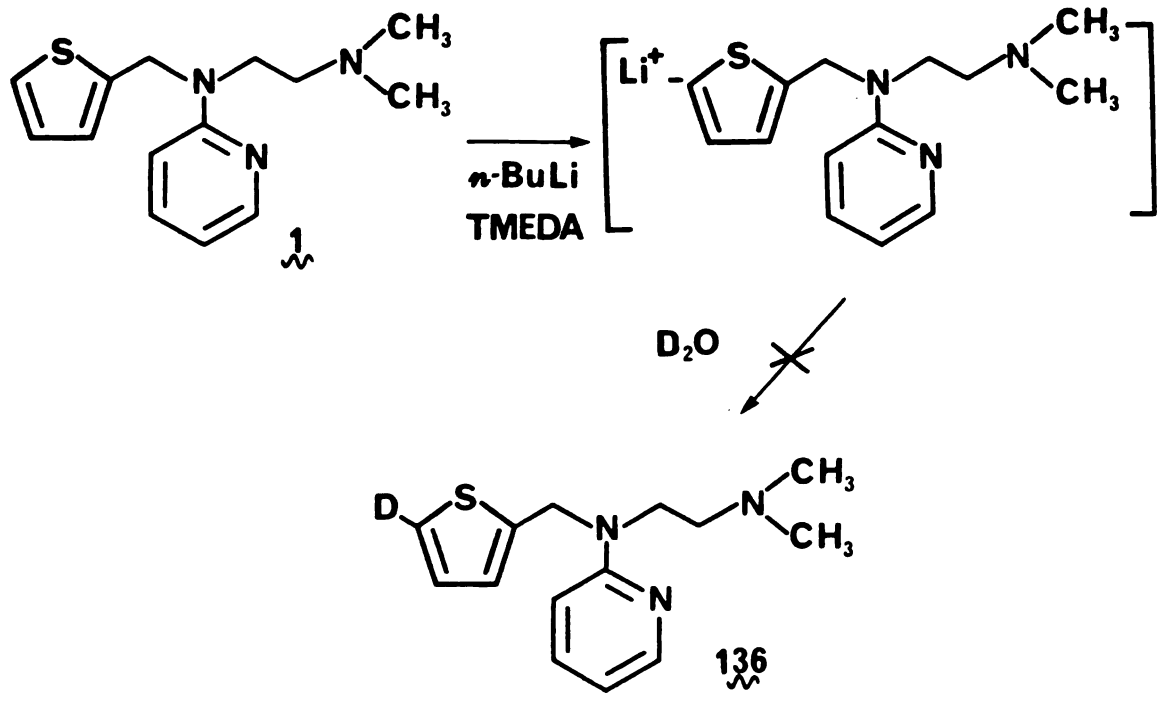

A. Organic Soluble Metabolites.

Mass spectral analysis of the organic soluble metabolite mixture was conducted on both low resolution and high resolution instruments and reproduced utilizing a 50:50 mixture of proteo:deutero methapyrilene. The metabolites will be discussed in the order of their elution from GC-EIMS with their chemical synthesis and HPLC characteristics. A representative GC-EIMS total ion curve is shown in Figure 21, where methapyrilene has been overloaded to enable the detection of the metabolites.

1). N-(N',N'-Dimethylaminoethyl)-2-aminopyridine (92).

The formation of N-(N',N'-dimethylaminoethyl) -2-aminopyridine (92) was previously undetected in the metabolic oxidation of methapyrilene. The potential metabolic pathway leading to this secondary amine is shown Scheme 12. Metabolic Formation of 92.

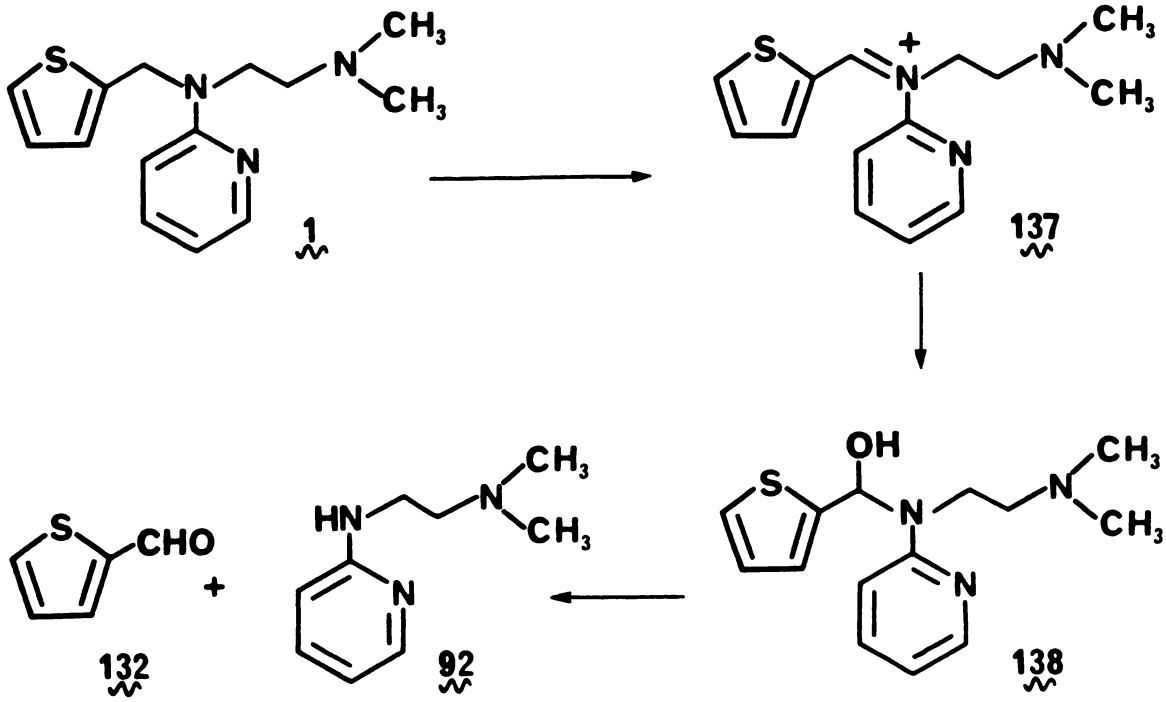

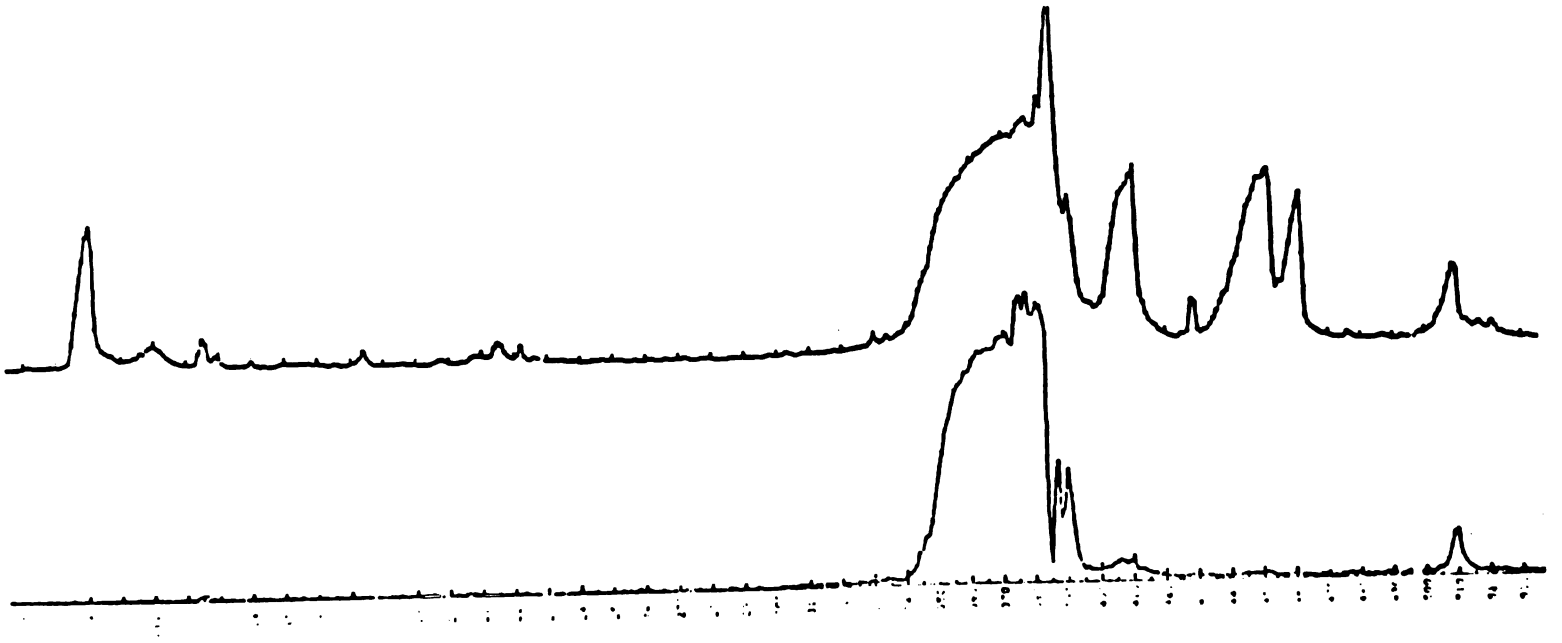

Figure 21. GC-EIMS Total Ion Current for Organic Soluble Metabolites

in Scheme 12.

Oxidation of methapyrilene to the benzylic iminium ion 137 followed by hydration could lead to the unstable carbinolamine 138. Dissociation of this carbinolamine would then yield the desired secondary amine 92 and thiophene-2-carboxaldehyde (133).

Scan 90 in Figure 21 shows a parent ion at m/e 165 (Figure 22) and does not contain the benzylic fragment ion at m/e 97. The mass spectral fragmentation pattern can be explained as follows. The pyridine ring leads to m/e 78 and the m/e 95 ion results from 2-aminopyridine. The m/e 107 and 58 ions are a result of α-cleavage as shown.

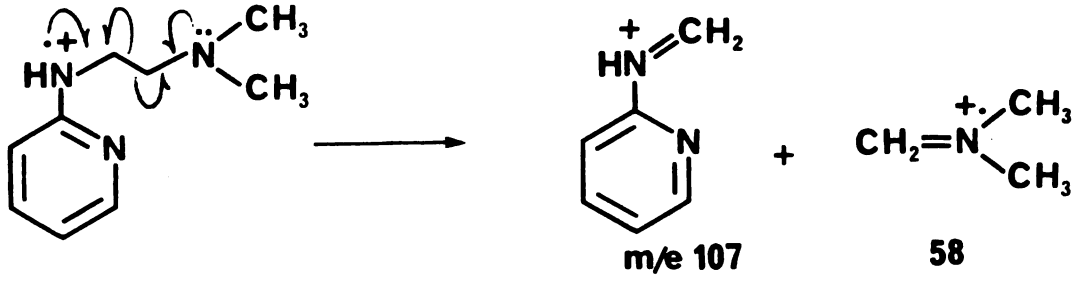

The ion at m/e 122 can be explained by the rearrangement depicted below.

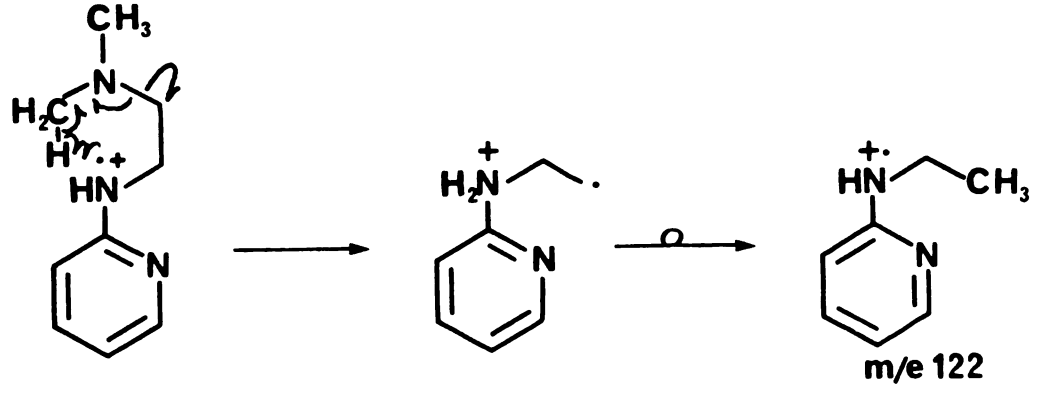

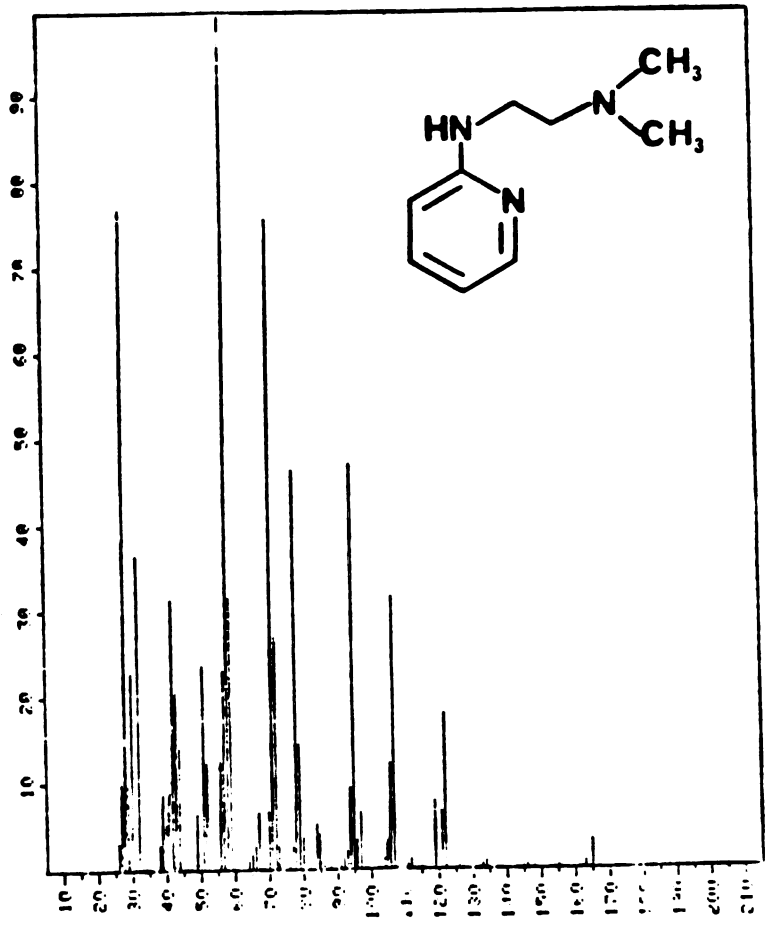

Figure 22. EIMS of 92.

Synthetic 92 has been prepared by the sodium hydride method described in Section V B. The high resolution mass spectrum resulted in nearly the identical mass spectrum as the biological amine with the differences due primarily to differences in instrumental conditions.

The retention time of 92 coincided with that of peak 1 in the HPLC chromatogram (Figure 15). The lack of ultraviolet absorption from the biological sample is a reflection of the relatively low absorptivity of the pyridine ring in addition to the small quantities present.

A strikingly similar mass spectrum was observed in scan 110 of Figure 21. As shown in Figure 23, the parent ion at mass 163 is very weak and the major fragmentation results in ions 122, 106 and 78. These ions are similar to that of 92 but the ions representing the dimethylaminoethyl fragment (m/e 71 and 58) are missing. Additionally, the strong peak at m/e 95 for the 2-aminopyridine ring of 92 is not present. For this reason, we believed that an analog structurally similar but two mass units less than 92 was present.

A similar spectrum was obtained from rabbit microsomal metabolism (Figure 24). Although 92 was not detected from rabbit microsomal metabolism, this mass spectrum clearly illustrates similar fragmentation but with much stronger ionization. The strongest ion at masses 163, 134, 118, 197, 93, 78 and 57 represent a cross-section of ions present in 92 and the unknown of scan 110. The presence of the ions at mass 177, 14 mass units above the strong 163 ion, may

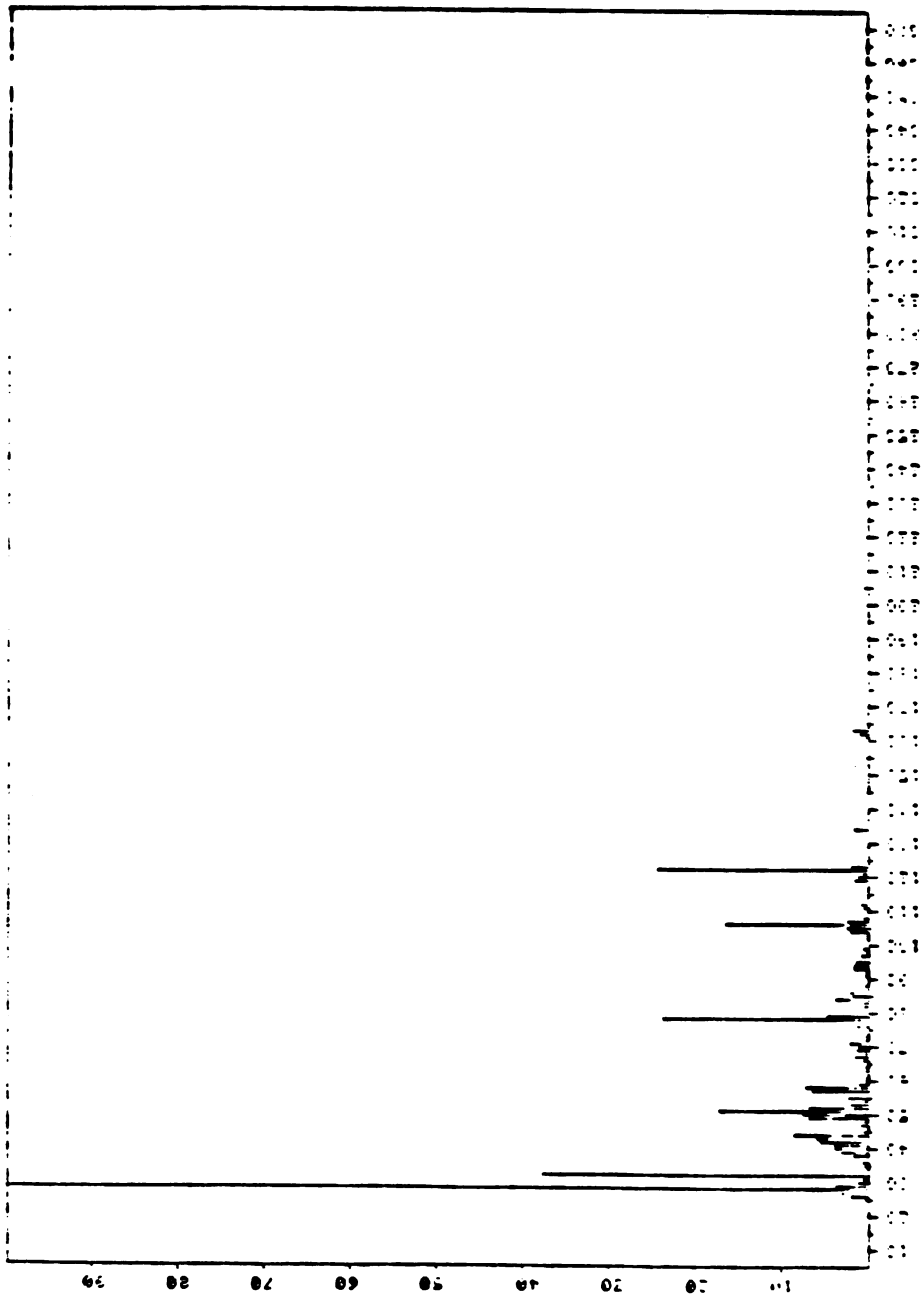

Figure 23. EIMS of Scan 110.

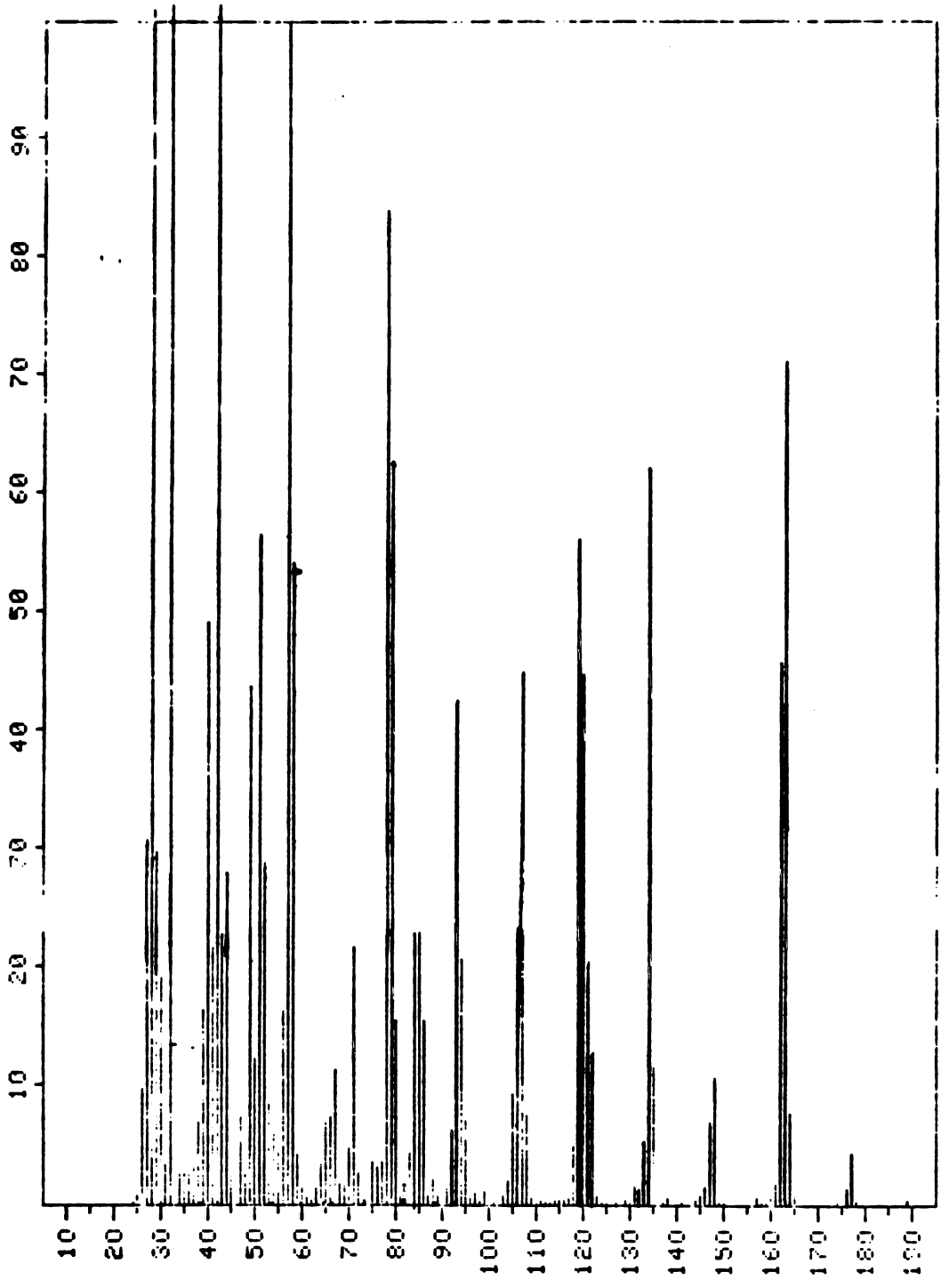

Figure 24. EIMS of Rabbit Unknown Metabolite

represent either a weak parent ion or an anomolous ion. Additionally, the spectrum occurred much later in the gas chromatogram than the unknown of scan 110, indicating a higher boiling point. Although both the rat unknown and this rabbit metabolite(s) represented extremely small quantities, we decided to explore the potential of these representing new metabolites of methapyrilene.

First, let us consider the spectrum for scan 110. The prominence of the ion at mass 78 denotes the presence of a pyridine ion but the usually present m/e 95 ion for the 2-aminopyridine moiety is missing. A cyclic structure 139 has been suggested to account for this spectrum where the ion at 106 is explained through the following fragmentation. This structure would explain the ions at m/e 163, 106 and 78 and the lack of an ion at m/e 71 for the dimethylaminoethyl fragment. However, the ion at m/e 122 is very difficult to explain without rearrangement of two protons.

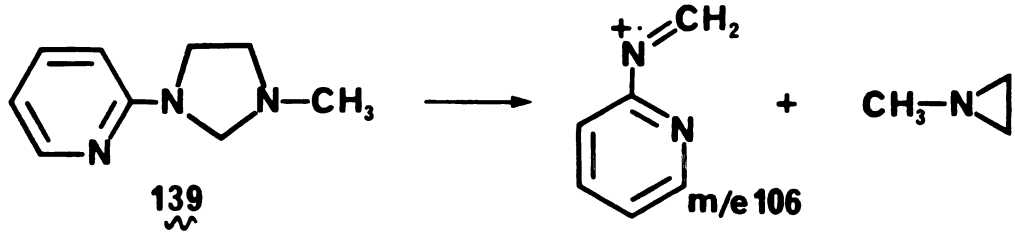

139 m/e 106

A different structure which also fits these results is the imidazolone 140 with molecular weight 163 and predicted fragment ions at 78 and 106. This structure could be produced metabolically through numerous oxidative steps as shown in Scheme 13. Unfortunately, the mass spectrum

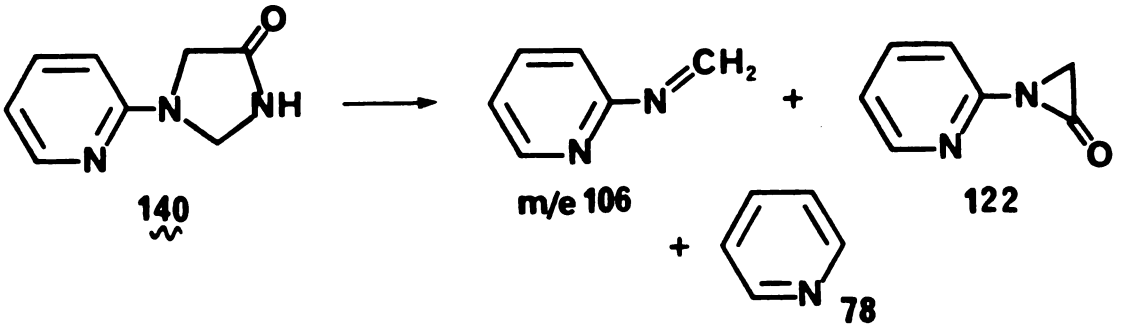

presented in Figure 23 is the only evidence that we have to support this structure, thus the relative importance of this argument is in question.

The only supporting evidence for a cyclized metabolite is that of the rabbit unknown in Figure 24. Assuming the parent ion to be mass 177, the following structures have

Scheme 13. Possible Oxidation to Form Imidazolone 140.

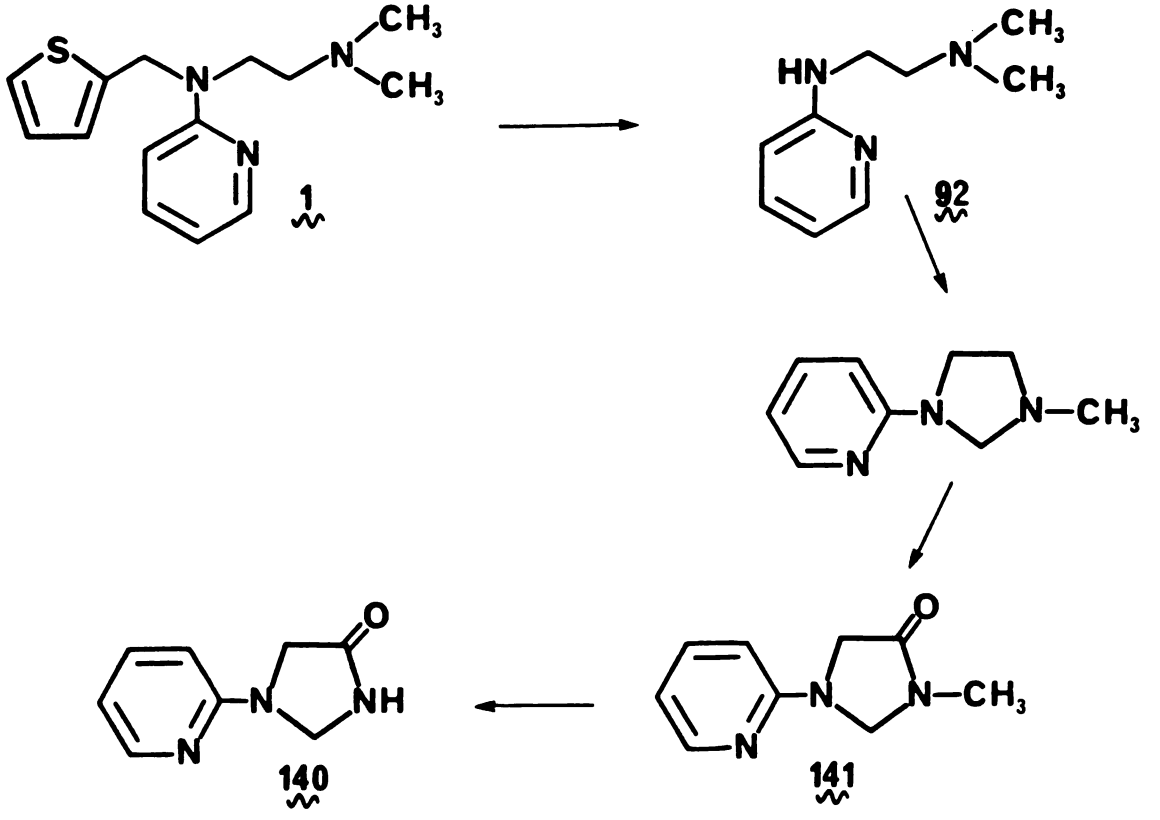

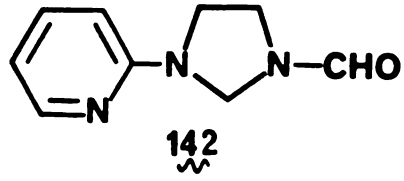

142

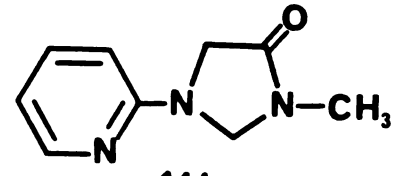

144

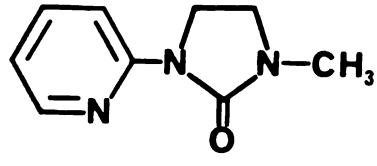

143

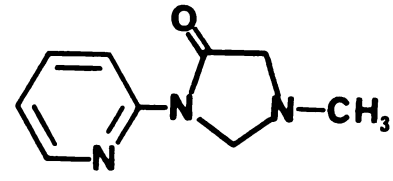

145

been proposed. Each of these structures should yield mass spectral fragments at m/e 78 for the pyridine ring and m/e 107 for the N-methylene-2-aminopyridine ion as discussed previously. The ion at mass 134 corresponds to a loss of $CH_2N\text{-}CH_3$, eliminating the N-formyl analog 142 as a possible structure. Additional information is required to distinguish between the remaining imidazolones. Although these are known ring structure, no mass spectra have been published to our knowledge. The 2-imidazolone 143 was eliminated as a possible structure through comparison with synthetic material. The N^1-methyl-N^3-pyridyl-2-imidazolone (143) was synthesized as shown in Scheme 14.[199] The 2-aminopyridine was condensed with α-chloroethylisocyanate and subsequently cyclized in the presence of base to give 146.[199] The unsubstituted nitrogen of the urea was

Scheme 14. Synthetic Approach to 143.

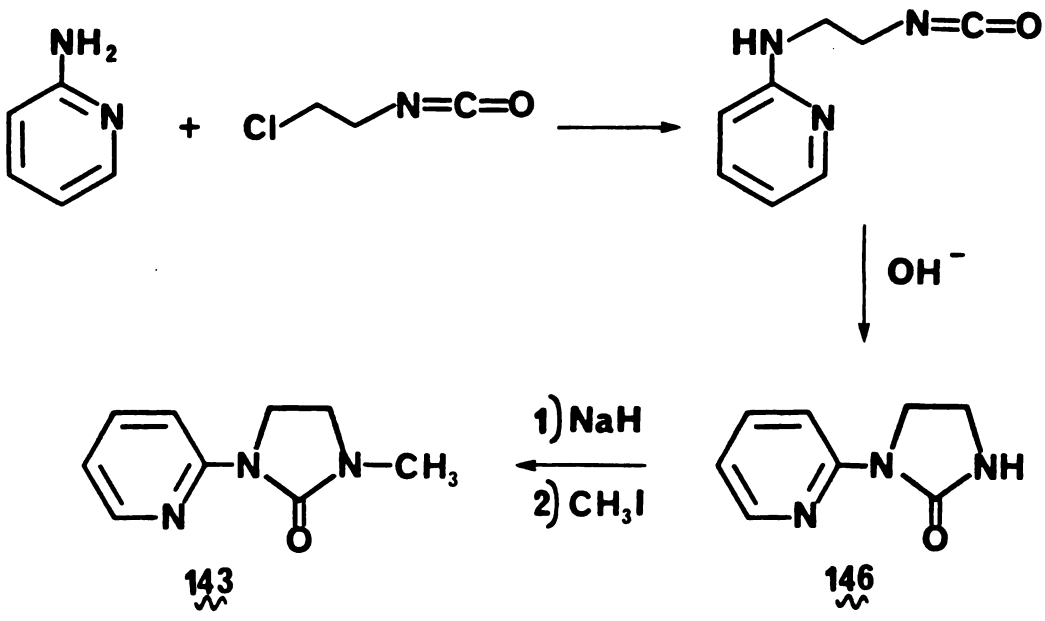

converted to its more nucleophilic anion and methylated with methyl iodide. The mass spectrum of this sample in no way resembled that of the rabbit unknown. This left the remaining two imidazolones 144 and 145 as possible structures. Unfortunately, efforts to synthesize these analogs were unsuccessful. The actual structure of the rabbit unknown thus remains unresolved. The importance of these two unknowns rests in their possible cyclized structures. This type of cyclized metabolites is of extreme importance as a measure of the iminium ions formed during metabolic activation of methapyrilene. Future studies might include the use of specifically deuterated drug to investigate the origin of these substances.

2). N-(2'-Thienylmethyl)-2-aminopyridine (91).

N-(2'-Thienylmethyl)-2-aminopyridine could be generated metabolically through the hydrolysis and dissociation of the iminium ion 147 shown in Scheme 15. The formation of 91 was observed from Pb-induced rabbit microsomal incubations.[71]

Scheme 15. Metabolic Formation of 91.

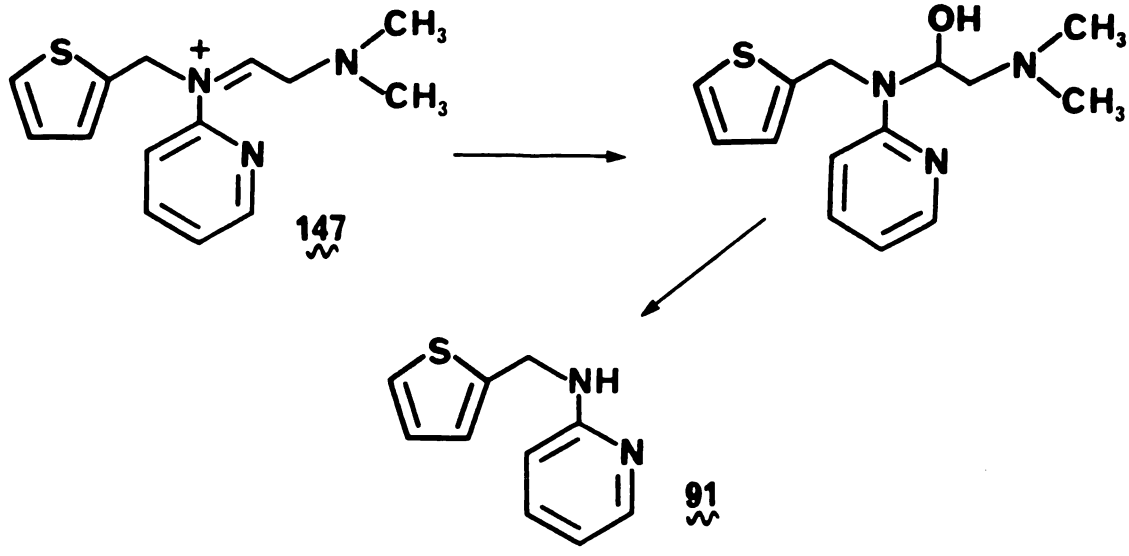

Scan 215 in Figure 21 is easily recognizable as the secondary amine. In the mass spectrum shown in Figure 25, the ion at m/e 190 represents the parent amine. The benzylic fragment was observed at m/e 97. In the deuteromethapyrilene metabolic sample, the spectrum shown in Figure 26 was obtained. The parent ion at m/e 190 is equally matched by the ion at m/e 191 as is the benzylic ion m/e 97 matched with m/e 98. In all other fragmentations, these spectra are identical with that obtained for the synthetic secondary amine.

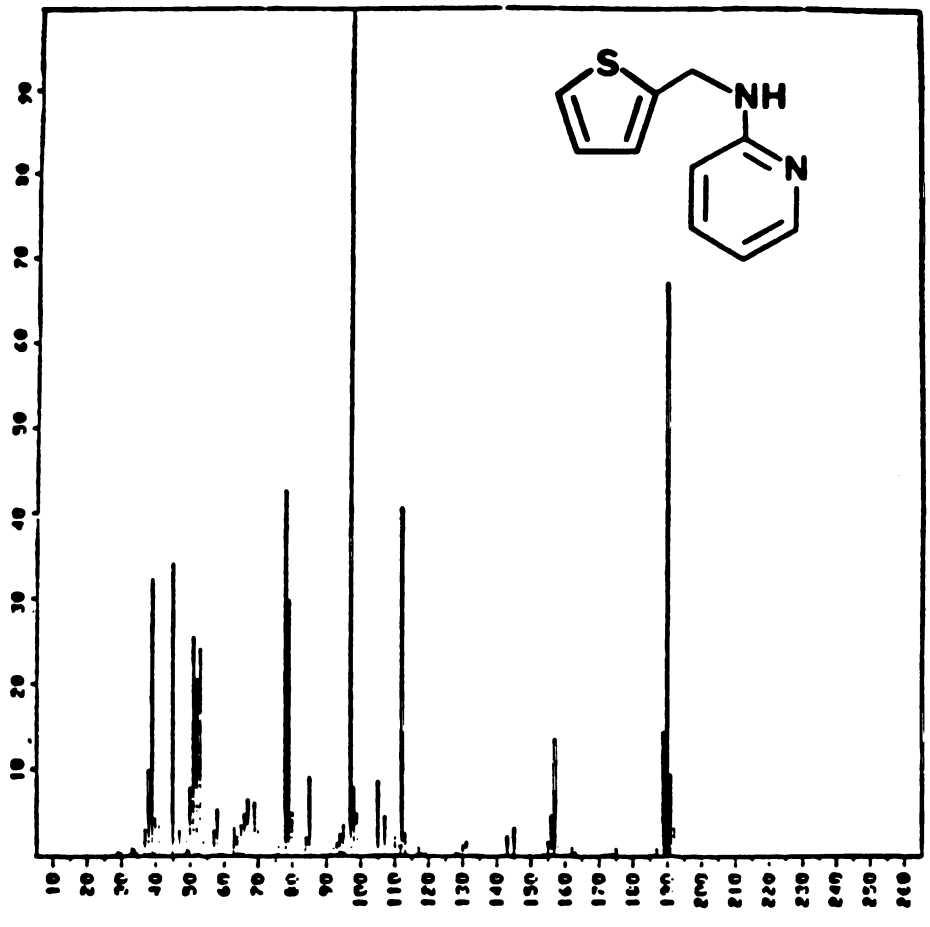

Figure 25. EIMS of 91.

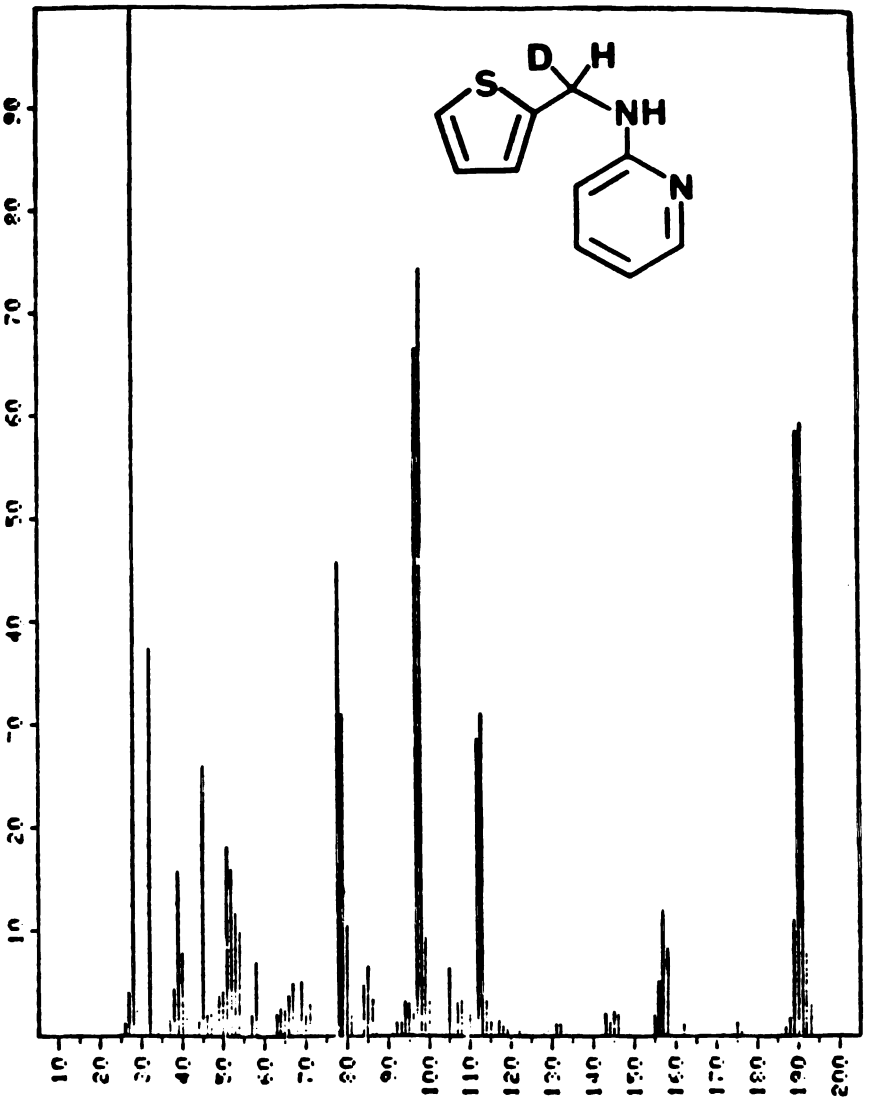

Figure 26.. EIMS of Deutero- 91.

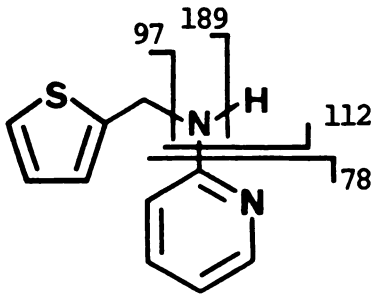

The chemical synthesis of N-(2'-thienyl-methyl)-2-aminopyridine was that given in the synthesis of deuteromethapyrilene (Section VI) except that the reduction of the imine was carried out with formic acid.[197] The EIMS is the same as that obtained from the metabolic 91. The synthetic amine had the same retention time as peak 3 in the HPLC chromatogram (Figure 15).

3). Methapyrilene (1).

The major peak on the total ion current was methapyrilene. The mass spectrum from scan 375 of Figure 21 corresponds to that of commercially available methapyrilene (Figure 27). The corresponding deuteromethapyrilene was similarly recorded (Figure 28). The mass spectral fragmentation has been summarized in the following structure. The largest peak eluting from the HPLC had the same retention time as methapyrilene (Figure 15).

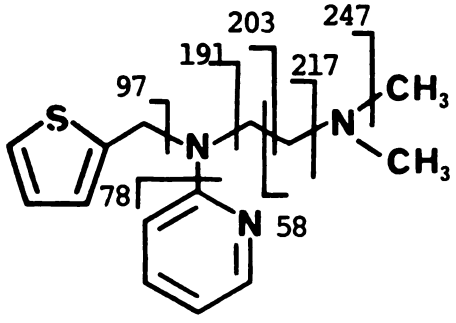

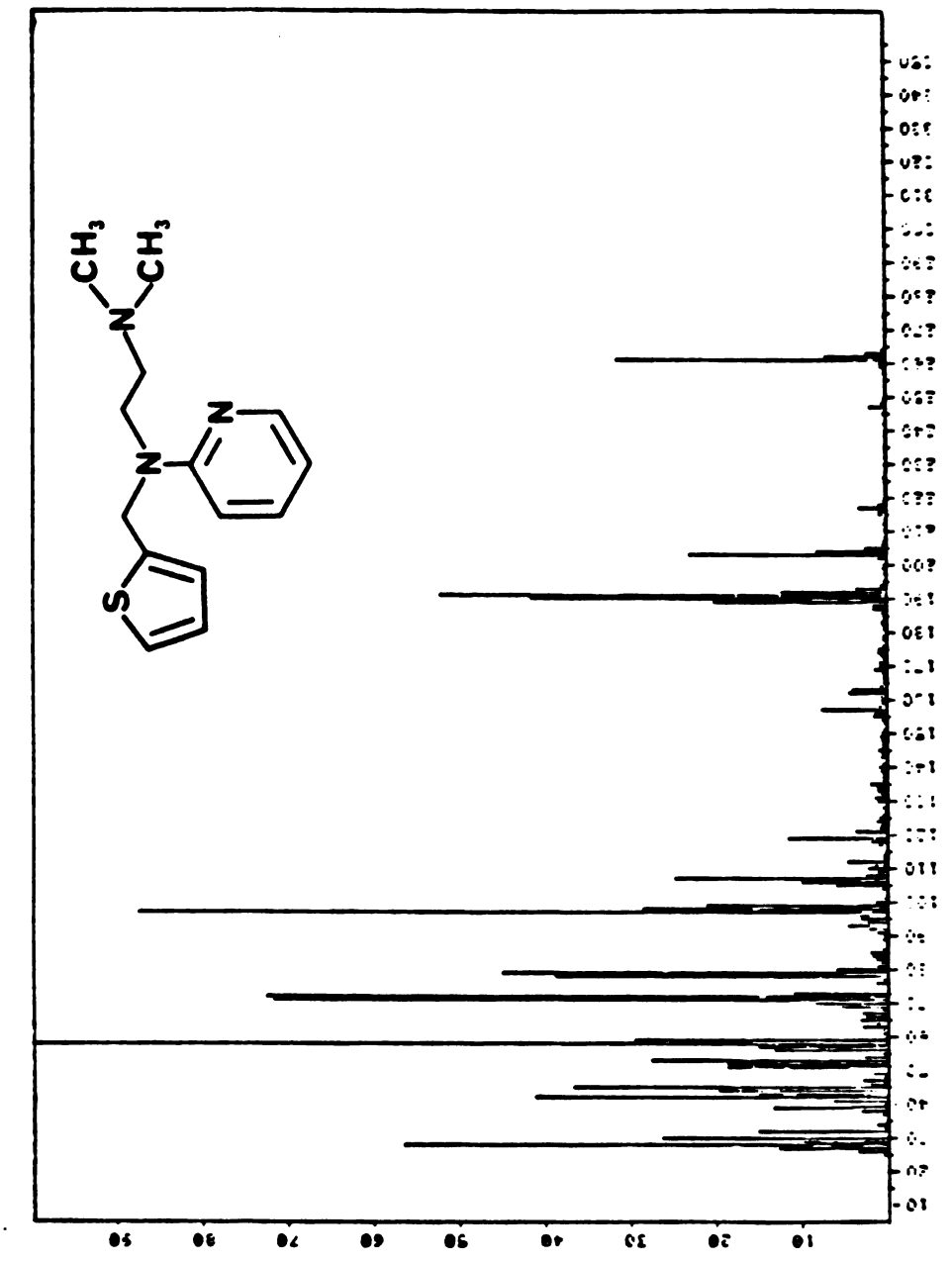

Figure 27. EIMS of 1.

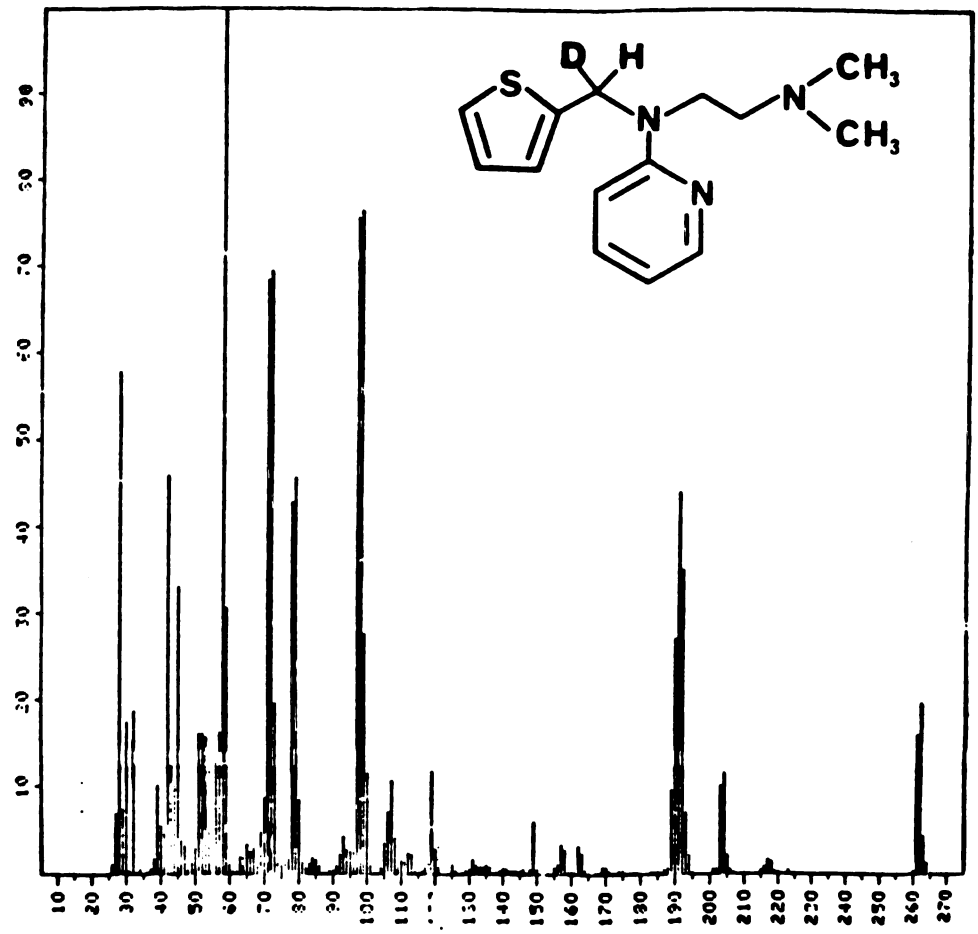

Figure 28. EIMS of Deutero- 1.

4). N-Desmethylmethapyrilene (127).

N-Demethylation of methapyrilene was found to be a major metabolic pathway in Pb-induced rabbits (Scheme 16).[71] The terminal iminium ion 148 was, in fact, trapped in metabolic incubates with inorganic cyanide.

Scheme 16. Metabolic Formation of 127.

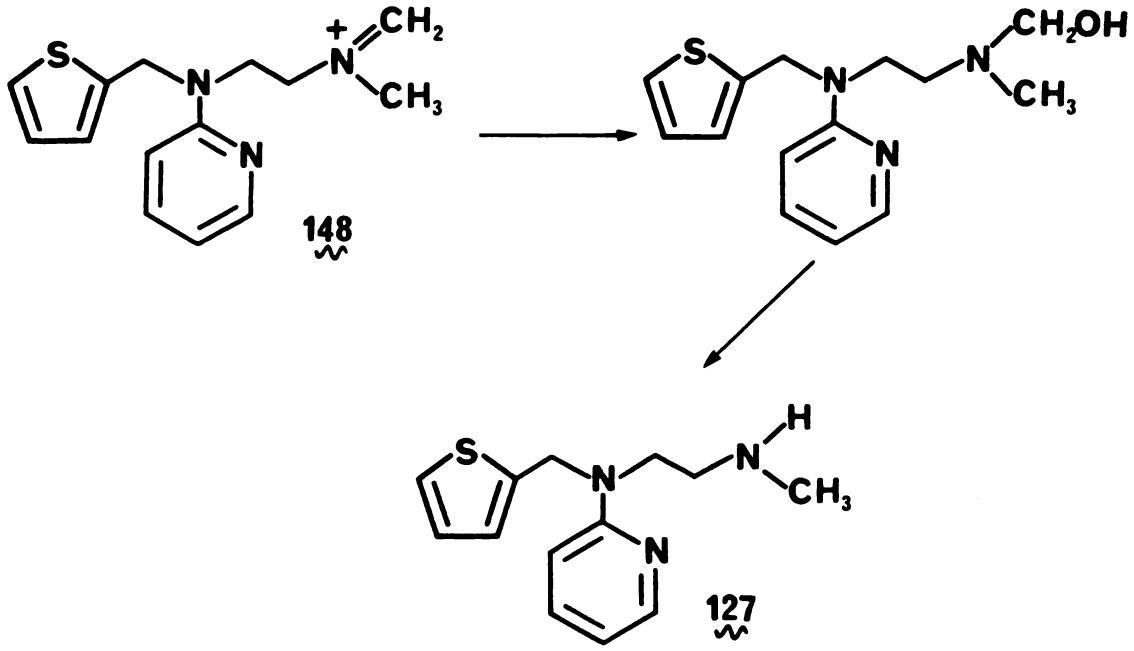

Scan 409 (Figure 29) and the corresponding spectrum from the deuteromethapyrilene incubates (Figure 30) show parent ions at m/e 247 and 247,248, respectively. The fragmentation can be explained as follows. The loss of the alkylamino side chain results in the ion at m/e 191 instead of the expected ion at m/e 189. This result is most likely due to hydrogen rearrangement from the terminal nitrogen and is present in both the metabolic and synthetic normethapyrilene spectra.

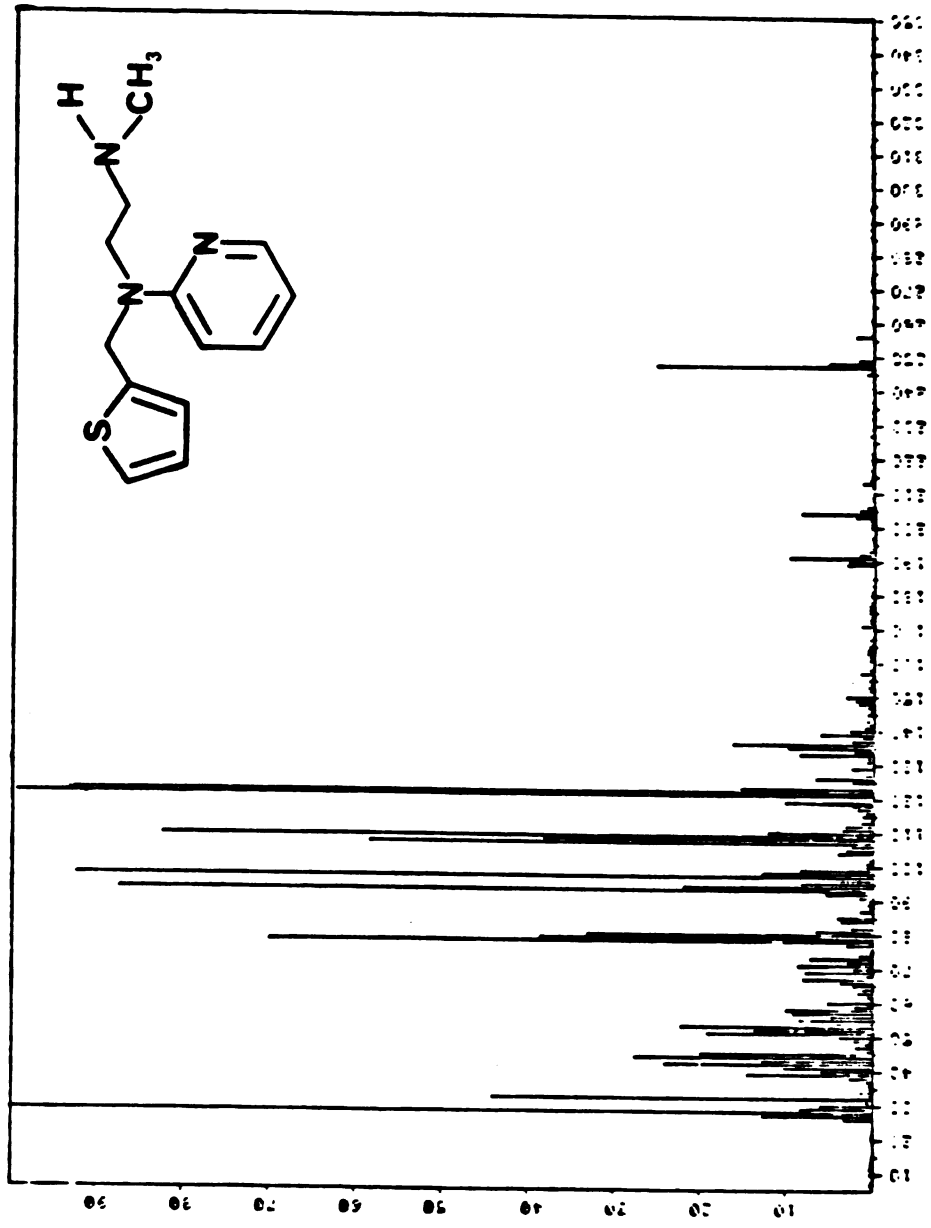

Figure 29. EIMS of 127.

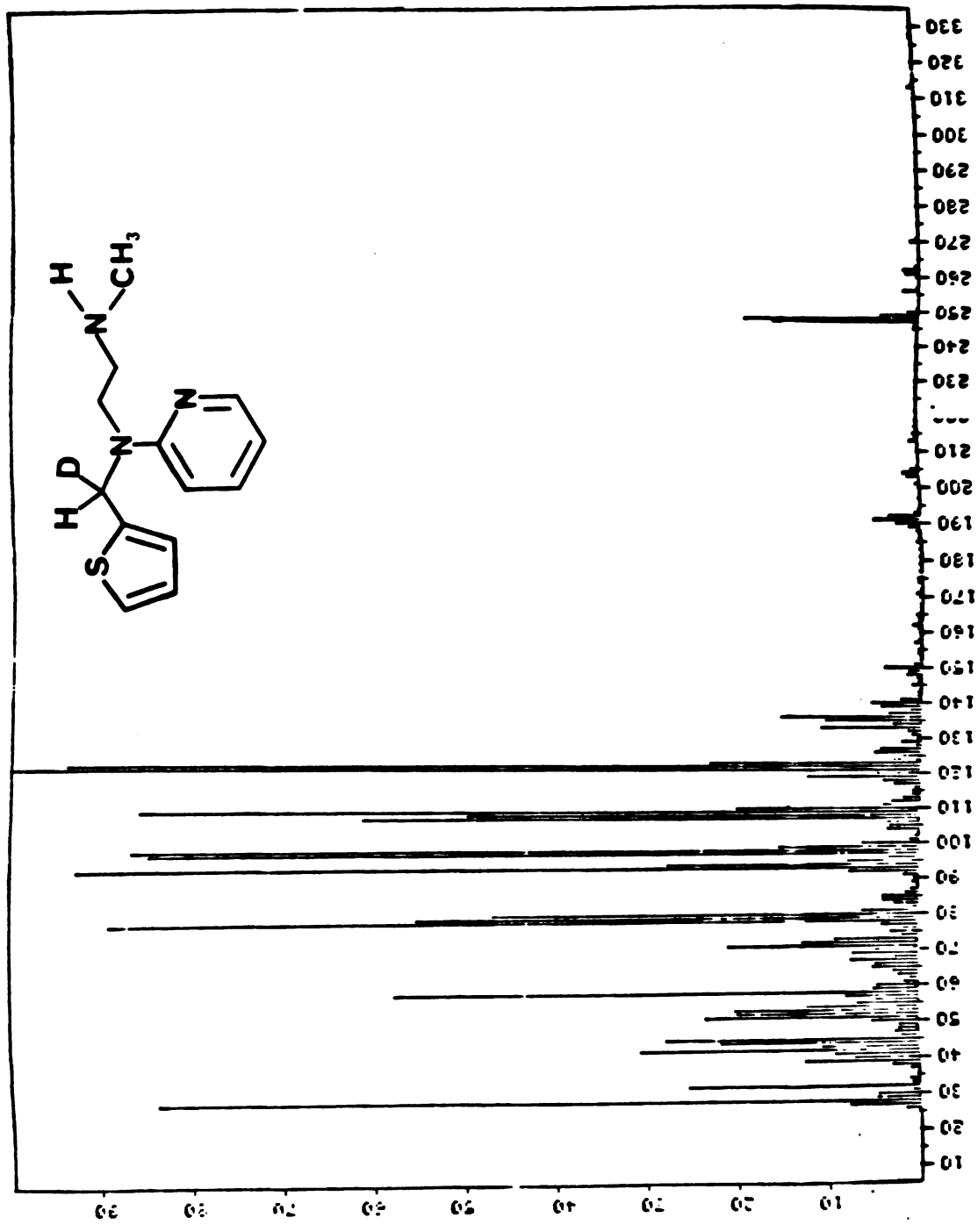

Figure 30. EIMS of Deutero- 127.

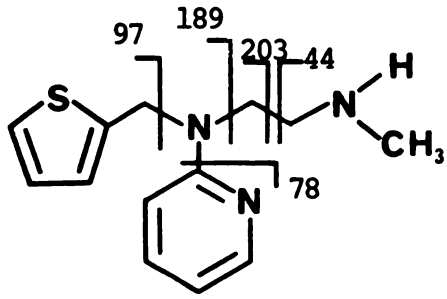

N-Desmethylmethapyrilene had been previously synthesized by R. Ziegler but the product was reported to be unstable under workup and purification conditions.[71] Therefore, slightly different conditions were utilized in the synthesis of 127 as shown in Scheme 17. N-Desmethylmethapyrilene was successfully synthesized in low but sufficient yield for product determination and HR-EIMS. The first step led to the diethylacetal 149 which when deprotected, yielded the cyclized carbinolamine 150. This was then neutralized with anhydrous potassium hydroxide to the aldehyde 131 and condensed with methylamine gas. Without isolation, the intermediate imine was reduced with sodium cyanoborohydride and the product isolated by chromatography. The reaction mixture, when acidified, extracted and then basified to extract the amine product, led to a very small quantity of oil. The material isolated in the acidic fraction was obtained in much higher quantity. Most likely, the condensation between methylamine and the aldehyde was not occurring to any appreciable extent, leaving the aldehyde to be reduced to the alcohol by sodium cyanoborohydride. The amine was chromatographed to give a

Scheme 17. Synthesis of N-Desmethylmethapyrilene.

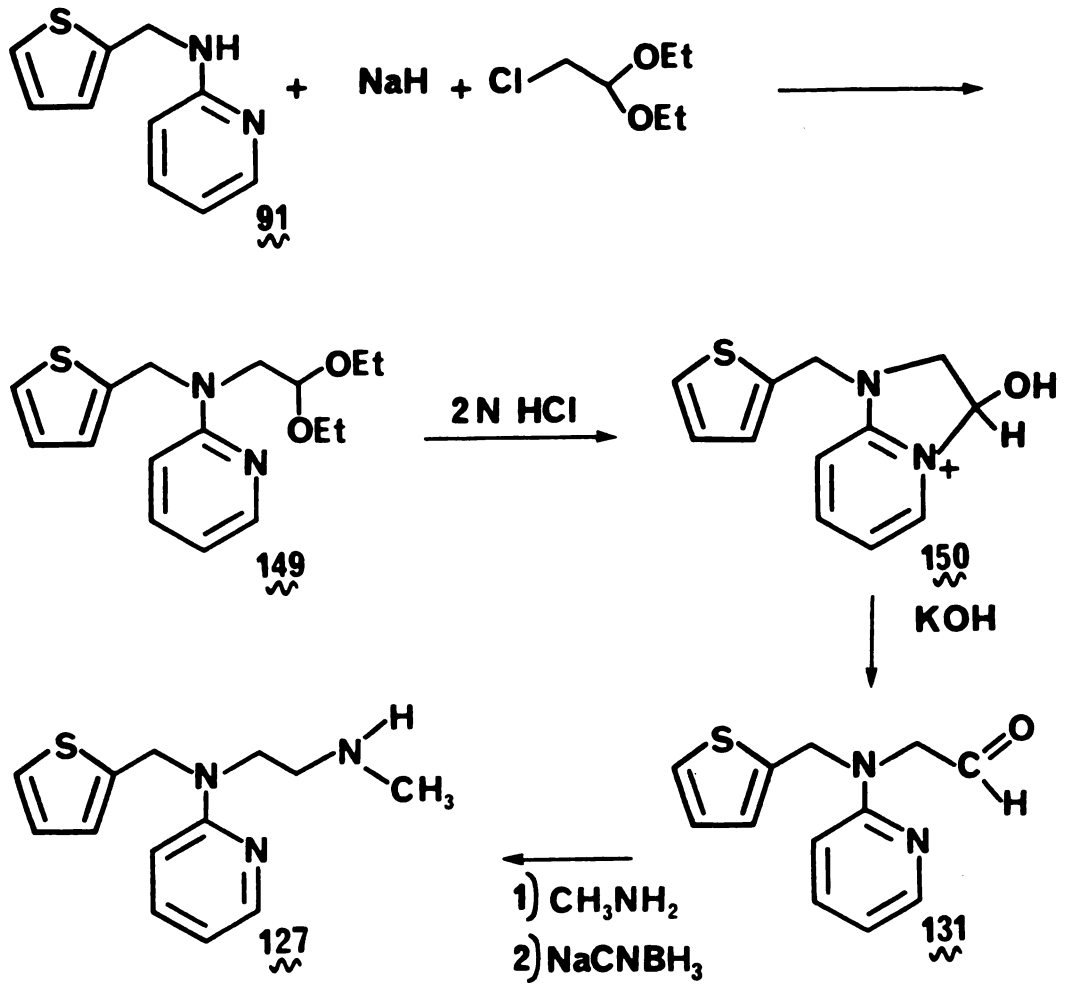

57% yield of slightly impure oil. The NMR spectrum (Figure 31) resembles that of methapyrilene except for the integration for only three protons for the N-CH_3 singlet at δ2.36. The HR-EIMS was consistent with $C_{13}H_{17}N_2S$.

Unfortunately, N-desmethylmethapyrilene is unstable upon standing, perhaps undergoing oxidation, and was therefore not available for HPLC analysis. As will be discussed later, N-desmethylmethapyrilene has the same retention time as peak 2 in Figure 15.

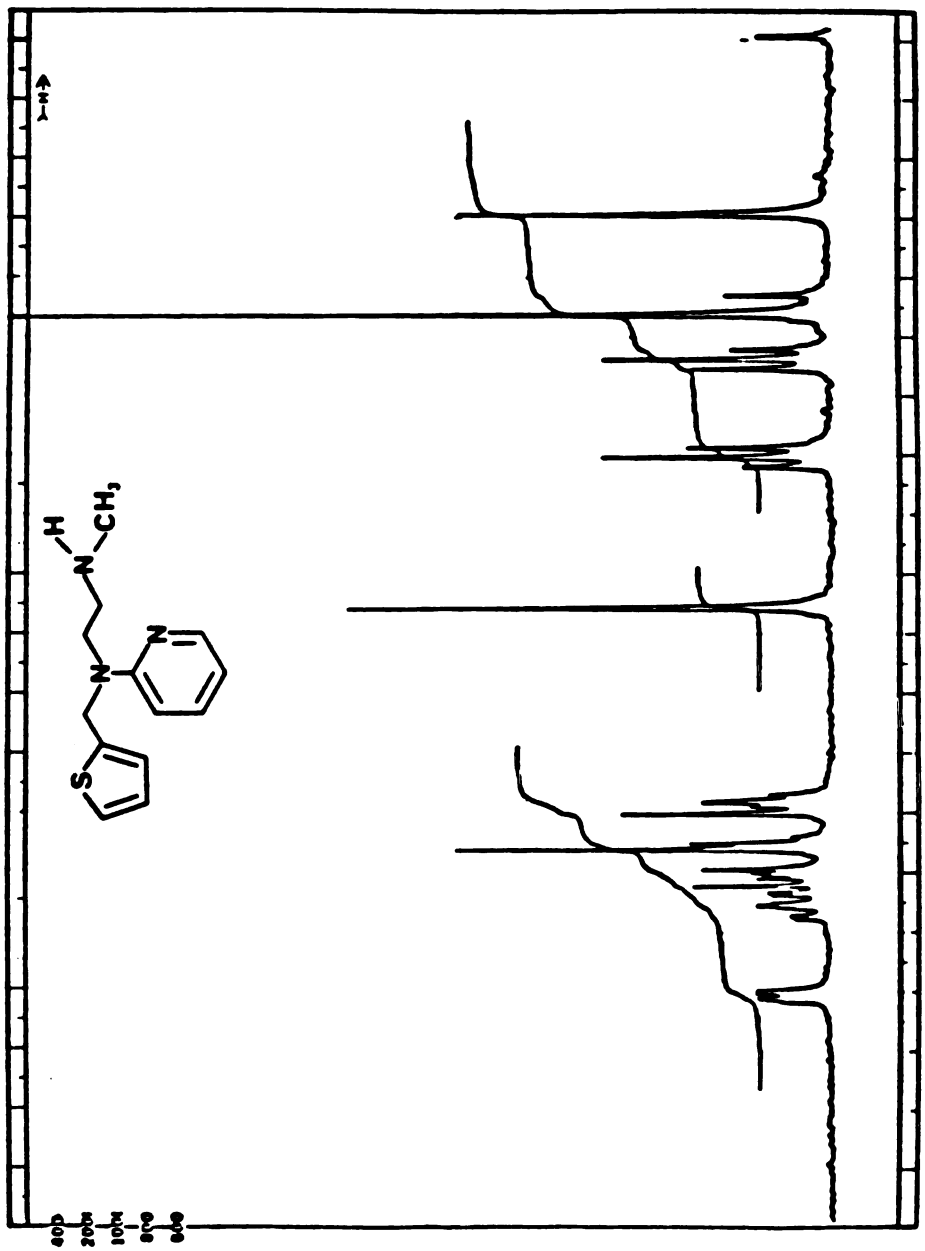

Figure 31. ^{1}H-NMR Spectrum of 127.

5). N-(N',N'-Dimethylacetamido)-N-(2'-thienylmethyl)-2-aminopyridine (129).

This final acetamide structure (129) was an isolated metabolite from rabbit microsomal incubates.[71] As discussed earlier, the carbinolamine 151 resulting from hydration of the iminium ion 152 is susceptible to further oxidation (Scheme 18).

Scheme 18. Metabolic Formation of Amide 129.

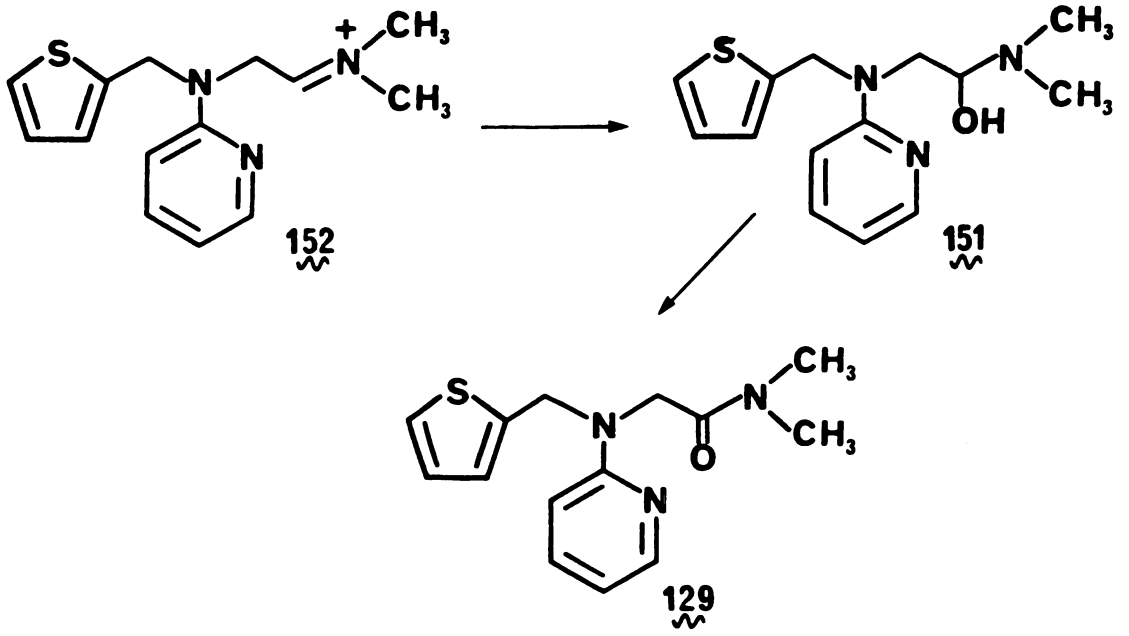

This amide was also isolated from rat liver microsomal incubates. The mass spectra from the proteo and deutero samples are identical (Figures 32 and 33), with the fragmentation occurring as shown.

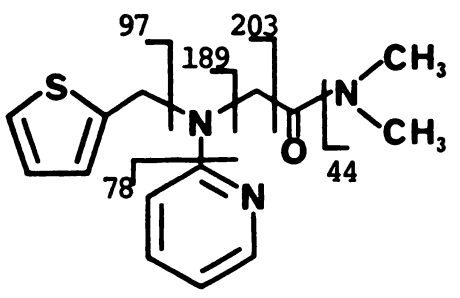

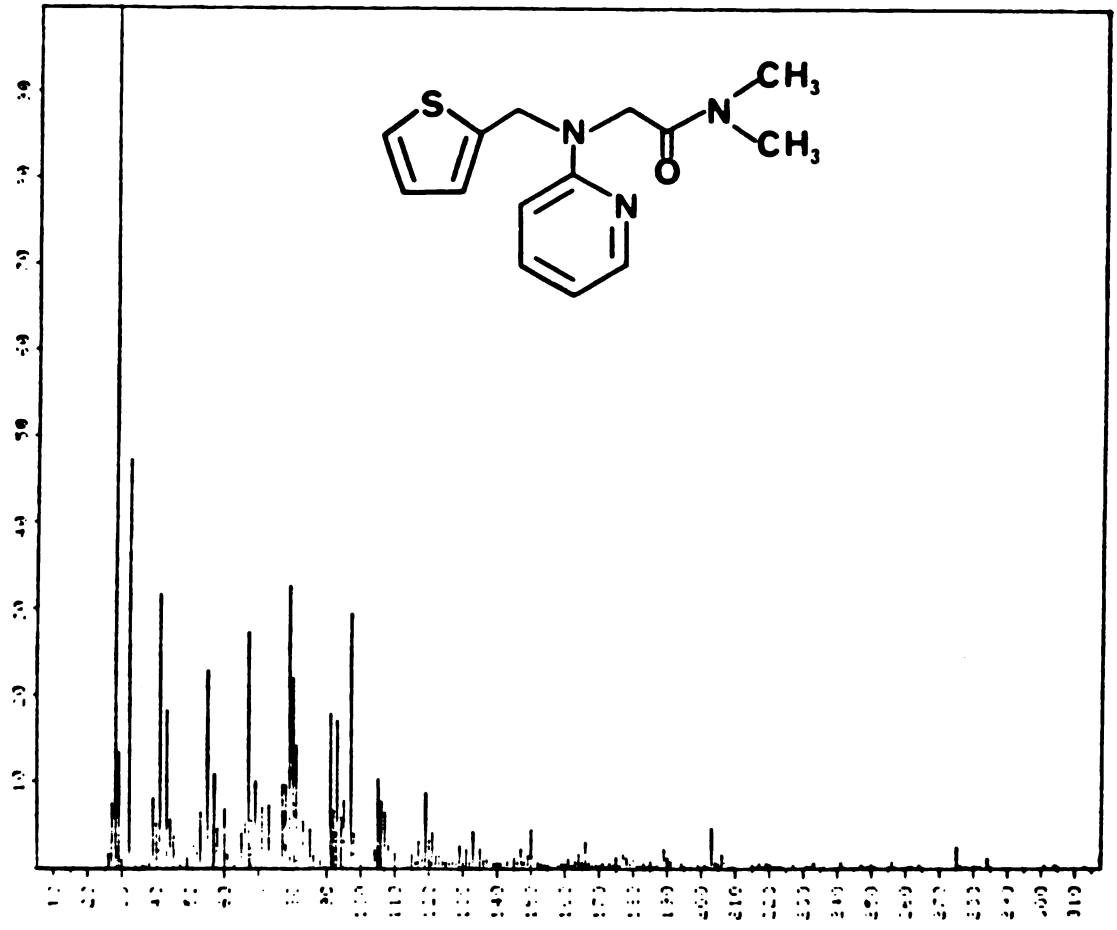

Figure 32. EIMS of 129.

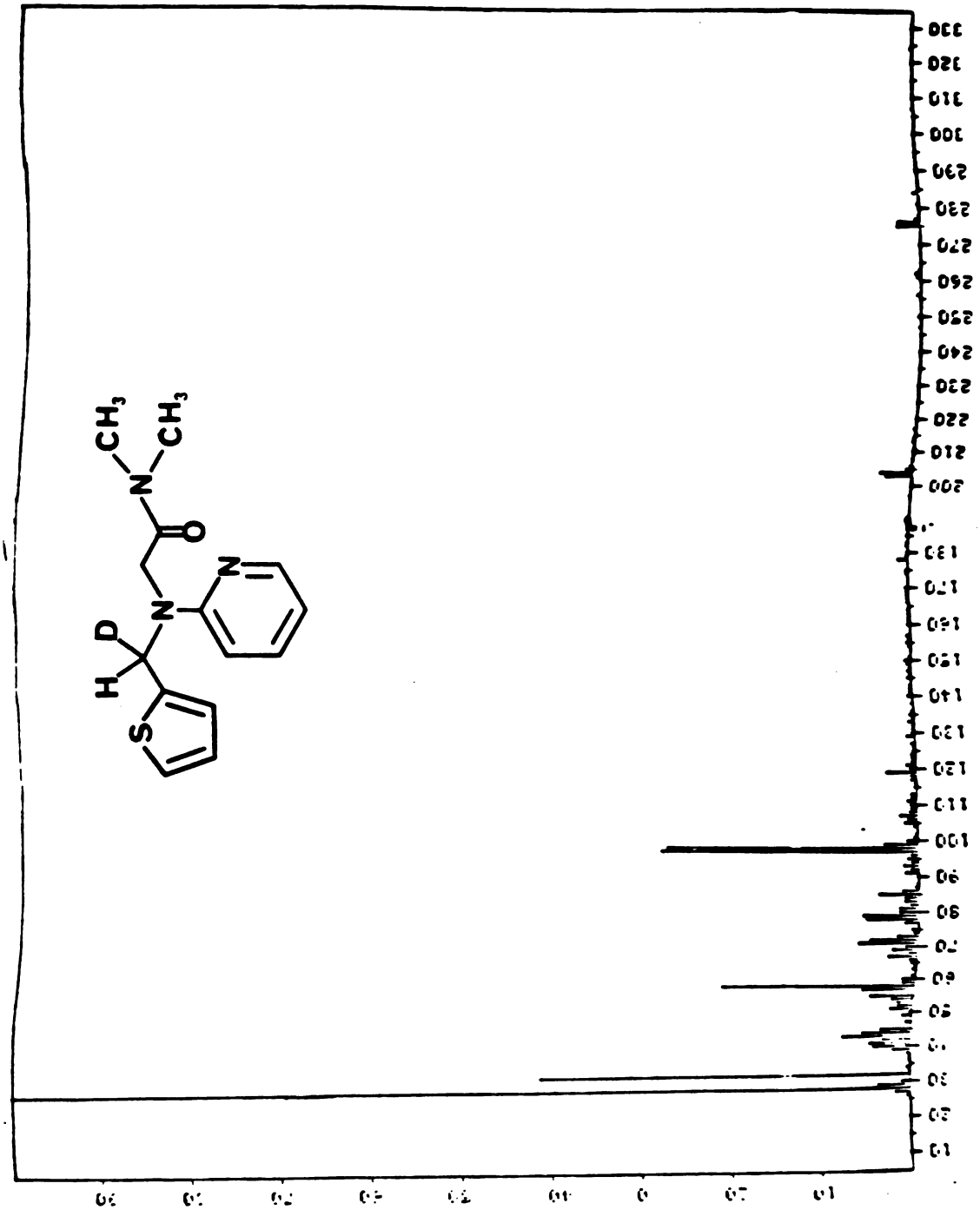

Figure 33. EIMS of Deutero- 129.

The chemical synthesis of amide 129 is illustrated in Scheme 19. N-(2'-Thienylmethyl)-2-aminopyridine (91) was treated with sodium hydride to generate the amine anion. This species was then alkylated with N,N-dimethyl-α -chloroacetamide to yield the desired product. After silica gel chromatography and crystallization, a 35% yield of the product was obtained. As noted during the numerous efforts at this synthesis, the product is sensitive to pH and tends to yield colored impurities when heated. Cyclization between the carbonyl and the pyridine ring nitrogen atom may be occurring. The mass spectrum of the synthetic 129 (Figure 34) is the same as that obtained from the biological sample. The retention time of 129 coincides with peak 3 in the HPLC chromatogram in Figure 15. Thus, N-desmethylmethapyrilene and amide 129 co-elute in this separation system.

Scheme 19. Synthesis of Amide 129.

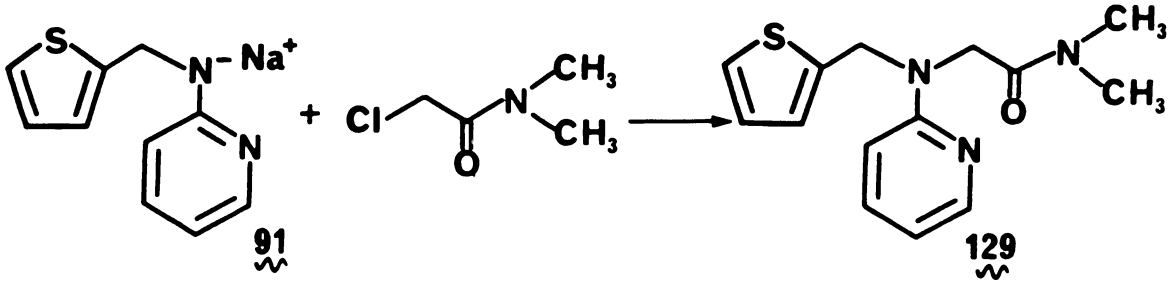

6). DMP High Resolution.

The total ion current shown in Figure 35 results from HR-EIMS. The spectra corresponded to those already found by low resolution and exact masses as well as elemental

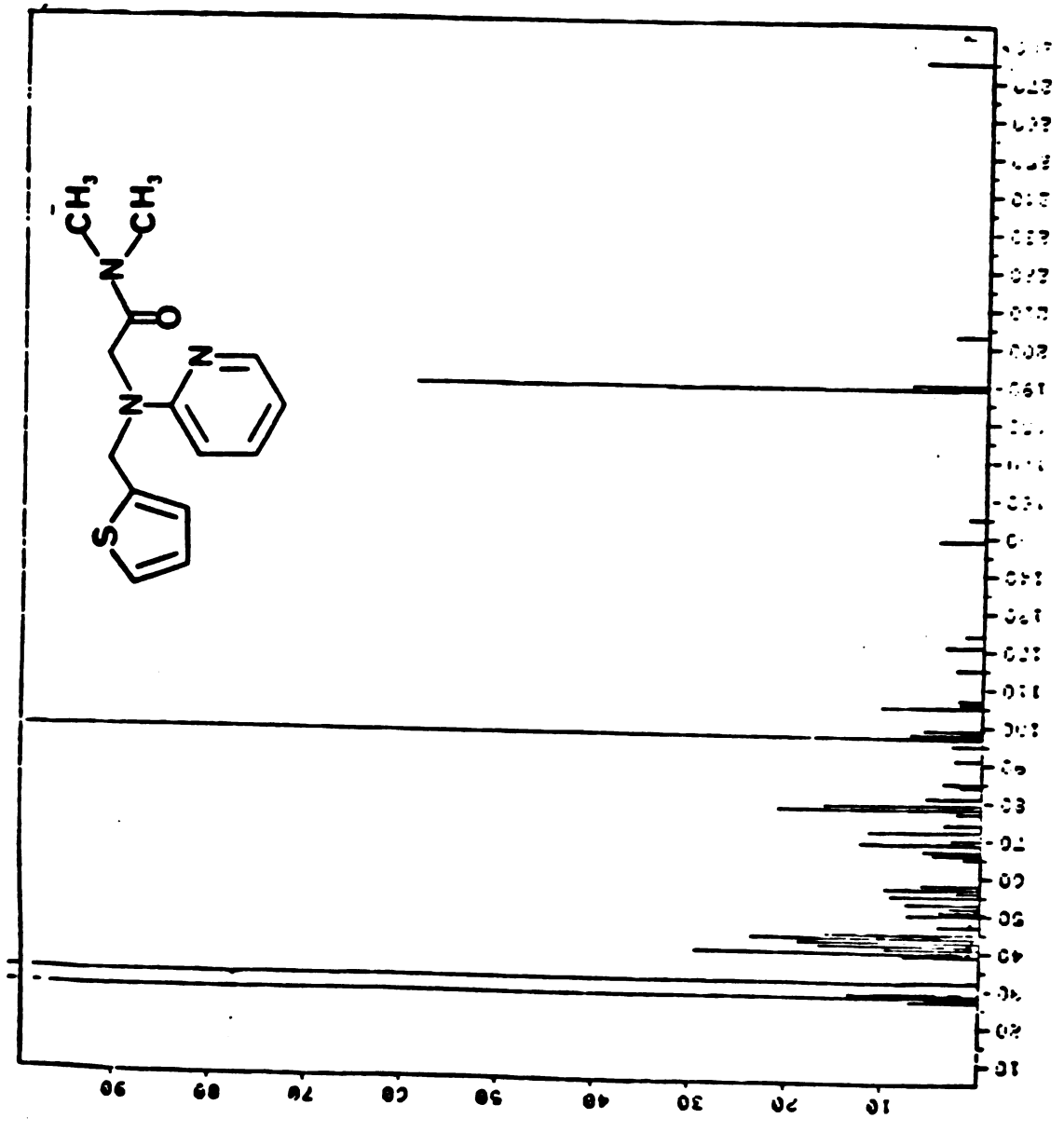

Figure 34. EIMS of Synthetic 129.

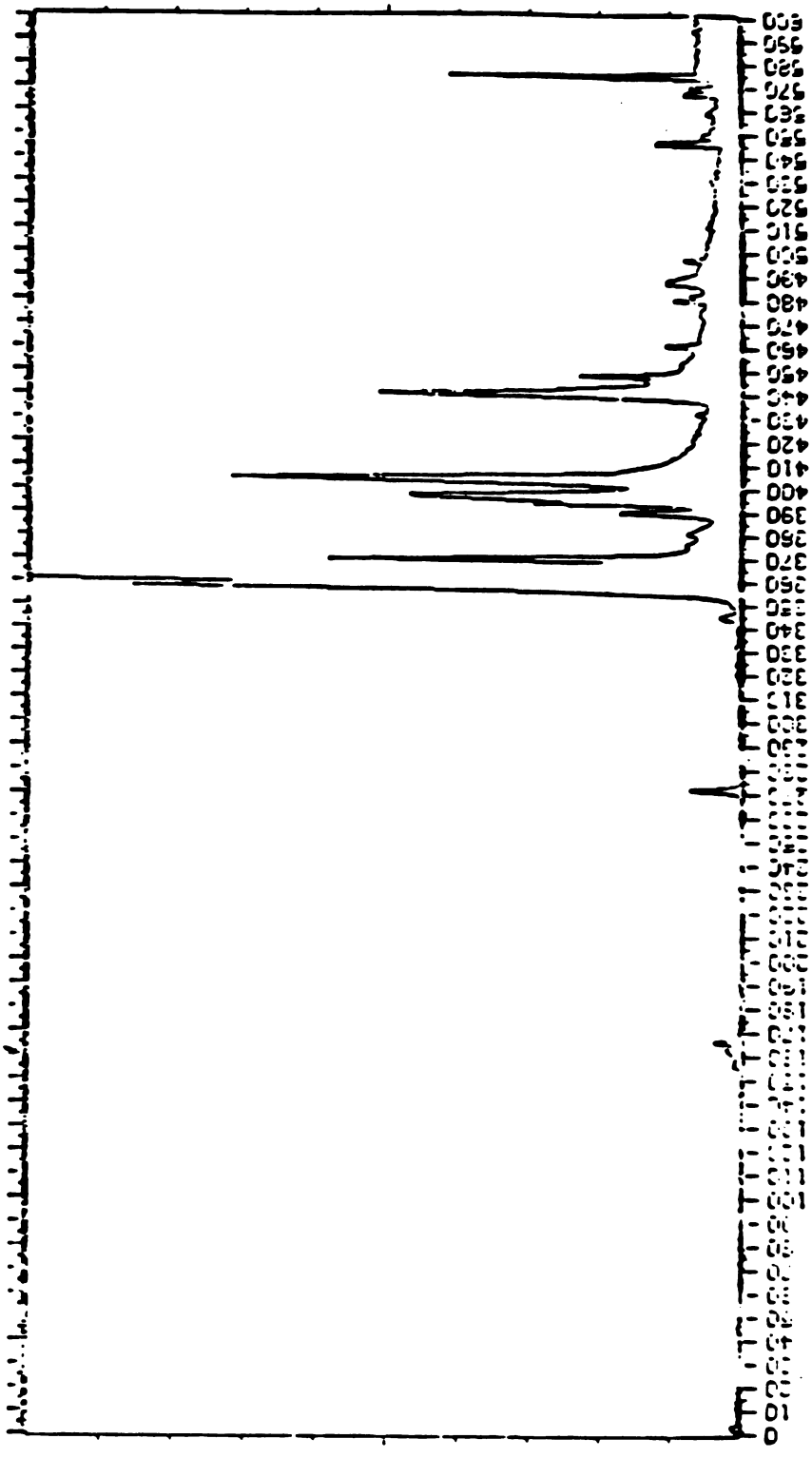

Figure 35. High Resolution GC-EIMS Total Ion Current

compositions confirm the structures previously assigned to the spectra. The ion current was also checked for all those specta containing the exact mass of the thienylmethyl fragment (m/e 97.011195, C_5H_5S) and only those peaks already identified as methapyrilene metabolites contained a mass 97 with composition $C5H_5S$. Other scans such as 696 and 704 may have had peaks at m/e 97 but upon checking, their compositions did not contain C_5H_5S. The scans have been identified by exact masses to be to metabolites illustrated in Table 8. In conclusion, it appears that all of the organic extractable metabolites have been identified. Each of the metabolites results from α-oxidation of an amine functionality.

Table 8. Organic Soluble Methapyrilene Metabolites.

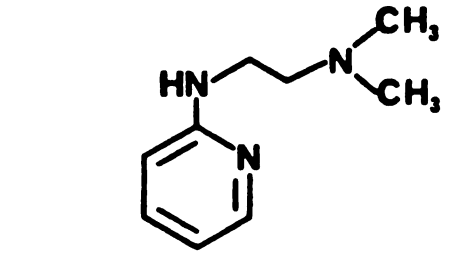

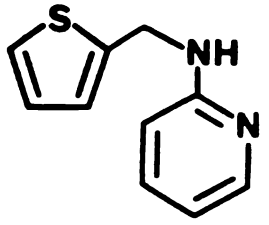

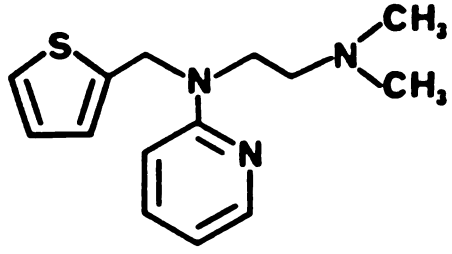

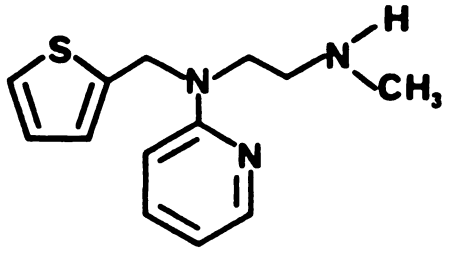

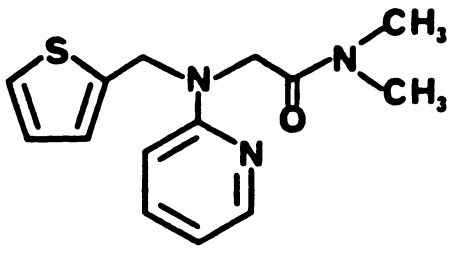

B. Water Soluble Metabolites

The radiochemical distribution studies determined that approximately 24% of the metabolized methapyrilene was distributed into the aqueous fraction after extraction of the incubate. In addition to the metabolites, the aqueous layer also contained the buffer, salts and other polar molecules which had to be removed prior to further analysis of the metabolites. The salts and other extremely polar molecules were removed by passing the aqueous fraction either through a reverse phase C-18 Sep Pak or a short column of XAD-2. Both of the packing materials have a hydrophobic attraction for organic material. Once the metabolites had been absorbed onto the support, the salts were removed by rinsing the support with distilled water (1-2 ml). The metabolites were then recovered by eluting the support with methanol. The total procedure is illustrated in Scheme 20. Analysis of the radioactivity distribution revealed that 29% passed through the Sep pak with the water phase, 40% eluted with the methanol and 31% remained bound to the Sep Pak. The radioactivity present in the water eluent would not adhere to a fresh Sep Pak indicating that this characteristic was not a result of overloading the Sep Pak but instead was due to the very polar properties of the radiolabeled material. Similarly, 54-61% of the radioactivity eluted from XAD-2 resin with methanol, with the rest residing in the aqueous phase (the

Scheme 20. Isolation of Water Soluble Metabolites.

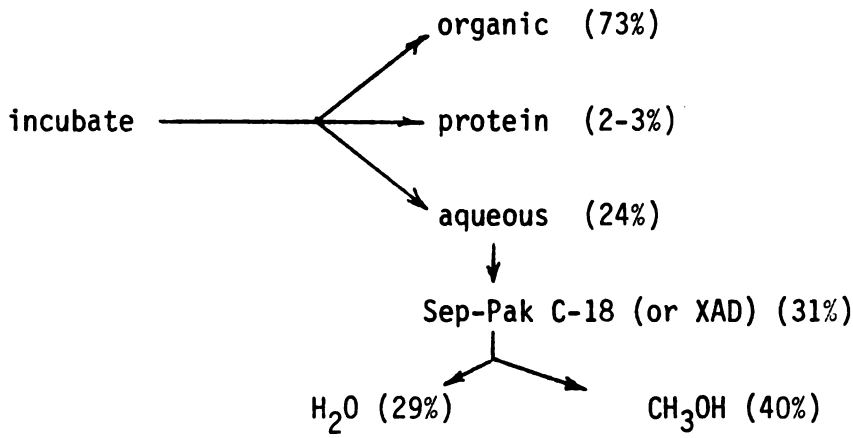

XAD-2 beads were not counted). Additionally, the aqueous layer was saturated with sodium chloride and extracted with n-butanol. This resulted in 32% extraction of the radioactivity into the butanol. The question arose as to whether the nonextractable aqueous soluble material was tritiated water. An aqueous aliquot was subjected to lyophilization and only 2% of the radioactivity distilled over with the water. From this information, we can conclude that the radioactivity eluting with water from the C-18 Sep Pak is not tritiated water but extremely polar tritiated metabolites. No information can be obtained on the radioactivity which binds to the C-18 support and we can only speculate that this is a result of nonspecific adsorption of metabolites.

The complexity of the methanol eluant mixture was illustrated in the HPLC chromatogram (Figure 16). The partitioning of the eluant into 0.5 ml fractions from a

radiolabeled sample showed that radioactivity was associated with only a few of the UV absorbing peaks. The compounds isolated from preparative scale HPLC will be discussed in the order of their elution.

1).N-(N',N'-Dimethylaminoethyl)-2-aminopyridine (92).

The first large radioactive peak was determined to be the known metabolite, 92. The NMR of the isolated sample (Figure 36) corresponded directly to that of the synthetic material as did the mass spectrum.

2) 2-Hydroxymethylthiophene (153).

The isolation of a thiophene containing fragment eliminated in the biochemical formation of N-(N',N'-dimethylaminoethyl)-2-aminopyridine was an unexpected pleasure. As shown in Scheme 12, thiophene-2-carboxaldehyde should be formed in the benzylic oxidative dealkylation of methapyrilene. Thus we hoped to isolate either thiophene-2-carboxaldehyde, or its corresponding reduction or oxidation products, 2-hydroxymethylthiophene or thiophene-2-carboxylic acid. Our isolation procedure would not extract thiophene-2-carboxylic acid due to its charged nature at pH 7.4.

Peak 9 off the HPLC was subjected to EIMS without success. Upon derivatization with BSTFA/pyridine (1:5) at 60^{0} for 30 minutes, the subsequent GC-EIMS yielded the

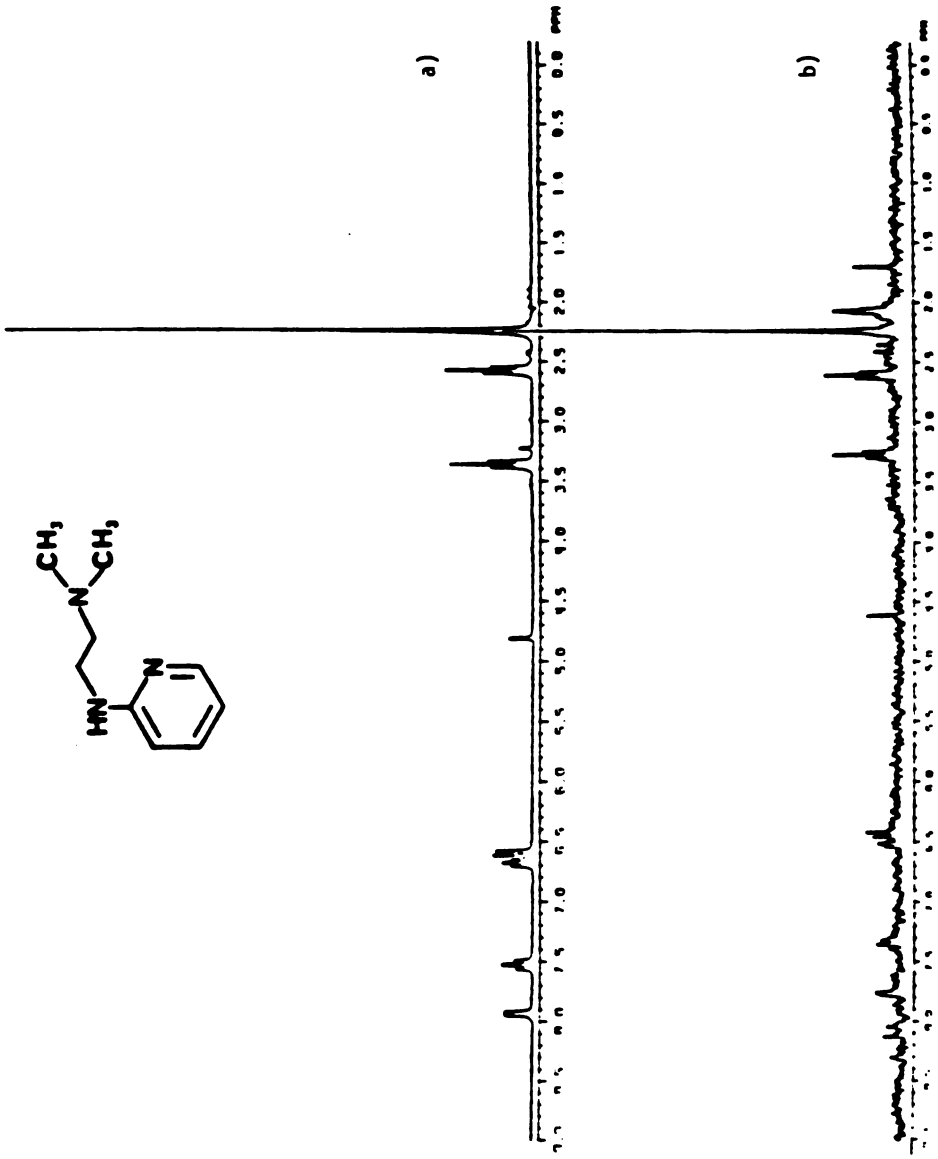

Figure 36. ^{1}H-NMR Spectrum of 92 a) synthetic b) metabolic

spectrum shown in Figure 37. The structure was assigned as O-trimethylsilyl-2-hydroxymethylthiophene (154). The initial loss of 15 mass units is a common loss of a methyl from the TMS group. The ion at m/e 97 was indicative of the benzylic unit observed numerous times before and represents a loss of 89 mass units from the parent, representative of O-Si-$(CH_3)_3$.

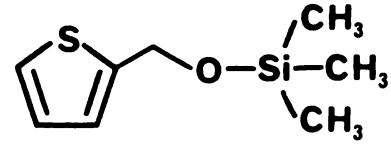

154

The structure assignment was confirmed by trimethylsilylation of the commercially available 2-hydroxymethylthiophene. As shown in Figure 38, the spectrum from the synthetic material closely corresponds to that of the biological sample.

Apparently the liberated thiophene-2-carboxaldehyde undergoes reduction microsomally to yield the corresponding alcohol. An aldehyde oxidase enzyme is most likely responsible for this reduction, which occurs in the presence of the excessive amounts of NADPH. This enzyme is usually considered to be a soluble enzyme, however, and should not be present in microsomal mixtures. Thus the microsomes are either slightly contaminated with soluble enzymes or there are other enzymes capable of oxidative/reductive transformations of carbonyls.

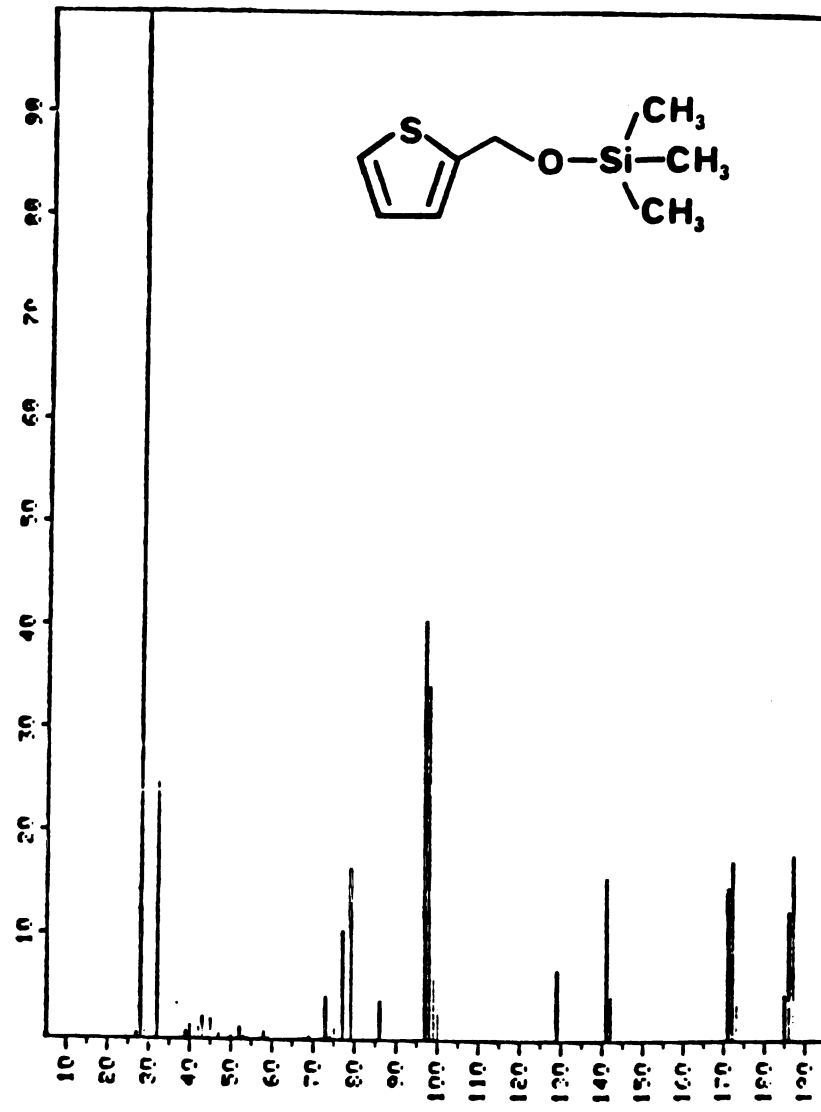

Figure 37. EIMS of 154.

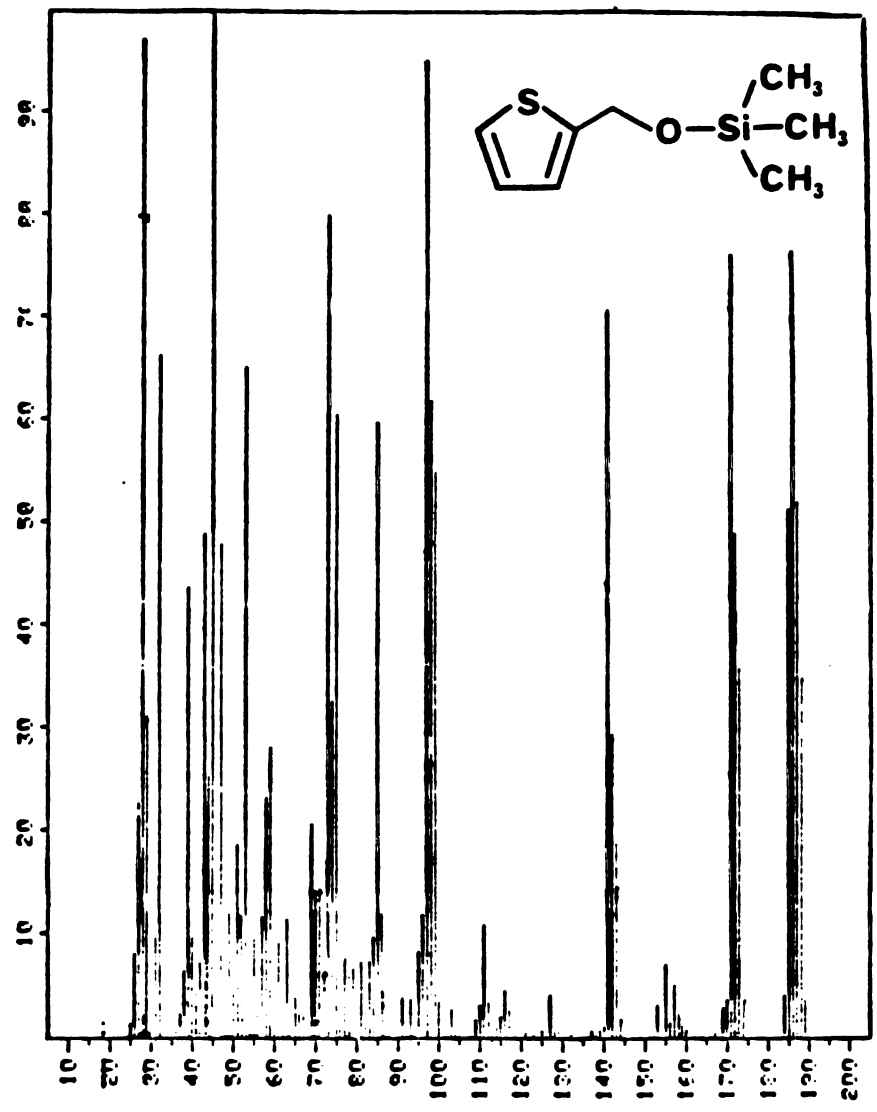

Figure 38. EIMS of Synthetic 154.

3). N-Desmethylmethapyrilene (127).

The formation of N-desmethylmethapyrilene (127) was previously discussed. Isolation of the N-demethylated metabolites from the aqueous fraction was not unexpected due to its polarity and possible distribution into both the aqueous and organic phases. The mass spectrum determined by probe EIMS of HPLC peak 11 had a parent ion at m/e 247 and in all ways corresponded to that of the synthetic N-desmethylmethapyrilene. As expected, the HPLC peak demonstrates both UV absorbance and radioactivity. The retention time, however, was found to be exactly that of the N,N-dimethylacetamide metabolite 129, which complicated the quantitation studies, as discussed in a later section.

4). 5-Hydroxymethapyrilene (155).

Oxidation of the pyridine ring within methapyrilene was expected based on tripelennamine metabolism.[185] The sample identified as peak 12 from HPLC yielded enough material to allow high field NMR. The 240 mHz NMR of peak 12 is shown in Figure 39. The sample was contaminated with a large amount of water causing the offscale peak at δ4.8. Additionally, some other peaks in the aliphatic region were due to impurities, as determined in many of the samples isolated in this manner. The aromatic region, however, was clearly that of a methapyrilene derived metabolite. A 240 mHz spectrum of methapyrilene is given in Figure 40 for comparison. The aromatic peak assignments for methapyrilene

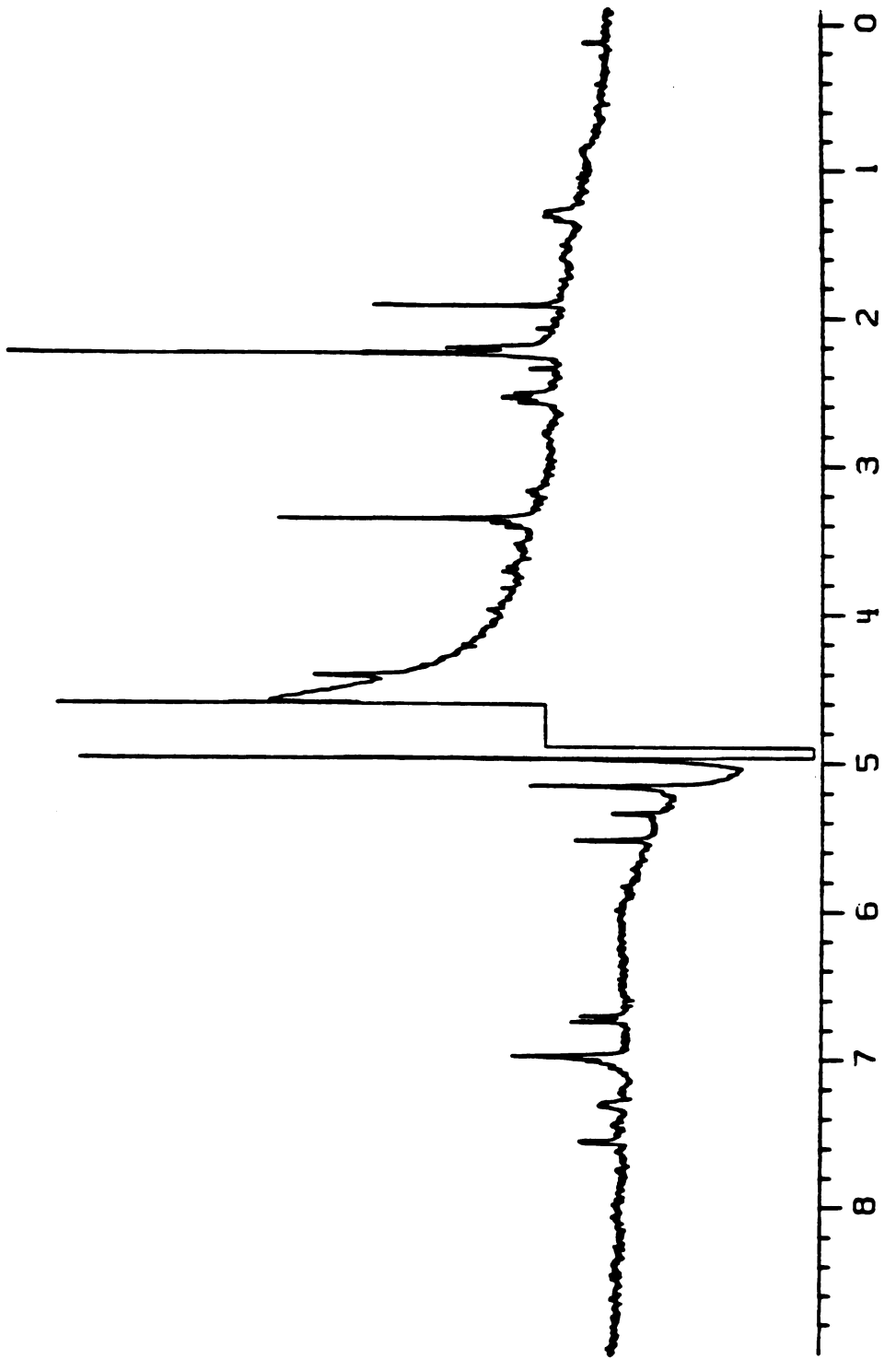

Figure 39. ^{1}H NMR Spectrum of 155.

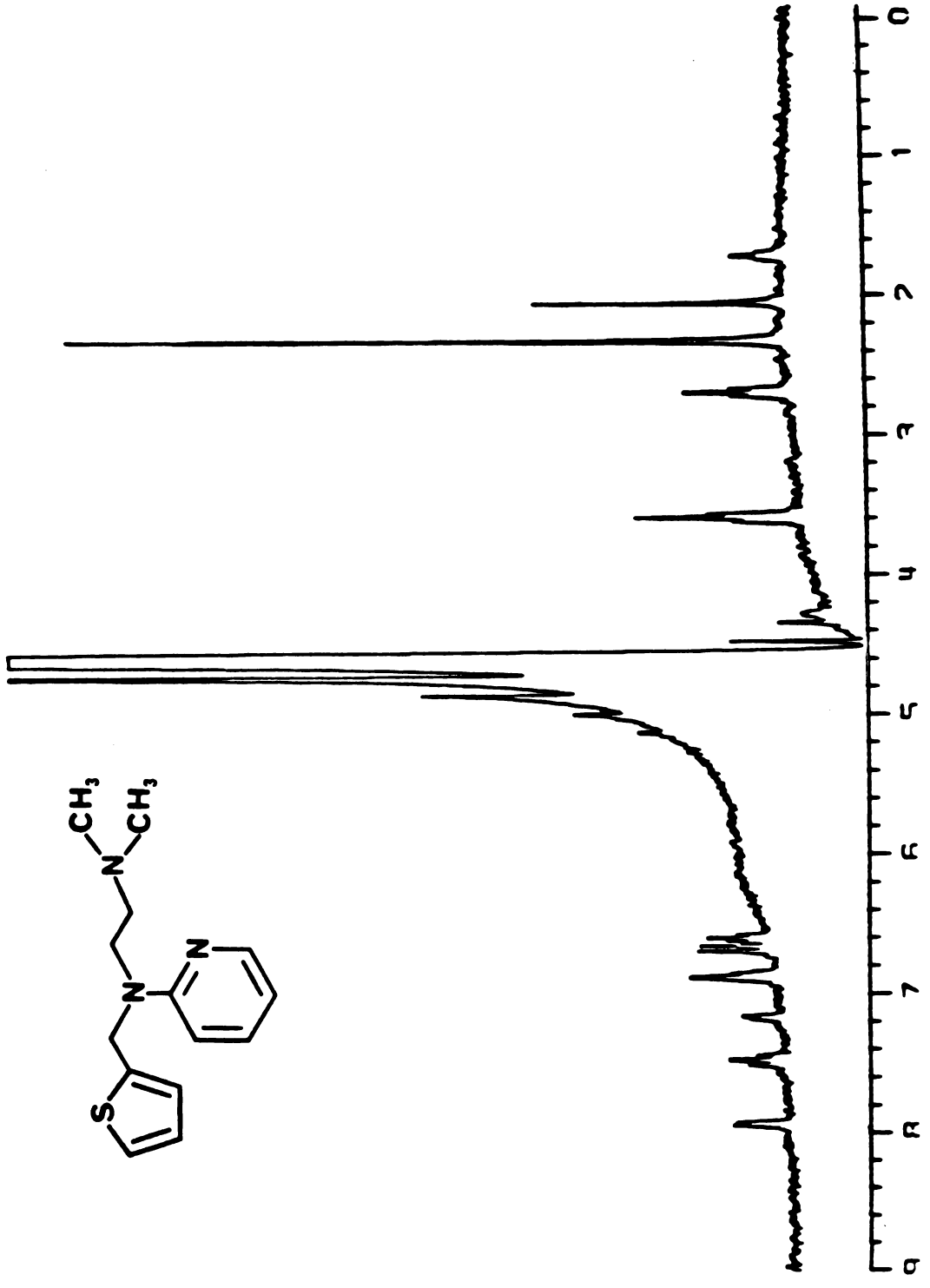

Figure 40. ^1H NMR Spectrum of 1.

have been made as follows. Clearly, the N-methyl and two methylene triplets are present in the unknown structure, although a contaminant singlet overlaps the triplet at δ 3.55. The downfield portion of the peak 12 spectrum decidedly lacks the C-5 triplet at δ6.6 while the doublet at 6.7 is still present. The peak at δ7.6 in the unknown exists as a singlet exhibiting ortho coupling. The remaining small peak and larger undefined peak represent the thiophene protons. Unfortunately, integration was not possible on this sample due to interference from the large water peak. Thus it was not clear if one of the pyridine proton peaks was hidden under the thiophene resonances. Attempts to remove the water by lyophilization resulted in loss of the sample. The volatility of this sample and most of the other water soluble metabolites was a consistent problem in the isolation and purification of metabolites.

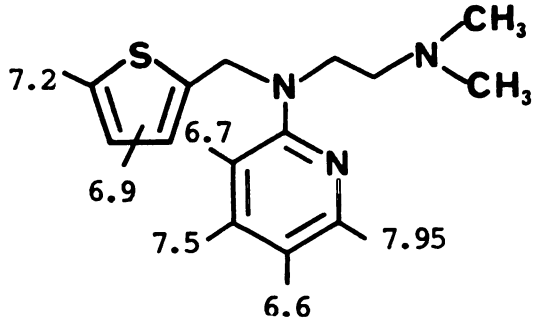

A portion of peak 12 was then subjected to probe EIMS for analysis. The mass spectrum, as shown in Figure 41, was extremely weak but the parent ion was 16 mass units higher than methapyrilene at m/e 277. The benzylic m/e 97 ion was still strong but the characteristic m/e 78 ion for the pyridine was missing. The loss of the

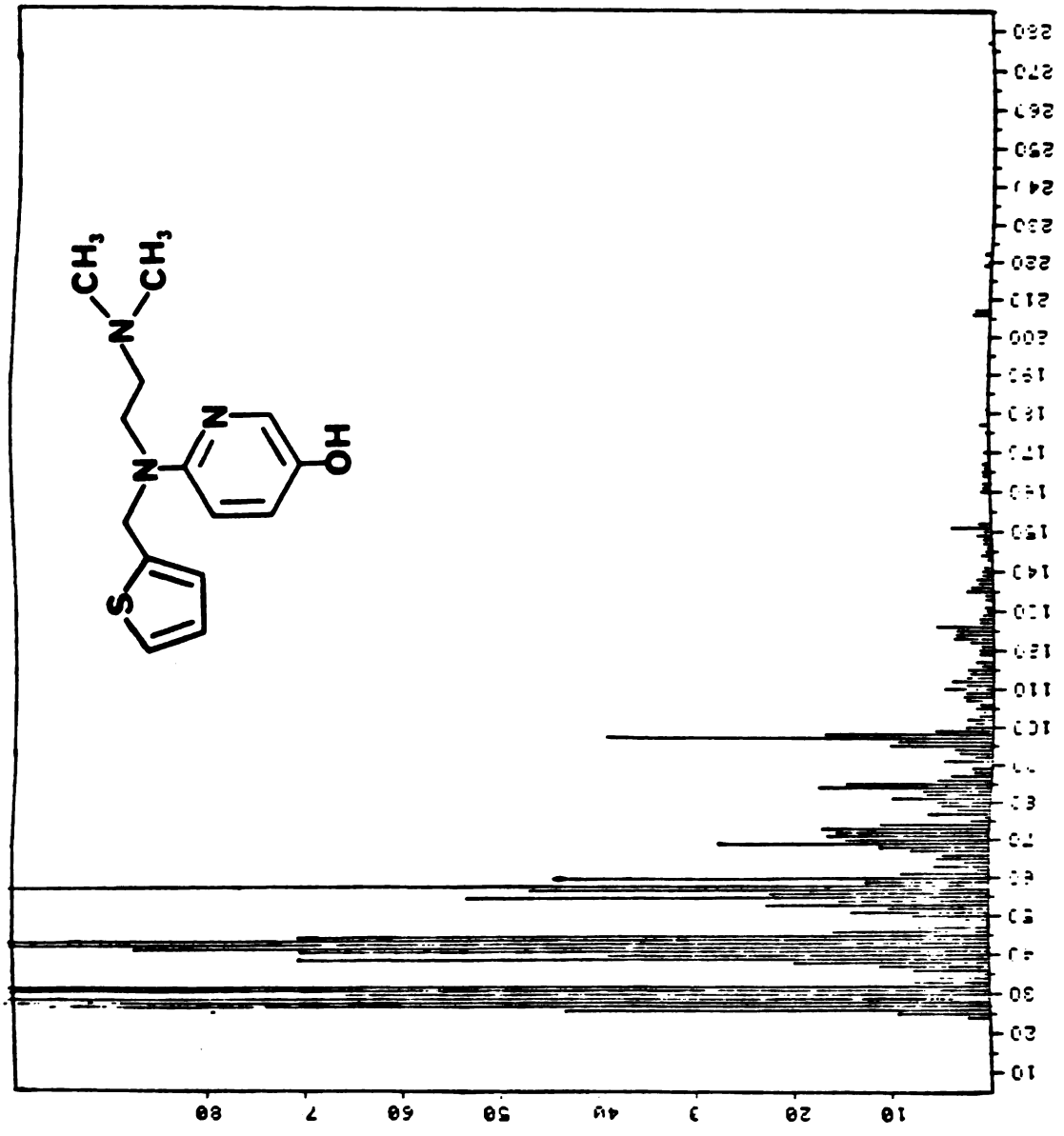

Figure 41. EIMS of 155.

N,N-dimethylaminoethyl fragment resulted in the ion at m/e 207. The peak assignments were made as follows.

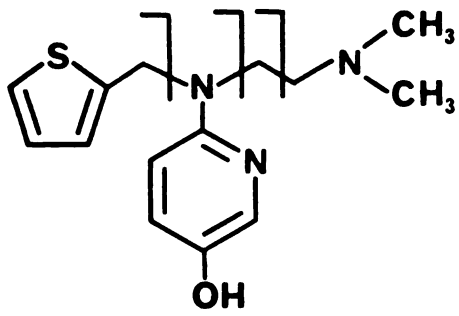

A secondary ionization mass spectrum (SIMS) was unsuccessful in detecting this sample. To confirm this structure, the aqueous mixture derived from incubates of deuterated methapyrilene was trimethylsilylated and then submitted to GC-EIMS. The spectrum of scan 476 (Figure 42) was analyzed as the O-TMS-ether of 5-hydroxymethapyrilene.

5). N-(2-Pyridyl)-N-(2-thienylmethyl)aminoacetaldehyde (131).

Oxidation alpha to the terminal nitrogen has been discussed previously in the formation of the dimethylacetamide metabolite (129). The intermediate carbinolamine, in that case, underwent additional oxidation to form the amide functionality. As shown in Scheme 21, however, the carbinolamine can undergo dissociation to form an aminoacetaldehyde. The overall reaction resulting in deamination of methapyrilene. This aldehyde could then act as a substrate for oxidation to the corresponding carboxylic acid or reduction to the alcohol. The aldehyde metabolite

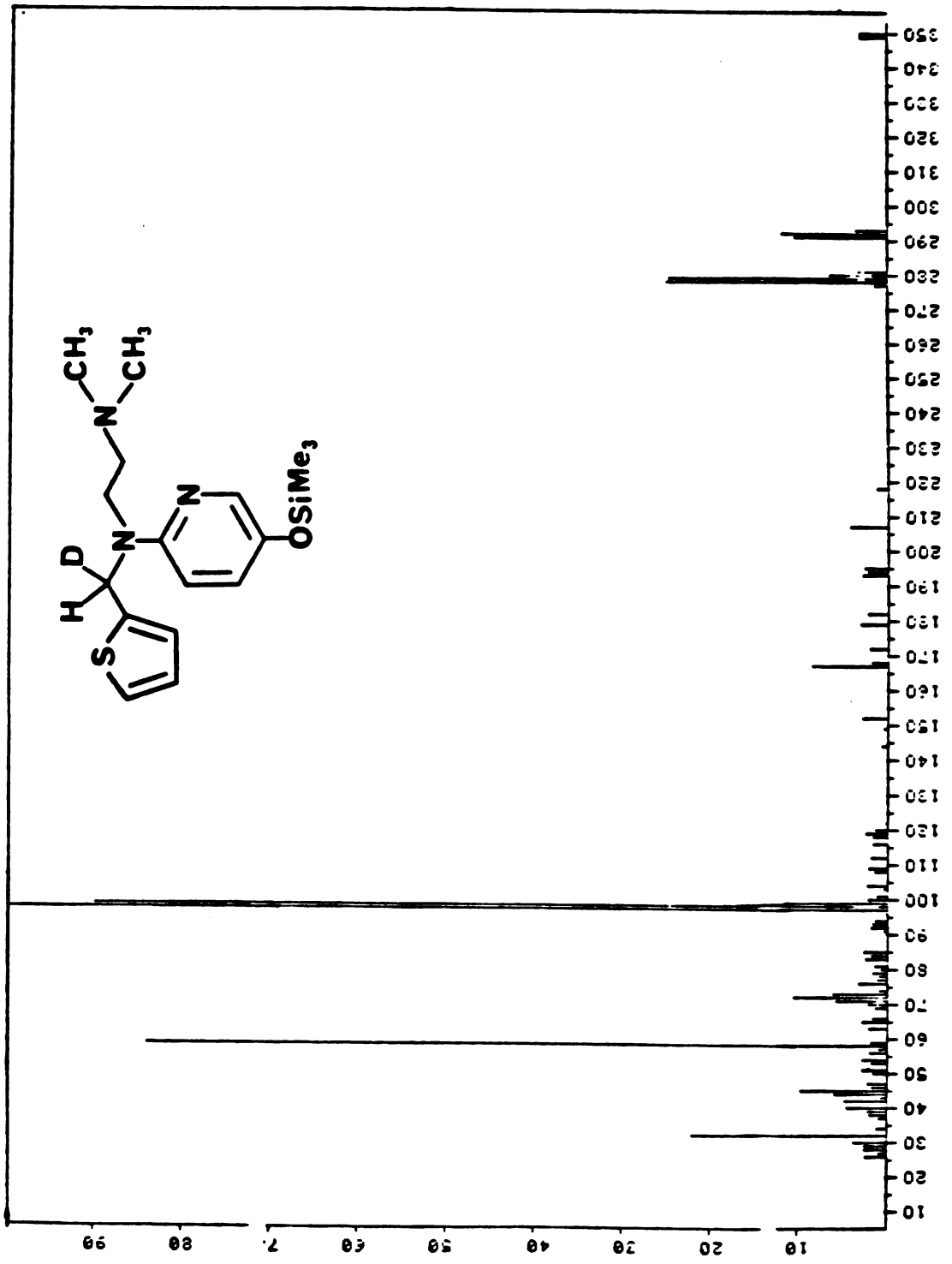

Figure 42. EIMS of O-TMS-Deutero 155.

Scheme 21. Metabolic formation of 131.

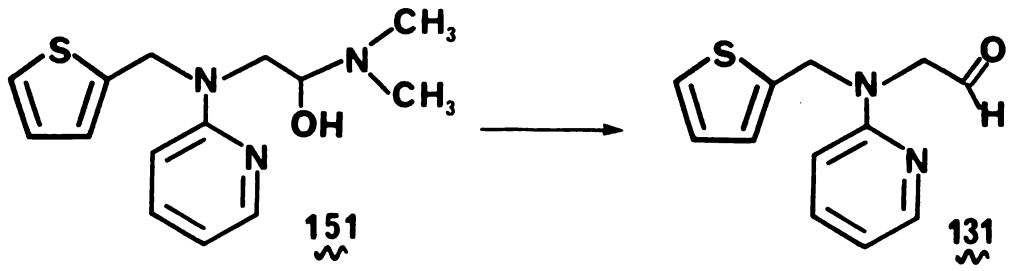

131 had never been isolated previously, suggesting that the carbinolamine preferred oxidation to the dimethylacetamide product.

Peak 13 in Figure 16, although sizable in UV, was found to have negligible radioactivity content. A sample isolated from preparative HPLC was concentrated and subjected to 500 mHz NMR. The proton spectrum is shown in Figure 43, where the predominant peaks reside in the aromatic region between δ 8.00 to 9.00. The water peak occurs at δ4.80 and was used as an internal standard.

An expanded plot of the downfield region of this spectrum is given in Figure 44. The first order spectrum yields a doublet at δ8.8 (J = 5.31 Hz) and two triplets at δ 8.59 (J = 7.90 Hz) and 8.06 (J = 6.94, 7.26 Hz), integrating for 3 : 1: 2 protons, respectively. The coupling constants for the triplets are confusing in that they appear not to be coupled to one another.

The same sample gave the HR-EIMS shown in Figure 45. With the parent ion at m/e 79 and only one fragment ion at m/e 52, the compound appeared to be pyridine. Pyridine

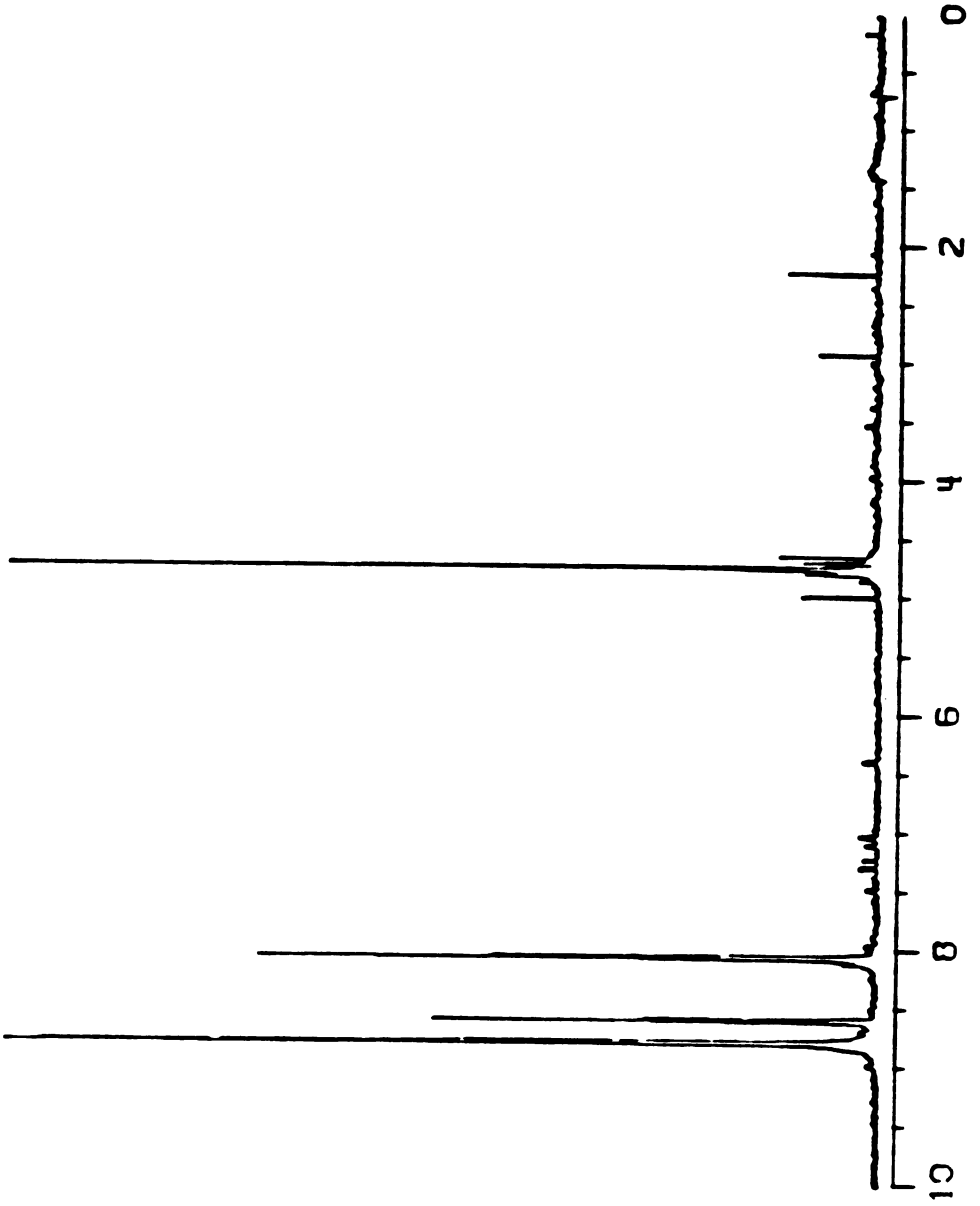

Figure 43. ^{1}H NMR Spectrum of Peak 13 of Figure 16.

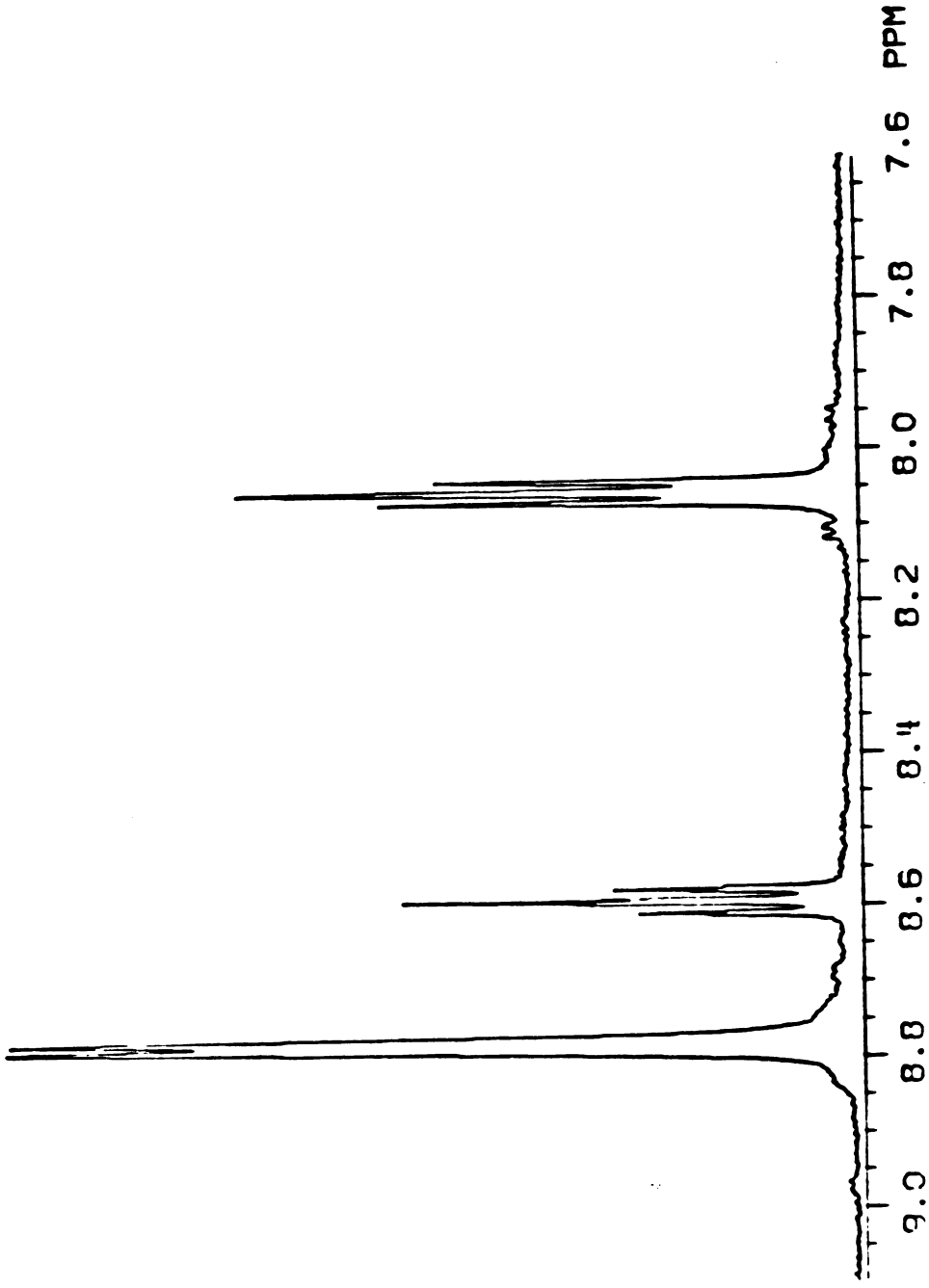

Figure 44. Expanded Region of Figure 43.

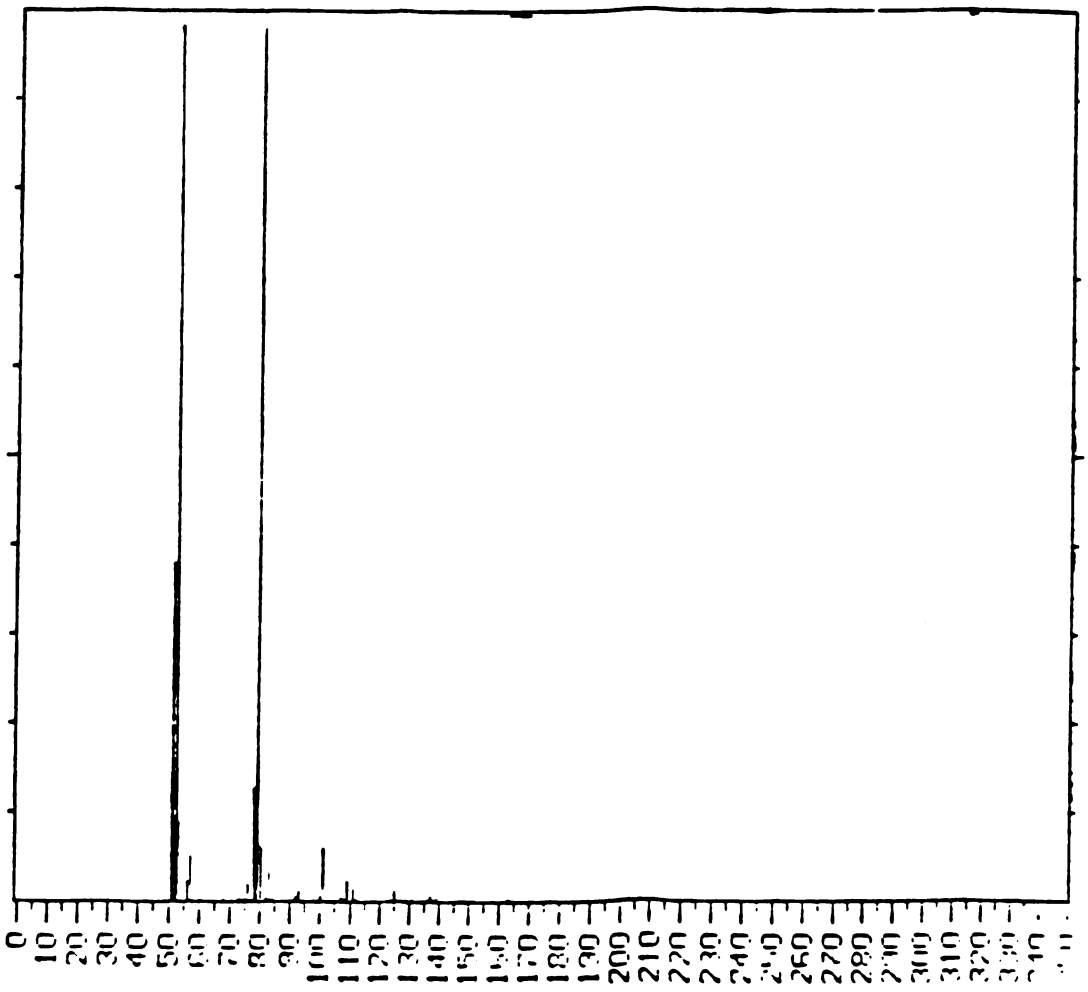

Figure 45. EIMS of Peak 13 of Figure 16.

fragments under mass spectral conditions to yield a loss of HC=N, leading to the only fragment observed at m/e 52.[200]

The proton NMR, although similar to that of pyridine, has a measurably lower chemical shift. The solvent system used to separate the metabolites was a perchlorate buffer and the downfield shift might be a result of isolating the perchlorate salt of pyridine. Authentic pyridinium perchlorate gave the same NMR spectrum as the HPLC sample. The incorrect integration of the spectrum was most likely due to the long relaxation time of a small molecule such as pyridine. Additionally, the observed coupling constants were confirmed in the literature.[200a] The formation of pyridine from metabolism of methapyrilene is highly unlikely and this material probably represents an artifact of the isolation procedures.

In the analysis of this sample, another compound was observed by HR-EIMS. As shown in Figure 46, the fragmentation was reminiscent of that from other methayrilene derivatives. Fragment ions at m/e 97, 107, 189 and 203 are indicative of the major portion of the methapyrilene structure. The parent ion at m/e 232 fragments to lose 29 mass units or a CHO group. N-(2-Pyridyl)-N-(2'-thienylmethyl)aminoacetaldehyde (131) was proposed for the structure of this metabolite. The exact mass of ion m/e 232 correlated to a composition of $C_{12}H_{12}N_2OS$.

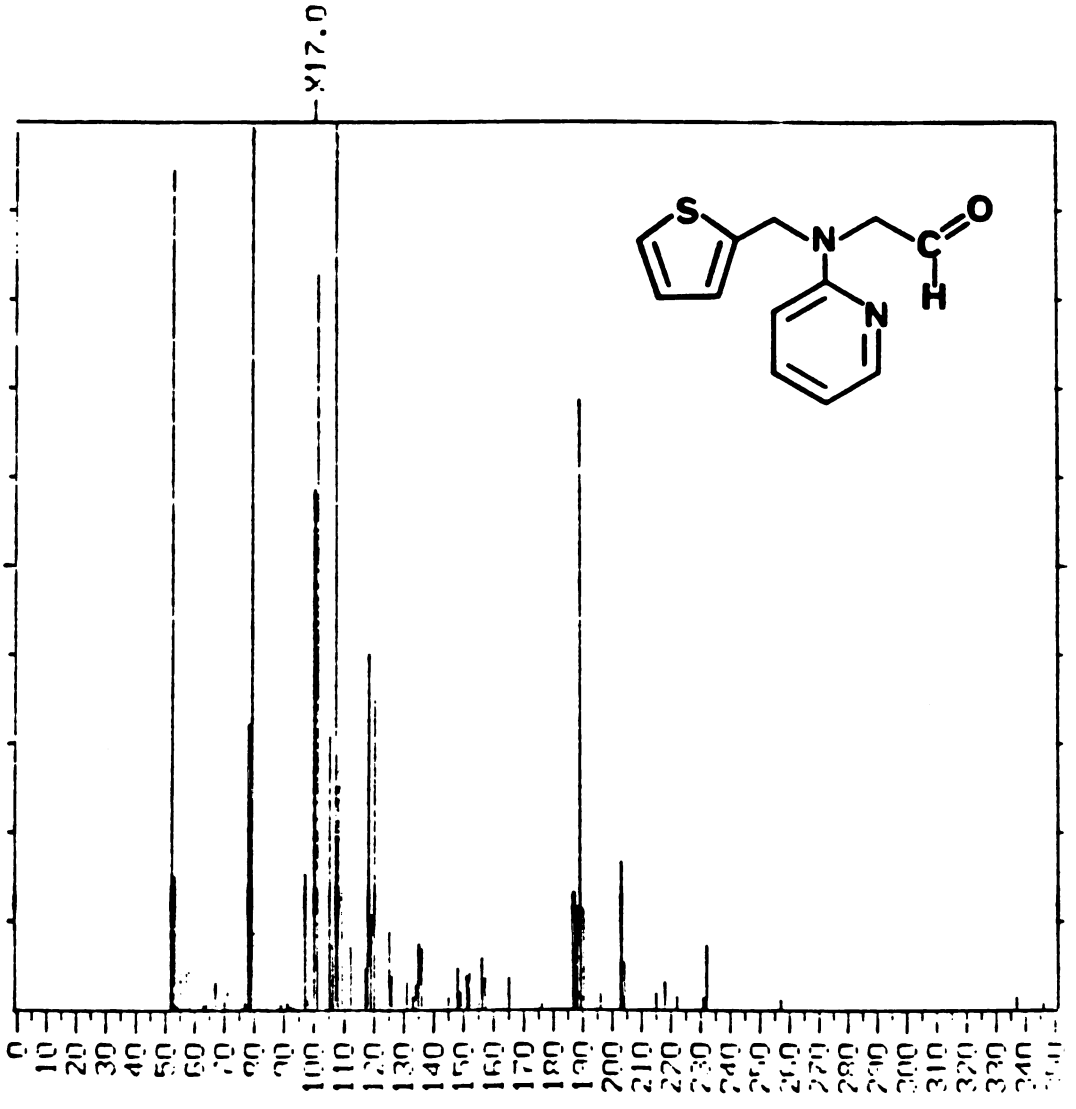

Figure 46. EIMS of Aldehyde 131.

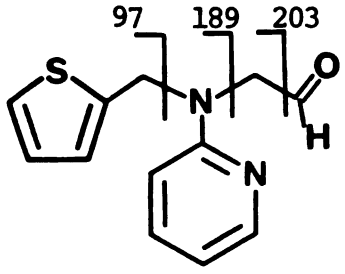

Total synthesis of this aminoactaldehyde had been previously achieved en route to synthetic N-desmethylmethapyrilene. The synthetic approach to the aldehyde is reviewed in Figure 47. The secondary amine 91 was treated with sodium hydride to generate the anion of the amine which was then condensed with bromoacetaldehyde diethylacetal to yield the protected aldehyde (149). The aldehyde was then liberated by treating the diethylacetal with 2 N HCl for one hour at room temperature and the product extracted into methylene chloride.

Figure 47. Synthesis of Aminoacetaldehyde Metabolite 131.

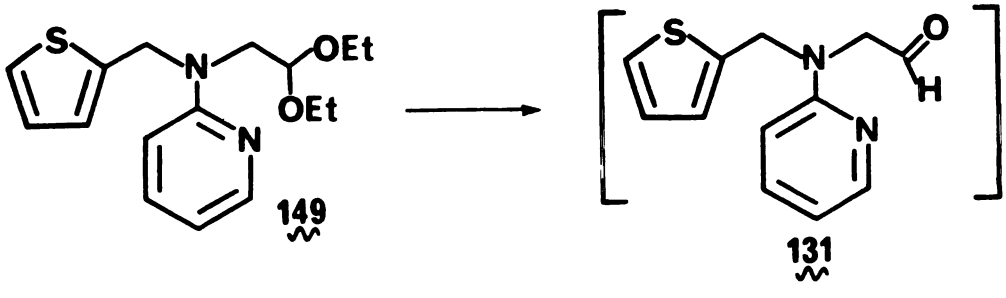

Very little material was isolated in the methylene chloride extract, none of which contained an aldehydic proton at δ 9- 10. For this reason, the reaction was repeated in D_2O and DCl in an NMR tube. The reaction progress is shown in Figure 48 where the spectrum at 5

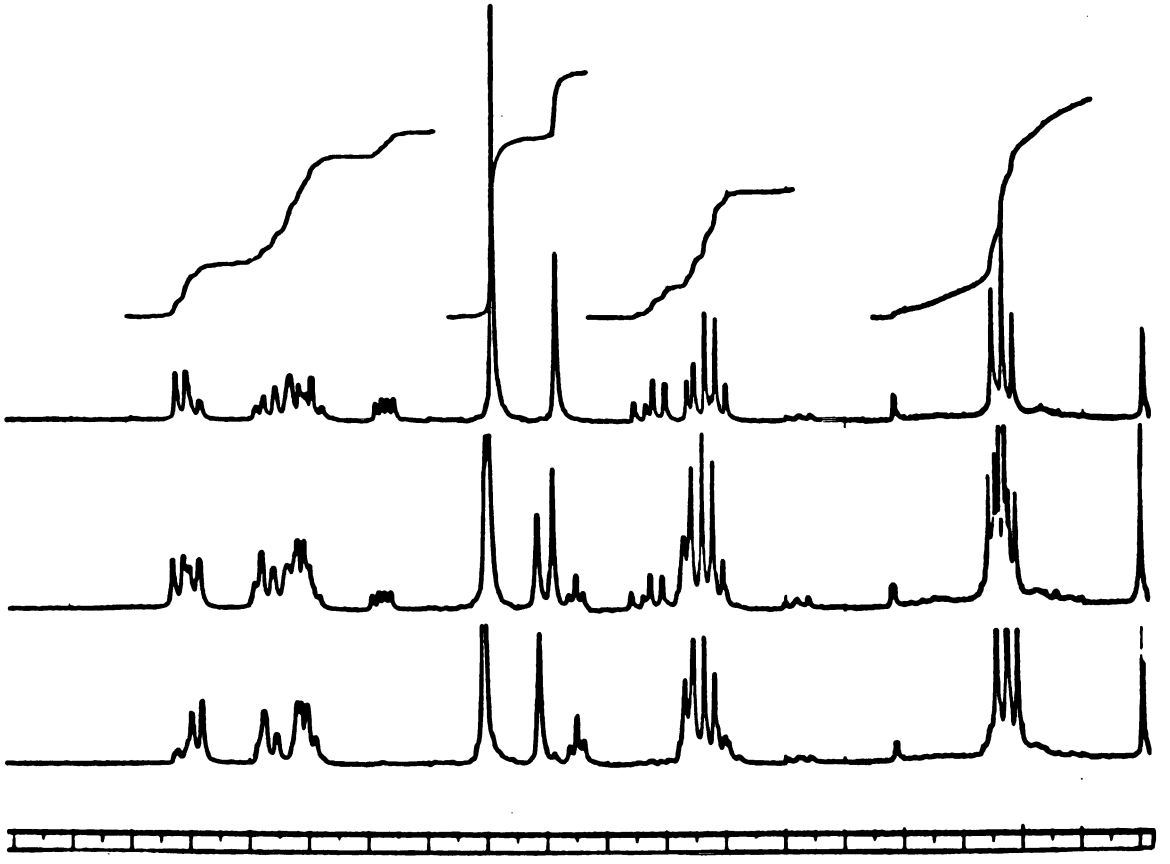

Figure 48. ^{1}H NMR Time Study of 149 Hydrolysis.

minutes is that of the diethylacetal. The triplet at δ1.18 represents the CH_3 protons of the two ethyl groups while the complex multiplet at δ3.62 represents the OCH_2- and N-CH_2-C hydrogens. The triplet at δ4.67 is the C-H which will become the aldehyde C-H after deprotection. The singlet at δ4.91 represents the benzylic CH_2 protons and the remaining multiplets from δ6.30 to 8.20 are characteristic of the thiophene and pyridine aromatic protons. The only peak which is easily monitored and has already changed by 5 minutes is the one at δ8.20 for the hydrogen on C-6 of the pyridine moiety. As shown in Figure 48, the acetal transforms to its product in approximately one half hour and no further change was observed at 24 hours. The proton of interest is that of the methine triplet at δ4.67. With time, this peak disappears and a new peak begins after 10 minutes at δ6.4. The doublet of doublets continues to grow along with the formation of new aliphatic shifts. The NMR spectrum after removal of the ethanol is illustrated in Figure 49. The previously hiden doublet for the N-CH_2-C protons at δ3.8 shifted downfield and split into a pattern for two nonequivalent protons. The aromatic region also spreads out but the resolution is too poor to make any definite assignments.

Based on these results, one must consider structures other than the desired aldehyde for the product. The observed changes in the aromatic region demonstrate that the aromatic rings are in some way interacting with the

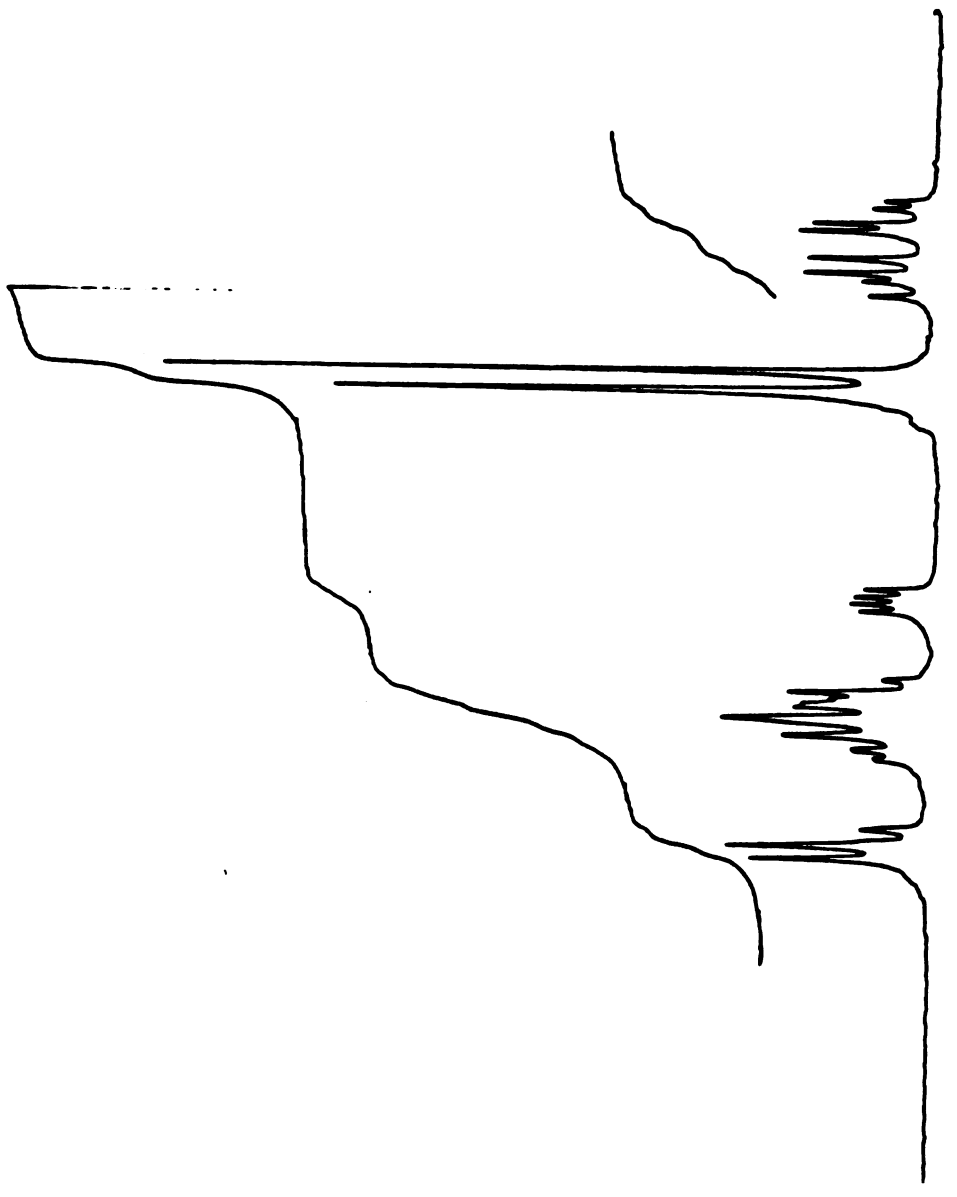

Figure 49. ^{1}H NMR Spectrum of Cyclized 131.

aldehydic carbon. The following structures have been proposed.

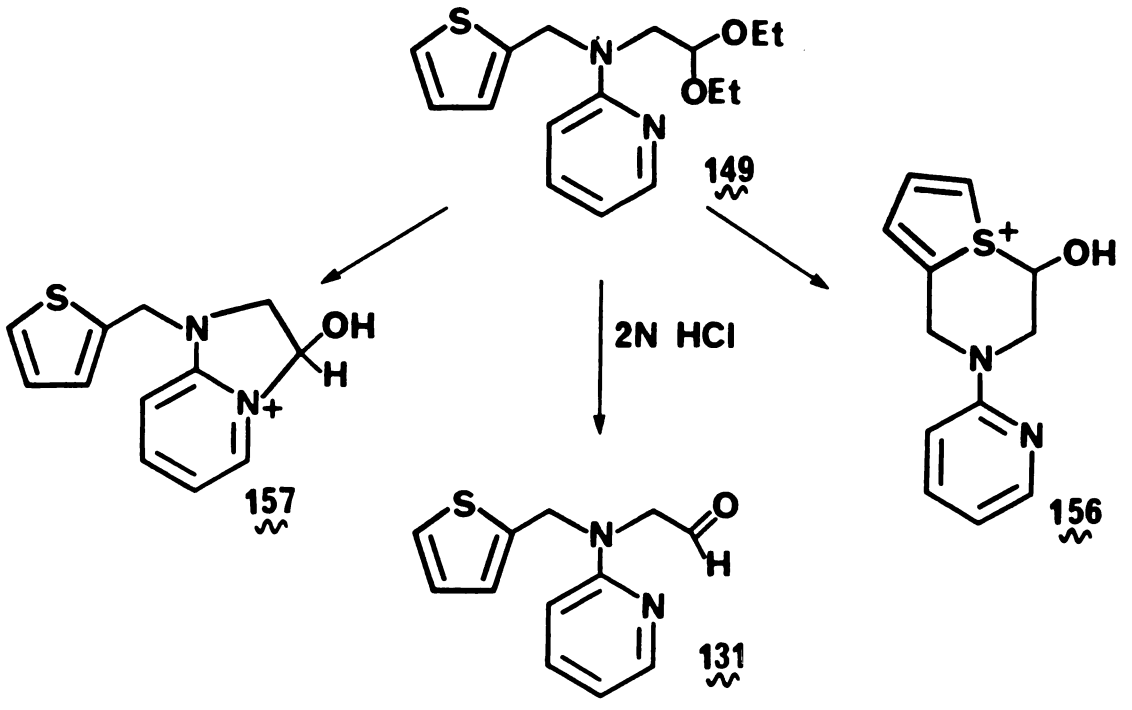

Stabilization of the carbonyl by interaction with a pyridine ring nitrogen has been previously investigated. A similar product was obtained from the treatment of the ketal 158 with 24% HBr to yield the imidazo-(1,2a)-pyridine 159 in 67% yield as a hygroscopic crystal.[201]

Imidazo-(1,2a)-pyridinium salts[202] have also been

synthesized from reactions of 2-(N-alkyl)aminopyridine and α -bromoketones.

The NMR spectrum of the "cyclized aldehyde" showed a slight downfield shift of the C-6 proton of the pyridine ring in the transformation from the diethylacetal to the cyclized structure. If the sulfur in the thiophene ring was involved in the carbonyl interaction, as in 156, no such effect should be observed in the pyridine ring. To characterize this interaction further, the same samples were dried and redissolved in DMSO-d_6. In Figure 50, the NMR spectra of the diethylacetal and the product of deprotection can be studied comparatively. The definite downfield shift of the C-6 proton signal (δ8.0 to 8.4) while maintaining the splitting by its neighboring proton on the aromatic ring is indicative of deshielding in the neighborhood of this proton. This downfield shift was maintained when the DMSO-d_6 was made acidic with DCl. Very little shifting of any of the peaks was observed upon acidification, leading one to conclude that no further protonation can occur.

Proton-proton decoupling demonstrated that the doublet of doublets at δ6.3 was coupled to the nonequivalent protons on the methylene attached to the nitrogen atom (see Figure 51). The arrows indicate the position of irradiation. In decoupling the methine proton a simple AB pattern (with some misleading residual O-CH_2 protons from ethanol) was seen for the methylene protons and no other peaks were affected. The reverse was observed in

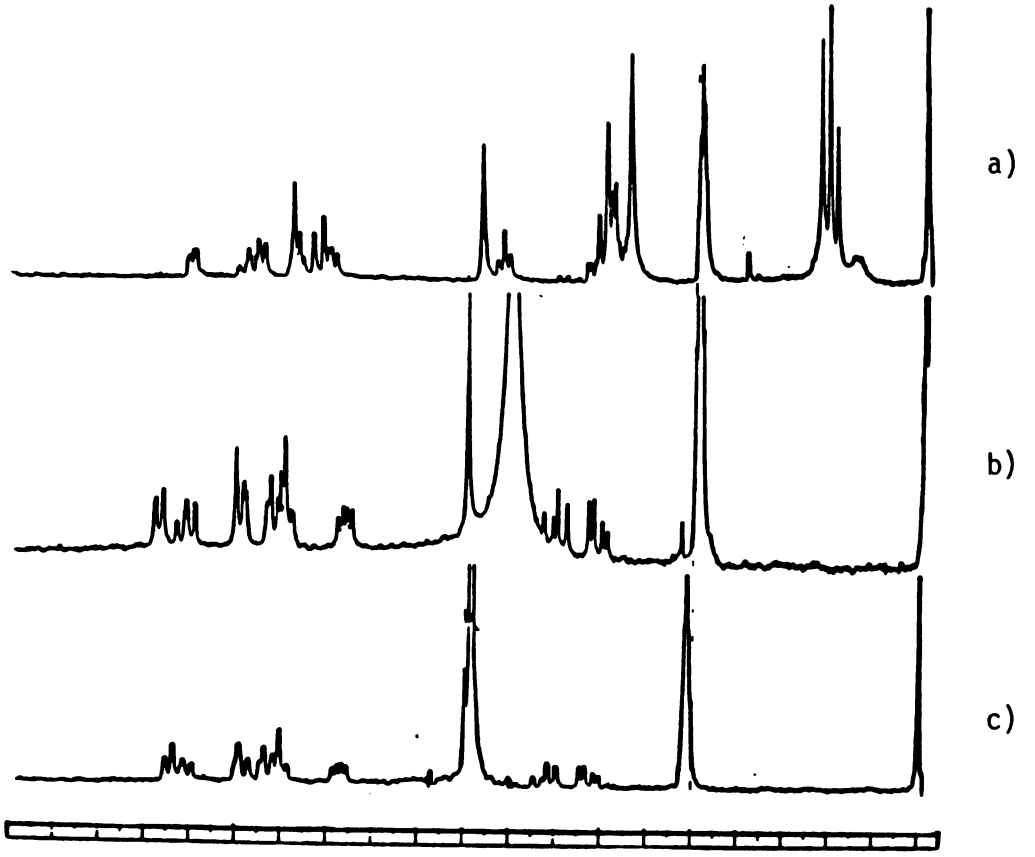

Figure 50. ^{1}H-NMR Spectrum of a) 149 b) Cyclized 131 c) 131 plus DCl in DMSO.

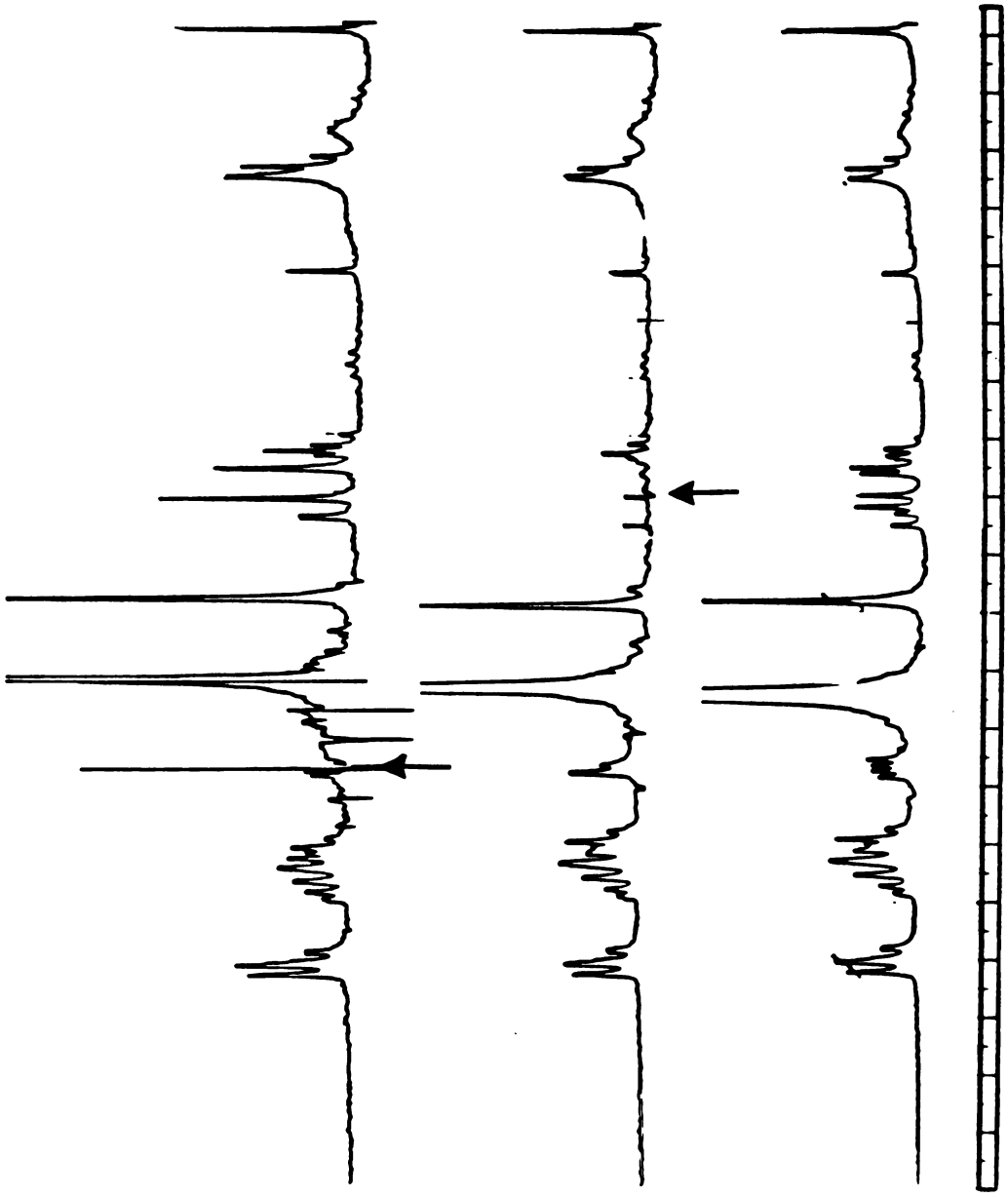

Figure 51. Proton-Proton Decoupling of Cyclized 131.

decoupling the methylene protons.

Upon neutralization of the cyclized sample with solid anhydrous potassium carbonate to approximately pH 7.0, the spectrum changes again to a non-aldehydic spectrum. As shown in Figure 52, the N-CH_2-C protons become equivalent and are coupled to the methine proton to yield a doublet. Conversely, the methine proton becomes a triplet but does not shift downfield to the expected aldehyde chemical shift. Further basification of the sample did not alter the spectrum. By extracting a neutral NMR sample with $CDCl_3$, the spectrum changes again (Figure 53) to yield an aldehydic proton at δ9.53 and the methylene changes to a singlet at δ4.5.

The explanation of these results may be simple acid/base chemistry, where the cyclized aldehyde (157) hydrates at neutral pH to form the aldehyde hydrate 160. The true aldehyde can only be liberated upon extraction into an organic solvent such as chloroform.

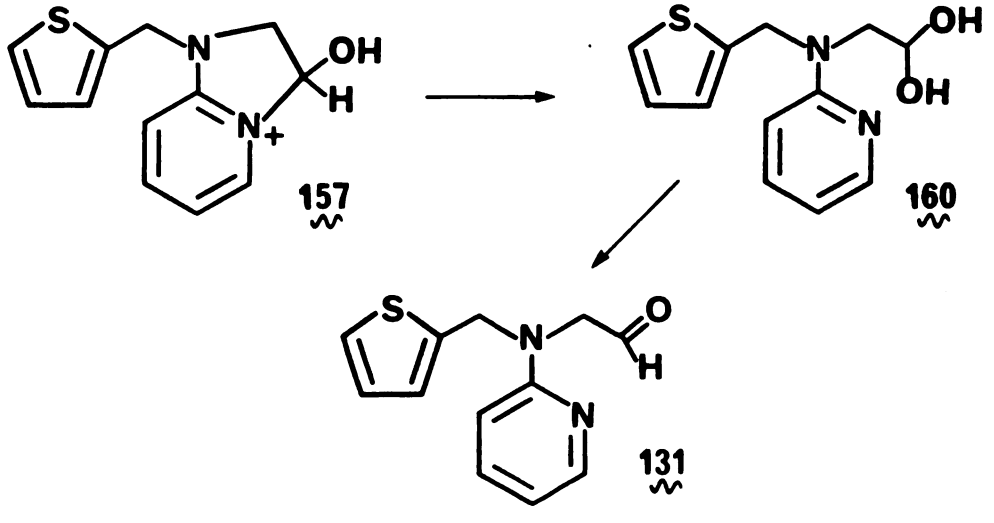

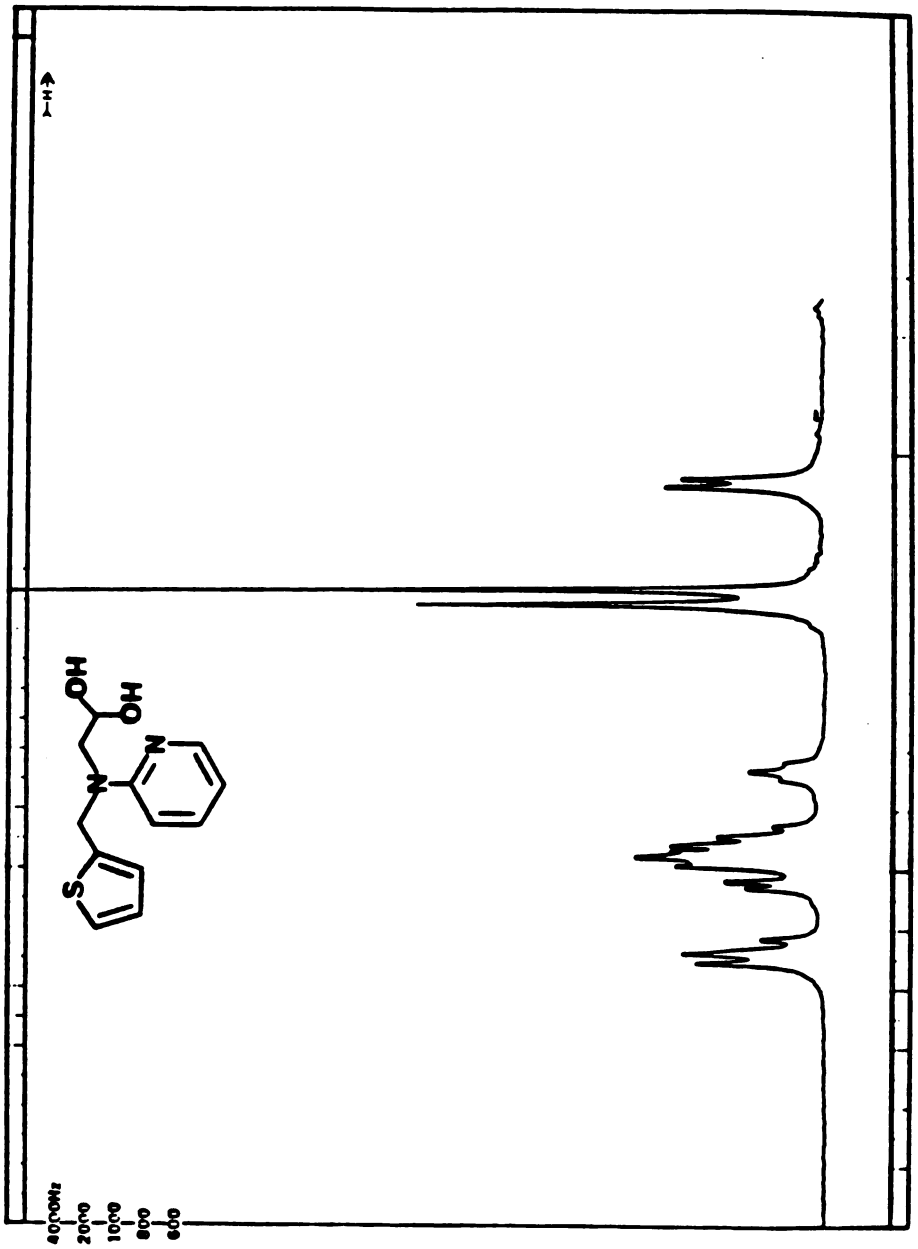

Figure 52. Aqueous ^{1}H-NMR Spectrum of 160.

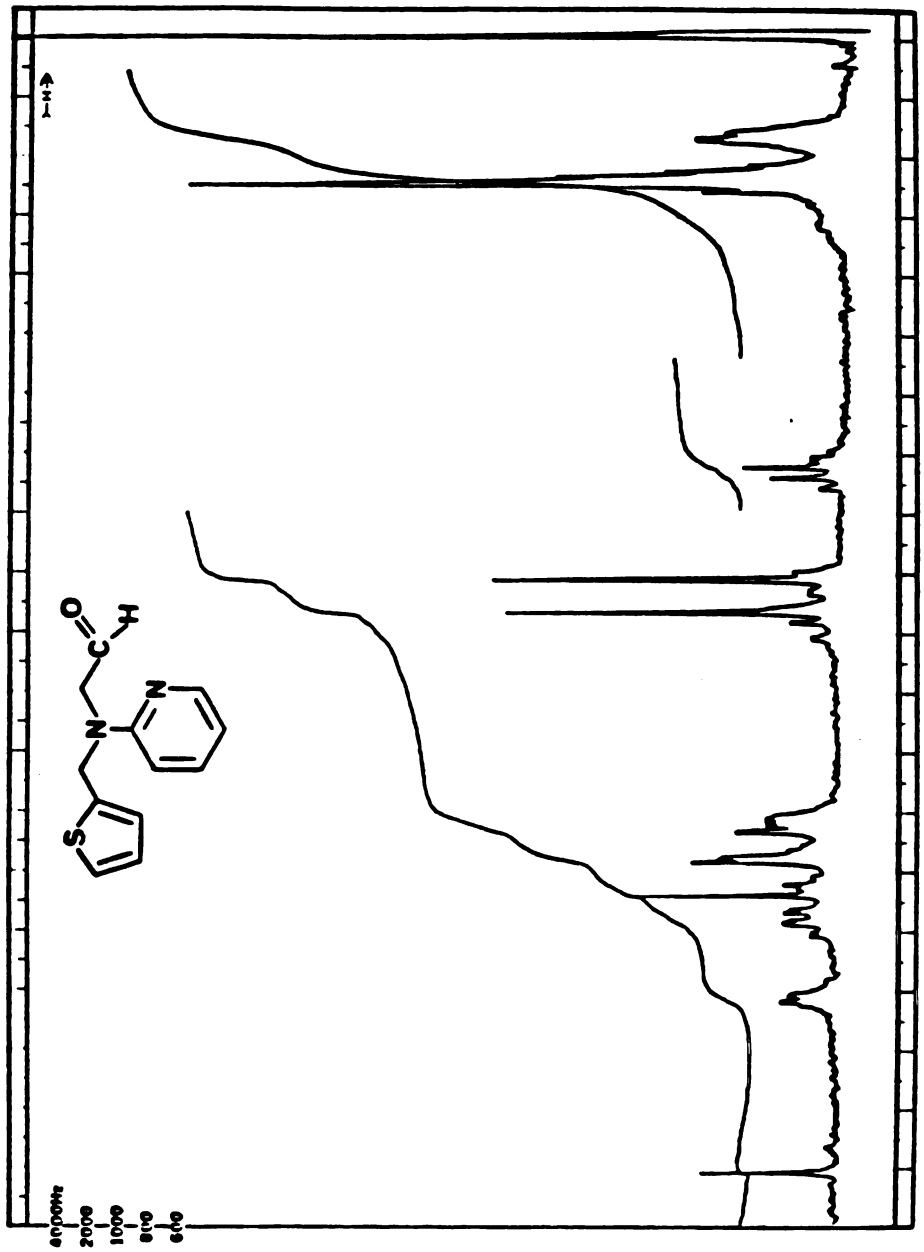

Figure 53. Organic ^{1}H-NMR Spectrum of 131.

The mass spectrum of the synthetic aminoacetaldehyde is exactly that obtained from the biological sample. The NMR of peak 13 (Figure 43) is dominated by pyridine peaks but if one looks closely at the baseline, one can see aromatic peaks resembling those of the cyclized aldehyde. From the NMR and mass spectral data, we conclude that the aminoacetaldehyde was formed in low but detectable levels from metabolic deamination of methapyrilene.

6). Methapyrilene (1).

Peak 14 was identified as methapyrilene by low resolution EIMS and HPLC retention time. The amount of methapyrilene present is very low, considering the amount of radioactivity associated with this peak. As determined by the GC assay, less than 3% of the methapyrilene distributes into the aqueous phase upon extraction of a microsomal incubate.

The remaining peaks gave anomalous NMR and/or mass spectra and appeared not to be resulting from methapyrilene metabolites. The analysis of the aqueous soluble metabolites led to the isolation and structure determination of four previously unknown metabolites. All of the metabolites resulted from the oxidation of methapyrilene in a position either alpha to a nitrogen or in the aromatic pyridine ring.

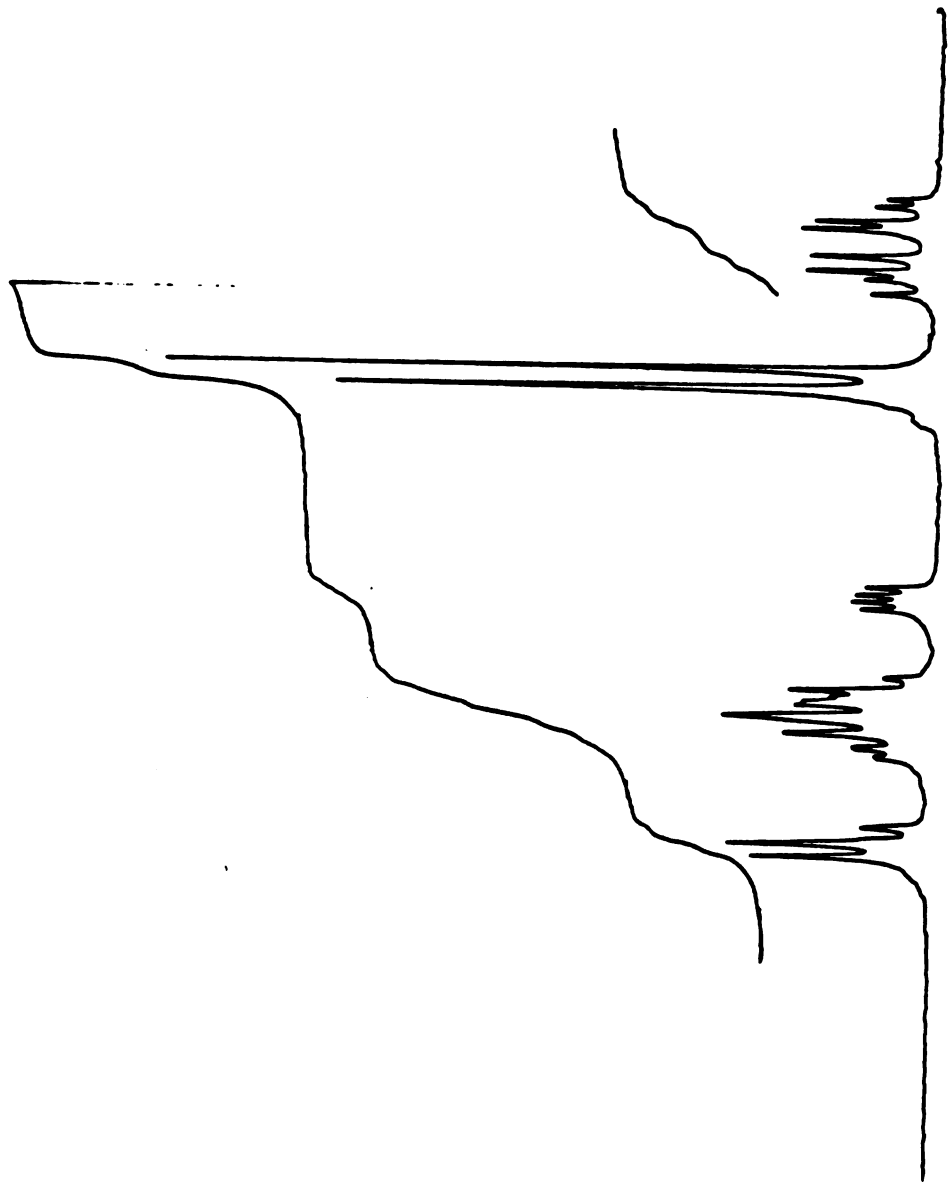

Figure 49. ^{1}H NMR Spectrum of Cyclized 131.

aldehydic carbon. The following structures have been proposed.

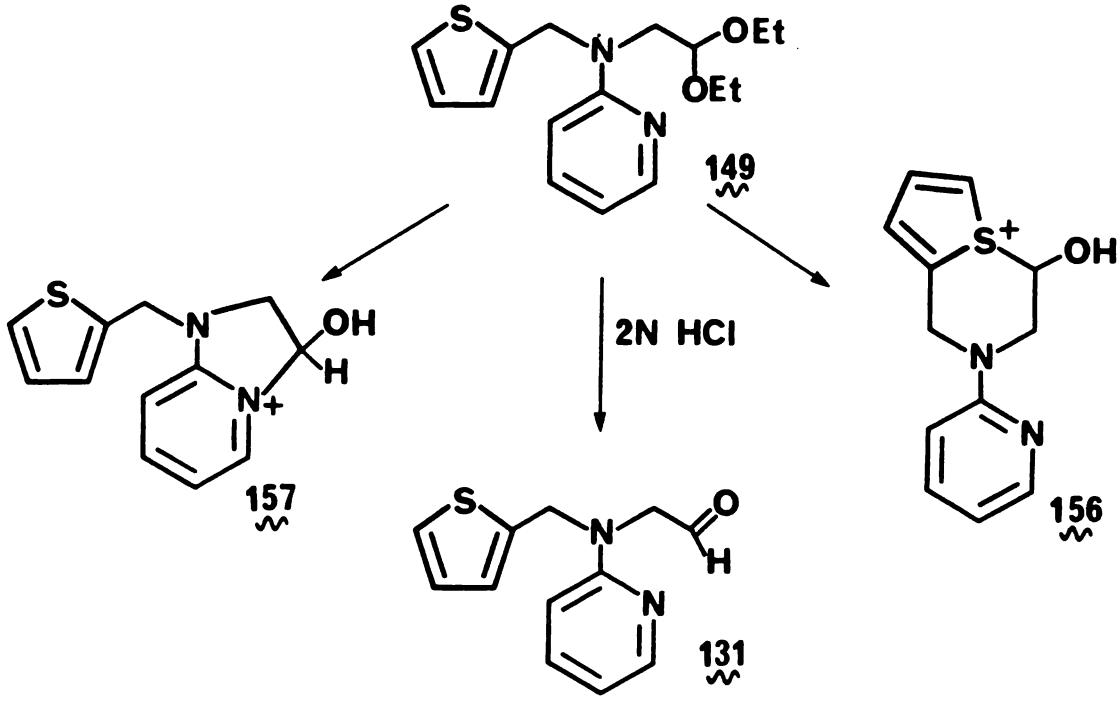

Stabilization of the carbonyl by interaction with a pyridine ring nitrogen has been previously investigated. A similar product was obtained from the treatment of the ketal 158 with 24% HBr to yield the imidazo-(1,2a)-pyridine 159 in 67% yield as a hygroscopic crystal.[201]

Imidazo-(1,2a)-pyridinium salts[202] have also been

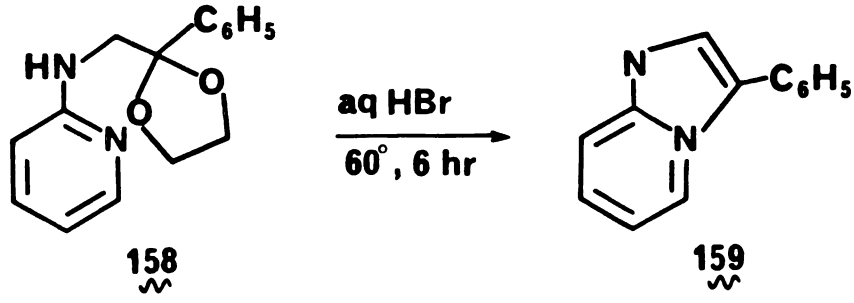

synthesized from reactions of 2-(N-alkyl)aminopyridine and α -bromoketones.

The NMR spectrum of the "cyclized aldehyde" showed a slight downfield shift of the C-6 proton of the pyridine ring in the transformation from the diethylacetal to the cyclized structure. If the sulfur in the thiophene ring was involved in the carbonyl interaction, as in 156, no such effect should be observed in the pyridine ring. To characterize this interaction further, the same samples were dried and redissolved in DMSO-d_6. In Figure 50, the NMR spectra of the diethylacetal and the product of deprotection can be studied comparatively. The definite downfield shift of the C-6 proton signal (δ8.0 to 8.4) while maintaining the splitting by its neighboring proton on the aromatic ring is indicative of deshielding in the neighborhood of this proton. This downfield shift was maintained when the DMSO-d_6 was made acidic with DCl. Very little shifting of any of the peaks was observed upon acidification, leading one to conclude that no further protonation can occur.

Proton-proton decoupling demonstrated that the doublet of doublets at δ6.3 was coupled to the nonequivalent protons on the methylene attached to the nitrogen atom (see Figure 51). The arrows indicate the position of irradiation. In decoupling the methine proton a simple AB pattern (with some misleading residual O-CH_2 protons from ethanol) was seen for the methylene protons and no other peaks were affected. The reverse was observed in

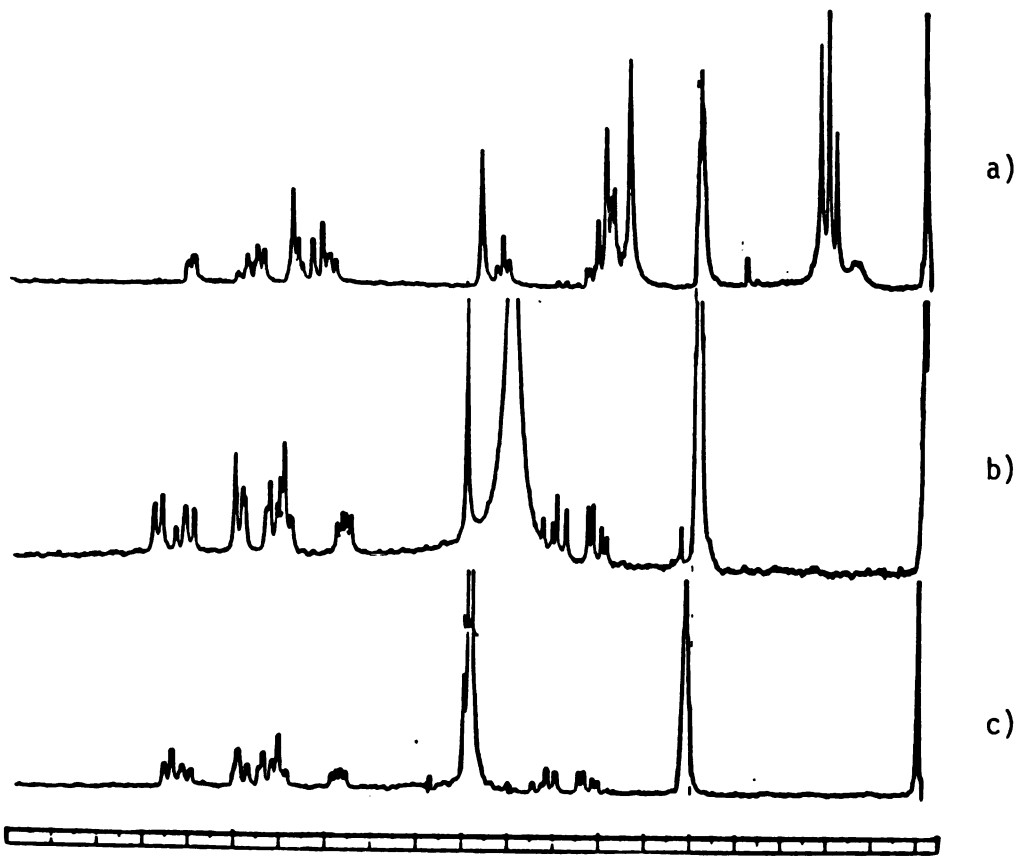

Figure 50. ^{1}H-NMR Spectrum of a) 149 b) Cyclized 131 c) 131 plus DCl in DMSO.

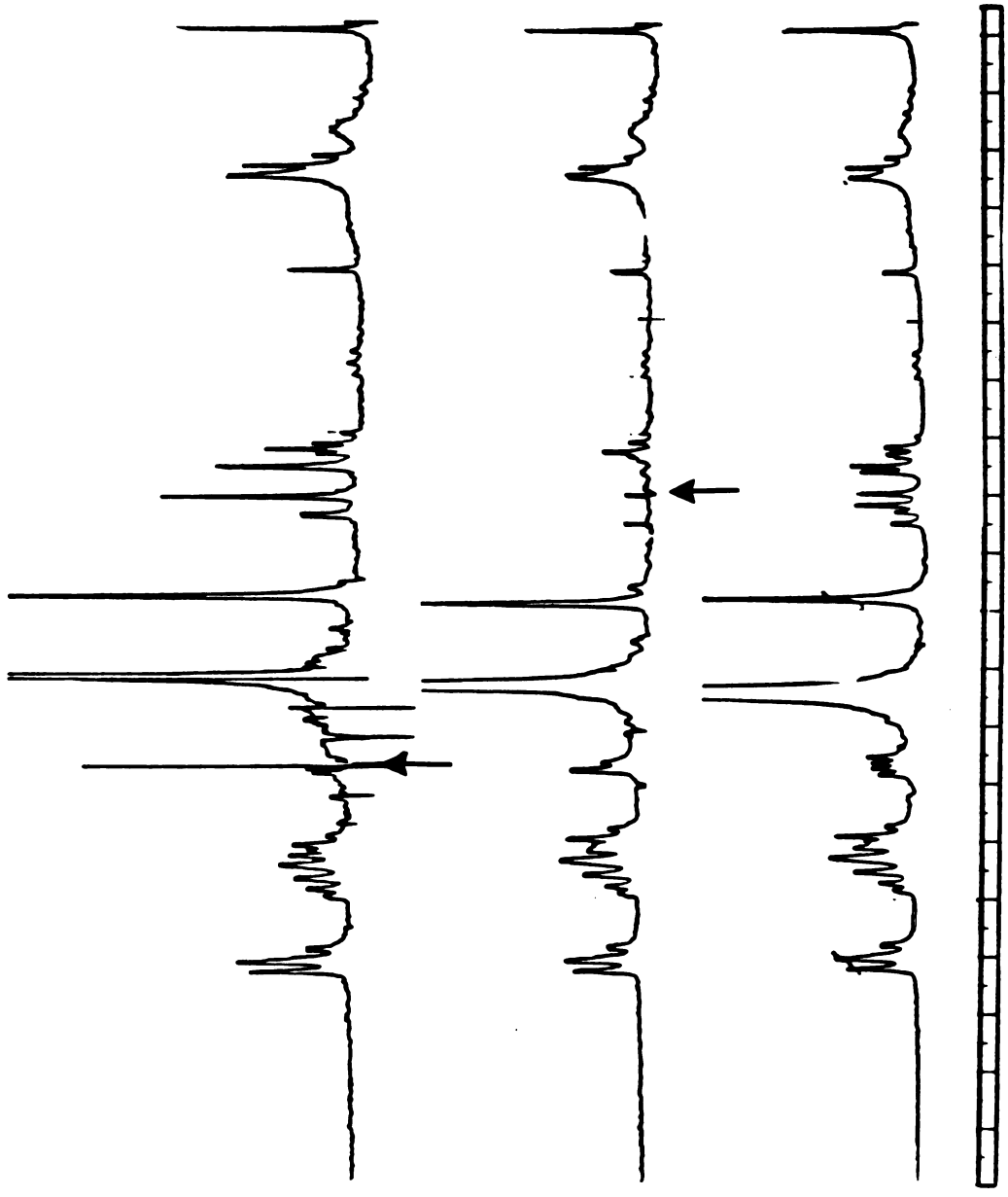

Figure 51. Proton-Proton Decoupling of Cyclized 131.

decoupling the methylene protons.

Upon neutralization of the cyclized sample with solid anhydrous potassium carbonate to approximately pH 7.0, the spectrum changes again to a non-aldehydic spectrum. As shown in Figure 52, the N-CH_2-C protons become equivalent and are coupled to the methine proton to yield a doublet. Conversely, the methine proton becomes a triplet but does not shift downfield to the expected aldehyde chemical shift. Further basification of the sample did not alter the spectrum. By extracting a neutral NMR sample with $CDCl_3$, the spectrum changes again (Figure 53) to yield an aldehydic proton at δ9.53 and the methylene changes to a singlet at δ4.5.

The explanation of these results may be simple acid/base chemistry, where the cyclized aldehyde (157) hydrates at neutral pH to form the aldehyde hydrate 160. The true aldehyde can only be liberated upon extraction into an organic solvent such as chloroform.

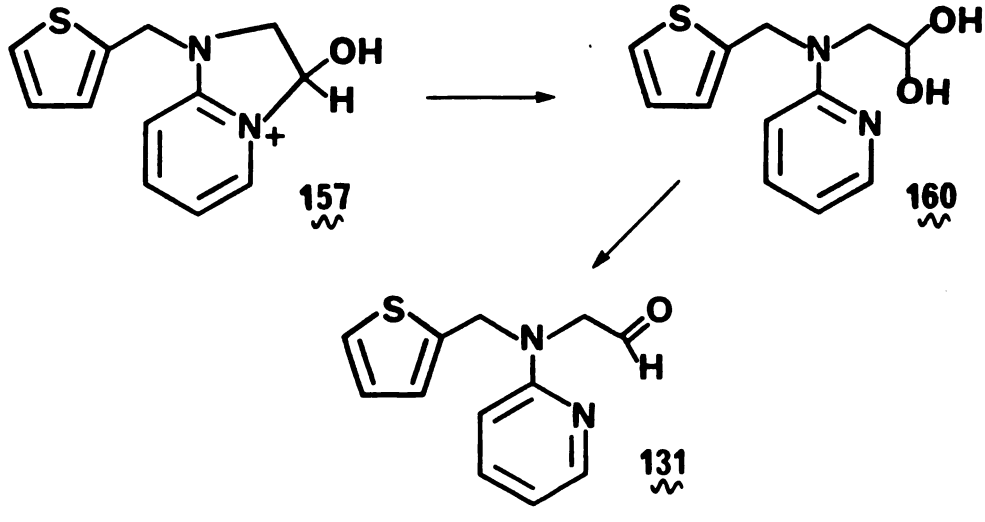

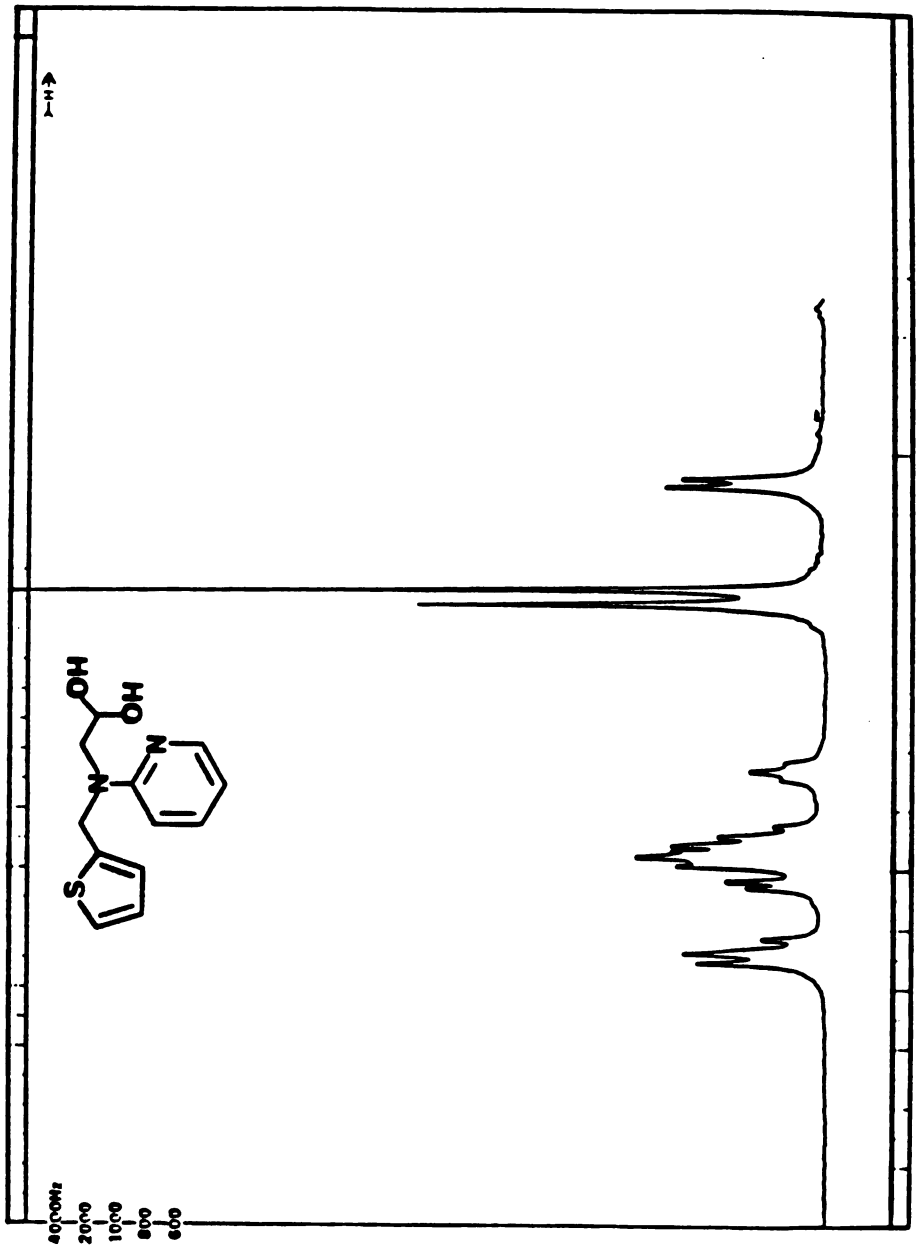

Figure 52. Aqueous ^{1}H-NMR Spectrum of 160.

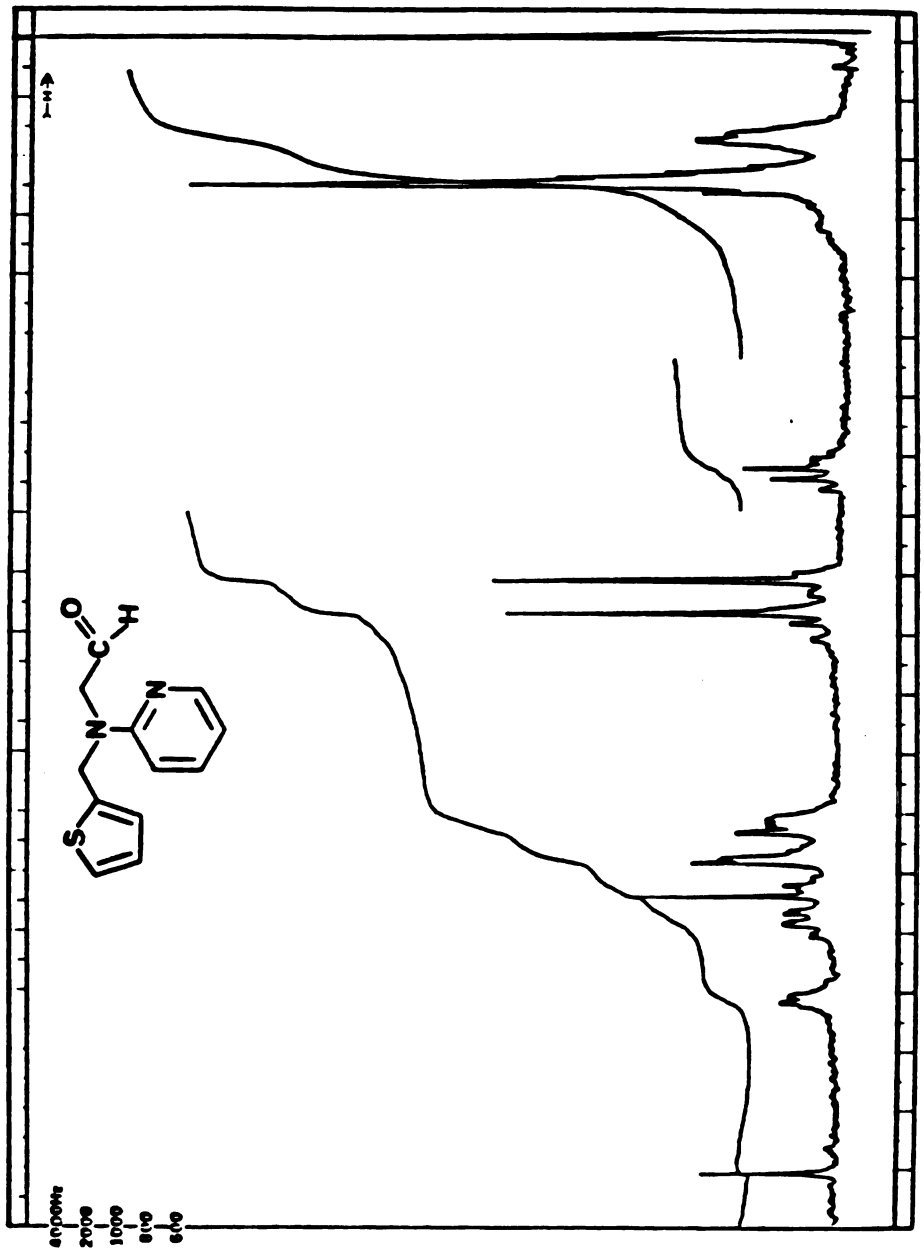

Figure 53. Organic ^{1}H-NMR Spectrum of 131.

The mass spectrum of the synthetic aminoacetaldehyde is exactly that obtained from the biological sample. The NMR of peak 13 (Figure 43) is dominated by pyridine peaks but if one looks closely at the baseline, one can see aromatic peaks resembling those of the cyclized aldehyde. From the NMR and mass spectral data, we conclude that the aminoacetaldehyde was formed in low but detectable levels from metabolic deamination of methapyrilene.

6). Methapyrilene (1).

Peak 14 was identified as methapyrilene by low resolution EIMS and HPLC retention time. The amount of methapyrilene present is very low, considering the amount of radioactivity associated with this peak. As determined by the GC assay, less than 3% of the methapyrilene distributes into the aqueous phase upon extraction of a microsomal incubate.

The remaining peaks gave anomalous NMR and/or mass spectra and appeared not to be resulting from methapyrilene metabolites. The analysis of the aqueous soluble metabolites led to the isolation and structure determination of four previously unknown metabolites. All of the metabolites resulted from the oxidation of methapyrilene in a position either alpha to a nitrogen or in the aromatic pyridine ring.

C. Metabolites Not Found

In addition to the metabolites discussed in the previous sections, a number of other potential metabolites were synthesized and characterized. Some of these compounds were found as metabolites in rabbit microsomal incubates and yet were not isolated in the present rat studies.

1). N-Formyl-N-(2'-thienylmethyl)-2-aminopyridine (130).

The formation of the N-formyl-N-(2'-thienylmethyl)-2-aminopyridine (130) was not observed as a rat microsomal metabolite of methapyrilene as it had been with rabbit microsomes.[71] Formylation of aromatic amines has been observed[203] but acylations of this type are not commonly found.

N-(2'-Thienylmethyl)-2-aminopyridine (91) was utilized in the synthesis of this N-formyl metabolite. Figure 54 shows several synthetic approaches to the N-formyl derivative. Initially, the amine was treated with formic acid in acetic anhydride.[204] The product isolated from preparative silica gel TLC gave a mass spectrum corresponding to that of the parent amine while the NMR spectrum demonstrated a downfield singlet at δ8.38. This downfield peak disappeared upon drying the sample under vacuum and the IR spectrum was indicative of a formate salt of the amine (161).

Alternatively 91 was heated under reflux with ethyl formate in xylenes equipped with a soxlet filled with molecular sieves to remove water.[205] After three days

at reflux, only starting material was obtained. The amine was heated under reflux for three days in freshly distilled ethyl formate and again only starting material was recovered. A more active formylating agent, chloral, was then used under amidation condition similar to those used with ethyl formate.[206] Again, only starting amine was obtained.

Figure 54. Synthetic Attempts at 130.

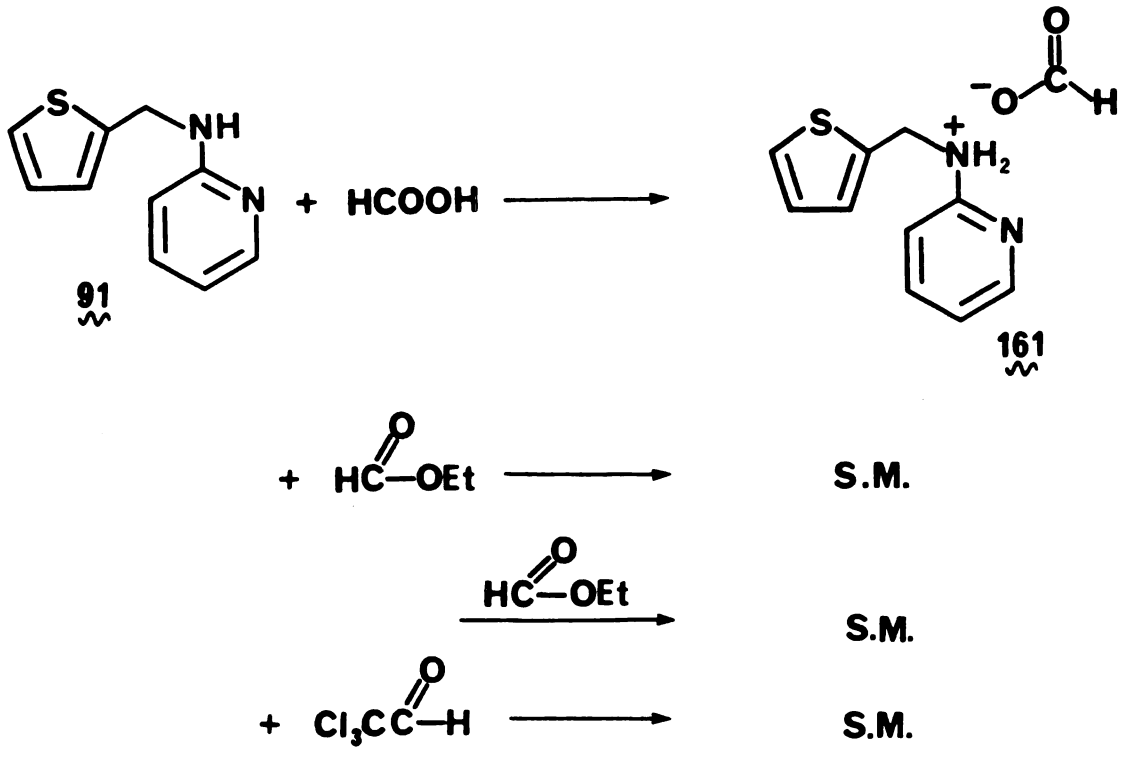

These studies were a good indication of the low nucleophilicity of 2-aminopyridine analogs. As discussed previously, the secondary amine was then treated with sodium hydride under anhydrous conditions to form the amine anion. One equivalent of chloral was then added and bulb to bulb

distillation of the resulting mixture gave the desired N-formyl compound in 72% yield. The NMR spectrum (Figure 55) showed the formyl proton signal at δ9.24 while the IR spectrum gave the characteristic carbonyl stretch at 1665 cm^{-1}. The EIMS showed a parent ion at mass 218 and the subsequent loss of CHO led to the base peak at m/e 189. The compound proved to be unstable over long periods of time resulting in the original secondary amine.

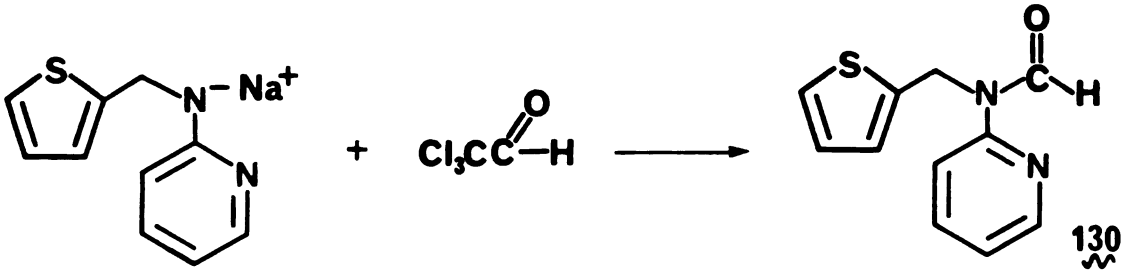

2). Methapyrilene N-Oxide (128).

The N-oxide of methapyrilene is a known metabolite from rabbit liver microsomes.[71] In analyzing the metabolites from rat studies, it was necessary to synthesize the N-oxide as a standard. The synthetic approach used was similar to that of Ziegler[71] Methapyrilene was dissolved in methanol and cooled to 0° at which time aqueous hydrogen peroxide was added. Additional aliquots of hydrogen

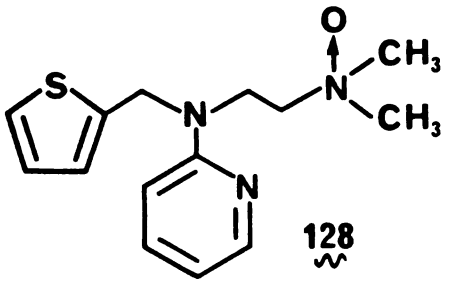

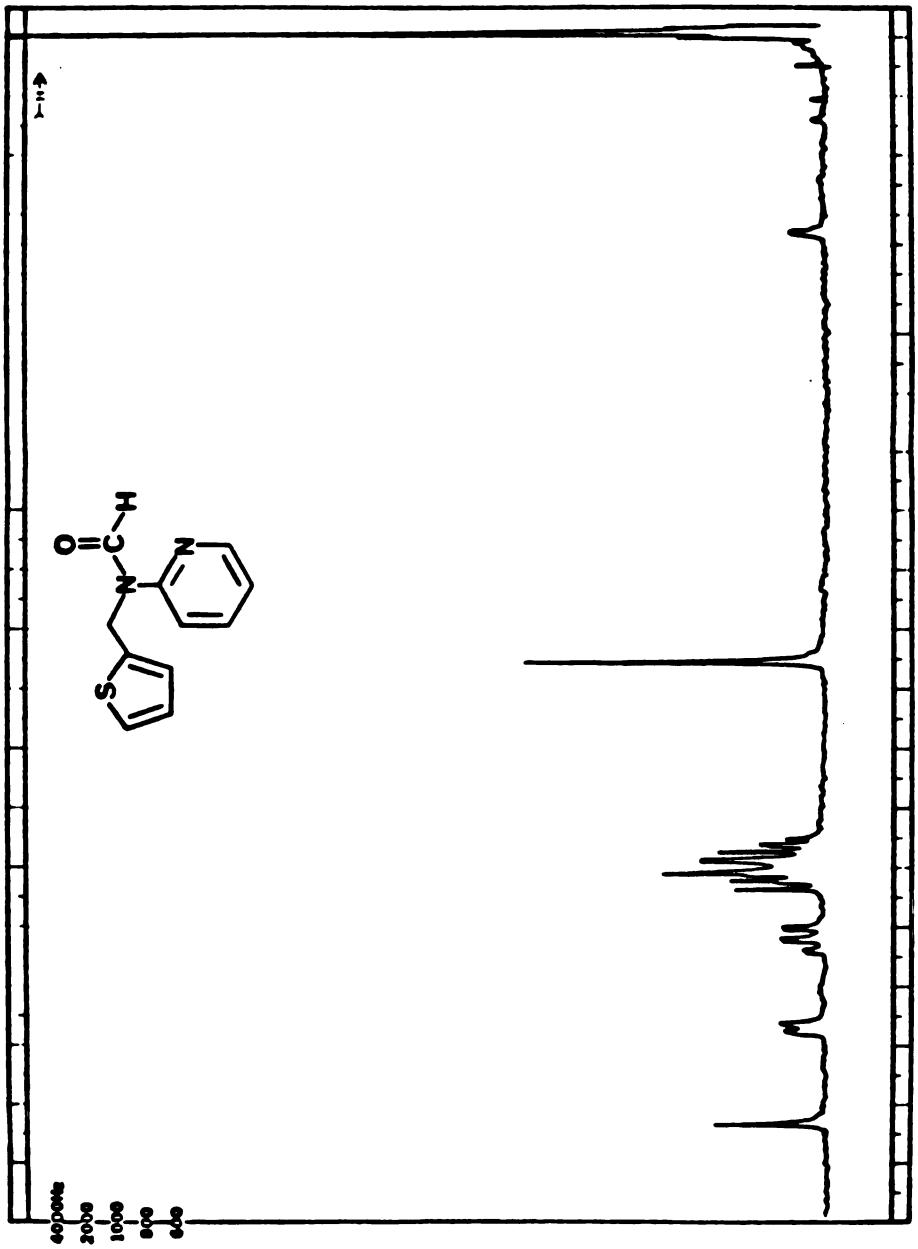

Figure 55. ^{1}H-NMR Spectrum of 130.

peroxide were added over the next three days as the reaction mixture stirred in a flask. The reaction was judged complete when no pink color was obtained when an aliquot was treated with aqueous phenolphthalein. Platinum on carbon mesh was added to destroy the excess H_2O_2 and the quenching considered complete when gas evolution ceased.[207] The catalyst was removed by filtration through celite and the product was concentrated under vacuum. The NMR spectrum of the N-oxide (Figure 56) corresponds directly with that previously reported.[71,78] The product was isolated as a monohydrate, in that C,H,N analysis yields one water molecule per methapyrilene N-oxide and removal of the water with K_2CO_3 led to an oil which would not crystallize.

3). N-(N',N'-Dimethylacetamido)-2-aminopyridine (162).

Since both oxidative debenzylation and amide formation were observed metabolically, the resultant product of multiple oxidation, namely N-(N',N'-dimethylacetamido)-2-aminopyridine (162) was synthesized as a potential methapyrilene metabolite. The synthesis proved to be more difficult than first expected. The usual coupling procedure involving the sodium salt of 2-aminopyridine and N,N-dimethylchloroacetamide led to a complex mixture of products, many of which were colored. The failure to form the sodium salt of 2-aminopyridine could

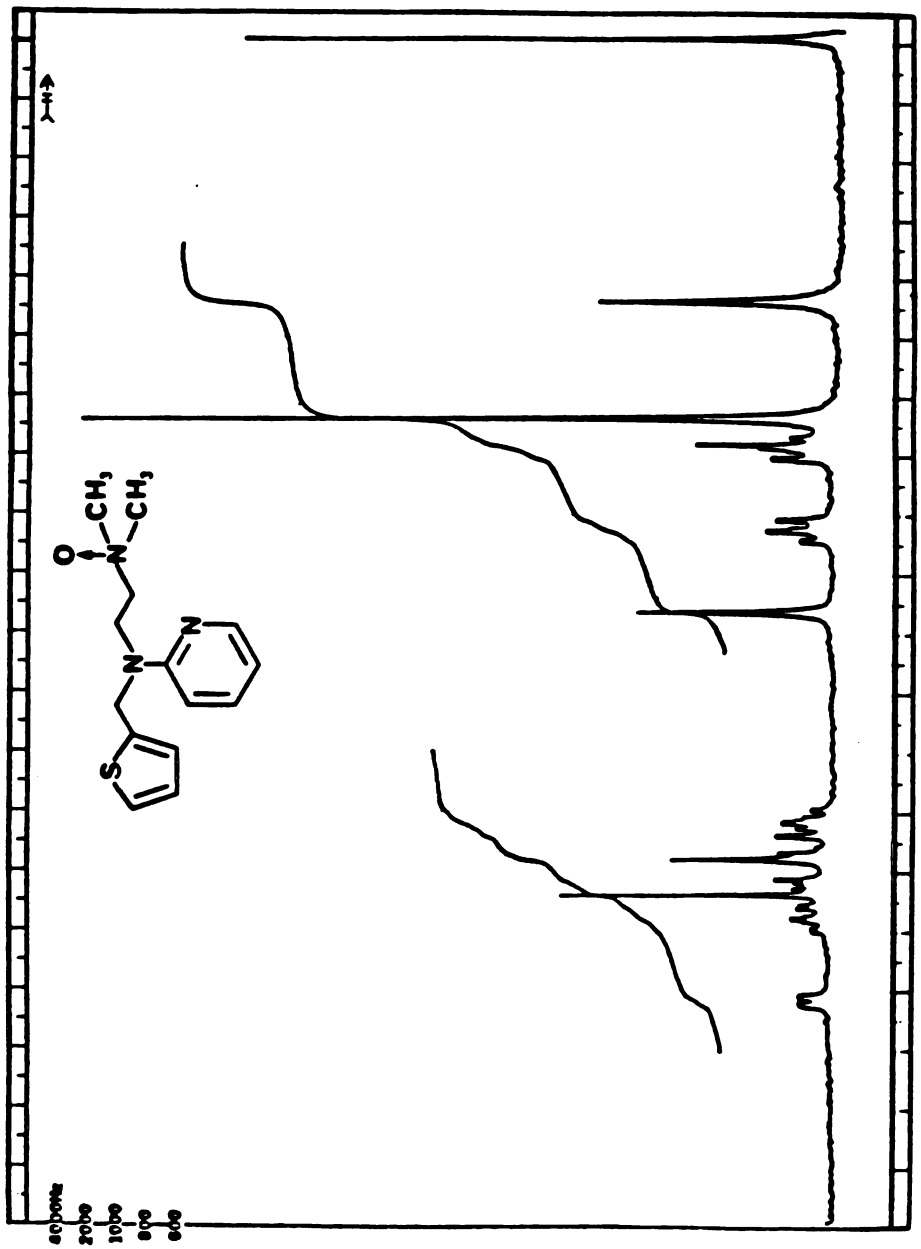

Figure 56. ^{1}H-NMR Spectrum of 128.

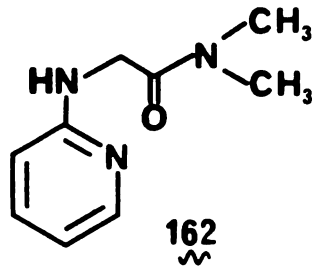

162

lead to a pyridine ring nitrogen alkylation which might then cyclize through the mechanism shown in Scheme 22. The final dehydration step of this reaction might lead to the imidazo-(1,2a)-pyridine species (163) which would be expected to demonstrate absorbance at long wavelength.

Scheme 22. Possible Cyclization to Form an Imidazo-(1,2a)-pyridine.

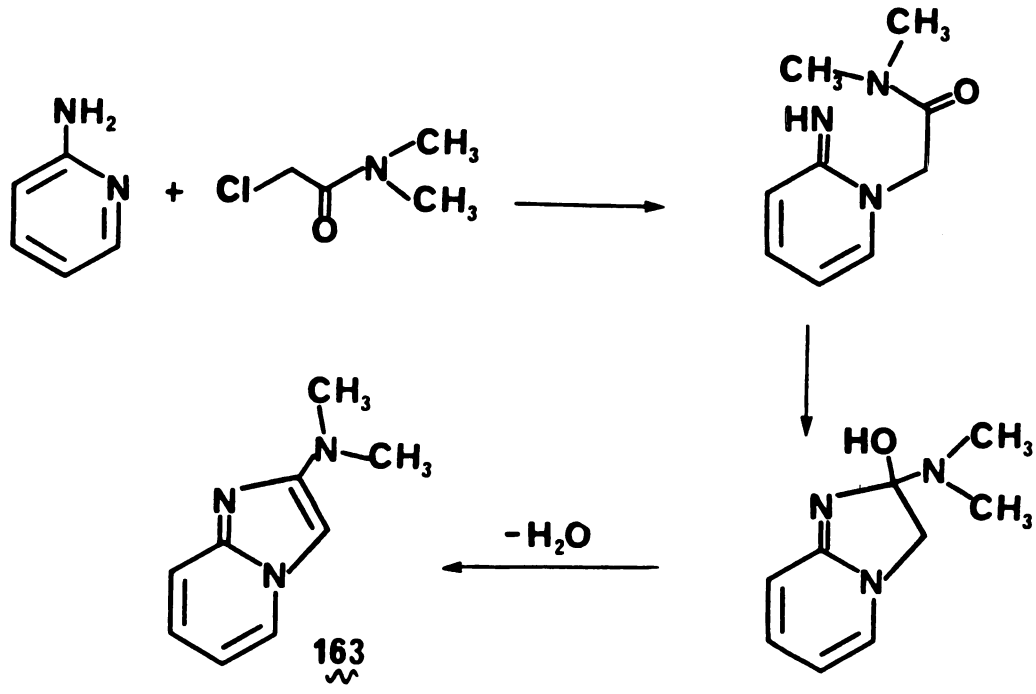

163

Alternatively, the anion of 2-aminopyridine was formed by reaction with N-butyllithium at -70°. The α -chloroacetamide was added to the salt at 0° and then the reaction mixture was allowed to come to room temperature

with stirring. A precipitate formed, presumably LiCl, which was removed by filtration after 18 hours. After concentration under vacuum, the resulting oil was distilled* by the Kugel Rohr technique. This treatment destroyed the product. In the next attempt, the reaction mixture was chromatographed and the desired prcduct crystallized directly from the column eluant fractions. The NMR spectrum and EIMS are shown in Figure 57 and 58, respectively. The N-methyl singlets are nearly equivalent at δ3.05 and the methylene protons occur as a doublet (δ4.15) coupled to the NH proton. The pyridine ring protons exhibit the expected chemical shifts. Upon addition of D_2O to the sample the N-H proton disappears and the methylene protons converge to a singlet.

The mass spectral fragmentation pattern is shown in Figure 58. The parent ion at mass 179 undergoes a loss of the $N-(CH_3)_2$ group to yield a fragment at m/e 134 and the amide group fragments to generate the base peak ion at m/e 107. The pyridine ring, as usual, results in an ion at m/e 79.

Neither this mass spectrum nor the NMR spectrum were observed in the analysis of microsomal incubates.

4). N-(2-Pyridyl)-N-(2'-thienylmethyl)glycine (164).

The aminoacetaldehyde metabolite (131) of methapyrilene was observed in such low quantities that the existence of either its oxidation or reduction product was in question.

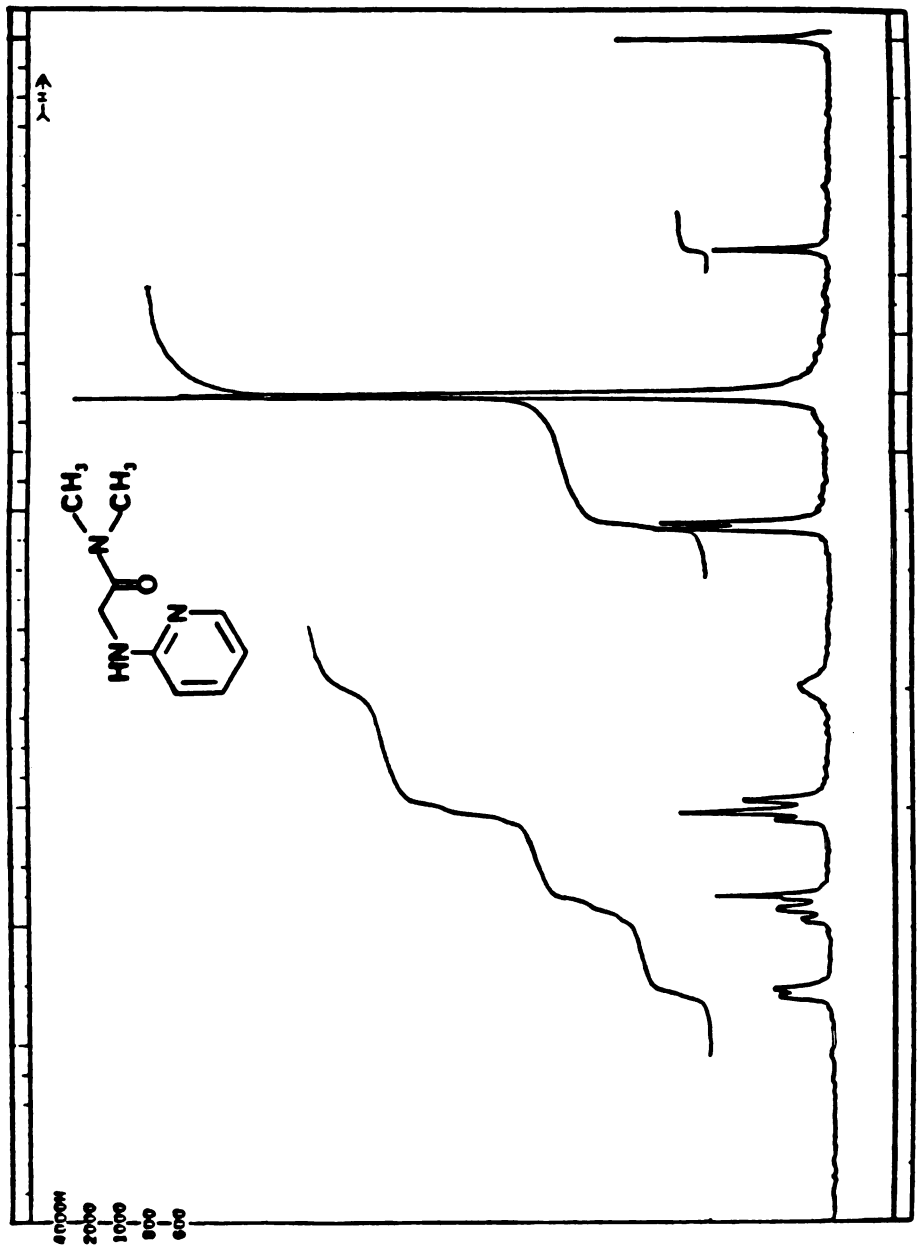

Figure 57. ^{1}H-NMR Spectrum of 162.

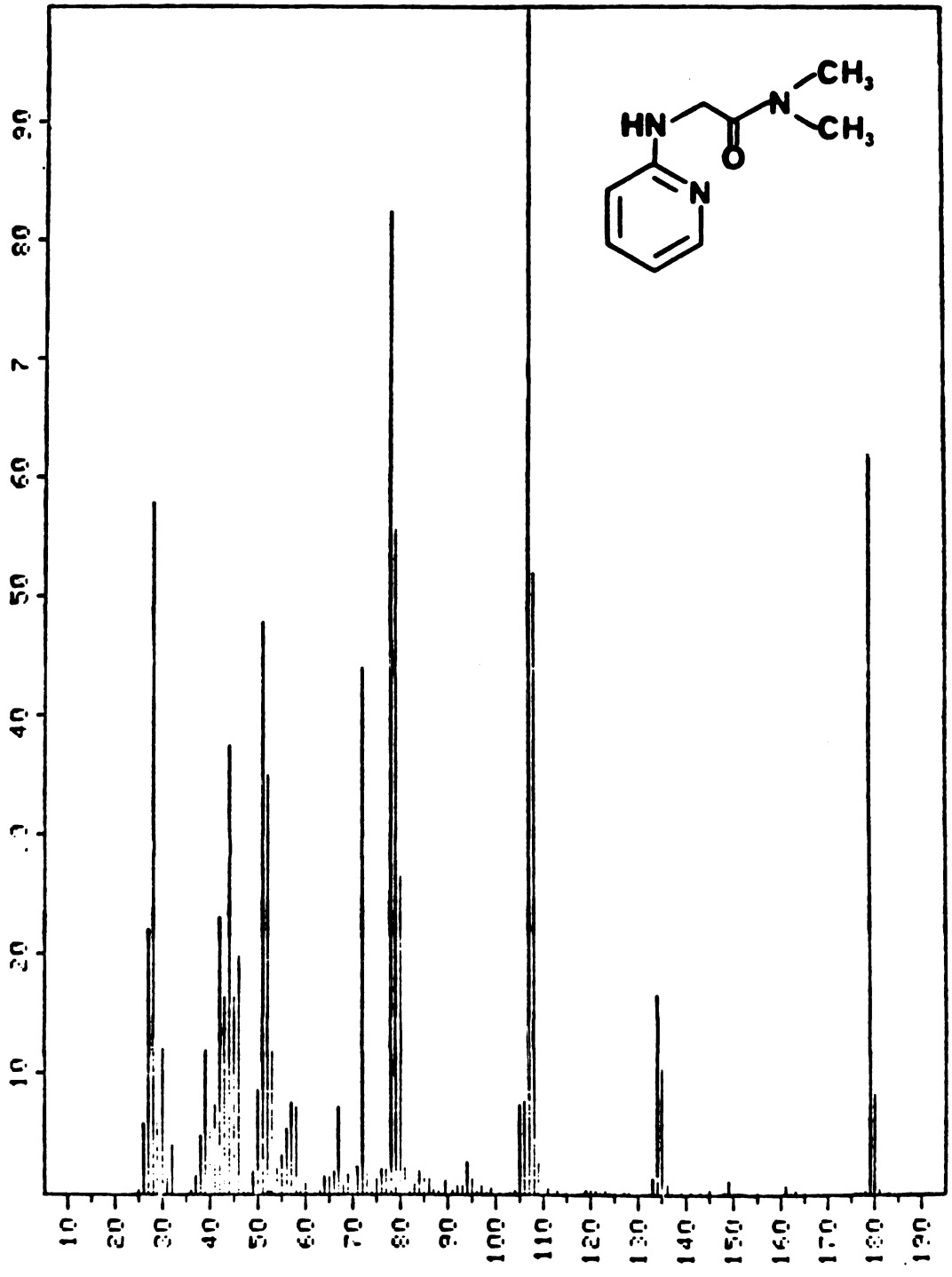

Figure 58. EIMS of 162.

The corresponding carboxylic acid derivative (164) was approached synthetically from numberous pathways.

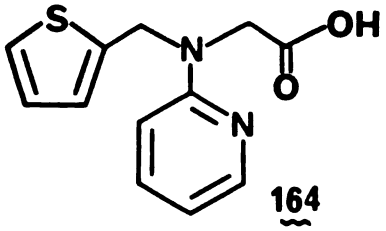

164

The first approach was to add a two carbon chain to the readily available N-(2'-thienylmethyl)-2-aminopyridine (91). Figure 59 illustrates the reactions run in the attempt to synthesize a carboxylic acid equivalent. Iodoacetic acid was first used in the coupling to the sodium salt of 2-aminopyridine with an additional equivalent of sodium hydride to neutralize the carboxylic acid. Starting amine was reisolated and most likely the iodoacetic acid salt was too insoluble in p-dioxane to react. Condensation with ethyl bromoacetate gave a poor yield of the desired product 165. As a synthetic intermediate much greater quantities

Figure 59. Reactions Leading to an Equivalent of 164.

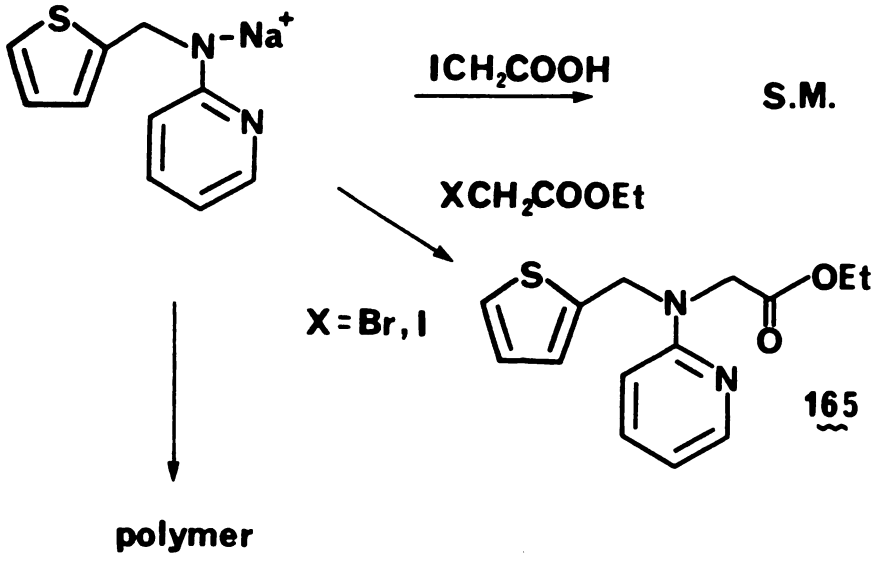

would be required, for which reason this reaction was not considered a viable route. Similar results were obtained with ethyl iodoacetate. The use of bromoacetonitrile produced polymeric material, presumably via carbanion condensation reactions.

An altogether different route to the cyanomethyl adduct was tried as shown below.[209] The reaction resembles a Strecker synthesis. First the formaldehyde and sodium bisulfite were allowed to react and the resulting intermediate was treated with the amine 91. After stirring two hours, the reaction mixture was treated with sodium cyanide. Unfortunately, only starting material was isolated although the NMR spectrum of the reaction mixture seemed to show two distinct CH_2-groups. Once again, the low nucleophilicity of 91 may be considered responsible for the low reaction rate.

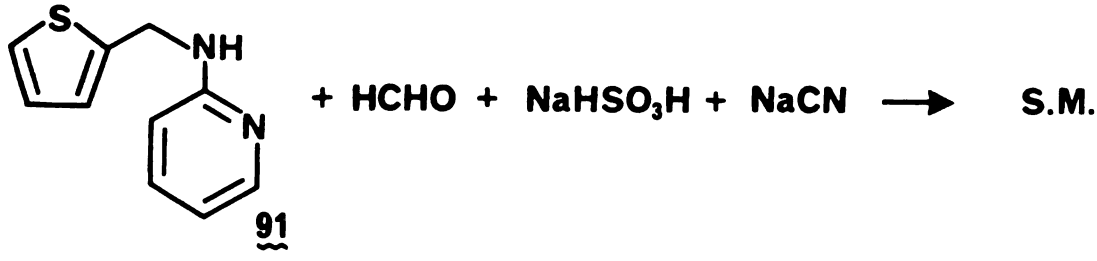

91

Based on these results, we tried to attach the two carbon chain to 2-aminopyridine first and then add on the thienylmethyl moiety. As shown below, the sodium salt of 2-aminopyridine was treated with ethyl bromoacetate to yield 10% of the desired N-(2-pyridyl)glycine ethyl ester (166). Because the yield again was too low to derive the needed

intermediate, we decided to look at the other reaction products. No single product occurred in large quantities and most of the NMR spectra were unintelligible. One poorly resolved spectrum resembled that of a cyclized material in which the ethyl group of the ester was absent.

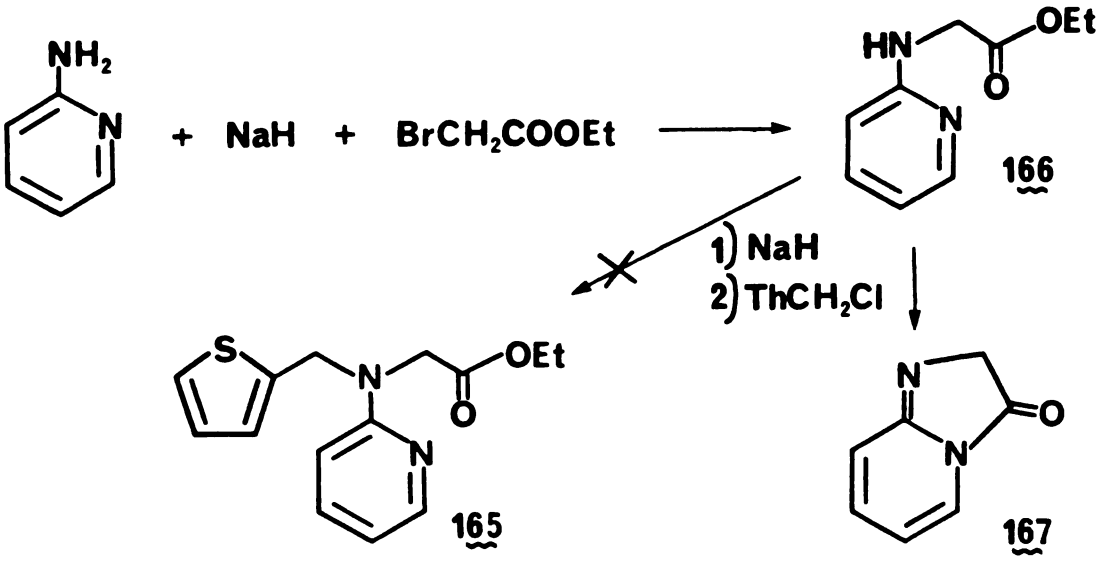

Nucleophilic displacement of the ethoxy group may have caused the low yield of the product in the appropriate reactions by producing a polar amide 167 that might be water soluble. If in fact this is the problem, then the ethyl ester would not be the correct approach to the carboxylic acid metabolite 164. However, the 300 mg of 166 in hand was treated with sodium hydride followed by addition of 2-chloromethylthiophene. Again, only starting amine was obtained.

To decrease the reactivity of the ester towards cyclization, synthesis of the ortho ester 168 was attempted. As shown in Scheme 23, trimethyl orthoacetate was treated

with bromine in pyridine[210] to give trimethyl bromoorthoacetate (169) in 28% yield. The sodium salt of N-(2'-thienylmethyl)-2-aminopyridine was then condensed with 169 but the reaction yielded only starting amine. Most likely, the ortho ester was too bulky to allow nucleophilic displacement of the bromine.

Scheme 23. Synthesis of the Orthoester 168.

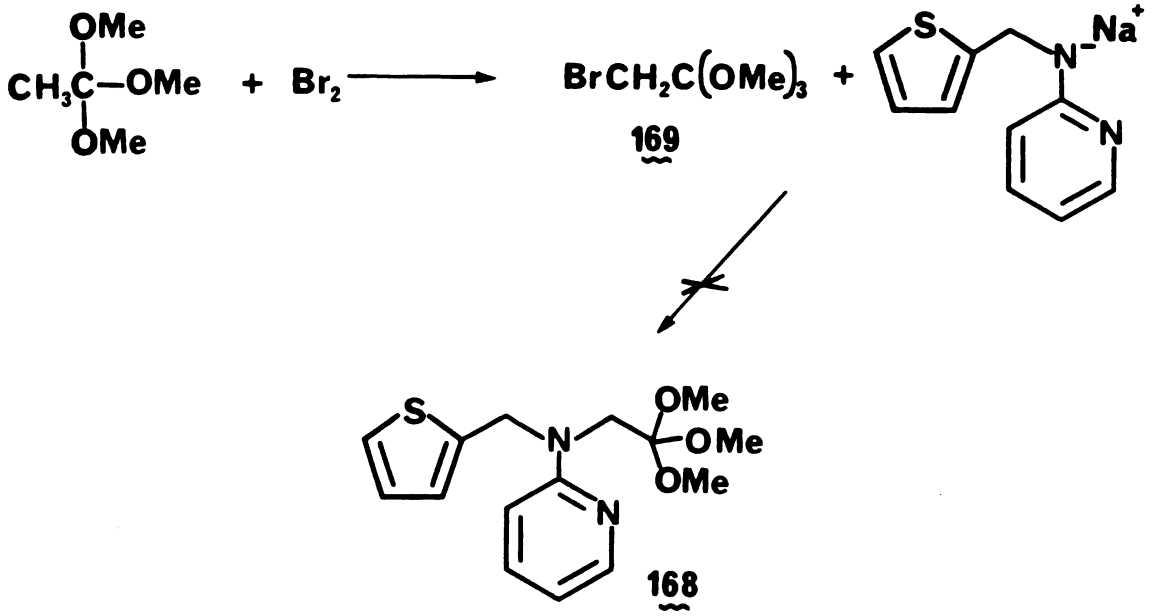

Direct oxidation of the synthetic aldehyde (131) was also attempted. The freshly prepared aldehyde was treated with CrO_3/C in toluene for 24 hours at reflux. No change was observed by TLC and reaction for an additional four days in the presence of excess CrO_3/C did not oxidize the aldehyde. Stronger oxidizing agents were not utilized so that pyridine ring oxidation could be avoided.

The carboxylic acid was finally synthesized through the dimethylacetamide 129. Hydrolysis of the amide with 2 N HCl for 5 minutes led to a green solution which, when extracted

with methylene chloride, yielded NMR spectrum (Figure 60) and CIMS indicative of the desired carboxylic acid. The NMR spectrum shows two methylene singlets at δ 4.28 and 4.26, corresponding to the N-CH_2-COOH and Th-CH_2-N protons, respectively. The complex multiplet between δ5.29 -8.09 is that expected for the methapyrilene aromatic protons. The carboxylic acid proton is present as a singlet at δ 9.51.

The CIMS gave the carboxylic parent ion at m/e 249 with the major fragmentations resulting from the loss of -CO_2 (m/e 204) and -CH_2COOH (m/e 189). Attempts to obtain this product on a larger scale have not as yet been conducted.

5). N-(2-Pyridyl)-N-(2'-thienylmethyl)-2-aminoethanol (170).

The cyclized aldehyde metabolite (157) was reduced to the proposed alcohol metabolite (170) by the method shown in Figure 61. The cyclized aldehyde was first converted to the

Figure 61. Synthesis of Alcohol 170.

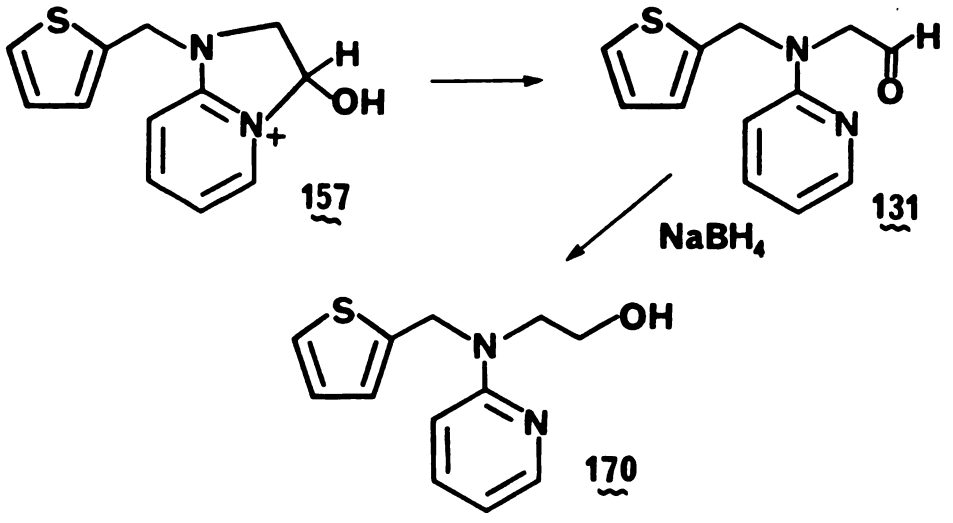

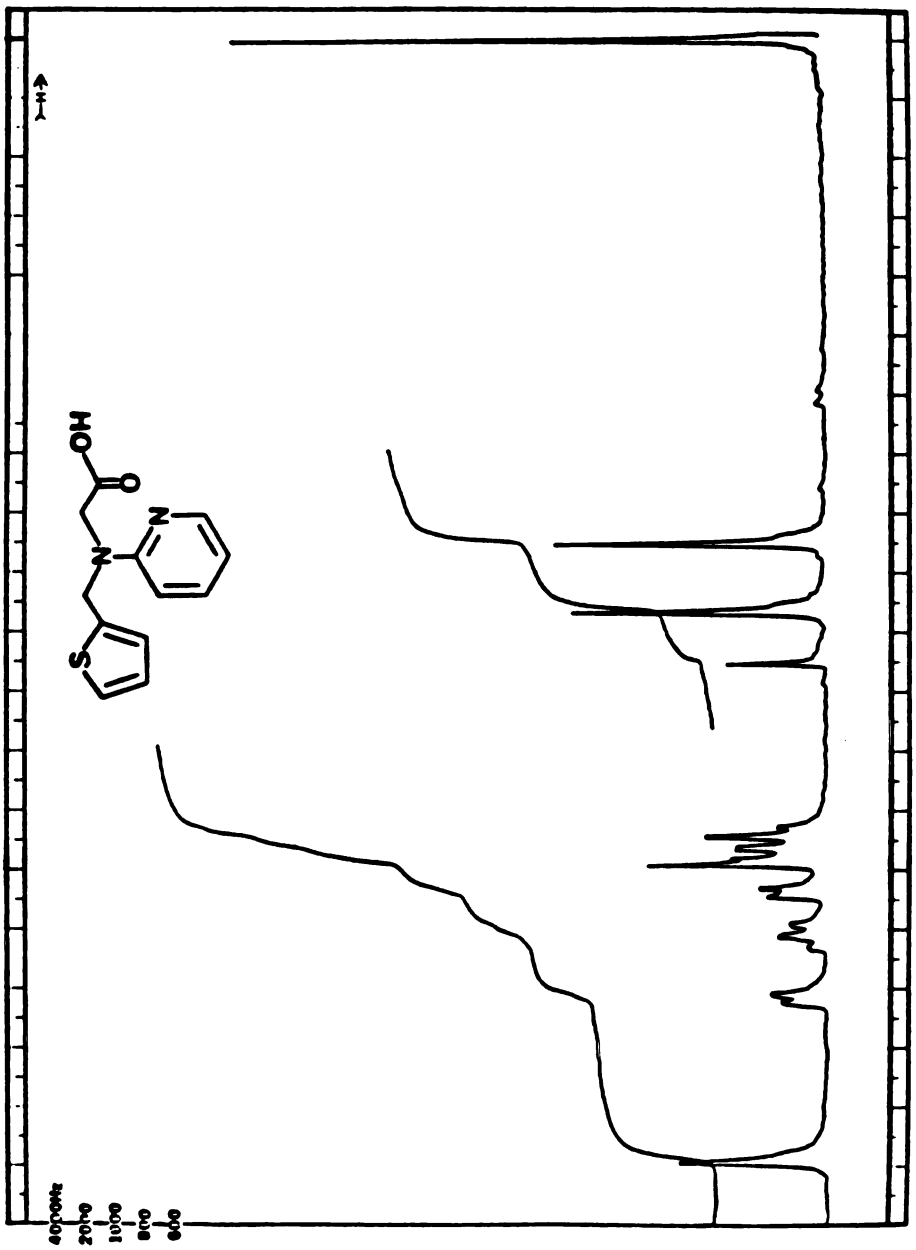

Figure 60. ^{1}H-NMR Spectrum of 164.

aldehyde by treatment with one equivalent of KOH and then sodium borohydride was added. After 5 days, the product was isolated from the reaction mixture by basic extraction and column chromatography. The reduction was slow and sodium cyanoborohydride was found to be ineffective in producing the alcohol from the aldehyde.

The NMR spectrum and EIMS of 170 are shown in Figures 62 and 63, respectively. The NMR spectrum of the alcohol shows a large singlet at δ3.8 integrating for four hydrogens. This peak has been assigned to the $N-CH_2-CH_2-O$ methylene protons. The benzylic methylene singlet at δ4.8 and the complex aromatic signals downfield are representative of methapyrilene metabolites.

The EIMS of 170 has its parent ion at mass 234, representing the molecular weight. Major fragmentations yielded the ion m/e 189 from the loss of C_2H_5O and the benzylic ion at m/e 97. Neither the mass spectrum nor NMR spectrum for alcohol 170 were observed from metabolic samples.

6). 1-Thienylmethylimidazo-(1,2a)-pyridinium chloride (171).

The aldehyde metabolite (131) was found to cyclize to a 3-hydroxy-2,3-dihydroimidazo-(1,2a)-pyridinium species (157). As reported by Adams and Dix,[201] ketones of a similar structure were found to cyclize and dehydrate to give a stable 3-alkylimidazo-(1,2a)-pyridine (173) under

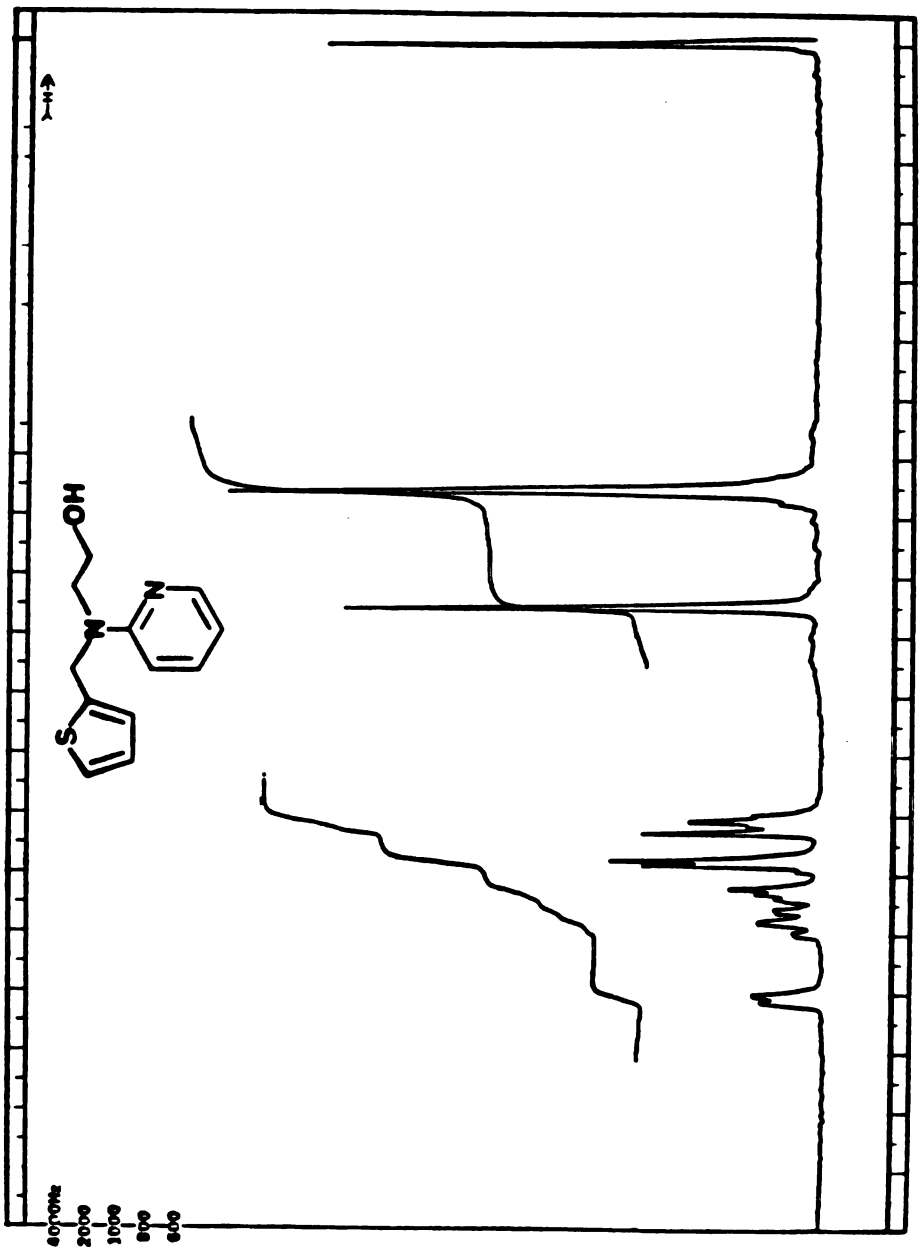

Figure 62. ^{1}H-NMR Spectrum of 170.

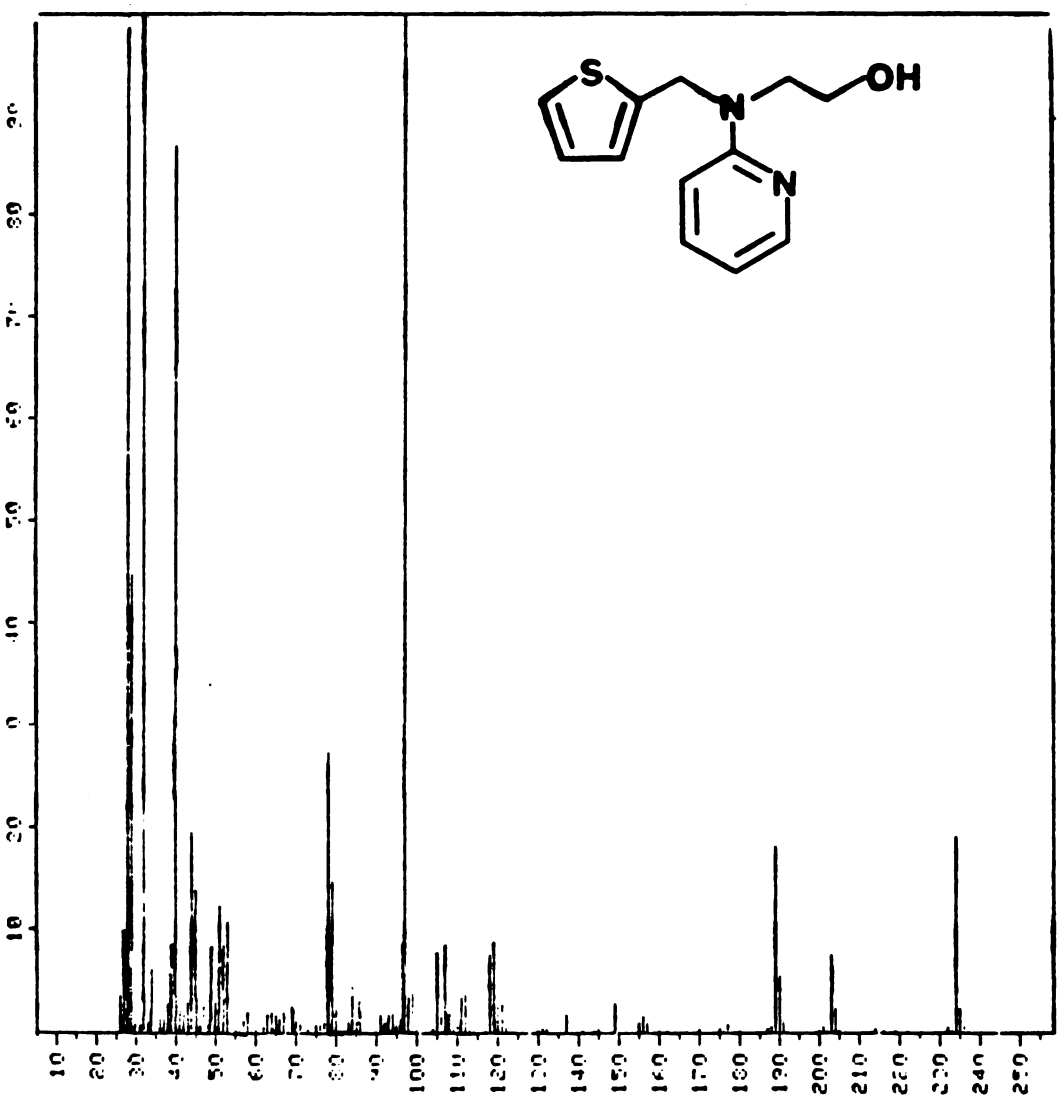

Figure 63. EIMS of 170.

dehydrating conditions, as shown below. Since many workup procedures require heating and drying under vacuum, we decided to investigate the possibility of dehydration of the cyclized aldehyde (157) during conditions even harsher than those involved in the workup of metabolic incubates.

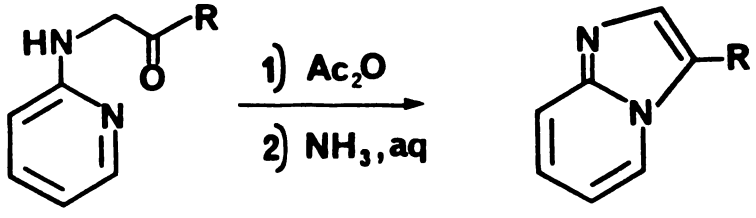

172 173

To achieve dehydration, 157 was heated under reflux in acetic anhydride for four hours. The reaction was quenched with ice cold ammonium hydroxide and the product was extracted into CH_2Cl_2. The TLC showed only one product which flouresced under UV light. Acetamide sublimed from this oil while the remaining material was found by NMR and TLC to be the cyclized aldehyde 157. The formation of 1-thienylmethylimidazo-(1,2a)-pyridinium salt (171) does not appear to be a facile transformation from the precursor carbinolamine, unless once formed, it rehydrates under basic conditions. Unlike the analogs used by Adams and Dix,[201] the exocyclic nitrogen is tertiary and cannot lose a proton, as shown below, to stabilize the product. Thus the leaving hydroxyl group generates a positive charge next to the positive charge on the pyridine ring as indicated. The electrostatic repulsion generated cannot be

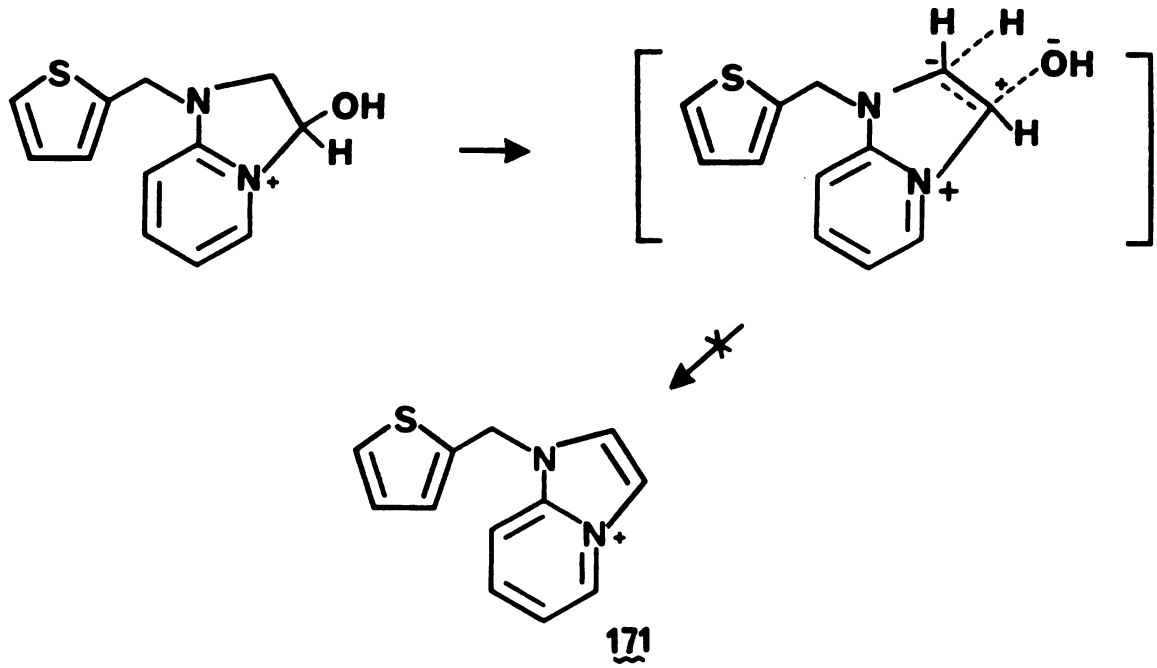

171

relieved by loss of a labile proton, therefore causing the reaction to be thermodynamically unfavorable. This is not to say that these types of reactions do not take place. Analogous dehydration of 1,2-dialkyl-2-hydroxy-2,3-dihydroimidazo-(1,2a)-pyridinium bromide compounds (174) yielded the desired imidazo-(1,2a)-pyridinium salts (175) as shown below.[202,211] In these cases, the hydroxyl was again next to a partially positively charged nitrogen. The delocalization of the charge, however, must be predominantly onto the ring nitrogen making the dehydration more favorable. These products were obtained in 50-65% yield. From these results, it appears that dehydration of the cyclized aldehyde metabolite to form the imidazo-(1,2a)-pyridinium species will not occur chemically.

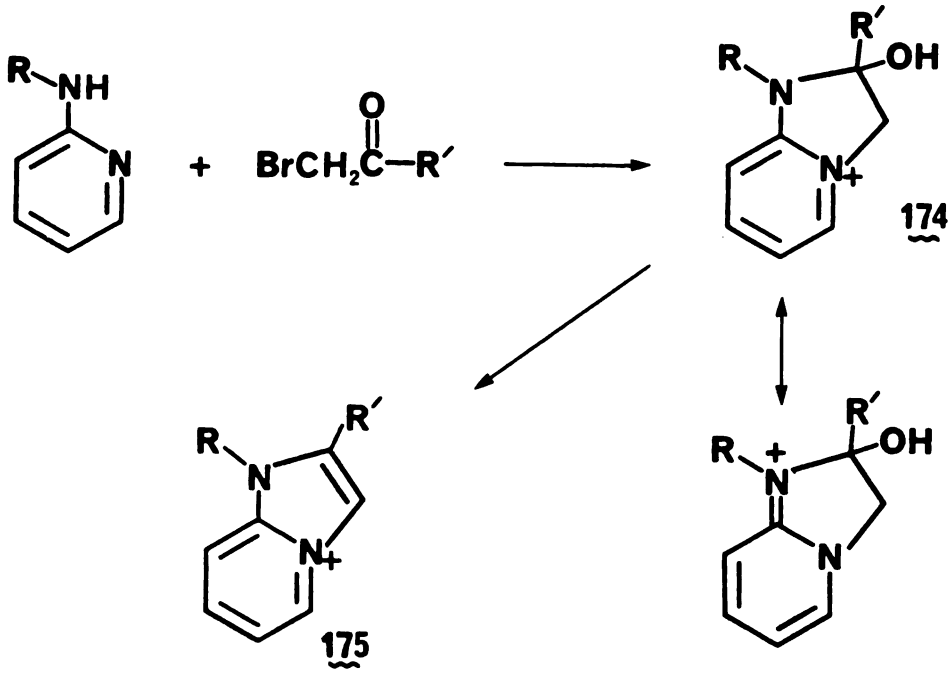

In addition to the synthesized metabolites, possible metabolites shown in Figure 64 were considered but not detected in the microsomal incubates.

Figure 64. Potential Metabolites not Detected in Rat Microsomal Incubates.

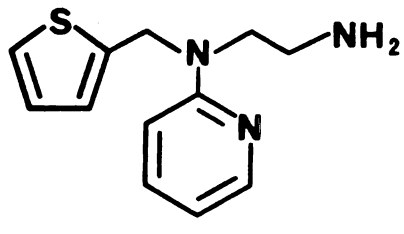

176

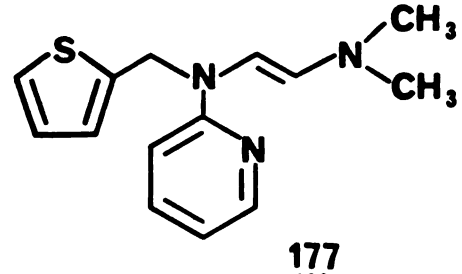

177

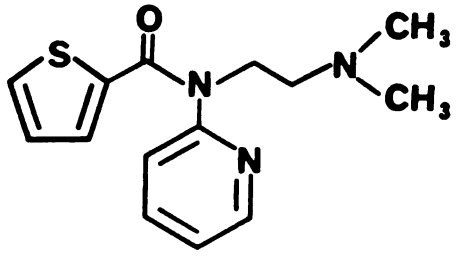

178

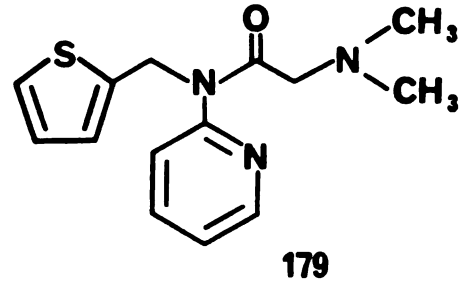

179

VII. Quantitation of Rat Microsomal Metabolites.

Of the methapyrilene incubated with rat liver microsomes, 65% remains unchanged while 2-3% binds to proteins. The remaining 32% distributed between the aqueous and organic phases in such a way that 24% was water soluble metabolites and 8% organic soluble metabolites. As discussed in the previous sections, some of the metabolites distributed into both the aqueous and organic fractions. For this reason, quantitation of the metabolites was achieved by extraction of known quantities of synthetic metabolites using the same procedure as that for incubates and analysis of the HPLC peaks heights. Standard curves were obtained and all synthetic analogues containing both the thiophene and pyridine ring gave identical peak height to concentation curves. Thus, the standard curves for compounds containing the same chromophores were used for those metabolites not synthetically available.

This analysis led to the approximate quantitation of most of the metabolites, as listed in Table 9. Unfortunately, N-desmethylmethapyrilene and the N,N-dimethylacetamide metabolite have the same retention time on the HPLC, but the two metabolites together account for 10% of the methapyrilene. N-(N',N'-dimethylaminoethyl)-2-aminopyridine (92), N-(2'-thienylmethyl)-2-aminopyridine (91) and 5-hydroxymethapyrilene (155) were each representative of approximately 1% of the methapyrilene. The aldehyde was

Table 9. Approximate Quantities of Known Metabolites.

129 + 127	10%
92	1%
91	1%
155	1%
protein bound	3%

present in negligible amounts. As discussed previously, the aqueous layer was subjected to lyophilization to determine if other water soluble metabolites resulted from ring hydroxylation. The amount of radioactivity which distilled over with the water represented only 2% of the total, in good agreement with the estimate of only 1% 5-hydroxymethapyrilene.

The totals here quantitate approximately 13% of a total 32% metabolized. We have not accounted for the remaining 16%. As illustrated in Scheme 20, 73% of the radioactivity distributed into the organic phase upon extraction of the incubate, of which 8% are metabolites. Of the 24% radioactivity which distributed into the aqueous phase, 9% of the radioactivity was isolated as metabolites in the methanol eluent of the Sep Pak. Approximately 60% of the water soluble radioactivity or 14% of the total radioactivity either passed through the Sep Pak or bound irreversibly to the Sep Pak. Thus, the unaccounted for methapyrilene derived materials remain in fractions not yet studied. In as much as the HPLC quantitation studies agree

closely with those from the radioactivity distribution, we feel that our data represent an accurate analysis of the isolated metabolites. The oxidatively metabolized centers of methapyrilene can be illustrated as follows, where oxidation of the dimethylamino moiety represents the majority of known metabolism.

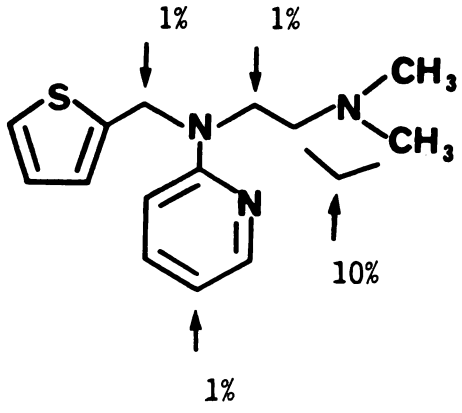

As a side note, the HPLC tracings from rat and rabbit liver microsomal metabolites have been compared. As illustrated in Figures 65 and 66, the rat organic soluble metabolites are fewer in number and lesser in quantity than those from the rabbit. No attempt at analyzing the metabolites unique to rabbits was made. In previous studies,[71] N-formyl-(2'-thienylmethyl)-2-aminopyridine and methapyrilene N-oxide were found as metabolites and could represent the compounds associated with two of the peaks unique to rabbit metabolism. Interestingly, N-demethylation occurs to a much greater extent in rabbit than rat as judged by peak height.

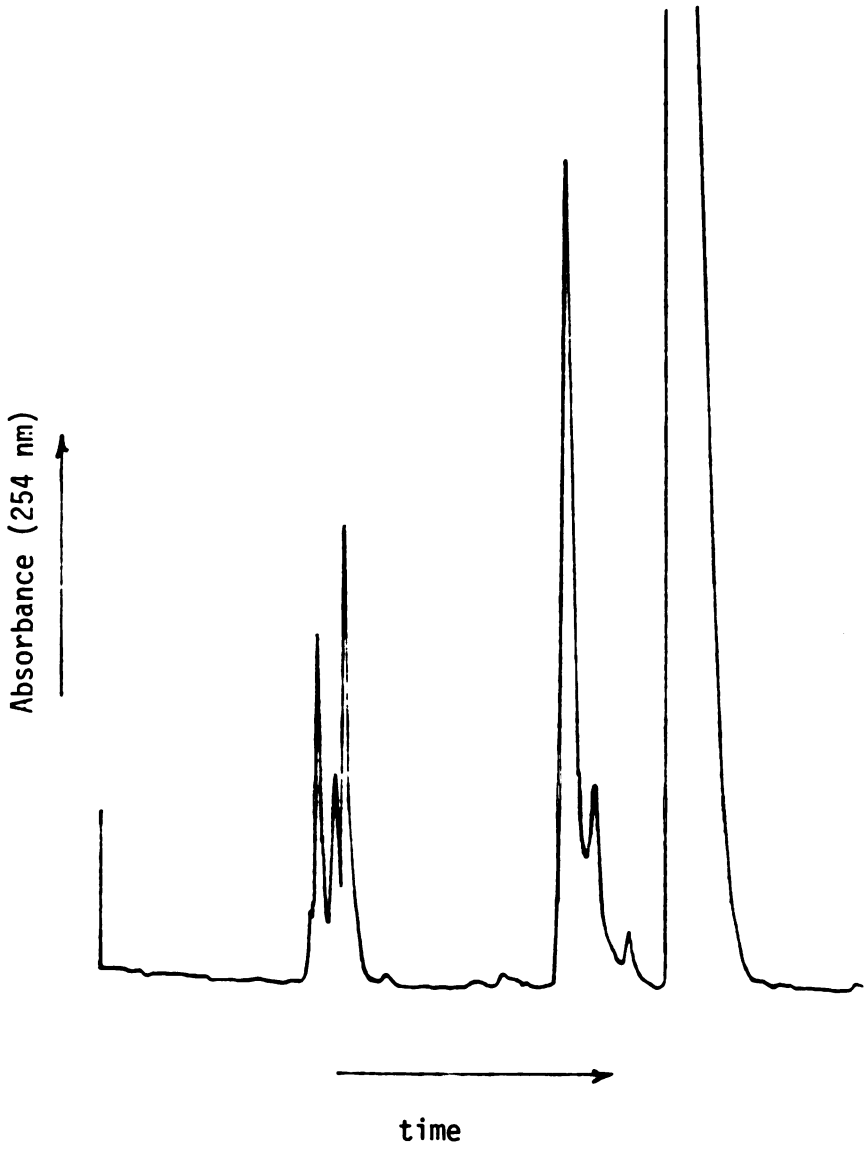

Figure 65. HPLC of Rat Organic Soluble Metabolites.

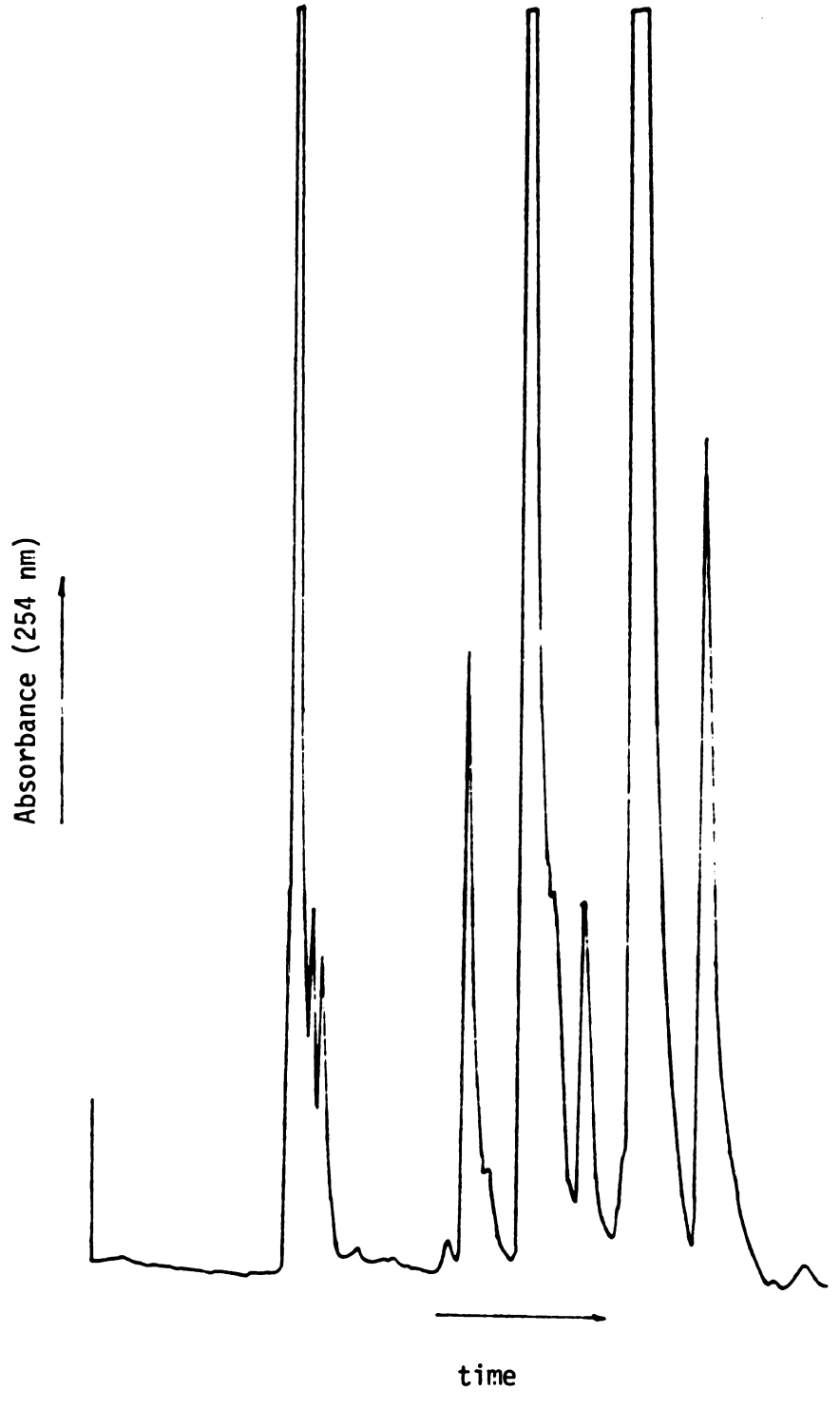

Figure 66. HPLC of Rabbit Organic Soluble Metabolites.

VIII. Macromolecular Binding

In vivo and in vitro binding of many carcinogens to macromolecules have been well established. As discussed in the Section I, many carcinogens are believed to undergo metabolic activation to electrophilic intermediates which are susceptible to nucleophilic attack by nucleophiles present on cellular macromolecules and small molecules. Different types of electrophilic intermediates are present in the various classes of carcinogens but, in some cases, the capacity of the carcinogen to bind to macromolecules is a measure of their carcinogenicity.[212] In a few cases, the type of electrophilic intermediate which binds to DNA is dependent on the tissue in which it is acting.[213] Thus, the macromolecular binding of carcinogens should be studied in the tissues where carcinogenesis begins.

The binding of carcinogens to microsomal proteins and exogenous DNA has been utilized as a convenient means for studying the nature of electrophilic intermediates and their reactivities under varying conditions. Diethylnitrosamine and N-nitrosopiperidine have been found to bind covalently to DNA with microsomal activation.[214] DNA alkylation was achieved, in this case, only in the presence of active microsomes and NADPH, and the alkylation was increased in the presence of either cytosolic enzymes or mitochondria.[214] Diethylnitrosamine bound to exogenous DNA to the extent of 3.5 pmol/mg DNA in 60 minutes and was

induced by pretreatment of the rat with phenobarbital but not with 3-methylcholanthrene. Similar results were obtained for N-nitrosopiperidine.[214] The potent mutagen resulting from pyrolysis of tryptophan (Trp-P-2, 180) binds to DNA after microsomal activation.[215,216] Increased binding was observed with N-hydroxy-Trp-P-2[217,218] and purified cytochrome P-448 readily mediated covalent binding of Trp-P-2 to DNA. The extent of DNA binding after P-448 activation was approximately 200 pmol/mg DNA.[217] Concomitant cytosolic activation increased the incorporation of Trp-P-2 into DNA.[218]

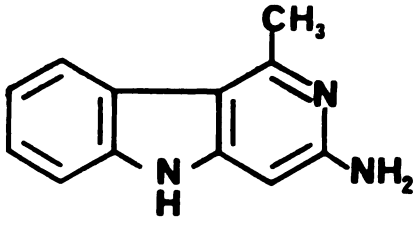

180

Analogously, various xenobiotics bind to microsomal proteins. N-Acetylaminofluorene binds to specific microsomal proteins presumably through the electrophilic intermediate 7 shown in Table I.[219] 4-Chlorobiphenyl[220] and various mixtures of polychlorinated biphenyls[94] have been found to bind to proteins as well as nuclic acids. The reactions of these halogenated biphenyls are believed to require P-450 activation and thought to involve an epoxide intermediate. In untreated rats, the rate of binding was found to be 24 pmol/mg protein per minute.[221] Benzene,[222]

phenol, benzo(a)pyrene, and 3-methylcholanthrene[223,224] each bind to a specific set of microsomal proteins upon metabolic activation. The profile of alkylated proteins is different for the different aromatic compounds and may be altered by 3-methylcholanthrene or phenobarbital induction.[224] In each case, however, the reaction may be inhibited by the presence of glutathione.

Recent studies demonstrated that 1-benylpyrrolidine binds to microsomal proteins to the extent of 180-330 pmol/mg protein.[53] Similarly, the tertiary amine, phencyclidine has been found to incorporate 6-8% of the incubated drug into microsomal proteins,[73] in agreement with a previous study that found 10% incorporation.[225] In this case, the covalent interaction with microsomal proteins required NADPH and was inhibited by the addition of inorganic cyanide.[73] Procainamide binds 650 pmol/mg protein in 15 minutes[226] and imipramine leads to 530 pmol/mg protein.[227] In each of these cases, metabolic activation in the presence of NADPH was required for binding. One or more intermediates may be involved in these instances but each structure contains both a tertiary amine (potential iminium ion) and an aromatic ring (potential arene oxide).

Methapyrilene was found to bind to proteins but not to nucleic acids in vivo.[228] This was not unexpected from previous results on the structural analog, tripelennamine (112) (Section VI). In the presence of active rat liver

microsomes, tripelennamine binds to proteins to the extent of 215 pmol/mg protein in 10 minutes.[185,186] No binding to nucleic acids was observed. Dual labeled tripelennamine, with ^{14}C in the benzylic methylene and ^{3}H in the N-methyl groups, as discussed earlier, incorporated the carbon and tritium labels equally into the protein.[186] The binding was increased by pretreatment with phenobarbital and decreased by 3-methylcholanthrene induction. An arene oxide intermediate was postulated as the alkylating species but again, the tertiary amine centers could yield an electrophilic iminium ion(s) which would also undergo nucleophilic attack.[185]

From these data, it seemed that 5-tritiomethapyrilene should bind to microsomal proteins and additional information could be gained by determining if the tritium label was retained in the C-5 position. As previously discussed in the section on radiochemical distribution, 2-3% of the radiolabel incubated was covalently incorporated into microsomal proteins. Table 10 demonstrates that NADPH, and therefore metabolic activation, was required for binding. The reaction was efficiently inhibited by the thiol nucleophiles cysteine ethyl ester and glutathione, while the nitrogen nucleophiles present in BSA had only a minor inhibitory effect. Likewise, inorganic cyanide inhibited binding only to a very limited extent. The actual extent of binding, with knowledge of the specific activity, was calculated to be approximately 5 nmol/mg protein in one

Table 10. Inhibition of Protein Binding.

incubation conditions	% bound	% inhibition
+ NADPH	2.4%	
- NADPH	----	
+ 1mM CysOEt HCl	0.9%	66%
+ 1mM GSH	1.3%	53%
+ BSA (10 mg/ml)	2.0%	14%
+ 1 mM CN^-	2.2%	8%

hour, much higher than that observed for other carcinogens.

As noted in Table 7 (Section V C), the protein-bound radiolabeled adduct is sensitive to acid and stable in the presence of base. In an effort to isolate the protein-bound adduct, a group of protein pellets was treated with aqueous acid and the resulting solutions were analyzed by HPLC. In each attempt, the control hydrolysate and incubate samples gave the same HPLC peaks (Figure 67). To insure that the tritium-label was not sensitive to strong acid, methapyrilene was treated with trichloroacetic acid in D2O. The following mechanism would explain deuterium incorporation or tritium loss in the protein-bound adduct. No deuterium was incorporated into methapyrilene by this method, as determined by NMR and EIMS.

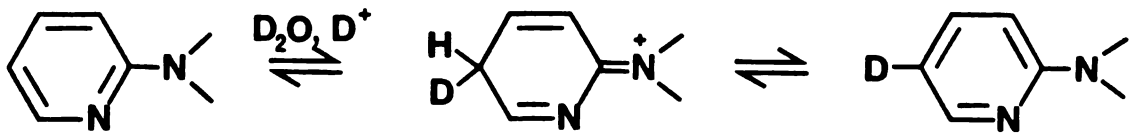

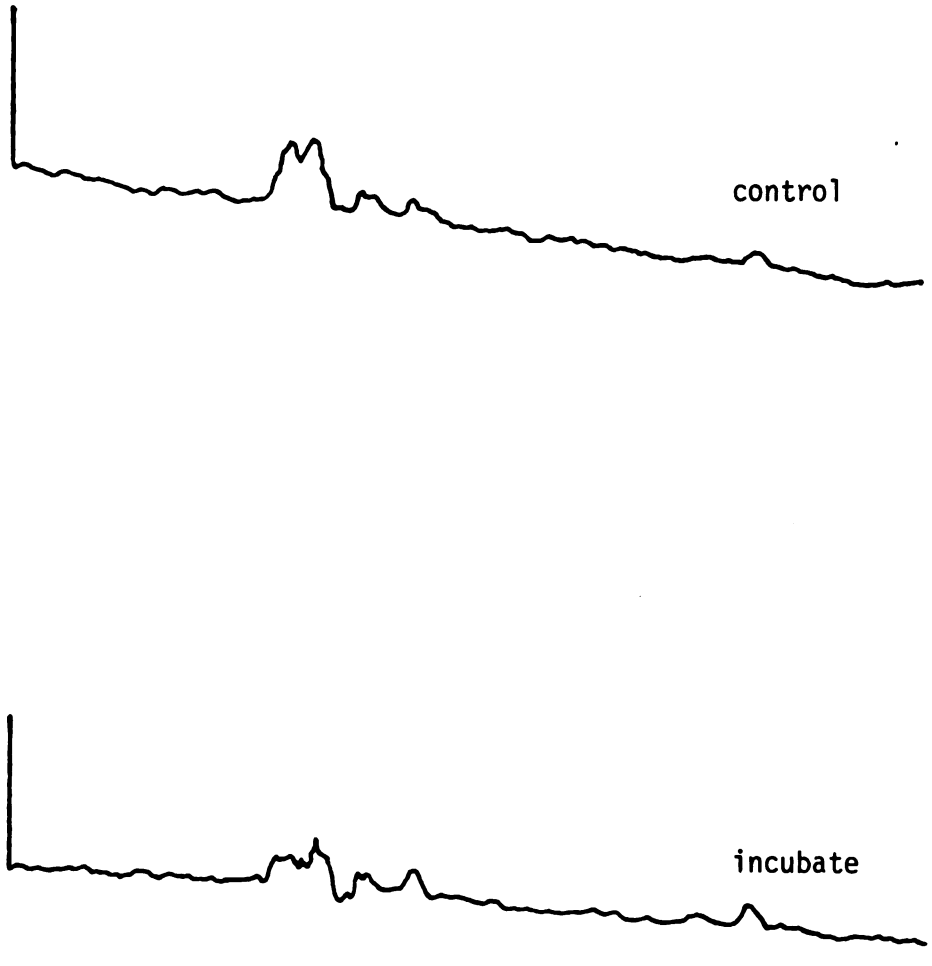

Figure 67. HPLC of Protein-Adduct Acid Hydrolysates.

The incorporation of 5 nmol/mg microsomal protein of metabolized methapyrilene is slightly higher but in agreement with the amounts of the previously mentioned protein-bound adducts of carcinogens and PCP. If a suicide-substrate type reaction of an activated metabolite with the activating enzyme were to occur, one might expect labeling of specific proteins. Alternatively, a reactive intermediate which dissociates from the activating enzyme would be expected to bind nonspecifically to proteins. To gain more information about the methapyrilene metabolite bound to microsomal protein, we decided to separate the proteins under mild conditions and to monitor the resulting radioactivity content.

Sodium dodecyl sulfate-polyacrylamide gel electrophoresis (SDS-PAGE) is particularly useful in the separation of microsomal proteins in that it separates by size only. The microsomal incubate (2ml of 5ml) was frozen at -70^{0}(dry ice/acetone) to quench the metabolism and then thawed and treated with 200 μl of 10% SDS. This was then dialysed against 2% SDS to remove the non-covalently associated radioactivity. The external dialysate was changed at 4, 18, and 72 hours. Before electrophoresis, the dialyzed samples was buffered with concentrated stacking gel buffer and placed in a boiling water bath to insure complete denaturation. This sample was then applied to a single slot of a 10% SDS-PAGE and electrophoresed at 10 mA/plate. A set of commercial proteins of known molecular weight

(BioRad) were electrophoresed as markers to aid in protein size approximation. After completion of the electrophoresis, the gel was cut in half, for each half was a mirror image of the other half and one side was stained with Coomassie Brilliant Blue for visualization of the protein bands (Figure 68). The other half was sliced into 2mm segments and counted in Aquasol. Removing the excess Coomassie Blue stain requires washing the gel extensively with aqueous acetic acid/methanol, and it was found that no radioactivity could be recovered from slices of stained gels. This result is in agreement with the lability of the protein-bound adduct to acidic conditions.

The radioactivity has been plotted against sample number and molecular weight in Figure 69. This plot shows a random distribution of the radioactivity amongst the microsomal proteins with the highest levels of incorporation coinciding directly with the bands of highest protein density (the cytochrome P-450 size range) and the noncovalently attached small molecule(s) at the bottom of the plate. The total amount of radioactivity present of the proteins was representative of 4% of the total radioactivity incubated, in agreement with the previous results. This preliminary evidence therefore suggests that activated methapyrilene can dissociate from the cytochrome P-450 or other activating enzyme to bind nonspecifically to microsomal proteins.

Preliminary results on methapyrilene binding to calf

Figure 68. SDS-PAGE of Microsomal Proteins.

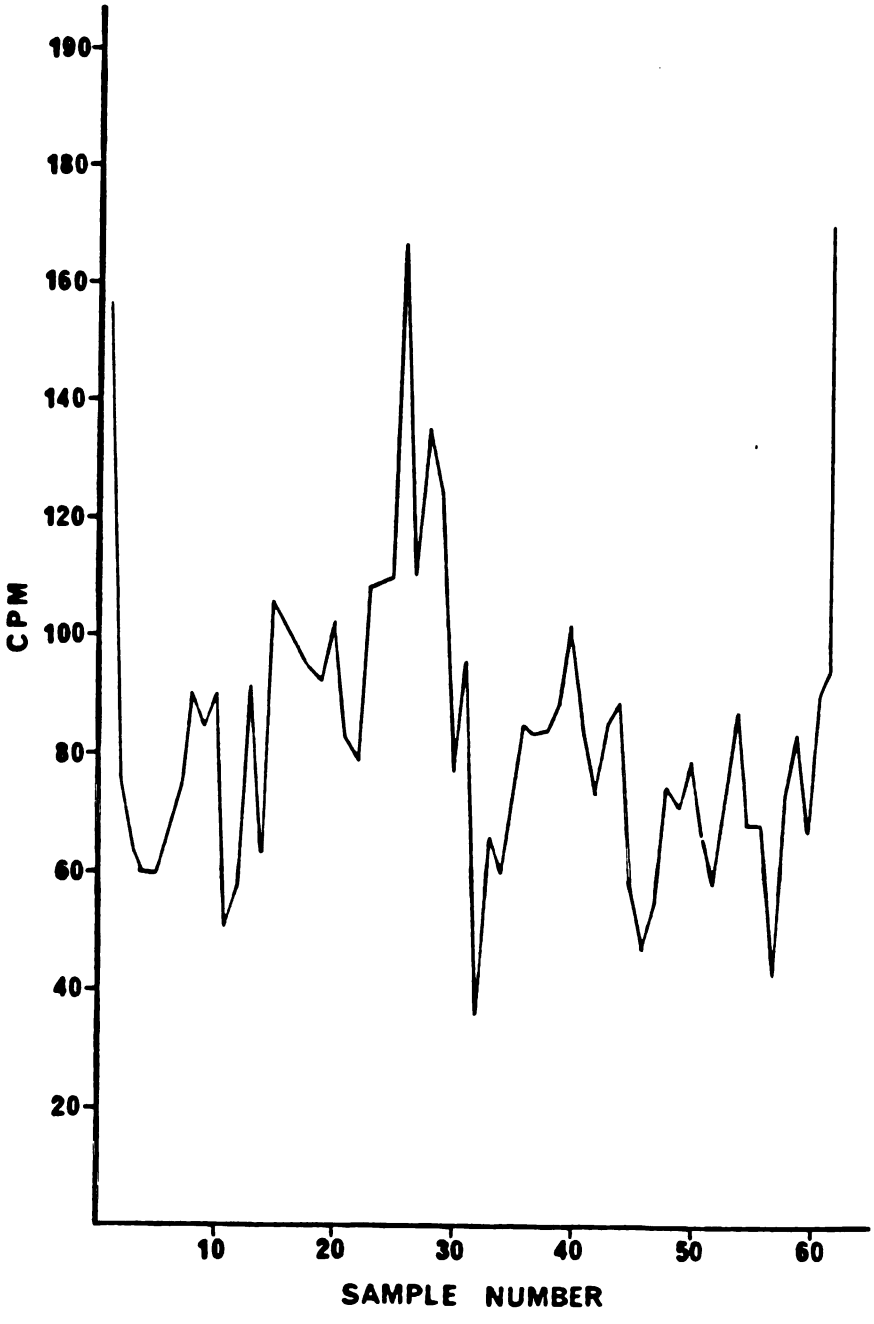

Figure 69. SDS-PAGE Sample Number versus CPM Incorporation.

thymus DNA in the presence of microsomal activation are presented in Table 11. Unfortunately, a large experimental error is expected due to the low specific activity of the tritiated methapyrilene and the low levels of incorporation. However, keeping this in mind, approximately 250 pmol/mg DNA was found with metabolic activation. At this level of incorporation, methapyrilene would well exceed those levels observed for diethylnitrosamine[214] and is in the same range as that for Trp-P-2. Thus, it appears that methapyrilene binds to DNA in quantities equivalent to that of other known DNA alkylators in vitro.

Table 11. Covalent Radiochemical Incorporation into DNA.

	dpm	pmol/mg DNA
Control 1, +NADPH,-DNA	90	----
Control 2, -NADPH,+DNA	81	
DNA + NADPH	1) 121	avg. + 247
	2) 158	
	0.05ml of 1 ml	

Covalent association of methapyrilene with proteins and DNA upon metabolic activation is a reproducible and significant result. Previous in vivo studies[153,228] with randomly labeled ^{3}H-methapyrilene found covalent associations with proteins but not with DNA or RNA. Additionally, many of the in vitro assays for DNA alkylation with methapyrilene (i.e. Ames test, cell transformation and unscheduled DNA synthesis) have been found to be

predominantly negative.[144-147] Only in one study[148] was methapyrilene found to cause unscheduled DNA synthesis in cultured rat hepatocytes. Our results on protein alkylation are consistent with those in vivo studies.[153,228] The preliminary results on microsomally activated DNA alkylation at 250 pmol/mg DNA, however, should also have been detected in vivo. At this point, more in vivo and in vitro studies on DNA alkylation by methapyrilene may determine whether the same mechanisms are involved in vitro and whether these same routes are possible in vivo. Future studies will help to clarify the definition of methapyrilene as a genotoxic or epigenetic carcinogen.

IX. Conclusion

This research in addition to those findings in other laboratories has led to some interesting ideas concerning methapyrilene carcinogenesis. Rat liver microsomal metabolism of methapyrilene resulted in a variety of metabolites in addition to protein and, to a much lesser extent, DNA alkylation. In this way, the metabolites and the enzymatically derived electrophilic intermediates involved in their formation must be considered as potentially carcinogenic.

The isolated metabolites represent various routes of oxidative dealkylation and aromatic hydroxylation. The most novel oxidation resulted in the formation of N-(N',N'-dimethylaminoethyl)-2-aminopyridine (92) and 2-hydroxymethylthiophene. Although oxidative N-debenzylation is known, the formation of thiophene-2-carboxaldehyde proved to be very important. Earlier research on morphological changes due to methapyrilene administration noted a proliferation of swollen and deformed mitochondria.[153] Mitochondrial swelling has also been observed in rats treated with substituted thiophenes such as thiophene-2-carboxylic acid[229] and others.[230,231] Although cytochrome oxidase activity was not inhibited,[231] the substituted thiophenes are inhibitors of mitochondrial oxidation and affect the ATPase activity.[231] This effect is

concomitant with a general decrease in overall Ca^{2+} and inorganic phosphate levels in rats.[229] A great number of causes of mitochondrial swelling have been noted[232] but the expression of morphological transformations due to benzo(a)pyrene has been linked to extracellular Ca^{2+} concentrations. Thus, perhaps the thiophene-2-carboxaldehyde metabolites of methapyrilene are important to carcinogenesis or in general, cellular toxicity. This result would confirm the findings on the non-toxicity of structurally similar analogs of methapyrilene (See Table 8).[154] Only the furan analog methafurylene (95) showed toxicity similar to methapyrilene.[154] Thus, perhaps metabolically generated substituted furans have similar mitochondrial activity compared to their thiophene analogs. In actuality, any one of the metabolites could be carcinogenic but those studies remain to be conducted.

As observed for many carcinogens, radiolabeled methapyrilene was found to bind covalently to both proteins and DNA. The structures of the metabolites provide evidence for the existence of electrophilic iminium ions 10, 11, 12 and 13, in addition to the pyridine epoxide 16. Formation of a thiophene epoxide 15 has not been detected but a fairly large quantity of highly polar metabolites remains to be studied (Section II B). Metabolic transformation of the thiophene ring of methapyrilene might lead to the ring opened 2-oxoglutarate, which would not be extractable at pH

7.4, due to its negative charge. The covalent interaction with proteins was inhibited by thiol nucleophiles such as cysteine ethyl ester and glutathione. Other nucleophiles such as BSA and inorganic cyanide demonstrated minimal inhibitory action. From these results, future experiments might be designed around trapping and isolating the alkylating specie(s) with cysteine ethyl ester. Ultimately, the structure of this intermediate could provide answers as to the "ultimate carcinogen" derived from methapyrilene. Additionally, further studies on the interaction of methapyrilene with DNA could provide evidence for defining methapyrilene as a genotoxic or epigenetic carcinogen.

X. Experimental

A. Materials and Methods

1). Chemistry

Melting points were obtained on a Thomas Hoover melting point apparatus and are uncorrected. Proton magnetic resonance spectra were recorded on a Varian FT-80 or a Nicolet model 1180 240 mHz spectrometer. Chemical shifts are recorded in parts per million (ppm) relative to tetramethylsilane (TMS) or 2,2-dimethyl-2-silapentane-5-sulfonic acid (DSS) as internal standard; s=singlet, d=doublet, t=triplet and m=multiplet. Infrared spectra were recorded on a Perkin Elmer model 257 grating infrared spectrometer.

Low resolution electron impact mass spectra (EIMS) were recorded on a Kratos MS 25 interfaced with a Varian model 3700 gas chromatograph (GC). GC-EIMS was carried out on a 0.2% OV-1 or 0.1% SE-50 capillary column (0.3mm idx 10 ft). Chemical ionization mass spectra (CIMS) were obtained on an AEI MS-9 instrument modified for chemical ionization. High resolution EIMS were obtained from the Bio-organic, Biomedical Mass Spectrometry Resource, Space Sciences Laboratory, University of California, Berkeley. Elemental analysis were performed by the Microanalytical Laboratory of the University of California, Berkeley.

Analytical gas chromatography was performed on a Varian Aerograph Series 2100 with an H_2-flame ionization detector utilizing a U-shape 2mx 2mm id glass column packed

with 3% OV-25 on acid washed DMCS Chromasorb W (mesh 100/120). Analytical high performance liquid chromatography (HPLC) was carried out with an Altex 110A pump equipped with a Hitachi model 100-10 spectrophotometer for detection at 254 nm. The HPLC column was an Altex Lichrosorb reverse phase C-18 (10μ, 4.6mmx 25cm). Preparative HPLC was performed with a Beckman model 100A pump utilizing a Whatman Partisil M9 ODS-3 (10mmx 50cm). A Gilson microfractionator was used to collect the fractions from chromatography. Analytical (250μ) and preparative (2000μ) silica gel TLC plates were purchased from Analtech. Silica gel 60 from Merck (70-230 mesh) was used for column chromatography.

Scintillation counting was performed on a Packard Tri-Carb model 3375 or a Beckman LS-3133T liquid scintillation spectrometer. SDS-gel elctrophoresis was performed with a Bio-Rad slab-gel setup equipped with an LKB 2103 power supply and LKB 2209 multitemperature temperature control bath.

Chemicals were purchased from Aldrich, Alfa, Mallincrodt, Pfaltz and Bauer, and Sigma. Aquasol for liquid scintillation was purchased from New England Nuclear. Burdick and Jackson solvents were used for HPLC.

2). Biology

Rat liver microsomes were prepared as described in reference 208. Control and induced animals were decapitated and the liver tissues subsequently homogenized at 0^{o}

using a Potter-Elvehjem Teflon pestle homogenizer. The liver homogenates were then centrifuged (10,000 x g, 20 min) on a refrigerated Sorvall RC-2. The resulting supernatant was centrifuged (100,000 x g, 60min) on a Beckman L2-65B ultracentrifuge and the microsomal pellet was resuspended and submitted to ultracentrifugation a second time (100,000 x g, 45-60 min). The protein content of the microsomes was determined by Lowry protein analysis[171] on a Varian Cary 118 and adjusted to 3mg protein/ml buffer. Metabolic incubations were carried out in a temperature regulated Dubnoff metabolic shaker/incubator with a 5 ml total volume containing the following concentrations of cofactors: Tris HCl buffer (pH 7.4, 0.2 M, 1.15% KCl), $MgSO_4$ (0.015 M), methapyrilene (1mg/incubate), NADPH (4 mg initially, 4 mg at 20 min). The incubates were quenched by extraction with freshly distilled methylene chloride.

The protein-binding assays were conducted in two ways: 1) The protein was pelleted by the addition of 10% trichloroacetic acid (9 ml) to the incubate. The resulting solid was pelleted by low speed centrifugation and the pellet was subsequently washed with MeOH (1 ml, 10 times). The pellet was dried under a flow of N_2 and hydrolyzed with 1.0 N NaOH (3 ml, 50^{o}, 2-3 hours). 2) The protein emulsion resulting from organic extraction of an incubate was isolated from the aqueous and organic solutions and then washed with MeOH as above. The same process of purification and hydrolysis was followed as in part 1.

The DNA binding studies were carried out by adding calf thymus DNA (2 mg, Sigma), dissolved in buffer, to a normal incubate. The incubates were extracted with 5 ml of a mixture of phenol (25): $CHCl_3$ (24): isoamyl alcohol (1). The extracts were subjected to low speed centrifugation and the supernatant was again extracted with the phenol mixture. The final supernatant was cooled in ice and ice cold EtOH (10 ml) was added without shaking and allowed to stand at room temperature over the weekend. The precipitated DNA was washed twice with EtOH (1 ml) and then redissolved in phosphate buffer (1 ml of 0.014 M, pH 6.8).

B. Synthetic Methods.

N-(N',N'-Dimethylaminoethyl)-2-aminopyridine (92): In flame dried glassware under N_2, a mixture of NaH (0.834g (61%), 0.0212 mol) in anhydrous dioxane (50 ml) was brought to reflux. The 2-aminopyridine (1.0g, 0.0106 mol) was then added batchwise and the solution was heated under reflux for two hours. 2-Dimethylaminoethyl chloride hydrochloride was then added in a batchwise manner and the reaction mixture was heated under reflux overnight. The reaction mixture was then cooled and the NaCl was filtered off by vacuum filtration. The filtrate was partitioned between ether and water. The aqueous solution was then washed with CH_2Cl_2 until no more yellow color was extracted. The combined organic layers were washed with water, then

dried (K_2CO_3), filtered and evaporated. Column chromatography (15g of silica gel) was performed with EtOAc as the eluant to remove the remaining 2-aminopyridine. The product was isolated by eluting with 5% MeOH/EtOAc with 2% Et_3N. Concentration of the eluent yielded 0.54g (25%) of 92 as a yellow oil: bp (0.05mm) 52°(lit[174] bp (0.1 mm) 100-106°); ^1H NMR ($CDCl_3$) δ 2.3 (s, 6H, N-CH_3), 2.5 (t, J=6.3 Hz, 2H, CH_2NMe_2), 3.3 (q, J=6.3 Hz, 2H, HN-CH_2) 4.95 (broad s, 1H, NH), 6.3-8.05 (complex m, 4H, arom.).

N-(N',N'-Dimethylaminoethyl)-2-amino-5-bromopyridine (100). A) A solution of bromine (0.051ml, 0.989 mmol) in glacial acetic acid (3.6ml) was added slowly with stirring to a solution of 92 (0.20g, 1.2 mmol) in glacial acetic acid (3.6ml) maintaining a constant temperature between 50-55°. The reaction mixture was allowed to stir for 1/2 hour after which the acetic acid was removed under reduced pressure. TLC with EtOAc as the developing solvent yielded less than 10 mg (3%) of a yellow oil at 95% purity. B) A suspension of sodium hydride (0.74g, 11.6mmol) in anhydrous dioxane (50ml) in flame dried glassware under N_2 was brought to reflux and 2-amino-5-bromopyridine (1.0g, 5.78mmol) was added batchwise. The reaction mixture was heated under reflux for two hours after which N,N-dimethylaminoethyl chloride hydrochloride (0.833g, 5.78 mmol) was added batchwise. The reaction mixture was then

heated under reflux overnight under N_2. After cooling the reaction mixture was filtered and the filtrate was partitioned between $CHCl_3$ and water. The aqueous layer was repeatedly extracted with $CHCl_3$ until no more yellow color was removed. The combined organic layers were then washed once with water and then dried over K_2CO_3. After filtration and concentration under reduced pressure, a brown oil was obtained. Silica gel chromatography (10g) was run with EtOAc as the eluent to yield 0.45g (32%) of 100 as a brown oil: ^1H NMR ($CDCl_3$) δ2.24 (s, 6H, N-CH_3), 2.51 (t, J=6 Hz, 2H, CH2-NMe_2), 3.31 (q, J=6 Hz, 2H, HN-CH_2), 5.05 (broad s, 1H, NH), 6.25-8.11 (complex m, 3H, arom.); EIMS m/e 245 (m+2, 3%), 243 (m+, 8%), 241 (m-2H, 8%), 187 (m - CH_2NMe_2, 27%), 185 (m - CH_2NMe_2, 20%), 157 (Br-Pyr, 35%), 155 (Br-Pyr, 33%), 78 (pyr, 45%), 71 (CH_2-CH=NMe_2, 100%). Anal. Clacd. for $C_9H_{14}N_3Br$: C, 44.26; H, 5.70; N, 17.20. Found: C, 44.43; H, 5.70; N, 16.90.

5-Bromomethapyrilene (103): A) Methapyrilene hydrochloride (1.5g, 5 mmol) was dissolved in glacial acetic acid and warmed to 50°. A solution of bromine (0.256ml, 5 mmol) dissolved in glacial acetic acid (15 ml) was added slowly to the methapyrilene solution with stirring. After addition was complete, the reaction was allowed to proceed for 1/2 hour at which time the acetic acid was removed under reduced pressure. The resultant oil was then dissolved in water and

basified. The product was extracted into CH_2Cl_2, dried (K_2CO_3), filtered and then concentrated under reduced pressure to an oily residue. The product was purified by bulb to bulb distillation to yield 0.60 g (35%) of a yellow oil: bp (0.40mm) 165°; ^1H NMR ($CDCl_3$) δ 2.26 (s, 6H, N-CH_3), 2.47 (t, J=7 Hz, 2H, CH_2-NMe_2), 3.61 (t, J=7 Hz, 2H, N-CH_2-C-), 4.92 (s, 2H, Ar-CH_2), 6.20-8.20 (complex m, 6H, arom.); CI-MS (direct probe) m/e 341 (m+2, 100%), 339 (m+, 100%), 177 (Br-Th-CH_2, 36%), 175 (Br-Th-CH_2, 36%). B). In 40 ml of anhydrous dioxane, NaH (0.262g, 4.1 mmol) was brought to reflux under N_2 and N-(N',N'-dimethylaminoethyl)-2-amino-5-bromopyridine (1.0 g, 4.1 mmol) was added. The reaction mixture was heated under reflux for 2 hours at which time freshly prepared 2-chloromethylthiophene (0.54 g, 4.1 mmol) was added. The reaction mixture was heated under reflux overnight. The reaction mixture was then cooled, filtered and partitioned between CH_2Cl_2 and water. The aqueous phase was repeatedly extracted with CH_2Cl_2 and the combined organic extracts were backwashed once with water. The CH_2Cl_2 solution was then dried (K_2CO_3), filtered and concentrated under reduced pressure. The resulting oil was purified by bulb to bulb distillation and then chromatographed on column and preparative thin layer chromatograhy to yield 0.15g (11%) of a brown oil 103. 5-Bromomethapyrilene hydrochloride: The oil of 103 (0.1g,

0.29 mmol) was then treated with one equivalent of HCl(g) in ethyl ether to form the hydrochloride salt. The salt was crystallized from MeOH/EtOAc/Et_2O to yield 0.04g (37%) of 103 as white needles: mp 138-140°(lit[175] mp of HBr salt 153-154°; ^1H NMR ($CDCl_3$) δ2.26 (s, 6H, $N-CH_3$), 2.46 (t, J=7.2 Hz, 2H, CH_2-NMe_2), 3.49 (t, J=7.2 Hz, 2H, $N-CH_2-C$), 4.87 (s, 2H, $Ar-CH_2$), 6.45 (d,J=9.1 Hz,1H, C3-H), 6.89-7.22 (complex m, 3H, thiophene arom.), 7.46 (dd, J_o=9.1,J_m=2.6 Hz, 1H, C4-H), 8.19 (d, J=2.5 Hz, 1H, C6-H); HR EIMS m/e 341.038791 (m+2, $C_{14}H_{18}BrN_3S$, 7.49%), 339.041177 (m+, $C_{14}H_{18}BrN_3S$, 7.41%), 268.976111 ($m-CH_2CH_2NMe_2$, 7.98%), 158.951021 (C_5H_4BrN, 5.35%), 156.953003 (C_5H_4BrN, 3.16%), 97.010747 (C_5H_5S, 100%), 72.080830 ($CH_2CH_2NMe_2$, 55.18%).

Anal. Calcd. for $C_{14}H_{20}N_3SBrCl_2$ (dihydrochloride): C, 40.68; H, 4.88; N, 10.17. Found: C, 40.90; H, 4.86; N, 10.24.

N-(N',N'-Dimethylaminoethyl)-2-amino-5-deuteropyridine (104): The amine 100 (0.100g, 0.409 mmol) was dissolved in 100% ethanol (5ml) and 10% Pd/C (50mg) was added. The reaction was flushed twice with deuterium gas and then stirred under an atmospheric pressure deuterium gas. The catalyst was removed by filtration through a celite pad and the product was obtained as a yellow oil by concentration of

the filtrate. The resulting mixture of amine and amine hydrobromide was redissolved in aqueous base and the product extracted into CH_2Cl_2, dried (K_2CO_3), filtered and concentrated under reduced pressure: ^1H NMR ($CDCl_3$) δ2.26 (s, 6H, N-CH_3), 2.54 (t, J=5.7 Hz, 2H, CH_2-NMe_2), 2.58 (q, J=5.4 Hz, 2H, NH-CH_2-C), 4.95 (broad s, 1H, NH), 6.39 (d, J=8.5 Hz, 1H, C3-H), 7.36 (d, J=8.5 Hz, 1H, C4-H), 8.07 (broad s, 1H, C6-H).

5-Deuteromethapyrilene (1-5D): A solution of 103 (0.012g, 0.0294mmol) in ethanol (95%, 1ml) was treated with 10% Pd/C (0.002g) and deaireated with N_2. The reaction vessel was flushed twice with D_2 gas and then stirred under an atmosphere of deuterium gas. Overnight hydrogenation yielded complete conversion. The catalyst was removed through filtration by a celite pad and the EtOH was concentrated to dryness under reduced pressure: ^1H NMR ($CDCl_3$) δ2.26 (s,6H, N-CH_3), 2.47 (t, J=8.0 Hz, 2H, CH_2-NMe_2), 3.61 (t, J=8.0 Hz, 2H, NCH_2-C), 4.92 (s, 2H, Th-CH_2), 6.48-8.19 (complex m, 6H, arom.); EIMS m/e 262 (m+, 13%) , 204 (m-$CH_2N(CH_3)_2$, 8%), 191 (m-$CH_2CH_2NMe_2$, 33%), 97 ($ThCH_2$, 95%), 71 ($CH_2CH{=}NMe_2$, 83%), 58 ($N(CH_3)_2$, 100%).

5-Tritiomethapyrilene (105): A solution of 103 (0.011g, 0.0025mmol) in 95% EtOH (1ml) was transferred to a round bottom flask and 10% Pd/C (5mg) was added. The sample was

frozen and degassed under vacuum. Tritium gas was added to approximately 1 atm and the hydrogenation was allowed to proceed for 4 hours with stirring. The sample was then frozen and evaporated to dryness under reduced pressure. The resulting material was suspended in EtOH (7ml) and centrifuged to remove the catalyst. The catalyst was washed with an additional 2 ml of EtOH and recentrifuged. The combined ethanolic solution was then lyopholized in a plastic scintillation vial. An aliquot of the oil was diluted with cold methapyrielene and treated with one equivalent of HCl(g) in ether. The resulting solid was crystallized from EtOAc/MeOH/Et_2O. Recrystallization to a constant specific activity led to 3.83 mCi/mmol. Purity was confirmed by TLC.

2-Chloromethylthiophene (106): A). Freshly distilled thiophene (5.25g, 0.062 mol) was dissolved in concentrated HCl (2.6ml, 0.031mol), cooled to 0^o, and the solution saturated with HCl(g). Formaldehyde (6.08ml (37%), 0.075mol) was added dropwise over a 10 minute period. Upon completion of the addition, the product was immediately extracted into Et_2O (3x 15ml). The combined ether extracts were washed with H_2O and saturated $NaHCO_3$ and then dried ($MgSO_4$) and concentrated under reduced pressure. The desired product 106 was purified by vacuum distillation to yield 4.1g (50%) as a clear liquid: bp (0.05 mm) 25^o(lit[181] bp (17mm) 73-75^o); ^1H

NMR ($CDCl_3$) δ 4.78 (s, 2H, benzylic CH_2), 7.09 (m, 3H, arom.); GC-EIMS m/e 134 (m+2, 41%), 132 (m+,76%), 97 (m-Cl, 100%).

2,5-Bischloromethylthiophene (107): 107 was isolated as a byproduct of the reaction to produce 106. This product easily polymerized and approximately 2.8g (25%) was isolated as a clear liquid: bp (0.05mm) 58°; ^1H NMR ($CDCl_3$) δ4.7 (s, 4H, benzylic CH_2), 6.87 (s, 2H, arom CH); GC-EIMS m/e 184 (m+4, 3%), 182 (m+2, 16%), 180 (m, 23%), 147 (m-^{37}Cl, 45%), 145 (m-^{35}Cl, 89%), 110 (m-2Cl, 100%).

B). Thiophene (1ml, 0.0118 mol) was dissolved in anhydrous diethyl ether (20 ml) at room temperature under nitrogen. A solution of nBuLi (7.35 ml of 1.6M in hexane, 0.0118 mol) and TMEDA (1.79 ml, 0.0118 mol) was added dropwise to the thiophene solution and allowed to stir for 1/2 hour after addition was complete to yield 2-lithiothiophene (108). Paraformaldehyde was freshly dried in a vacuum oven for 2 hours at 100°, 15mm. The anhydrous paraformaldehyde (0.356g, 0.0118 mol) was then added in one batch to the anhydrous ethereal solution of 108. The reacton mixture was allowed to stir overnight under nitrogen after which the reaction became reddish in color. The reaction was quenched by addition of water. The ethereal reaction mixture was extracted with dilute HCl (0.2N), H_2O, and then dried ($MgSO_4$), filtered and concentrated under reduced

pressure. The desired product 0.53 ml (40%) of 2-hydroxymethylthiophene (109) was isolated as a clear liquid: ^{1}H NMR ($CDCl_3$) δ1.93 (broad s, 1H, -OH), 4.81 (s, 2H, CH_2), 6.94-7.31 (complex m, 3H, arom.); IR 3330 cm^{-1} (O-H). The alcohol 109 (0.53 ml, 4.2 mmol) was dissolved in ethyl ether (4 ml) and thionyl chloride (0.34 ml, 4.6 mmol) was added dropwise with stirring. After 5 minutes, the reaction mixture was poured into water (25 ml) and extracted with ether (2 x 20 ml). The ether was dried ($MgSO_4$), filtered and concentrated under reduced pressure without heating to yield 0.55g (19%) of 106: bp (0.05mm) 25°.

Methapyrilene (1): In flame dried glassware, a suspension of NaH (0.192g. 3.2 mmol) in anhydrous dioxane (25ml) was brought to reflux under N_2 atmosphere. A solution of 92 (0.5g, 3 mmol) in dioxane (5ml) was added dropwise to the refluxing suspension. The reaction mixture was heated under reflux for 2 hours and then cooled to room temperature. 106 (0.4g, 3mmol) was then added dropwise and the alkylation was heated under reflux overnight. The reaction mixture was cooled to room temperature and filtered. The filtrate was acidified and extracted with CH_2Cl_2 (25ml). Subsequently, the aqueous layer was basified and the product extracted into CH_2Cl_2 (2x 25ml). The basic CH_2Cl_2 extract was dried (K_2CO_3), filtered and concentrated under reduced pressure. The residual brown

oil was subjected to preparative TLC (2x 2000μ) developed with 10% methanol in CH_2Cl_2 to yield 40mg (5%) of 1 as a yellow oil. The ^1H NMR spectrum and EIMS were that of commercially available methapyrilene.

N-(2-Thienylmethyl)-2-aminopyridine (91): 2-Aminopyridine (20g, 0.2125mol) was heated under reflux in toluene (60ml) in the presence of thiophene-2-carboxaldehyde (19.8g, 0.2125mol) for 24 hours with a Dean Stark trap to remove water. The reaction was then cooled to room temperature and the solvent was removed under reduced pressure. The resulting oil was then treated with formic acid (11.3g, 95%) and heated on the steam bath for 1.5 days. A solution of 5% HCl was then added (100ml) and the reaction was extracted with ether. The aqueous layer was basified and the product was partitioned into CH_2Cl_2. The basic organic layers were dried (K_2CO_3), filtered and concentrated under reduced pressure. Vacuum distillation yielded 22.35g (55%) of 91 as a white solid. The product was crystallized from EtOAc/hexanes: mp 77-78°(lit[197] mp 80-83°); bp (0.25mm) 135-136°; ^1H NMR ($CDCl_3$) δ 4.71 (s, 2H, Th-CH_2), 6.3-8.1 (complex m, 7H, arom.).

N-(2-Thienyl-(1D)-2-aminopyridine (134). A solution of the intermediate imine 133 (4g, 0.021mol) in anhydrous THF (10ml) was added dropwise to a stirred suspension of $LiAlD_4$ (0.81g, 0.019mol) in anhydrous THF (10ml) under

inert atmosphere. The reaction mixture was stirred overnight at room temperature and quenched by the addition of 1 ml of H_2O, 1ml of 15% NaOH, and the 3ml of water with vigorous stirring. The salts were removed by vacuum filtration and the filtrate was concentrated under reduced pressure. The product was crystallized from EtOAc/hexanes. Pure 134 (2.28g, 57%) was obtained as white crystals: mp 77-78°; ^{1}H NMR ($CDCl_3$) δ4.66 (broad s, 1H, Th-CHD), 4.78 (broad s, 1H, NH), 6.46-8.07 (complex m, 7H, arom.).

2'-Deuteromethapyrilene Hydrochloride (135): The sodium salt of 134 was condensed with N,N-dimethylaminoethylchloride hydrochloride as described for 1. After workup, the resulting oil was chromatographed on silica gel with a gradient of MeOH/CH_2Cl_2. The product was isolated as a yellow oil which when treated with one equivalent of HCl(g) dissolved in ether yielded a white solid. The salt was crystallized with EtOAc/ MeOH/ Et_2O to yield 0.18g (16%) of 135: mp 161-162°; ^{1}H NMR (D_2O) δ2.93 (s, 6H, $N(CH_3)_2$), 3.37 (t, J=5.8 Hz, 2H, CH_2-NMe_2), 3.94 (t, J=5.8 Hz, 2H, NCH_2-C), 4.87 (s, 1H, ThCHD), 6.75-8.18 (complex m, 7H, arom.); EIMS m/e 262 (m+, 17%), 204 (m-CH_2NMe_2, 18%), 192 (m-$CH_2CH_2NMe_2$ +2H, 58%), 98 (Th-CHD, 88%), 58 (CH_2NMe_2, 100%).

N'-(2-Pyridyl)-2-imidazolone (146). A solution of 2-aminopyridine (0.5g, 5.31mmol) and β-chloroethylisocyanate (0.56g, 5.31mmol) in dioxane (25 ml) was stirred for 3 days at room temperature under N_2. The solvent was removed under reduced pressure. The resulting solid was then treated with 75 ml of aqueous 1 N KOH and warmed until no more solid went into solution. The reaction was filtered and the filtrate extracted with CH_2Cl_2. The CH_2Cl_2 solution was dried (K_2CO_3), filtered and concentrated under reduced pressure to yield the desired product as a solid. The product was crystallized from EtOAc/hexanes to yield 0.34g (40%) of 146 as white crystals: mp 164-165°(lit.[199] mp 165-166°); ^1H NMR ($CDCl_3$) δ3.55 (t, J= 7.5 Hz, 2H, $-HNCH_2-$), 4.18 (t, J=7.2, 8.5 Hz, 2H, $Ar-N-CH_2$), 5.30 (bs, 1H, NH), 6.91 (t, J=6.1 Hz, 1H, C4-H), 7.62 (t, J=8.7 Hz, 1H, C5-H), 8.2, 8.3(d, 2H, C3,C6-H); EIMS m/e 163 (m+, 75%), 162 (m-1, 100%), 149 ($m-CH_2$, 27%), 119 (m-NHCO, 85%), 78 (pyr, 95%).

Anal. Calcd. for $C_8H_9N_3O$: C, 58.88.; H, 5.56; N, 25.75. Found: C, 58.81; H, 5.56; N, 25.75.

N^1-Methyl-N^3-(2-pyridyl)-2-imidazolone (143). A solution of 146 (0.20g, 1.23mmol) and NaH (0.05g,(61%), 1.23mmol) in anhydrous DMF was stirred under N_2 until gas evolution had stopped (45min). A solution of methyl iodide (0.172g, 1.23mmol) in DMF (2ml) was added dropwise to

the reaction mixture and stirred for 2 hours. The solvent was removed under reduced pressure and the product was dissolved in CH_2Cl_2 and extracted with ice cold H_2O. The CH_2Cl_2 solution was subsequently dried (K_2CO_3), filtered and concentrated under reduced pressure. Crystallization from EtOAc/hexanes gave 0.05g (35%) of 143 as white needles: mp 101-102°; ^1H NMR ($CDCl_3$) δ2.91 (s, 3H, N-CH_3), 3.45 (t, J=7.8 Hz, 2H, CH_2-NCH_3), 4.05 (t, J=7.8 Hz, 2H, ArN-CH_2-), 6.86-8.32 (complex m, 4H, arom.); EIMS m/e 177 (m+, 88%), 176 (m-H, 75%), 119 (m-CO-NCH_3, 100%), 107 (pyr-NH=CH_2, 13%), 78 (pyr, 51%).

N-(2,2-Diethoxyethyl)-N-(thienylmethyl)-2-aminopyridine (149): A suspension of sodium hydride (0.336 (61%), 5.26mmol) in anhydrous dioxane (26ml) was brought to reflux under N_2 in flame dried glassware. The amine 91 (1.0g, 5.26mmol) was then added batchwise and heated under reflux for two hours. Bromoacetaldehyde diethylacetal (1.036g, 5.26mmol) was then added dropwise and the reaction heated under reflux overnight. The resulting precipitate was removed by filtration and the filtrate diluted with diethyl ether and washed with water. The aqueous phase was then extracted with CH_2Cl_2 (3x 25ml) and the combined CH_2Cl_2 extracts were washed once with water. The organic phase was then dried (K_2CO_3), filtered and concentrated under reduced pressure. The product was

purified by bulb to bulb distillation to give a yellow oil. This was then further purified by column chromatography (10g) with hexanes as the eluent to yield 0.69g (43%) of 149: bp (0.5mm) >200°(lit[208] bp (0.25 mm) 120-125°); The NMR spectrum and EIMS were identical with those reported previously.

N-(2-Pyridyl)-N-(2'-thienylmethyl)aminoacetaldehyde hydrochloride (150): The diethylacetal 149 (0.150g ,0.49 mmol) was treated with 2N HCl (15ml) for 45 minutes at room temperature. The aqueous acid was removed under vacuum to yield the cyclized aldehyde as a clear oil in approximately 100% yield: ^{1}H NMR ($CDCl_3$) δ4.18 (d, J=6.5 Hz, 2H, CH_2CHO), 4.88 (s, 2H, $ThCH_2$), 6.62-8.16 (complex m, 7H, arom.), 9.47 (s, 1H, CHO); EIMS m/e 232 (m+, 7%), 203 (m- CHO, 10%), 189 (m- CH_2CHO, 23%), 97 ($ThCH_2$, 100%), 78 (pyr., 24%); IR ($CHCl_3$) 1675 cm^{-1} (C=O).

N-(N',N'-Dimethylacetamido)-N-(thienylmethyl)-2-aminopyridine (129): As in the synthesis of 1, a solution of 91 (2.4g, 0.0127 mol) was treated with NaH (0.5g, 0.0127mol) and then N,N-dimethylacetamidochloride (1.53 g, 0.0127 mol) was added. The product was purified by silica gel chromatography (75g) with EtOAc/hexanes gradient as the eluent. The resulting solid was then crystallized from EtOAc/hexanes to yield 1.15g (35%) of 129 as white crystals. Product 129 appears to be sensitive to heat: mp

102-103°; ^{1}H NMR ($CDCl_3$) δ2.95 (s, 3H, N-CH_3), 3.03 (s, 3H, N-CH_3), 4.42 (s, 2H, N-CH_2CONMe_2), 4.89 (s, 2H, $ThCH_2$), 6.49-8.18 (complex m, 7H, arom.); IR (KBr) 1650 cm^{-1} (C=O); EIMS m/e 275 (m+, 7%), 203 (m- $CONMe_2$, 4%), 189 (m- CH_2CONMe_2, 59%), 97 ($ThCH_2$, 100%), 78 (pyr, 20%).

Anal. Calcd. for $C_{14}H_{17}N_3OS$: C, 61.04; H, 6.22; N, 15.27. Found: C, 61.22; H, 6.31; N, 15.19.

N-Formyl-N-(2-thienylmethyl)-2-aminopyridine (130): A solution of amine 91 (1.0g, 5.2 mmol) in dioxane (5ml) was added to a refluxing suspension of NaH (0.145g, 5.79mmol) in anhydrous dioxane (5ml) with stirring under N_2. The reaction mixture was heated under reflux for 2 hours and then Cl_3CCHO (0.51ml, 5.26mmol) was added. The reaction mixture was stirred overnight under reflux, after which it was quenched by the addition of water. The reaction mixture was basified and extracted with CH_2Cl_2 (2x 50ml). The combined organic extracts were dried (K_2CO_3), filtered and concentrated to an oil. Kugel Rohr distillation yielded 0.83g (72%) ofthe product as a pale orange oil: bp (0.05mm) 143-150°; ^{1}H NMR ($CDCl_3$) δ 5.33 (s, 2H, $ThCH_2$), 6.86-7.68 (complex m, 7H, arom.), 9.24 (s, 1H, CHO); IR (neat) 1665 cm^{-1} (C=O); EIMS m/e 218 (m+, 75%), 189 (m- CHO, 100%), 105 (pyr-N=CH, 50%), 97 ($ThCH_2$, 85%), 78 (pyr, 65%).

Anal. Calcd. for $C_{11}H_{10}N_2OS$: C, 60.54; H, 4.62; N, 12.84. Found: C, 60.15; H, 4.59; N, 12.66.

Methapyrilene N-oxide (128): In an Erlenmeyer flask, methapyrilene (1.0g, 3.8mmol) was dissolved in methanol (5ml) and cooled to 0°. To this was added H_2O_2 (0.422ml of 31%, 3.8mmol) and after 2 hours the reaction was allowed to come to room temperature. Another aliquot of H_2O_2 (0.422ml) was added and after 19 hours a third aliquot of H_2O_2 was added. The reaction mixture was allowed to stir for 3 days or until the solution no longer tested positive with phenolphthalien. A small amount of Pt of 4-8 carbon mesh was added and the reaction mixture allowed to stir until H_2 evolution had stopped. The catalyst was then removed by filtration through a celite pad and the filtrate was concentrated under reduced pressure. The product was crystallized from EtOAc to yield 0.77g (73%) of a white powder: mp 74-75°; ^{1}H NMR ($CDCl_3$) δ 3.24 (s, 6H, NCH_3), 3.49 (t, J=7.5 Hz, 2H, CH_2NMe_2), 4.20 (t, J=7.5 Hz, 2H, N-CH_2C-N), 4.88 (s, 2H, ThCH_2), 6.55-8.19 (complex m, 7H, arom.); CIMS m/e 276 (m- 2H, 35%), 262 (m- O +H, 99%), 248 (m- O, CH_2, 44%), 217 (m-$NOMe_2$,75%) 191 (m-$C_2H_2NOMe_2$, 35%), 166 (m- ThCH_2, 74%), 97 (ThCH_2, 100%).

Anal. Calcd. for $C_{14}H_{18}N_3OS\ H_2O$: C, 56.92; H, 7.17; N, 14.23. Found: C, 56.90; H, 7.12; N, 14.15.

N,N-Dimethylacetamido-2-aminopyridine (162): A suspension of NaH (0.33g, 0.0136 mol) in anhydrous dioxane (5ml) was brought to reflux and 2-aminopyridine (1.28g, 0.0136mol) in anhydrous dioxane (5ml) was added dropwise with stirring under N_2. After heating at reflux for 30 minutes, a solution of α-chlorodimethylacetamide (1.5g, 0.0124mol) in dioxane (2ml) was added and the reaction mixture heated under reflux for 2 hours. The reaction mixture was acidified with aqueous dilute HCl and extracted with ether. The aqueous layer was basified with saturated K_2CO_3 and extracted with CH_2Cl_2. The CH_2Cl_2 was dried (K_2CO_3), filtered and concentated under reduced pressure. Preparative TLC with EtOAc(85%):hexanes (15%) as the developing solvent yielded 162 as isolated from the blue band. White crystalline 162 (50mg, 2%) was obtained from cyclohexane recrystallization: mp 96-97°; ^{1}H NMR ($CDCl_3$) δ3.05 (s, 6H, NCH_3), 4.15 (d, J=4.0 Hz, 2H, NCH_2-CO), 5.5 (broad s, 1H, NH), 6.46-8.12 (complex m, 4H, arom.); EIMS m/e 179 (m+, 63%), 134 (m- NMe_2, 17%), 107 (pyr-NH=CH_2, 100%), 79 (pyr, 83%).

N-(2-Pyridyl)-N-(2-thienylmethyl)glycine (164). The amide 129 (0.100g, 0.364mmol) was treated with 4N HCl (0.8mmol) and warmed on a steam bath for 5 minutes. The reaction mixture turned green and the product was extracted into CH_2Cl_2. The CH_2Cl_2 was concentrated under

reduced pressure to yield a green oil: ^{1}H NMR ($CDCl_3$) δ 4.28 (s, 2H, NCH_2COOH), 4.86 (s, 2H, $ThCH_2$), 5.29-8.09 (complex m, 7H, arom.), 9.51 (s, 1H, COOH); CIMS m/e 249 (m+H, 100%), 204 (m- CO_2, 72%), 189 (m- CH_2COOH, 70%), 107, pyr-N=CH_2, 53%), 97 ($ThCH_2$, 65%).

N-(2-Hydroxyethyl)-N-(2-thienylmethyl)-2-aminopyridine (17̲0̲): The cyclized aldehyde 15̲0̲ (1.3g, 4.9mmol) was dissolved in isopropanol (15ml) and neutralized with KOH (0.27g, 4.9mmol) to yield the aldehyde. The salts were removed by filtration and the filtrate was treated with $NaBH_4$ (0.185g, 4.9mmol) and stirred for 5 days. The reaction mixture was then basified and extracted with CH_2Cl_2. The combined organic extracts were dried (K_2CO_3), filtered and concentrated under reduced pressure. After column chromatography (30g) with hexanes/EtOAc gradient elution, the product (0.61g, 54%) was obtained as a yellow oil: ^{1}H NMR ($CDCl_3$) δ 3.80 (broad s, 4H, NCH_2CH_2OH), 4.78 (s, 2H, $ThCH_2$), 7.15-8.11 (complex m, 7H, arom.); EIMS m/e 234 (m+, 20%), 203 (m- CH_2OH, 8%), 189 (m- CH_2CH_2OH, 18%), 97 ($ThCH_2$, 100%), 78 (pyr, 27%).

Anal. Calcd. for $C_{12}H_{14}N_2OS$: C, 61.51; H, 6.02; N, 11.96. Found: C, 61.43, H, 6.04; N, 11.96.

References

(1) Lijinsky,W.; Taylor,H.W. Fd. Cosmet. Toxicol. 1977, 15, 269.

(2) Lancet 1979, 2, 108.

(3) Redmond,Jr.,D.E. New Engld. J. Med. 1970, 282, 18.

(4) Pott,P. Natl. Cancer Inst. Monographs 1963, 10, 7.

(5) Miller,J.A.; Miller,E.C. in "Biological Reactive Intermediates"; Jollow,D.J.; Kocsis,J.J.; Snyder,R.; Vainio,H.,Eds.; Plenum Press; New York,1977; Ch.2.

(6) a) Yang,S.K.; Roller,P.P.; Gelboin,H.V. in "Microsomes and Drug Oxidations"; Ullrich,V.; Roots, I; Hildebrandt,A.; Estabrook,R.W.; Conney,A.H.,Eds.; Pergamon Press: Oxford,1977; p 403. b) Thakker,D.R.; Yagi,H.; Akagi,H.; Koreeda,M.; Lu,A.Y.H.; Levin,W.; Wood,A.W.; Conney,A.H.; Jerina,D.M. Chem.-Biol.Interac. 1977, 16, 281.

(7) Levin,W.; Wood,A.W.; Chang,R.L.; Slaga,T.J.; Yagi,H.; Jerina,D.W.; Conney,A.H. Cancer Res. 1977, 37, 2721.

(8) Weinstein,I.B.; Jeffrey,A.M.; Jennette,K.W.; Blobstein,S.H.; Harvey,R.G.; Harris,C.; Autrup,H.; Kasai,H.; Nakanishi,K. Science 1976, 193, 592.

(9) a) Gurtoo,H.L.; Dave,C.V. Cancer Res. 1975, 35, 382. b) Miller,J.A.; Miller,E.C. Cancer Res. 1975, 35, 3811.

(10) a) Swenson,D.H.; Miller,E.C.; Miller,J.A. Biochem. Biophys. Res. Comm. 1974, 60, 1036. b) Swenson,D.H.; Miller,J.A.; Miller,E.C. Biochem. Biophys. Res. Comm. 1973, 53, 1260.

(11) Miller,E.C.; Miller,J.A. in "The Molecular Biology of Cancer"; Busch,H., Ed.; Academic Press: New York,1974; p 377. b) Irving,C.C. in "Metabolic Conjugation and Metabolic Hydrolysis"; Vol. 1; Fishman,W.H., Ed.; Academic Press: New York, 1970; p 53.

(12) Miller,E.C. Cancer Res. 1978, 38, 1479.

(13) Lai,D.Y.; Arcos,J.C. Life Sci. 1980, 27, 2149.

(14) Weisburger,J.H.; Williams,G.M. Science 1981, 214, 401.

(15) McMahon,R.E. J. Pharm. Sci. 1966, 55, 457.

(16) Bickel,M.H. Xenobiotica 1971, 1, 313.

(17) Bickel,M.H. Pharmacological Revs. 1969, 21, 325.

(18) Lockwood,G.F.; Houston,J.B. J. Pharm. Pharmacol. 1980, 32, 619.

(19) Hlavica,P; Aichinger,G. Biochem. Biophys. Acta 1978, 544, 185.

(20) Beckett,A.H. Xenobiotica 1971, 1, 365.

(21) Brookman,S.; Kourounakis,P. J. Pharm. Sci. 1977, 66, 1492.

(22) Buening,M.K.; Franklin,M.R. Drug Met. Disp. 1976, 4, 244.

(23) Bickel,M.H. Arc. Biochem. Biophys. 1971, 148, 54.

(24) Matsubara,T.; Touchi,A. Jpn. J. Pharmacol. 1977, 27, 701.

(25) Gorrod,J.W.; Temple,D.J.; Beckett,A.H. Xenobiotica 1975, 5, 465.

(26) Devereux,T.R.; Fouts,J.R. Chem.-Biol. Interac. 1974, 8, 91.

(27) Willi,P.; Bickel,M.H. Arc. Biochem. Biophys. 1973, 156, 772.

(28) Ohmiya,Y.; Mehendale,H.M. Life Sci. 1980, 26, 1411.

(29) Hucker,H.B.; Balletto,A.J.; Stauffer,S.C.; Zacchei,A.G.; Arison,B.H. Drug Met. Disp. 1974, 2, 406.

(30) Nash,T. Biochem. J. 1953, 55, 416.

(31) Adams,H.K.;Douglas,E.J.; Kemp,J.V. Biochem. Pharmacol. 1979, 27, 145.

(32) Foster,A.B.; Griggs,L.J.; Jarman,M.; van Maanen,J.M.S.; Schulten,H.-R. Biochem. Pharmacol. 1980, 29, 1977.

(33) Bast,A.; Noordhoek,J. Biochem. Pharmacol. 1981, 30, 19.

(34) Goromaru,T.; Noda,A.; Matsuyama,K.; Iguchi,S. Chem. Pharm. Bull. 1976, 24, 1376.

(35) Iguchi,S.; Goromaru,T.; Noda,A. Chem. Pharm. Bull. 1975, 23, 932.

(36) Noda,A.; Tsubone,N.; Mihara,M.; Goromaru,T.; Iguchi,S. Chem. Pharm. Bull. 1976, 24, 3229.

(37) McMahon,R.E.; Culp,H.W.; Occolowitz,J.C. J. Am. Chem. Soc. 1969, 91, 3389.

(38) Karim,A.; Ranney,R.E.; Kraychy,S. J. Pharm. Sci. 1972, 61, 888.

(39) Porter,C.C.; Arison,B.H.; Gruber,V.F.; Titus,D.C.; Vandenhuevel,W.J.A. Drug Met. Disp. 1975, 3, 189.

(40) Huizing,G.; Beckett,A.H.; Segura,J.; Bakke,O.M. Xenobiotica 1980, 10, 211.

(41) Huizing,G.; Beckett,A.H. Xenobiotica 1980, 10, 593.

(42) Cho,A.H.; Miwa,G.T. Drug Met. Disp. 1973, 2, 477.

(43) Gorrod,J.W. Chem.-Biol. Interac. 1973, 7, 289.

(44) Henderson,P.T.; Vree,T.B.; vanGinneken,C.A.M.; van Rossum,J.M. Xenobiotica 1974, 4, 121.

(45) Johnson,E.F. in "Reviews in Biochemical Toxicology"; Vol. 1; Hodgson,E.; Bend,J.R.; Philpot,R.M., Eds.; Elsevier/North Holland, Inc.: New York, 1979; pp1-27.

(46) White,R.E.; Coon,M.J. Ann. Rev. Biochem. 1980, 49, 315.

(47) Gorrod,J.W.; Temple,D.J. Xenobiotica, 1976, 6, 265.

(48) Schwartz,M.A.; Kolis,S.J. J. Pharmacol. Exp. Ther. 1972, 180, 180.

(49) Gescher,A.; Hickman,J.A.; Stevens,M.F.G. Biochem. Pharmacol. 1979, 28, 3235.

(50) Gescher,A.; D'Incalci,M.; Fanelli,R.; Farina,P. Life Sci. 1980, 26, 147.

(51) Ames,M.M.; Sanders,M.E.; Tiede,W.S. Life Sci. 1981, 29, 1591.

(52) Nguyen,T.-L.; Dagne,E.; Gruenke,L.; Bhargava,H.; Castagnoli,Jr,N. J. Org. Chem. 1981, 46, 758.

(53) Ho,B.; Castagnoli,Jr.,N. J. Med. Chem. 1980, 23, 133.

(54) Sadee,W.; Garland,W.; Castagnoli,Jr.,N. J. Med. Chem. 1971, 14, 643.

(55) Thompson,J.A.; Shioshita,G.W. Drug Met. Disp. 1981, 9, 5.

(56) Osterloh,J.D.; Karakaya,A.; Carter,D.E. Drug Met. Disp. 1980, 8, 12.

(57) Cowan,D.A.; Huizing,G.; Beckett,A.H. Xenobiotica 1976, 6, 605.

(58) Beckett,A.H.; Hutt,A.J. J.Pharm. Pharmacol. 1982, 34, 614.

(59) Nguyen,T.-L.; Gruenke,L.D.; Castagnoli,Jr.,N. J. Med. Chem. 1979, 22, 259.

(60) Kammerer,R.C.; Schmitz,D.A.; DiStefano,E.W.; Cho,A.K. Drug Met. Disp. 1981, 9, 274.

(61) Kadlubar,F.F.; Morton,K.C.; Ziegler,D.M. Biochem. Biophys. Res. Comm. 1973, 54, 1255.

(62) Werringloer,J.; Kawano,S.; Estabrook,R.W. in "Microsomes, Drug Oxidations and Chemical Carcinogenesis"; Coon,M.J.; Conney,A.H.; Estabrook,R.W.; Gelboin,H.V.; Gillette,J.R.; O'Brien,P.J.,Eds.; Academic Press: New York, 1980; p 403.

(63) Ashley,P.L.; Griffin,B.W. Molec. Pharmacol. 1981, 19, 146.

(64) Griffin,B.W.; Ting,P.L. Biochemistry 1978, 17, 2206.

(65) Nordblom,G.D.; White,R.E.; Coon,M.J. Arc. Biochem. Biophys. 1976, 175, 524.

(66) Lichtenberger,F.; Nastainczyk,W.; Ullrich,V. Biochem. Biophys. Res. Comm. 1976, 70, 939.

(67) O'Brien,P.J. Pharmac. Ther. A. 1978, 2, 517.

(68) Kirmse,W. "Carbene Chemistry"; Academic Press: New York, 1971; Ch. 7.

(69) Griffin,B.W. in "Microsomes, Drug Oxidations and Chemical Carcinogenesis"; Coon,M.J.; Conney,A.H.; Estabrook,R.W.; Gelboin,H.V.; Gillette,J.R.; O'Brien, P.J., Eds.; Academic Press: New York, 1980; p 72.

(70) Nguyen,T.-L., Gruenke,L.D.; Castagnoli,Jr.,N. J. Med. Chem. 1976, 19, 1168.

(71) Ziegler,R.; Ho,B.; Castagoli,Jr.,N. J. Med. Chem. 1981, 24, 1133.

(72) Murphy,P.J. J. Biol. Chem. 1973, 248, 2796.

(73) Ward,D.; Kalir,A.; Trevor,A.; Adams,J.; Baillie,T.; Castagnoli,Jr.,N. J. Med. Chem. 1982, 25, 492.

(74) Brandage,S.; Lindblom,L. Acta Chem. Scand. B. 1979, 33, 187.

(75) Hucker,H.B.; Gillette,J.R.; Brodie,B.B. J. Pharmacol. Exp. Ther. 1960, 129. 94.

(76) Brandange,S.; Lindblom,L. Biochem. Biophys. Res. Comm. 1979, 91, 991.

(77) Ruenitz,P.C.; McLennon,T.P.; Sternson,L.A. Drug Met. Disp. 1979, 7, 204.

(78) Schraven,E.; Koss,F.W.; Keck,J., Beisenherz,G.; Bucheler,A.; Lindner,W. Eur. J. Pharmacol. 1967, 1, 445.

(79) Nelson,J.O.; Kearney,P.C.; Plimmer,J.R.; Menzer,R.E. Pest. Biochem. Physiol. 1977, 7, 73.

(80) Ketterer,B.; Srai,S.K.S.; Waynforth,B.; Tullis,D.L.; Evans,F.E.; Kadlubar,F.F. Chem.-Biol. Interac. 1982, 38, 287.

(81) Abdel-Monem,M.M. J. Med. Chem. 1975, 18, 427.

(82) Nelson,S.D.; Pohl,L.R.; Trager,W.F. J. Med. Chem. 1975, 18, 1062.

(83) Thompson,J.A.; Holtzman,J.L. Drug Met. Disp. 1974, 2, 577.

(84) Miwa,G.T.; Garland,W.A.; Hodshon,B.J.; Lu,A.Y.H.; Northrop,D.B. J. Biol. Chem. 1980, 255, 6049.

(85) Miwa,G.T.; Zweig,J.S.; Walsh,J.S.A.; Lu,A.Y.H. in "Microsomes, Drug Oxidations and Chemical Carcinogenesis"; Coon,M.J.; Conney,A.H.; Estabrook,R.W.; Gelboin,H.V.; Gillette,J.R.; O'Brien,P.J., Eds.; Academic Press: New York, 1980; p 363.

(86) Miwa,G.T.; West,S.B.; Huang,M.-T.; Lu,A.Y.H. J. Biol. Chem. 1979, 254, 5695.

(87) Walsh,C. "Enzymatic Reaction Mechanisms"; W.H. Freeman and Company: San Francisco, 1979; p 118.

(88) vonBahr,C.; Hedlund,I.; Karlen,B.; Backstrom,D.; Grasdalen,H. Acta Pharmacol. et. Toxicol. 1977, 41, 39.

(89) Nyberg,G.; Karlen,B.; Hedlund,I.; Grundin,R.; vonBahr,C. Acta Pharmacol. et. Toxicol. 1977, 40, 337.

(90) Duquette,P.H.; Erickson,R.R.; Holtzman,J.L. in "Microsomes, Drug Oxidations and Chemical Carcinogenesis"; Coon,M.J.; Conney,A.H.; Estabrook,R.W.; Gelboin,H.V.; Gillette,J.R.; O'Brien,P.J., Eds.; Academic Press: New York, 1980; p 311.

(91) Miwa,G.T.; West,S.B.; Lu,A.Y.H. J. Biol. Chem. 1978, 253, 1921.

(92) Kitada,M.; Omori,S.; Igarashi,T.; Kanakubo,Y.; Kitagawa,H. Biochem. Biophys. Res. Comm. 1980, 97, 1527.

(93) Beckett,A.H.; Hewick,D.S. J. Pharm. Pharmacol. 1967, 19, 135.

(94) Baker,J.; Chaykin,S. Biochim. Biophys. Acta 1960, 41, 548.

(95) Baker,J.R.; Chaykin,S. J. Biol. Chem. 1962, 237, 1309.

(96) Kuntzman,R.; Phillips,A.; Tsai,I.; Klutch,A.; Burns,J.J. J. Pharmacol. Exp. Ther. 1967, 155, 337.

(97) McMartin,C.; Simpson,P. Clin. Pharmacol. Ther. 1970, 12, 73.

(98) Ishida,T.; Oguri,K.; Yoshimura,H. Drug Met. Disp. 1979, 7, 162.

(99) Ziegler,D.M.; Mitchell,C.H. Arc. Biochem. Biophys. 1972, 150, 116.

(100) Ruenitz,P.C. Drug Met. Disp. 1981, 9, 456.

(101) Gorrod,J.W.; Jenner, P.; Keysell,G.; Beckett,A.H. Chem.-Biol. Interac. 1971, 3, 269.

(102) Booth,J.; Boyland,E. Biochem. Pharmacol. 1970, 19, 733.

(103) Booth,J.; Boyland,E. Biochem. Pharmacol. 1971, 20, 407.

(104) Testa,B.; Jenner,P.; Beckett,A.H.; Gorrod,J.W. Xenobiotica 1976, 6, 553.

(105) Duffel,M.W.; Poulson,L.L.; Ziegler,D.M. Fed. Proc. 1979, 38, 732.

(106) Ziegler,D.M.; Poulson,L.L. in "Methods of Enzymology",Vol. 52; Fleischer,S.; Packer,L., Eds.; Academic Press: New York, 1978; p 142.

(107) Miller,B.S.S.; Ziegler,D.M. Arc. Biochem. Biophys. 1971, 145, 358.

(108) Hlavica,P.; Kehl,M. Biochem. J. 1977, 164, 487.

(109) Hlavica,P.; Hulsmann,S. Biochem. J. 1979, 182, 109.

(110) Hlavica,P.; Hulsmann,S. in "Microsomes, Drug Oxidations and Chemical Carcingenesis"; Coon,M.J.; Conney,A.H.; Estabrook,R.W.; Gelboin,H.V.; Gillette,J.R.; O'Brien,P.J., Eds.; Academic Press: New York, 1980; p 217.

(111) Beaty,N.; Ballou,D. in "Microsomes, Drug Oxidations and Chemical Carcinogenesis"; Coon,M.J.; Conney,A.H.; Estabrook,R.W.; Gelboin,H.V.; Gillette,J.R.; O'Brien,P.J., Eds.; Academic Press: New York, 1980; p 299.

(112) Beaty,N.B.; Ballou,D.P. J. Biol. Chem. 1980, 255, 3817.

(113) Poulson,L.L.; Ziegler,D.M. J. Biol. Chem. 1979, 254, 6449.

(114) Ball,S.; Bruice,T.C. J. Am. Chem. Soc. 1979, 101, 4017.

(115) Ball,S.; Bruice,T.C. J. Am. Chem. Soc. 1980, 102, 6498.

(115A) Nee,M.W.; Bruice,T.C. J. Am. Chem. Soc. 1982,104, 6123.

(116) Shimokawa,O.; Ishimoto,M. J. Biochem. 1979, 86, 1709.

(117) Rajagopalan,K.V. in "Enzymatic Basis of Detoxication", Vol. 1; Jakoby,W.B., Ed.; Academic Press: New York, 1980; Ch. 14.

(118) Sugiura,M.; Iwasaki,K.; Noguchi,H.; Kato,R. Life Sci. 1974, 15, 1433.

(119) Iwasaki,K.; Noguchi,H.; Kato,R.; Imai,Y.; Sato,R. Biochem. Biophys. Res. Comm. 1977, 77, 1143.

(120) Shannon,P.; Bruice,T.C. J. Am. Chem. Soc. 1981, 103, 4580.

(121) Bickel,M.H.; Weder,H.J.; Aebi,H. Biochem. Biophys. Res. Comm. 1968, 33, 1012.

(122) Nagy,A.; Hansen,T. Acta Pharmacol. et. Toxicol. 1978, 42, 58.

(123) Gorrod,J.W.; Damani,L.A. Xenobiotica 1979, 9, 219.

(124) Gorrod,J.W.; Damani,L.A. Xenobiotica 1979, 9, 209.

(125) Gorrod,J.W.; Damani,L.A. Eur. J. Drug Met. Pharmacokin. 1980, 5, 53.

(126) Damani,L.A.; Crooks,P.A.; Cowan,D.A. Drug Met. Disp. 1981, 9, 270.

(127) Dagne,E.; Castagnoli,Jr.,N. J. Med. Chem. 1972, 15, 840.

(128) Burns,J.; Duncan,W.A.M.; Scales,B. Biochem. Pharmacol. 1967, 16, 463.

(129) Crew,M.C.; DiCarlo,F.J. Drug Met. Disp. 1976, 4, 147.

(130) Bachur,N.R.; Felsted,R.L. Drug Met. Disp. 1976, 4, 239.

(131) Lee,Y.C.; Gholson,R.K.; Raica,N. J. Biol. Chem. 1969, 244, 3277.

(132) Stubley,C.; Subryan,L.; Stell,J.G.P; Perrett,R.H.; Ingle,P.B.H.; Mathieson,D.W. J. Pharm. Pharmacol. 1977, 29, 77p.

(133) Bray,H.G.; Carpanini,F.M.B Biochem. J. 1968, 109, 11p.

(134) Bray,H.G.; Carpanini,F.M.B.; Waters,B.D. Xenobiotica 1971, 1, 157.

(135) Cripps,R.E. Biochem. J. 1973, 134, 353.

(136) Meshi,T.; Nakamura,S.; Sato,Y. Chem. Pharm. Bull. 1972, 20, 1687.

(137) Robbins,J.D.; Bakke,J.E.; Feil,V.J. J. Agr. Food Chem. 1970, 18, 130.

(138) Harrison,Jr.,S.D.; Bosin,T.R.; Maickel,R.P. Drug Met. Disp. 1974, 2, 228.

(139) Bosin,T.R.; Bickers,R.G.; Dinner,A. Drug Met. Disp. 1978, 6, 31.

(140) Traficante,L.J.; Siekierski,J.; Sakalis,G.; Gershon,S. Biochem. Pharmacol. 1979, 28, 621.

(141) Breyer-Pfaff,U.; Kreft,H.; Rassner,H.; Prox,A. Drug Met. Disp. 1978, 6, 114.

(142) Winek,C.L.; Fochtman,F.W.; Trogus,Jr.,W.J.; Fusia,E.P.; Shanor,S.P. Clin. Toxicol. 1977, 11, 287.

(143) Ainsworth,C.A.;Biggs,J.D. Clin. Toxicol. 1977, 11, 281.

(144) Andrews,A.W.; Fornwald,J.A.; Lijinsky,W. Toxicol. Appl. Pharmacol. 1980, 52, 237.

(145) a) Pienta,R.J. in "The Predictive Value of Short Term Screening Tests in Carcinogenicity Evaluation"; Williams,G.M. etal., Eds.; Elsevier/North Holland/Biomedical Press: Amsterdam, 1980; p 149-169. b) Pienta,R.J.; Poiley,J.A.; Lebherz,W.B. Int. J. Cancer 1977, 19, 642.

(146) Iype,T. personal communication in Reznik-Schuller,H.M.; Lijinsky,W. Ecotoxicol. Environ. Safety 1982, 6, 328.

(147) Probst,G.S.; Neal,S.B. Cancer Letters 1980, 10, 67.

(148) Althaus,F.R.; Lawrence,S.D.; Sattler,G.L.; Pitot,H.C.

Mutation Res. 1982, 103, 213.

(149) Couri,D.; Wilt,S.R.; Milks,M.M. Res. Commun. Chem. Path. Pharmacol. 1982, 35, 51.

(150) Lijinsky,W. Cancer Res. 1974, 34, 255.

(151) Mergens,W.J.; Vane,F.M.; Tannenbaum,S.R.; Green,L.; Skipper,P.L. J. Pharm. Sci. 1979, 68, 827.

(152) Lijinsky,W.; Reuber,M.D.; Blackwell,B.-N. Science 1980, 209, 817.

(153) Reznik-Schuller,H.M.; Lijinsky,W. Arch. Toxicol. 1981, 49, 79.

(154) Reznik-Schuller,H.M.; Lijinsky,W. Ecotoxicol. Environ. Safety 1982, 6, 328.

(155) Lefkowitch,J.H.; Arborgh,B.A.M.; Scheuer,P.J. Am. J. Clin. Pathol. 1980, 74, 432.

(156) Williams,G.M. Biochim. Biophys. Acta 1980, 605, 167.

(157) Wilkie,D.; Gooneskera,S. Chem. Ind. 1980, 21, 847.

(158) Egilsson,V.; Evans,I.H.; Wilkie,D. Molec. Gen. Genet. 1979, 174, 39.

(159) Patel,R.; Wilkie,D. Mutation Res. 1982, 100, 179.

(160) Wunderlich,V.; Schutt,M.; Bottger,M.; Graffi,A. Biochem. J. 1970, 118, 99.

(161) Allen,J.A.; Coombs,M.M. Nature 1980, 287, 244.

(162) Backer,J.M.; Weinstein,I.B. Science 1980, 209, 297.

(163) Niranjan,B.G.; Bhat,N.K.; Avadhani,N.G. Science 1982, 215, 73.

(164) Wilkie,D.; Evans,I. Trends in Biochem. Sci. 1982, 7, 147.

(165) Williams,G.M. Fd. Cosmet. Toxicol. 1981, 19, 577.

(166) Weiner,M.; Olson,J.W. Drug Met. Disp. 1980, 8, 139.

(167) Naranjo,P.; Naranjo,E.B. Arch. Int. Pharmacodyn. 1953, 94, 383.

(168) Dusci,L.J.; Hackett,L.P. Clin. Toxicol. 1979, 14, 587.

(169) Schirmer,R.E.; Pierson,R.J. J. Pharm. Sci. 1973, 62, 2052.

(170) Calandre,E.P.; Alferez,N.; Hassanein,K.; Azarnolff, D.L. Clin. Pharmacol. Ther. 1981, 29, 527.

(171) Lowry,O.H.; Rosebrough,N.J.; Farr,A.L.; Randall,R.J. J. Biol. Chem. 1951, 193, 265.

(172) Ziegler,D.M. in "Enzymatic Basis of Detoxication", Vol. 1; Jakoby,W.B.,Ed.; Academic Press: New York, 1980; Ch. 9.

(173) Chaudhuri,N.K.; Servando,O.A.; Manniello,M.J.; Luders,R.C.; Chao,D.K.; Bartlett,M.F. Drug Met. Disp. 1976, 4, 372.

(174) a) Clark, J.H.; Clapp,R.C.; Vaughan, Jr.,J.R.; Sutherland,L.H.; Winterbottom,R.; Anderson,G.W.; Forsythe,J.D.; Blodinger,J.; Eberlin,S.L.; English,J.P. J. Org. Chem. 1949, 14, 216. b) Hutter,C.P.; Djerassi,C.; Beears, W.L.; Mayer,R.L.; Scholtz,C.R. J. Am. Chem. Soc. 1946, 68, 1999.

(175) Marrian,D.H.; Hill,S.J.; Sanders,J.K.M.; Young,J.M. J. Pharm. Pharmacol. 1978, 30, 660.

(176) Meyer,V. Ber. 1883, 16, 1465.

(177) Major,R.T.; Peterson,L.H. J. Org. Chem. 1957, 22, 579.

(178) Stewart,R.; Harris,M.G. J. Org. Chem. 1978, 43, 3123.

(179) Horning,E.C. Org. Syn.; Wiley: New York, 1955; Collect. Vol. III, p 519.

(180) House,H.O. "Modern Synthetic Reactions", 2nd ed; W.A. Benjamin, Inc.: California, 1972; Ch. 1.

(181) Horning,E.C. Org. Syn.; Wiley: New York, 1955; Collect. Vol. III; p 197.

(182) Chadwick,D.J; Willbe,C. J.C.S. Perkin I 1977, 887.

(183) Rao,G.S.; Krishna,G.; Gillette,J.R. Toxicol. Appl. Pharmacol. 1975, 34, 264.

(184) Weinman,E.O.; Geissman,T.A. J. Pharmacol. Exp. Ther. 1959, 125, 1.

(185) Rao,G.S.; Krishna,G.; Gillette,J.R. J. Pharmacol. Exp. Ther. 1975, 195, 433.

(186) Rao,G.S.; Krishna,G.; Gillette,J.R. Biochem. Pharmacol. 1975, 24, 1707.

(187) Bruce,R.B.; Turnbull,L.B.; Newman,J.H.; Pitts, J.E. J. Med. Chem. 1968, 11, 1031.

(188) Kabasakalian,P.; Taggart,M.; Townley,E. J. Pharm. Sci. 1968, 57, 856.

(189) Peets,E.A.; Jackson,M.; Symchowicz,S. J. Pharmacol. Exp. Ther. 1972, 180, 464.

(190) Peets,E.A.; Weinstein,R.; Billard,W.; Symchowicz,S. Arch. int. Pharmacodyn. 1972, 199, 172.

(191) Hespe,W.; deRoos,A.M.; Nauta,W.T. Arch. int. Pharmacodyn. 1965, 156, 180.

(192) Drach,J.C.; Howell,J.P. Biochem. Pharmacol. 1968, 17, 2125.

(193) King,C.T.G.; Weaver,S.A.; Narrod,S.A. J. Pharmacol. Exp. Ther. 1965, 147, 391.

(194) Gaertner,H.J.; Breyer,U. Liomin,G. J. Pharmacol. Exp. Ther. 1973, 185, 195.

(195) Snyder,L.R.; Kirkland,J.J. "Introduction to Modern Liquid Chromatography"; J. Wiley & Sons, Inc.: New York, 1979; Ch. 11.

(196) Knox,J.H.; Jurand,J. J. Chrom. 1975, 110, 103.

(197) a) U.S. Patent #2,713,048. b) U.S. Patent #673,633.

(198) Hallberg,A.; Gronowitz,S. Chemica Scripta 1980, 16, 42.

(199) British Patent #1,441,440.

(200) "Mass Spectrometry of Organic Compounds"; Budzikiewicz,H.; Djerassi,C.; Williams,D.H., Eds.; Holden-Day, Inc.:San Francisco, 1967; p 566.

(200A) Becker,E.D. "High Resolution NMR"; Academic Press: New York, 1980; p.97.

(201) Adams,R.; Dix,J.S. J. Am. Chem. Soc. 1958, 80, 4618.

(202) Bradsher,C.K.; Litzinger,E.F.; Zinn,M.F. J. Heterocyclic Chem. 1965, 2, 331.

(203) Gothoskar,S.V.; Benjamin,T.; Roller,P.P.; Weisburger,E.K. Xenobiotica 1979, 9, 533.

(204) duVigneaud,V.; Dorfmann,R.; Loring,H.S. J. Biol. Chem. 1932, 98, 577.

(205) Lombardino,J.G. J. Med. Chem. 1981, 24, 39.

(206) Blicke,F.F.; Lu,C.-J. J. Am. Chem. Soc. 1952, 74, 3933.

(207) Cope,A.C.; Ciganek,E. "Organic Synthesis"; J. Wiley & Sons: New York,1957; Coll. Col. IV; p 612.

(208) Ho,B. Ph.D. Thesis, University of California, San Francisco, 1980.

(209) Bristow,N.W.; Charlton,P.T.; Peak,D.A.; Short,W.F. J. Chem. Soc. 1954, 616.

(210) Beyerstadt,F.; McElvain,S.M. J. Am. Chem. Soc. 1937, 59, 1273.

(211) Kahla,D.E.; Watson,Jr.,H.A. J. Heterocyclic Chem. 1978, 15, 1149.

(212) Baird,W.M.; Brooks,P. Cancer Res. 1973, 33, 2378.

(213) Bigger,C.A.H.; Tomaszewski,J.E.; Dipple,A. Biochem. Biophys. Res. Comm. 1978, 80, 229.

(214) Lai,D.Y.; Arcos,J.C.; Argus,M.F. Biochem. Pharmacol. 1979, 28, 3545.

(215) Hashimoto,Y.; Takeda,K.; Shudo,K.; Okamoto,T.; Sugimura,T.; Kosuge,T. Chem.-Biol. Interac. 1978, 23, 137.

(216) Hashimoto,Y.; Shubo,K.; Okamoto,T. Chem. Pharm. Bull. 1979, 27, 1058.

(217) Mita,S.; Ishii,K.; Yamazoe,Y.; Kamataki,T.; Kato,R.; Sugimura,T. Cancer Res. 1981, 41, 3610.

(218) Yamazoe,Y.; Shimada,M.; Kamataki,T.; Kato,R. Biochem. Biophys. Res. Comm. 1982, 107, 165.

(219) Kaderbhai,M.A.; Bradshaw,T.K.; Freedman,R.B. Chem.-Biol. Interac. 1981, 36, 211.

(220) Wyndham,C.; Safe,S. Biochemistry 1978, 17, 208.

(221) Shimada,T.; Sato,R. Toxicol. Appl. Pharmacol. 1980, 55, 490.

(222) Tunek,A.; Platt,K.L.; Bentley,P.; Oesch,F. Molec. Pharmacol. Ther. 1978, 14, 920.

(223) Tunek,A.; Schelin,C.; Jergil,B. Chem.-Biol. Interac. 1979, 27, 133.

(224) Schelin,C.; Tunek,A.; Jergil,B. Acta Chemica Scand. B. 1979, 33, 603.

(225) Law,F.C.P. Toxicol. Appl. Pharmacol 1981, 57, 263.

(226) Freeman,R.W.; Uetrecht,J.P.; Woosley,R.L.; Oates, J.A.; Harbison,R.D. Drug Met. Disp. 1981, 9, 188.

(227) Kappus,H.; Remmer,H. Biochem. Pharmacol. 1975, 24, 1079.

(228) Lijinsky,W.; Muschik,G.M. J. Cancer Res. Clin. Oncol. 1982, 103, 69.

(229) Raman,A.; Chong,Y.K. Clin. Exp. Pharmacol. Physiol. 1975, 2, 147.

(230) Peter,J.B.; Lee,L.D. Biochem. Biophys. Res. Comm. 1967, 28, 1053.

(231) Franklin,T.J.; Jones,C.W.; Redfearn,E.R. Biochim. Biophys. Acta 1967, 131, 240.

(232) Judah,J.D. Biochim. Biophys. Acta 1961, 53, 375.

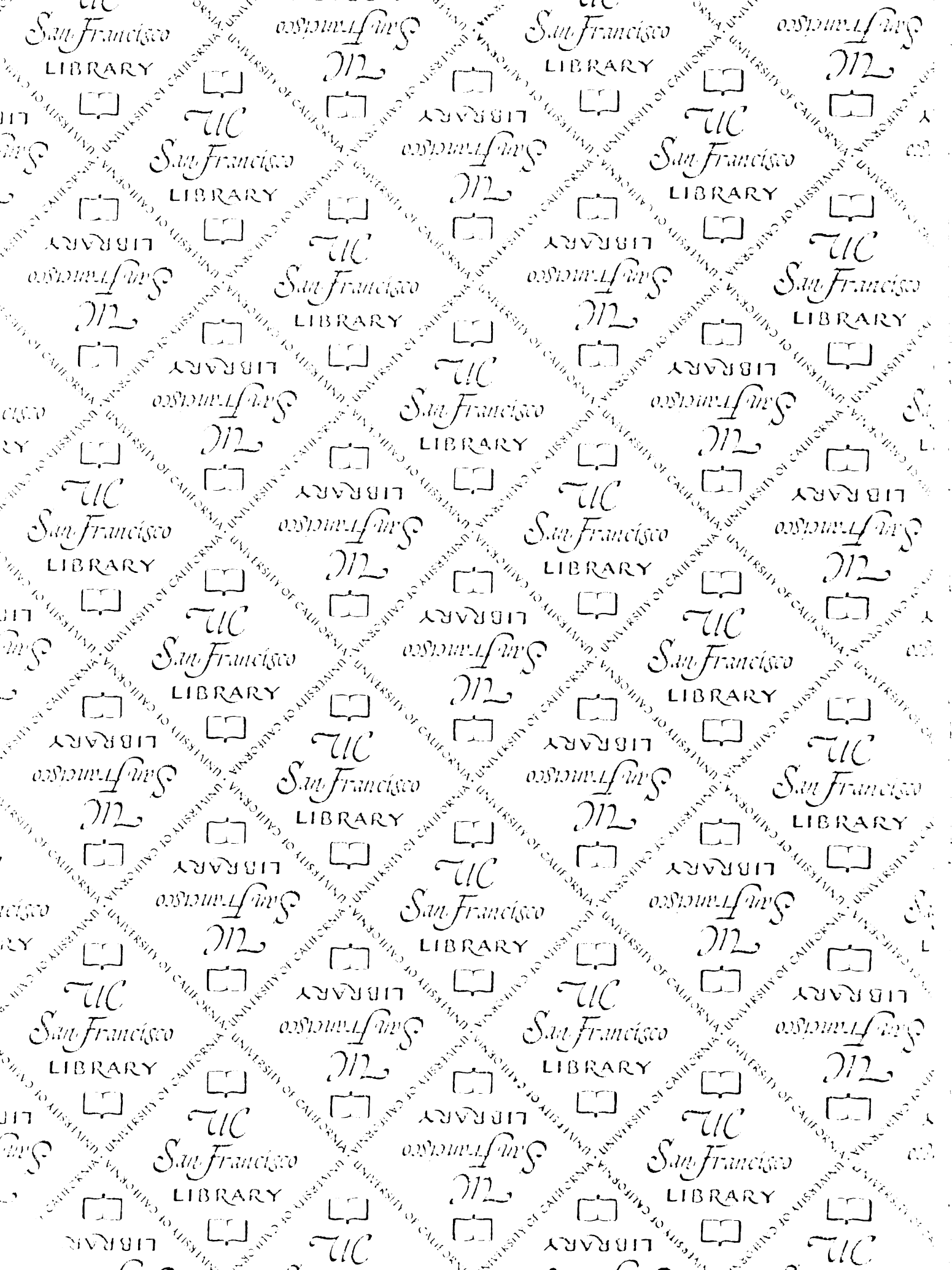
UC
San Francisco
LIBRARY
UNIVERSITY OF CALIFORNIA · UNIVERSITY OF CALIFORNIA